

UNIVERSIDADE FEDERAL DO PARANÁ

GUSTAVO JABOR GOZZI

DERIVADOS 1,3,4-TIADIAZÓIS MESOIÔNICOS E INDENO[1,2-*b*]INDÓIS:
CITOTOXICIDADE E EFEITOS SOBRE TRANSPORTADORES ABC

CURITIBA
2015

GUSTAVO JABOR GOZZI

DERIVADOS 1,3,4-TIADIAZÓIS MESOIÔNICOS E INDENO[1,2-*b*]INDÓIS:
CITOTOXICIDADE E EFEITOS SOBRE TRANSPORTADORES ABC

Tese apresentada como requisito parcial à obtenção do grau de Doutor em Ciências-Bioquímica, no curso de Pós-graduação em Ciências-Bioquímica, Setor de Ciências Biológicas, Universidade Federal do Paraná.

Orientadora: Prof^a. Dr^a. Silvia Maria Suter Correia Cadena

Colaborador: Prof. Dr. Attilio Di Pietro

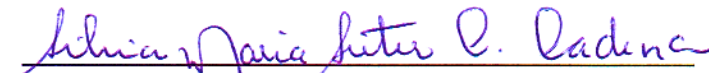
CURITIBA
2015


TERMO DE APROVAÇÃO

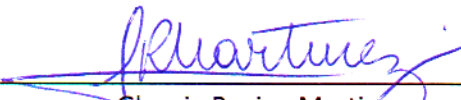
GUSTAVO JABOR GOZZI

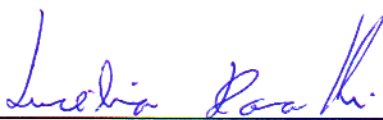
Derivados 1,3,4-Tiadiazóis Mesoiónicos e Indenoindóis: Citotoxicidade e Efeitos sobre Transportadores ABC


Tese aprovada como requisito parcial para obtenção do grau de Doutor no curso de Pós-Graduação em Ciências-Bioquímica, Setor de Ciências Biológicas, Universidade Federal do Paraná, pela seguinte banca examinadora:


Prof.ª Dr.ª Silvia Maria Suter Correia Cadena – Orientador
Departamento de Bioquímica, UFPR


Prof.ª Dr.ª Sheila Maria Brochado Winnischofer
Departamento de Bioquímica, UFPR


Glaucia Regina Martinez
Departamento de Bioquímica, UFPR


Prof.ª Dr.ª Lucélia Donatti
Departamento de Biologia Celular, UFPR


Prof. Dr. Antonio F. Pereira
Departamento de Microbiologia Geral - Instituto de Microbiologia - UFRJ

Curitiba, 16 de outubro de 2015.

AGRADECIMENTOS

Agradeço primeiramente aos meus pais, que fizeram o possível e o impossível para que eu concluísse meus estudos, desejando apenas minha felicidade como retorno.

À minha orientadora Prof^a. Dr^a. Silvia M. S. C. Cadena, que foi muito paciente, gentil e compreensiva durante estes quatro anos (além do mestrado). Serei eternamente grato pelo incentivo, confiança e todo precioso ensinamento.

Ao Dr. Attilio Di Pietro, meu orientador na França, que me acolheu sem restrições em seu laboratório e não poupou esforços para realização deste trabalho. Je vous remercie, Attilio, pour être toujours à l'écoute et pour l'opportunité que vous m'avez donné. Ça a été un plaisir de travailler dans votre laboratoire.

Às professoras do grupo de oxidação biológicas e cultivo celular, em especial à Prof^a. Dr^a. Glauca R. Martinez e Prof^a. Dr^a. Sheila M. B. Winnischofer pelas discussões e correções do projeto, e à Prof^a. Dr^a. Maria E. M. Rocha, pelo conforto emocional e incentivo.

À Dr^a. Amanda R. A. Pires, pelas discussões do trabalho e risadas nos momentos mais difíceis. Ao Dr. Glauco Valdameri, pelo grande incentivo no início do meu doutorado, pelas colocações críticas e pela recomendação ao Dr. Attilio Di Pietro.

Aos amigos do laboratório, em especial às amigadas que se fortaleceram além do laboratório: Anna, Aninha, Lyvia, Monique e Stephane.

Aos amigos do laboratório da França, em especial a Nathalia, pelas discussões e cafés, e Evelyn, pelos procedimentos iniciais no laboratório e discussões.

À minha tia Rosana, sempre apontando os lados positivos nos momentos mais difíceis.

Ao programa de Pós-graduação em Ciências-Bioquímica e às agências financiadoras brasileiras e francesas.

*“E aqueles que foram vistos dançando foram julgados insanos por aqueles
que não podiam escutar a música”*

Friedrich Nietzsche

RESUMO

O carcinoma hepatocelular (CHC) possui uma alta taxa de mortalidade e apenas um quimioterápico, com eficiência limitada, está disponível para seu tratamento. Buscando potenciais drogas para o tratamento do CHC, neste estudo foram avaliados os efeitos de derivados 1,3,4-tiadiazóis mesoiônicos (MI-D, MI-J, MI-F e MI-2,4diF) em células de hepatocarcinoma humano (HepG2) e em hepatócitos de rato em cultura. A viabilidade das células HepG2, avaliada pelo método do MTT, foi reduzida em ~50% pelos derivados (25 μ M para MI-J, MI-F, MI-2,4diF e 50 μ M para MI-D - 24h). Esta citotoxicidade foi confirmada pelo aumento da atividade da enzima lactato desidrogenase (LDH) no meio extracelular, em ~ 55, 24 e 16% após incubação com MI-D, MI-J e MI-F (25 μ M - 24 h), respectivamente. Nestas condições, análises por citometria de fluxo mostraram um aumento no número de células marcadas com anexina V e iodeto de propídio, de ~11, 76, 25 e 25 para MI-D, MI-J, MI-F e MI-2,4diF, respectivamente. O aumento na fragmentação do DNA também foi observado, em ~12, 9 e 8% para MI-J, MI-F e MI-2,4diF, respectivamente. Alterações morfológicas características de indução de apoptose foram observadas após incubação com todos os derivados (3h - 5 μ M). Nenhuma citotoxicidade foi observada quando células não-tumorais (hepatócitos de ratos) foram tratadas com os compostos na concentração de 25 μ M por 24 h. Neste estudo também se investigou a interação destes derivados com os principais transportadores responsáveis pela resistência aos tratamentos quimioterápicos: Pgp, ABCG2 e MRP1. MI-D, MI-4F e MI-2,4diF foram substratos de Pgp (RR= 2,4; 2,8 e 5,2), cuja atividade transportadora foi inibida por MI-J (~ 13% - 30min). Todos os derivados inibiram tanto a atividade de ABCG2 (~ 37, 21, 12 e 18 % para MI-D, MI-J, MI-4F e MI-2,4diF - 30min) quanto de MRP1 (~ 8, 36, 10 e 20% para MI-D, MI-J, MI-4F e MI-2,4diF -30min). Ainda neste estudo, novos inibidores de ABCG2 foram desenvolvidos através de substituições apropriadas nos anéis do núcleo indeno[1,2-b]indol. Foram obtidos potentes inibidores de ABCG2 (4c, 4h, 4i, 4j, 4k - IC₅₀= 0,21-0,49 μ M - N⁵ = fenetila) ou da caseína quinase II (CK2) (4a, 4p, 4e - IC₅₀= 0,0025-0,36 μ M N⁵ = isopropila) quando o núcleo cetônico indeno[1,2-b]indol foi utilizado. Os derivados 4h, 4j, 4l e 4d apresentaram baixa citotoxicidade intrínseca (IG₅₀ 28-100 μ M), o que resultou em índices terapêuticos (IT) aceitáveis para utilização em modelos *in vivo* (IT= 98-430), entretanto, 4h, 4j, 4k não foram seletivos em relação à atividade inibitória em MRP1 (44, 87 e 86% - 10 μ M). A utilização de um núcleo fenólico indeno[1,2-b]indol resultou em inibidores com maior potência (5c, 5f, 5h- IC₅₀= 0,15-0,16 μ M) e seletividade em CK2, Pgp e MRP1. Baixa citotoxicidade intrínseca (5c, 5f, 5h- IG₅₀= 42-54 μ M) e alto IT (267-360) também foram encontrados. A partir dos resultados obtidos, conclui-se que derivados 1,3,4-tiadiazóis mesoiônicos e indeno[1,2-b]indóis fenólicos são candidatos promissores para futuras investigações *in vivo* visando o tratamento do CHC e a quimiosensibilização de tumores superexpressando ABCG2, respectivamente.

Palavras-chave: Carcinoma hepatocelular. Células HepG2. Cultura primária de hepatócitos. Derivados 1,3,4-tiadiazóis mesoiônicos. Derivados indeno[1,2-b]indóis. Inibidores de ABCG2.

ABSTRACT

Hepatocellular carcinoma (HCC) has a high mortality rate and only one chemotherapy drug is available for its treatment, which has limited efficacy. Aiming to find potential drugs for HCC treatment, in this study the effects of 1,3,4-thiadiazolium mesoionic derivatives (MI-D, MI-J, MI-F and MI-2,4diF) were evaluated on human hepatocellular carcinoma cells (HepG2) and primary rat hepatocytes. The viability of HepG2 was reduced by ~ 50% after treatment with derivatives (25 μ M for MI-J, MI-F and MI-2,4diF and 50 μ M for MI-D- 24h), as shown by MTT assay. The cytotoxicity was confirmed by the increase of lactate dehydrogenase (LDH) in cells supernatant at 55, 24 and 16% for MI-J, MI-4F and MI-2,4diF, respectively (at 25 μ M after 24 h). Under same conditions, all compounds increased the number of cell doubly-stained with annexin V and PI (76% for MI-J, 25% for MI-4F and MI-2,4diF, and 11% for MI-D), as demonstrated by flow cytometry. DNA fragmentation was also observed upon MI-J, MI-4F and MI-2,4diF treatment (by 12%, 9% and 8%, respectively). Morphological features of apoptosis induction were observed after incubation with all derivatives (3h – 5 μ M). It was not observed cytotoxicity when non-tumor hepatocytes were treated with derivatives (25 μ M – 24h). This study also investigated the interaction of these derivatives with the main transporters related to chemotherapy resistance: Pgp, ABCG2 and MRP1. MI-D, MI-4F e MI-2,4diF were Pgp substrates (RR = 2.4; 2.8 and 5.2), and MI-J inhibited the transporter activity of Pgp by 13% (30 min). All derivatives inhibited both ABCG2 (by ~ 37, 21, 12 and 18 % for MI-D, MI-J, MI-4F e MI-2,4diF - 30min) and MRP1 (~ 8, 36, 10 and 20% for MI-D, MI-J, MI-4F e MI-2,4diF - 30min) transporter activity. New ABCG2 inhibitors were developed through substitutions in indeno[1,2-b]indoles scaffold. Potent ABCG2 (4c, 4h, 4i, 4j, 4k - IC₅₀= 0.21-0.49 μ M - N⁵ = phenethyl) or casein kinase II (CK2) (4a, 4p, 4e - IC₅₀= 0.0025-0.36 μ M N⁵ = isopropyl) inhibitors were obtained with a cetonic indeno[1,2-b]indoles scaffold. The derivatives 4j, 4l and 4d showed low intrinsic cytotoxicity (IG₅₀ 28-100 μ M), resulting in therapeutic ratio (TR) suitable for use on *in vivo* models (TR = 98-430). However, the derivatives 4h, 4j, 4k were not selective to ABCG2, also inhibiting MRP1 activity (44, 87 e 86% - 10 μ M). The derivatives of phenolic indeno[1,2-b]indoles were more potent (5c, 5f, 5h- IC₅₀= 0.15-0.16 μ M) and selective to ABCG2 than cetonic derivatives. Low intrinsic cytotoxicity (5c, 5f, 5h- IG₅₀= 42-54 μ M) and high TR (267-360) were also observed. These results suggest that 1,3,4-thiadiazolium mesoionic derivatives and indeno[1,2-b]indoles are promising candidates for future investigations on *in vivo*, targeting HCC treatment and chemosensitization of tumors overexpressing ABCG2, respectively.

Keywords: Hepatocellular carcinoma. HepG2 cells. Primary rat hepatocytes. 1,3,4-thiadiazolium mesoionic derivatives. Indeno[1,2-b]indoles derivatives. ABCG2 inhibitors.

LISTA DE FIGURAS

REVISÃO BIBLIOGRÁFICA

FIGURA 1: CLASSIFICAÇÃO CLÍNICA DO CHC E ESTRATÉGIA DE TRATAMENTO.....	22
FIGURA 2: ESTRUTURA MOLECULAR DO SORAFENIBE.....	25
FIGURA 3: ESTRUTURA MOLECULAR E NUMERAÇÃO DOS ÁTOMOS DO SISTEMA HETEROCÍCLICO 1,3,4-TIADIAZOL.....	26
FIGURA 4: ESTRUTURA QUÍMICA DOS DERIVADOS 1,3,4-TIADIAZÓIS.....	30
FIGURA 5: TOPOLOGIA E ESTRUTURA DE TRANSPORTADORES ABC.....	34
FIGURA 6: ESTRUTURA MOLECULAR DO Ko143.....	37
FIGURA 7: ESTRUTURA MOLECULAR DO MBLII-141.....	39

ARTIGO 1

FIGURE 1: CHEMICAL STRUCTURE OF THE 4-PHENYL-5-(2-Y-4-X-CINNAMOYL)-1,3,4-THIADIAZOLIUM-2-PHENYLAMINE CHLORIDE DERIVATIVES.....	48
FIGURE 2: CYTOTOXIC EFFECTS OF 1,3,4-THIADIAZOLIUM DERIVATIVES ON HEPG2 CELLS.....	56
FIGURE 3: CYTOTOXIC EFFECTS OF 1,3,4-THIADIAZOLIUM DERIVATIVES ON HEPATOCYTES.....	57
FIGURE 4: DNA FRAGMENTATION IN HEPG2 CELLS, AS INDUCED BY 1,3,4-THIADIAZOLIUM DERIVATIVES.....	58
FIGURE 5: ANNEXIN V-FITC AND PROPIDIUM IODIDE STAINING OF HEPG2 TREATED WITH 1,3,4-THIADIAZOLIUM DERIVATIVES.....	59
FIGURE 6: EFFECTS OF 1,3,4-THIADIAZOLIUM DERIVATIVES ON HEPG2 CELL MORPHOLOGY.....	60
FIGURE 7: ANNEXIN V-FITC AND PROPIDIUM IODIDE STAINING OF HEPATOCYTES TREATED BY 1,3,4-THIADIZOLIUM DERIVATIVES.....	61
FIGURE 8: EFFECTS OF 1,3,4-THIADIAZOLIUM DERIVATIVES ON HEPATOCYTES MORPHOLOGY.....	62

ARTIGO 2

FIGURE 1: SUBSTITUTION PATTERNS OF 4a-r.....	78
FIGURE 2. VIEW OF THE CRYSTAL STRUCTURE OF 4c WITH OUR NUMBERING SCHEME, DISPLACEMENT ELLIPSOIDS ARE DRAWN AT THE 30% PROBABILITY LEVEL.....	79
FIGURE 3: CONCENTRATION DEPENDENCE FOR THE MOST POTENT INHIBITORS OF CK2 ACTIVITY.....	81
FIGURE 4: FLUORESCENCE IMAGES OF MCF-7 CELLS TREATED WITH DIFFERENT CONCENTRATIONS OF THE INHIBITOR 4p FOR 24 H.....	82
FIGURE 5: ANTIPROLIFERATIVE EFFECT OF THE INHIBITOR 4p ON MCF-7 CELLS.....	83
FIGURE 6: CONCENTRATION DEPENDENCE FOR THE MOST POTENT INDENOINDOLE INHIBITORS OF ABCG2 TRANSPORT ACTIVITY.....	86
FIGURE 7: RELATIONSHIPS BETWEEN CK2 INHIBITORS AND ABCG2 INHIBITORS.....	88

ARTIGO 3

FIGURE 1: STRUCTURAL ARRANGEMENT OF ABCG2.....	109
FIGURE 2: PREPARATION OF THE TARGET COMPOUNDS 5 AND 6 FROM KETONES	110
FIGURE 3: REAGENTS AND CONDITIONS.....	120
FIGURE 4: STRUCTURES OF THE INVESTIGATED INDENOINDOLE SERIES 5 AND 6.....	121
FIGURE 5: VIEW OF THE CRYSTAL STRUCTURE OF 5c WITH OUR NUMBERING SCHEME.....	122
FIGURE 6: STRUCTURES OF KETONIC INDENOINDOLES (SERIES 4).....	123
FIGURE 7: ABILITY OF LEADS OF THE DIFFERENT SERIES OF INDENOINDOLES TO INHIBIT DRUG EFFLUX BY ABCB1 OR ABCC1.....	126
FIGURE 8. PHENOLIC INDENOINDOLES AS BETTER ABCG2 INHIBITORS OVER KETONIC- AND P-QUINONIC- DERIVATIVES.....	128
FIGURE 9: MODULATION OF BASAL ATPase ACTIVITY BY INDENOINDOLES.....	129

FIGURE 10: TENTATIVE REPRESENTATION OF PARTLY-OVERLAPPING SITES FOR INDENOINDOLES.....	132
-------------------------------------------------------------------------------------------	-----

LISTA DE TABELAS

REVISÃO BIBLIOGRÁFICA

TABELA 1. ANTITUMORAIS SUBSTRATOS DE TRANSPORTADORES ABC. 35

ARTIGO 1

TABLE 1. EFFECTS OF 1,3,4-THIADIAZOLIUM DERIVATIVES ON MDR CELL PARAMETERS..... 63

ARTIGO 2

TABLE 1. INHIBITION OF HUMAN CK2 HOLOENZYME..... 81

TABLE 2. INHIBITION OF MITOXANTRONE EFFLUX IN ABCG2-TRANSFECTED CELLS..... 85

ARTIGO 3

TABLE 1. INHIBITION OF MITOXANTRONE EFFLUX IN ABCG2-TRANSFECTED CELLS, AND CYTOTOXICITY..... 124

TABLE 2. INHIBITION OF HUMAN CK2 HOLOENZYME AND COMPARISON WITH ABCG2..... 127

LISTA DE SIGLAS

REVISÃO BIBLIOGRÁFICA

ABCG2-	Proteína de resistência ao câncer de mama
CHC-	Carcinoma hepatocelular
CK2-	Caseína quinase II
FDA-	Administração Federal para Drogas e Alimentos - EUA
IC₅₀-	Concentração necessária para inibir em 50% a atividade da proteína
IG₅₀-	Concentração necessária para inibir em 50% a proliferação celular
IPE-	Injeção percutânea de etanol
IT-	Índice terapêutico
I.P.	Intraperitoneal
LDH-	Lactato desidrogenase
MDR-	Resistência a múltiplas drogas
mRNA-	RNA mensageiro
MRP1-	Proteína1 associada à resistência a múltiplas drogas
NBD-	Domínio de ligação do nucleotídeo
Pgp-	Glicoproteína P
QET-	Químico-embolização transarterial
RF-	Radiofrequência
TMD-	Domínio transmembrana

ARTIGO 1

ABCG2-	ATP-binding cassette sub-family G member 2
ADMET-	Absorption, distribution, metabolism, excretion and toxicity
ASA-	Acetylsalicylic acid
BSA-	Bovine serum albumin
DMEM-	Dulbecco's modified Eagle's medium
DMSO-	Dimethylsulfoxide
FDA-	Food and drug administration

HCC-	Hepatocellular carcinoma
HBSS-	4-(2-hydroxyethyl)-1-piperazine ethanesulfonic acid
HEPES-	3-(4,5-dimethylthiazol-2-yl)-2,5-diphenyltetrazolium bromide
LDH-	Lactate dehydrogenase
MDR-	Multiple drugs resistance
MTT-	4-phenyl-5-(4-nitrocinnamoyl)-1,3,4-thiadiazolium-2-phenylamine chloride
MI-D-	4-phenyl-5-(4-nitrocinnamoyl)-1,3,4-thiadiazolium-2-phenylamine chloride
MI-J-	4-phenyl-5-(4-hydroxycinnamoyl)-1,3,4-thiadiazolium-2-phenylamine chloride
MI-4F-	4-phenyl-5-(4-fluorocinnamoyl)-1,3,4-thiadiazolium-2-phenylamine chloride
MI-2,4diF-	4-phenyl-5-(2,4-fluorocinnamoyl)-1,3,4-thiadiazolium-2-phenylamine chloride
MRP1-	Multidrug resistance protein 1
PBS-	Phosphate buffered saline
Pgp-	P-glycoprotein
PI-	Propidium iodide

ARTIGO 2

ABC-	ATP-binding cassette
ABCG2-	Breast cancer resistance protein (BCRP)
ARS-	aromatic ring system
CK2-	casein kinase II
DMA-	Dimethylacetamide
HBA-	hydrogen-bond acceptor
HP-	hydrophobic part
LCIA-	lithium cyclohexylisopropylamide
SAR-	Structure-Activity Relationship
TETA-	N,N,N',N'-tetraethylthionylamide

ARTIGO 3

ABC-	ATP-binding cassette
BCRP-	Breast cancer resistance protein (ABCG2)
CK2-	Casein kinase II
MRP1-	Multidrug resistance protein 1 (ABCC1)
Pgp-	P-glycoprotein (ABCB1)
TR-	Therapeutic ratio

SUMÁRIO

1 INTRODUÇÃO	19
2 REVISÃO BIBLIOGRÁFICA	21
2.1 TRATAMENTOS DO CARCINOMA HEPATOCELULAR	21
2.2 ATIVIDADE CITOTÓXICA E ANTITUMORAL DE DERIVADOS DE 1,3,4-TIADIAZÓIS	26
2.3 RESISTÊNCIA À MULTIPLAS DROGAS (MDR)	31
2.3.1 Inibidores de transportadores ABC	36
2.3.1.1 Inibidores de ABCG2	36
2.4 ATIVIDADES BIOLÓGICAS DE INDENO[1,2- <i>b</i>]INDÓIS	41
3 JUSTIFICATIVA E OBJETIVOS	44
4 ARTIGOS CIENTÍFICOS	45
4.1 ARTIGO 1.	45
ABSTRACT	46
4.1.1 Introduction	46
4.1.2 Materials and Methods	48
4.1.2.1 Chemicals	48
4.1.2.2 HepG2 cell culture	49
4.1.2.3 Primary culture of rat hepatocytes	49
a) Animals	49
b) Isolation and culture of hepatocytes	49
4.1.2.4 Culture of multiple drugs resistant cells	50
4.1.2.5 Cell viability assays	51
a) MTT reduction	51
b) Lactate dehydrogenase release	51
c) Annexin-V and propidium iodide staining	52
4.1.2.6 Morphology assays	52
4.1.2.7 DNA fragmentation	53
4.1.2.8 Protein concentration assay	53
4.1.2.9 Inhibition of drug efflux in multiple drug resistant cells	54
4.1.2.10 Statistical Analysis	54
4.1.3 Results	55

4.1.3.1 Cytotoxicity of 1,3,4-thiadiazolium derivatives on HepG2 and rat hepatocytes	55
4.1.3.2 Apoptosis induction by 1,3,4-thiadiazolium derivatives in HepG2 cancer cells but not in control hepatocytes.....	57
4.1.3.3 Effects of 1,3,4-thiadiazolium derivatives on multiple drugs resistant (MDR) cells.....	62
4.1.4 Discussion and conclusions.....	64
REFERENCES	67
4.2 ARTIGO 2.	72
ABSTRACT	73
4.2.1 Introduction	73
4.2.2 Chemistry.....	74
4.2.3 Biological evaluation, SARs and discussion	80
4.2.3.1 Inhibition of human CK2 holoenzyme	80
4.2.3.2 Inhibition of MCF-7 cell proliferation by the CK2 inhibitor 4p	82
4.2.3.3 Inhibition of ABCG2-Mediated Drug Efflux.....	84
4.2.4 Experimental section.....	89
4.2.4.1 Chemistry	89
4.2.4.2 General Procedure for the Synthesis of Compounds 2.....	90
4.2.4.3 General Procedure for the Synthesis of Compounds 3.....	91
4.2.4.4 General Procedure for the Synthesis of Compounds 4i-n.....	93
4.2.4.5 General Procedure for the Synthesis of Compounds 4q and 4r.	96
4.2.4.6 X-ray Data	97
4.2.4.7 Biology and Biochemistry	98
a) Preparation of recombinant human CK2 holoenzyme	98
b) Capillary electrophoresis based assay for the testing of inhibitors of the human CK2	98
c) Cell culture and proliferation.....	99
d) Compounds.....	100
e) Cell Cultures.....	100
f) ABCG2-Mediated Mitoxantrone Efflux and Inhibition	100
g) Intrinsic Cytotoxicity of the Inhibitory Compounds.....	101
4.2.5 Acknowledgements.....	101
REFERENCES	102

4.3 ARTIGO 3	107
ABSTRACT	108
4.3.1 Introduction	108
4.3.2 Material and Methods	110
4.3.2.1 Chemistry	110
a) General procedure for the synthesis of compounds 5.....	111
b) General procedure for the synthesis of compounds 6.....	113
c) X-ray data.....	116
4.3.2.2 Biology and biochemistry.....	116
a) Compounds.....	116
b) Cell cultures	116
c) ABCG2-mediated mitoxantrone efflux and inhibition.....	117
d) Intrinsic cytotoxicity of the inhibitory compounds.....	117
e) Inhibition of Pgp- and MRP1-mediated drug efflux.....	117
f) Effects on ABCG2 ATPase activity	118
g) Preparation of recombinant human CK2 holoenzyme and assay of inhibitors activity.....	118
4.3.3 Results.....	119
4.3.3.1 Chemistry	119
4.3.3.2 Biological evaluation and SARs.....	122
a) Inhibition of ABCG2-mediated mitoxantrone efflux, and cytotoxicity	122
b) Selectivity toward ABCG2 inhibition	125
c) Effects on ABCG2 basal ATPase activity	128
4.3.4 Discussion	130
4.3.4.1 Phenolic indenoindoles as better ABCG2 inhibitors than ketonic derivatives	130
4.3.4.2 Molecular mechanism and polyspecificity.....	131
4.3.5 Acknowledgments.....	132
REFERENCES	133
5. CONCLUSÕES	137
REFERÊNCIAS	138
ANEXOS	153

1 INTRODUÇÃO

O carcinoma hepatocelular (CHC) é um câncer com altas incidência e taxa de mortalidade. Isto decorre, respectivamente, da característica multifatorial de sua patogênese e da reduzida eficácia dos tratamentos empregados em pacientes diagnosticados nos estágios mais avançados da doença (MENDEZ-SANCHEZ *et al.*, 2014; SINGAL; EL-SERAG, 2015). São descritas na literatura científica muitas moléculas promissoras quanto à indução de morte de células de CHC, entretanto poucas são caracterizadas em relação à toxicidade em células não tumorais. Antitumorais com baixa seletividade para células tumorais promovem toxicidade sistêmica, levando frequentemente o paciente a abandonar o tratamento antes da erradicação do tumor (MAHATO *et al.*, 2011). Particularmente para o CHC, existe apenas um medicamento (Sorafenibe) aprovado para seu tratamento clínico e, o mau prognóstico observado após sua utilização tem estimulado a busca por novos compostos que possam representar uma melhor alternativa (BUPATHI *et al.*, 2015; FITZMORRIS *et al.*, 2015; KALYAN *et al.*, 2015). Com isto em mente, neste trabalho investigou-se a ação citotóxica de 4 derivados 1,3,4-tiadiazóis mesoiônicos na linhagem de carcinoma hepatocelular humano (células HepG2) e hepatócitos de ratos (ARTIGO 1). Trabalhos anteriores demonstraram que estes derivados induzem alterações em mitocôndrias de fígado de rato relacionadas à indução de apoptose (CADENA *et al.*, 1998; PIRES *et al.*, 2010), também sugerida para linhagens de câncer de cérvix (CADENA, 1999) e melanoma (SEFFF-RIBEIRO *et al.*, 2004a) submetidas ao tratamento com um destes derivados (MI-D). Além disto, alguns destes compostos possuem importante atividade antitumoral *in vivo* (melanoma, sarcoma 180 e tumor de Erlich) (GRYNBERG *et al.*, 1997; SEFFF-RIBEIRO *et al.*, 2004b), com ausência de alterações hematológicas indicativas de toxicidade, evidenciando uma possível ação seletiva em células tumorais.

Alguns trabalhos têm sugerido que a ineficiência do sorafenibe no tratamento do CHC deve-se, pelo menos em parte, a sua interação com transportadores ABC (SUN *et al.*, 2010; HUANG *et al.*, 2013). Estes transportadores localizam-se em membranas celulares, principalmente membranas citoplasmáticas, e promovem o efluxo de diversas moléculas, reduzindo suas concentrações

celulares. Em geral, possuem importantes funções fisiológicas, como diminuir o acúmulo intracelular ou promover a excreção de substâncias tóxicas ou, ainda, transportar moléculas sinalizadoras. Entretanto, algumas células tumorais podem superexpressar estes transportadores, resultando num fenótipo denominado resistência a múltiplas drogas (MRD), que é considerado um dos principais mecanismos responsáveis pela resistência à quimioterapia antitumoral (ECKFORD; SHAROM, 2009; KATHAWALA *et al.*, 2015). Neste estudo também foi avaliada a interação dos 1,3,4-tiadiazóis mesoiônicos com os principais transportadores ABC (ARTIGO 1).

Visando contribuir para a reversão do fenótipo MDR, novos inibidores de ABCG2, uma proteína pertencente à família dos transportadores ABC (STACY *et al.*, 2013), foram desenvolvidos e caracterizados quanto a sua atividade. A síntese destes compostos foi realizada a partir de modificações estruturais no núcleo indeno[1,2-b]indol presente em moléculas inicialmente desenvolvidas como inibidores da proteína caseína quinase II (CK2) (HUNDSDORFER *et al.*, 2012a; HUNDSDORFER *et al.*, 2012b), uma vez que diversos trabalhos têm demonstrado que certos inibidores de quinases podem interagir com transportadores ABC e reverter o fenótipo MDR *in vivo* e *in vitro* (WANG *et al.*, 2014). Desta forma, ainda neste estudo as influências positivas e negativas de alguns substituintes em núcleos cetônicos (ARTIGO 2), fenólicos e quinônicos (ARTIGO 3) para a atividade inibitória em ABCG2 e CK2 são demonstradas. Também foram investigados alguns parâmetros essenciais para utilização prática destes novos inibidores, como citotoxicidade e especificidade em outros transportadores.

2 REVISÃO BIBLIOGRÁFICA

2.1 TRATAMENTOS DO CARCINOMA HEPATOCELULAR

O carcinoma hepatocelular (CHC) é o tipo de câncer mais frequente do fígado, compreendendo 60-70% dos tumores primários originários deste órgão (HATZARAS *et al.*, 2014). Anualmente são observadas mais de 600.000 mortes em decorrência desta doença (WOO; HEO, 2015), sendo considerada a terceira causa mais comum de morte relacionada ao câncer no mundo (CHENG *et al.*, 2014; LEE *et al.*, 2014; BUPATHI *et al.*, 2015; WOO; HEO, 2015). São estimados aproximadamente 700 mil novos casos de CHC anualmente (ALVES *et al.*, 2011; CHENG *et al.*, 2014), o que o posiciona como o sexto tipo de câncer mais prevalente no mundo (LEE *et al.*, 2014; WOO; HEO, 2015).

Os tratamentos considerados curativos geralmente são recomendados para os estágios iniciais do CHC (CHENG *et al.*, 2014; YU; KIM, 2015), entretanto apenas 20-30% dos diagnósticos são realizados nesta fase (BUPATHI *et al.*, 2015), o que resulta em prognóstico desfavorável para estes pacientes (CHENG *et al.*, 2014; YU; KIM, 2015). Diversos fatores são considerados para a escolha da terapêutica, como tamanho e localização tumoral, relação tumor/estruturas adjacentes, número de lesões, presença de invasão vascular e doenças hepáticas e extra-hepáticas (HATZARAS *et al.*, 2014). Atualmente, a classificação de Barcelona é amplamente utilizada para eleição do tratamento e predição do prognóstico, utilizando como base o grau de evolução clínica do CHC (ALVES *et al.*, 2011) (FIGURA 1).

Em geral, a ressecção cirúrgica é o tratamento padrão para pacientes com CHC em estágios iniciais e função hepática preservada (CHENG *et al.*, 2014; TABRIZIAN *et al.*, 2014), proporcionando uma taxa de sobrevida em cinco anos de 42-62% (HATZARAS *et al.*, 2014), ou até 70% quando nenhum fator de risco, como pressão portal e bilirrubina aumentadas, está associado (TABRIZIAN *et al.*, 2014). Altas taxas de recorrência são observadas após a ressecção cirúrgica, acometendo em média 70% dos pacientes, cinco anos após o procedimento (CHENG *et al.*, 2014; FITZMORRIS *et al.*, 2015). Os principais mecanismos de reincidência do CHC são a disseminação do tumor primário e desenvolvimento de novos tumores

(MENDEZ-SANCHEZ *et al.*, 2014; ATTWA; EL-ETREBY, 2015), este último ocorrendo geralmente 4 anos após o procedimento (HATZARAS *et al.*, 2014). A maioria das recorrências deve-se à invasão vascular e disseminação, estabelecendo-se nos primeiros 2 ou 3 anos após a ressecção (FITZMORRIS *et al.*, 2015). Apenas uma pequena porcentagem de pacientes (6-12%) apresenta metástase extra-hepática (HATZARAS *et al.*, 2014).

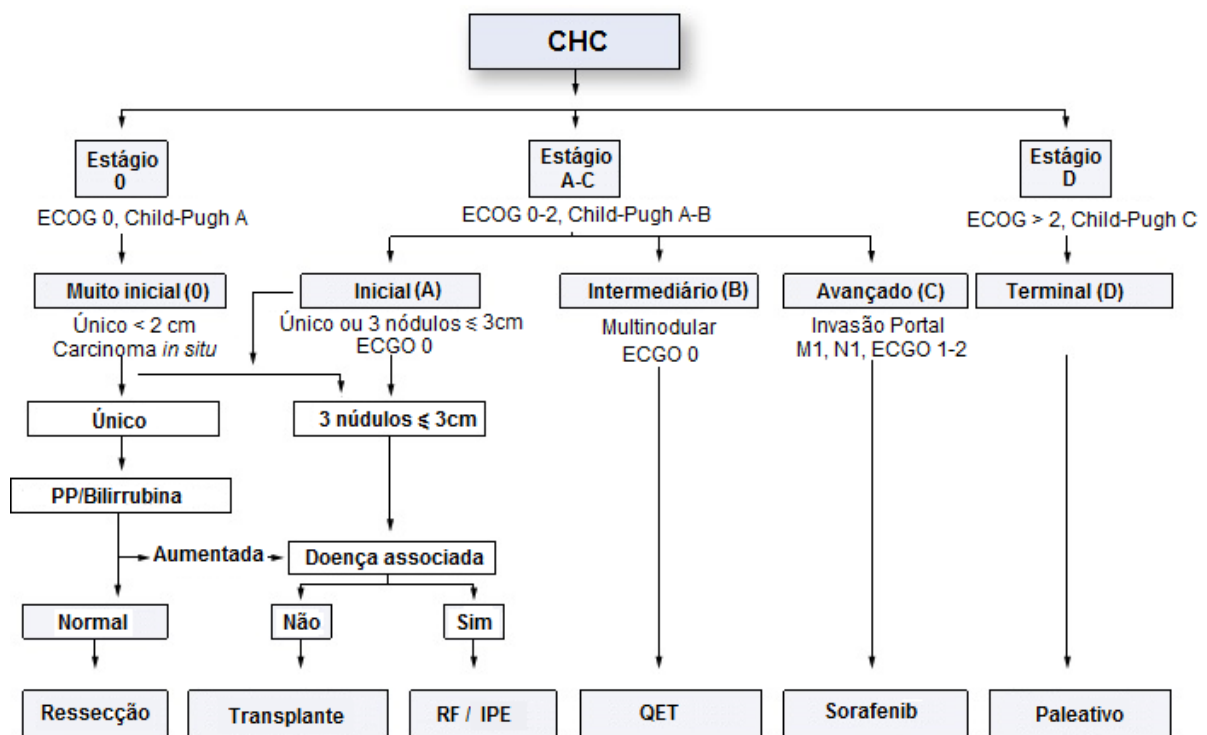


FIGURA 1: CLASSIFICAÇÃO CLÍNICA DO CHC E ESTRATÉGIA DE TRATAMENTO

FONTE: Adaptado de EASL-EORTC, 2012

NOTA: A classificação do CHC proposta pela Clínica de Câncer Hepático de Barcelona divide os pacientes em 5 estágios (A-D), considerando variáveis do tumor (sistema TNM), função hepática (escala Child-Pugh) e estado de saúde do paciente (ECGO). ECOG: escala de desempenho desenvolvida pelo Grupo Oriental de Oncologia Cooperativa, pontuando de 0 (totalmente ativo, desempenhando funções sem restrições) a 5 (morte) (HSU *et al.*, 2013); Child-Pugh: classificação utilizada para avaliar o prognóstico da doença hepática crônica, pontuando de 1 a 3 ao considerar os níveis de albumina, bilirrubina, tempo de protrombina, ascite e grau de encefalopatia (GE *et al.*, 2014); M1 e N1: Estágios pertencentes ao sistema TNM (tamanho, presença em linfonodos, metástases) de classificação de tumores, onde M1 indica presença de metástase distante e N1 metástase em linfonodos (MARSH *et al.*, 2000); RF: radiofrequência; IPE: injeção percutânea de etanol; QET: quimio-embolização transarterial; PP: pressão portal.

O transplante de fígado é o tratamento de primeira escolha para pacientes com pequenos tumores multinodulares (≤ 3 nódulos ≤ 3 cm) ou tumores únicos (≤ 5 cm) e disfunção hepática avançada (EASL-EORTC, 2012). Além destas, outras condições devem estar presentes para elegibilidade do transplante, como nível reduzido de invasão vascular e ausência de doenças extra-hepáticas (HATZARAS *et al.*, 2014). Ao seguir estes critérios, estima-se uma taxa de sobrevida em cinco anos de 70% e recorrência menor que 15% (EASL-EORTC, 2012; TABRIZIAN *et al.*, 2014). A principal desvantagem relacionada ao transplante, além da indução da imunossupressão ao longo da vida, é o grande tempo de espera por um doador. Estima-se que ao exceder 12 meses na fila de espera por um órgão, mais de 25% dos pacientes tornam-se inelegíveis para o transplante devido à progressão do carcinoma (ATTWA; EL-ETREBY, 2015; FITZMORRIS *et al.*, 2015).

A ablação local é considerada a primeira linha de tratamento para pacientes em estágios iniciais do CHC, não elegíveis para terapias cirúrgicas (EASL-EORTC, 2012; HATZARAS *et al.*, 2014). Nesta abordagem, são realizadas injeções locais de substâncias químicas ou modificações na temperatura do microambiente, induzindo necrose tumoral com efeitos reduzidos no parênquima hepático (MENDEZ-SANCHEZ *et al.*, 2014).

Atualmente, a injeção percutânea de etanol (IPE) e o aquecimento por radiofrequência (RF) são as terapias ablativas utilizadas com maior frequência (FITZMORRIS *et al.*, 2015). Estima-se que 50% dos tumores entre 3 e 5 cm são totalmente necrosados após a IPE, elevando-se para 90% ao considerar os tumores menores que 2 cm (MENDEZ-SANCHEZ *et al.*, 2014). Entretanto, as altas taxas de reincidência representam um fator limitante na utilização deste tratamento (KHAN *et al.*, 2000), podendo alcançar 34%, dois anos após o procedimento, em pacientes que apresentam tumores menores ≤ 3 cm. Com a utilização de RF, por outro lado, a taxa de reincidência, nas mesmas condições de análise, cai para 14% (LIN *et al.*, 2005). Além disso, o efeito antitumoral promovido pela RF é superior quando comparado a IPE (EASL-EORTC, 2012), com taxas de sobrevivências de 63-81% versus 48-67% ao final de três anos após o tratamento (CHO *et al.*, 2009; FITZMORRIS *et al.*, 2015).

A quimioembolização transarterial (QET) é um tratamento bem estabelecido para o HCC em estágios intermediários (EASL-EORTC, 2012; TABRIZIAN *et al.*, 2014), sendo elegível em casos de tumores múltiplos e de grandes tamanhos,

incluindo pacientes com disfunção hepática moderada (MURATA *et al.*, 2014; ATTWA; EL-ETREBY, 2015). Importantes resultados também têm sido demonstrados com a sua utilização na forma de terapia adjuvante após ressecção cirúrgica de tumores maiores que 5 cm (CHENG *et al.*, 2014). A ação antitumoral da QET baseia-se na aplicação local de um agente citotóxico, seguido por indução de isquemia através de embolização dos vasos sanguíneos responsáveis pelo suprimento tumoral (EASL-EORTC, 2012; MENDEZ-SANCHEZ *et al.*, 2014). Em geral, a taxa de resposta após a QET está entre 15 e 55% (BRUIX *et al.*, 2004), refletindo num aumento de 2-3 vezes sobre a taxa de sobrevivência 2 anos após o tratamento, quando comparado ao controle que recebe tratamento apenas sintomático (taxa de 11-27%) (LLOVET *et al.*, 2002; LO *et al.*, 2002; TABRIZIAN *et al.*, 2014).

Para pacientes com estágios avançados de CHC ou tumores recorrentes após terapias loco-regionais e com função hepática bem preservada, a quimioterapia sistêmica é o tratamento mais indicado (EASL-EORTC, 2012). Em geral, esta abordagem é bastante limitada devido à natureza refrataria do tumor (EASL-EORTC, 2012; ATTWA; EL-ETREBY, 2015), decorrente principalmente da expressão aumentada ou mutações de proteínas promotoras de resistência, como p53, glutatona-S-transferase, glicoproteína P (NG *et al.*, 2000; AKIMOTO *et al.*, 2006) e chaperonas. Além disso, a ação pouco seletiva de determinados compostos para células tumorais, e a consequente toxicidade para células hepáticas, são fatores que frequentemente determinam a interrupção do tratamento devido à perda da função hepática de reserva (ATTWA; EL-ETREBY, 2015).

Sorafenibe foi o primeiro composto a demonstrar aumento nas taxas de sobrevivência em pacientes com CHC em estágio avançado (ALVES *et al.*, 2011) (FIGURA 2), permanecendo o único medicamento aprovado pela *Food and Drug Administration* (FDA) desde 2007 (EASL-EORTC, 2012; BUPATHI *et al.*, 2015). O efeito antitumoral desta molécula é proveniente de sua ação inibitória em algumas quinases responsáveis pela sinalização da proliferação celular e angiogênese, dentre as quais os receptores de membrana com atividade intrínseca de tirosina-quinase, como os receptores para o fator de crescimento endotelial vascular (VEGFR-1, 2 e 3), fator de crescimento derivado de plaquetas (PDGFR- β), fator de célula-tronco (c-Kit), fator estimulador de colônia de macrófagos (FLT3) e fatores neurotróficos derivados de linhagem de célula glial (RET). Além disso, sorafenibe

inibe as isoformas Raf-1 e B-Raf da serina/treonina-quinase RAF, interferindo na sinalização intracelular da cascata de proteínas quinases ativadas por mitógeno (MAPK) (WILHELM *et al.*, 2004; ALVES *et al.*, 2011).

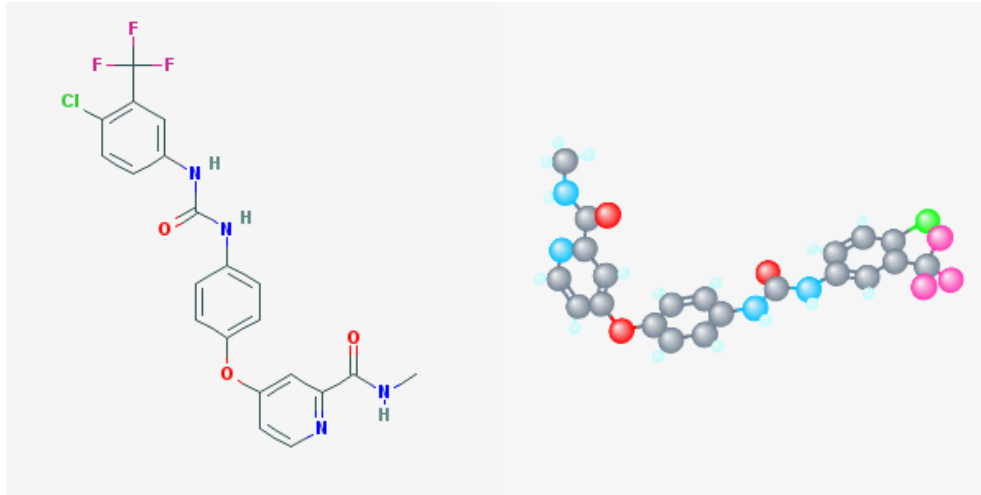


FIGURA 2: ESTRUTURA MOLECULAR DO SORAFENIBE

FONTE: Adaptado de NCBI, 2015a

NOTA: Nome químico: 4-[4-[[4-cloro-3-(trifluorometil)fenil]carbamoilamino]fenoxi]-N-metilpiridina-2-carboxamida. Representação da estrutura molecular em 2D (esquerda) e 3D(direita).

Estima-se que o uso de sorafenibe diminua em 31% a possibilidade de morte associada ao CHC em estágio avançado (LLOVET *et al.*, 2008), aumentando em 2 ou 3 meses a média geral de sobrevivência destes pacientes (LLOVET *et al.*, 2008; CHENG *et al.*, 2009). Alguns indivíduos, entretanto, apresentam resistência à ação antitumoral deste composto (HUANG *et al.*, 2013; BUPATHI *et al.*, 2015); efeito que pode relacionar-se com a presença dos transportadores Pg-p e ABCG2 (SUN *et al.*, 2010; HUANG *et al.*, 2013). Embora esta relação não tenha sido demonstrada diretamente, sabe-se que a expressão destas proteínas está significativamente aumentada em amostras de tumores humanos de CHC resistentes (SUN *et al.*, 2010), e que inibidores de ABCG2 podem restaurar a sensibilidade ao sorafenibe em linhagens de HCC superexpressando ABCG2 (HUANG *et al.*, 2013).

A quimioterapia empregada para o tratamento do CHC pode ser considerada, em geral, de baixa eficácia (BUPATHI *et al.*, 2015), sendo fundamental o desenvolvimento de novos medicamentos que apresentem maior eficácia e reduzida toxicidade sistêmica (ALVES *et al.*, 2011).

2.2 ATIVIDADE CITOTÓXICA E ANTITUMORAL DE DERIVADOS DE 1,3,4-TIADIAZÓIS

Os derivados do sistema heterocíclico 1,3,4-tiadiazóis (FIGURA 3) têm ganhado destaque nas pesquisas médicas em decorrência de sua diversidade de efeitos farmacológicos, tais como: atividade antimicrobiana, antifúngica, antiviral, anti-inflamatória, analgésica, anticonvulsivante, antioxidante, antidepressiva, ansiolítica, anti-hipertensiva e antineoplásica (JAIN *et al.*, 2013; HU *et al.*, 2014). Este sistema é composto por 2 átomos de carbono, 2 átomos de nitrogênio interconectados e 1 átomo de enxofre, o que resulta em uma estrutura aromática com pouca reatividade. Entretanto, determinadas substituições nas posições 2' e 5' podem ativar o anel, tornando-o altamente reativo e permitindo a síntese de diversos derivados (HU *et al.*, 2014).

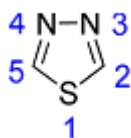


FIGURA 3: ESTRUTURA MOLECULAR E NUMERAÇÃO DOS ÁTOMOS DO SISTEMA HETEROCÍCLICO 1,3,4-TIADIAZOL

FONTE: Adaptado de HU *et al.*, 2014 .Copyright 2014 American Chemical Society.

O anel 1,3,4-tiadiazol é importante para a atividade antitumoral de seus derivados pois é capaz de estabelecer ligações de hidrogênio com alvos celulares. Ainda, a inserção de diferentes substituintes permite uma diversificação destas interações, resultando no amplo espectro de mecanismos de ação destes compostos (HU *et al.*, 2014).

A atividade citotóxica de derivados 1,3,4-tiadiazóis já foi demonstrada em diferentes linhagens tumorais humanas, incluindo câncer de próstata, pulmão, mama, útero, bexiga, fígado, além de cânceres retal, neuronal, e colorretal (JAIN *et al.*, 2013).

Em 2003, Chou *et al.* sintetizaram compostos utilizando piridinas, quinolinas, quinazolininas, pirimidinas, tiadiazóis e tiadiazinas como estrutura de base. Dentre as diversas moléculas obtidas, o derivado tiadiazólico (E,E)-2,5-bis[4-(3-dimetilaminopropoxi)estiril]-1,3,4-tiadiazol (GO-13) exerceu uma significativa atividade antiproliferativa para carcinoma de pulmão A549 ($IG_{50} \sim 6,8 \mu\text{g/mL} - 24\text{h}$) e hepático HA22T ($IG_{50} \sim 9,7 \mu\text{g/mL}$), além de adenocarcinoma de próstata PC-3 ($IG_{50} \sim 6,3 \mu\text{g/mL}$). Os autores demonstraram que os mecanismos envolvidos na citotoxicidade promovida por GO-13 na linhagem A549 incluem: inibição da fosforilação de Akt/PKB, uma quinase serina/treonina inibidora de apoptose; aumento da expressão de BAX, uma proteína apoptótica; diminuição da expressão da proteína antiapoptótica Bcl-X_L e ativação de caspase 3. Estes efeitos resultaram na parada no ciclo celular na fase G₀/G₁ e indução de apoptose, que foi prevenida na presença de antioxidantes, indicando a participação de espécies reativas de oxigênio para iniciação dos eventos.

Matysiak *et al.* (2006a) analisaram o efeito citotóxico de uma série de 2-amino-5-(2,4-dihidroxifenil)-1,3,4-tiadiazóis, substituídos por grupos alquila, arila ou morfolina. Após incubação de 72 horas, os autores encontraram compostos altamente citotóxicos para carcinomas de bexiga HCV-29T ($IG_{50} \sim 4,2 \mu\text{g/mL}$), mama T47D ($IG_{50} \sim 1,5 \mu\text{g/mL}$) e de pequenas células de pulmão A549 ($IG_{50} \sim 5,3 \mu\text{g/mL}$), além de adenocarcinoma colorretal SW707 ($IG_{50} \sim 2,8 \mu\text{g/mL}$). Em outro estudo, os autores testaram uma série de 2-(2,4-dihidroxifenil)-1,3,4-tiadiazóis, substituídos na posição 5, nas mesmas linhagens, demonstrando compostos com potenciais citotóxicos similares ou superiores ($IG_{50} \sim 1,1 \mu\text{g/mL}$ para HCV-29T) aos da série anterior (MATYSIAK *et al.*, 2006b).

Em 2010, Kumar *et al.* sintetizaram uma série de compostos com diferentes substituições na posição 2' do anel tiadiazol e um anel indol (contendo bromo exocíclico ou não) na posição 5'. Algumas destas moléculas demonstram importante atividade citotóxica, após incubação de 24 horas, nas linhagens de câncer de próstata LnCaP ($IG_{50} = 8,9 \mu\text{M}$), Du145 ($IG_{50} = 3,6 \mu\text{M}$) e PC3 ($IG_{50} = 7,5 \mu\text{M}$), além de adenocarcinomas mamários MCF-7 ($IG_{50} = 6,5 \mu\text{M}$) e MDA-MB-231 ($IG_{50} = 6,2 \mu\text{M}$) e carcinoma pancreático PaCa2 ($IG_{50} = 1,5 \mu\text{M}$). Em trabalho posterior, os mesmos autores sintetizaram uma série de derivados com grupos arilaminas na posição 2' e arilas em 5' e realizaram uma seleção dos mais efetivos nas mesmas

linhagens. Embora alguns compostos tenham apresentado significativa atividade citotóxica, a magnitude de seus efeitos não superou a dos compostos anteriormente sintetizados (KUMAR *et al.*, 2011).

A ação inibitória de derivados 1,3,4-tiadiazóis em quinases também tem sido investigada como estratégia para o desenvolvimento de compostos antitumorais. Neste contexto, Sun *et al.* (2012) demonstraram indução de apoptose, ativação de caspase 3 e poli (ADP-ribose) polimerase (PARP), na linhagem de hepatocarcinoma celular humano HepG2 tratada com uma molécula contendo um grupo 1,4-benzodioxano na posição 5' do anel 1,3,4-tiadiazol e uma acetamida substituída com ácido fenilpropiónico na posição 2'. Este efeito foi associado à inibição da quinase de adesão focal FAK ($IC_{50} \sim 10 \mu M$), responsável pela ativação da divisão celular, resultando numa atividade antiproliferativa ($IG_{50} \sim 10 \mu g/mL$). Outro potente inibidor de FAK ($IC_{50} \sim 13 \mu g/mL$) da mesma série também exerceu intensa atividade antiproliferativa em células HepG2 ($IG_{50} \sim 15 \mu g/mL$), SW116 (adenocarcinoma colorretal - $IG_{50} \sim 16 \mu g/mL$) e BGC823 (câncer gástrico - $IG_{50} \sim 14 \mu g/mL$).

Utilizando-se de uma nova abordagem, Rajak *et al.* (2011) sintetizaram e selecionaram inibidores de histonas deacetilases (HDACs), baseando-se em 1,3,4-tiadiazóis substituídos com grupos de reconhecimento e ligação à proteína, e avaliaram seus potenciais antitumorais *in vitro* e *in vivo*. A inibição de HDACs está relacionada com a redução do crescimento celular, diferenciação e promoção de apoptose via ativação transcricional de uma série de genes envolvidos no controle da divisão celular. A superexpressão desta proteína está relacionada com a patogênese de alguns cânceres; fato que tem impulsionado a busca por seus inibidores para utilização como agente antitumoral. Os derivados obtidos naquele trabalho exerceram intensa atividade inibitória sobre HDACs (IC_{50} entre 0,007 e 0,018 μM), que resultou em alta citotoxicidade para células de carcinoma colorretal HCT-116 (IG_{50} entre 0,08 e 0,31 μM). Em carcinomas ascíticos de Ehrlich, os autores observaram inibição de até 78% no crescimento celular em camundongos tratados intraperitonealmente por 7 dias com 0,2 mM/kg/dia.

A ação citotóxica em células tumorais já foi sugerida para pelo menos dois compostos derivados de 1,3,4-tiadiazóis: FABT (2-(4-fluorofenilamino)-5-(2,4-dihidroxifenil)-1,3,4-tiadiazol) e 4CIABT (2-(3-clorofenilamino)-5-(2,4-dihidroxifenil)-

1,3,4-tiadiazol. Rzeski *et al.* (2007) demonstraram a atividade citotóxica de FABT nas linhagens humanas de neuroblastoma SK-N-AS ($IG_{50} \sim 54 \mu M$), rabdiosarcoma TE671 ($IG_{50} \sim 26 \mu M$); adenocarcinoma colorretal HT-29 ($IG_{50} \sim 31 \mu M$), carcinoma de pulmão A549 ($IG_{50} \sim 22 \mu M$) e glioma de rato C6 ($IG_{50} \sim 27$). Nenhuma alteração significativa foi observada na viabilidade de culturas primárias de neurônios e células da glia de ratos, ou em linhagem de hepatócitos de rato (Fao). No entanto, é importante ressaltar que o tempo de tratamento utilizado para as células não-tumorais foi inferior (48h) ao das células tumorais (96h). O derivado substituído com cloro (4CIABT), por sua vez, foi capaz de inibir a proliferação de HT-29, TE671 e C6 com eficiência superior ao FABT, alcançando IG_{50} de 6, 15 e 12 μM com o mesmo tempo e tratamento. O composto 4CIABT, somente em concentrações maiores que 50 μM , reduziu a viabilidade de células humanas de fibroblasto de pele HSF, Fao e culturas primárias de neurônios e células da glia de ratos. Como ocorrido no trabalho anterior, o tempo de tratamento das células não-tumorais foi inferior (24 ou 48h para cultura de neurônios) ao das células tumorais (96h). Além disto, metodologias diferentes foram utilizadas para determinação da viabilidade (JUSZCZAK *et al.*, 2011).

Uma classe particular de compostos contendo o sistema 1,3,4-tiadiazol, denominada 1,3,4-tiadiazóis mesoiônicos, tem demonstrado destacada atividade antitumoral (HU *et al.*, 2014). Em geral, esta classe apresenta um átomo (ou grupo de átomos) com carga negativa ligado ao anel, que possui carga positiva. Embora com alto momento dipolar, estas moléculas possuem caráter globalmente neutro, sendo capazes de atravessar membranas biológicas e interagir com biomoléculas como proteínas e DNA (KIER; ROCHE, 1967; OLLIS; RAMSDEN, 1976; PAIVA *et al.*, 2015).

Grynberg *et al.* (1997) e Santos (2001) sintetizaram quatro derivados do cloreto de 4-fenil-5-[2-Y, 4-X-cinamoil]-1,3,4-tiadiazólio-2-fenilamina (FIGURA 4) com atividade antitumoral *in vivo* e *in vitro* (FIGURA 4). Os compostos MI-D (Y=H e X=NO₂) e MI-J (Y=H e X=OH) inibiram o crescimento de carcinoma de Erlich e Sarcoma 180 em ratos tratados intraperitonealmente com 30 e 10 mg/Kg, respectivamente, sem causar alterações nos parâmetros hematológicos de toxicidade. Em outro trabalho, MI-D, MI-2,4diF (Y=X=F) e MI-4F (Y=H; X=F) reduziram em $\sim 77\%$, 55% e 40% , respectivamente, o crescimento de melanoma

B16-F10 em camundongos tratados com 57 $\mu\text{M}/\text{Kg}$ destes derivados, ainda que para MI-4F essa redução não tenha sido estatisticamente significativa (SENFF-RIBEIRO *et al.*, 2004b). Interessantemente, Romão *et al.* (2009) estimaram que a concentração de MI-D necessária para promoção de seu efeito antitumoral em melanoma B16-F10 foi sete vezes inferior a de sua dose letal ($\text{DL}_{50} \sim 181 \text{ mg}/\text{Kg}$), sugerindo que os efeitos tóxicos sistêmicos associados à sua utilização possam ser reduzidos (ROMAO *et al.*, 2009).

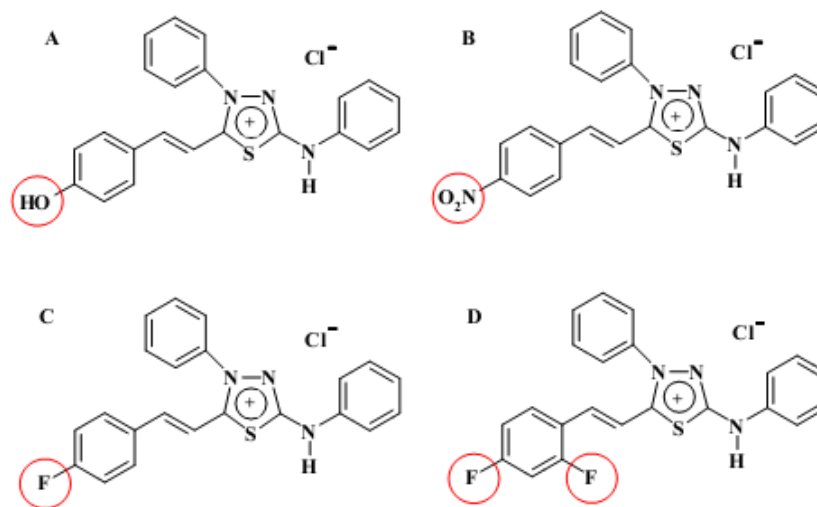


FIGURA 4: ESTRUTURA QUÍMICA DOS DERIVADOS 1,3,4-TIADIAZÓIS

FONTE: PIRES, 2011

Nota: A. cloreto de 4-fenil-5-[hidroxi-cinamoil]-1,3,4-tiadiazólio-2-fenilamina (MI-J); B. cloreto de 4-fenil-5-[4-nitrocinaoimil]- 1,3,4-tiadiazólio-2-fenilamina (MI-D); C. cloreto de 4-fenil-5-[4-fluorcinaoimil]-1,3,4-tiadiazólio-2-fenilamina (MI-F); D. cloreto de 4-fenil-5-[2,4-difluorcinaoimil]- 1,3,4-tiadiazólio-2-fenilamina (MI-2,4diF). Os círculos destacam os substituintes do anel cinamoil.

A atividade citotóxica do MI-D já foi caracterizada em diferentes células de melanoma humano. O composto reduziu a viabilidade das linhagens MEL-85, SK-MEL, A2058 e MEWO para 40, 30, 12 e 8%, após incubação com 25 μM por 24 h. Quando a concentração e o tempo de tratamento com o derivado foram aumentados para 50 μM e 48 h, observou-se de 90-100% de comprometimento na viabilidade destas células. Análises morfológicas das células MEL-85 sugeriram que a apoptose foi a via de morte induzida pelo MI-D. Além disto, houve diminuição da adesão destas células às proteínas de matriz extracelular laminina (65%- 5 μM por 2h), fibronectina (34%) e matrigel (71%) (SENFF-RIBEIRO *et al.*, 2004b). Cadena (1999)

também sugeriu, após análise de alterações morfológicas e fragmentação do DNA (TUNEL), que a apoptose seria a via de morte induzida por MI-D em células HeLa (CADENA, 1999).

Diversos trabalhos têm sugerido que os efeitos citotóxicos promovidos por estes derivados estejam relacionados com as alterações na bioenergética mitocondrial, como a dissipação do potencial de membrana, aumento da atividade da ATPase, inibição dos complexos transportadores de elétrons e desacoplamento da fosforilação oxidativa, efeitos relacionados a diminuição da fluidez das membranas mitocondriais (CADENA *et al.*, 1998; 2002; PIRES, A. R. A. *et al.*, 2011).

2.3 RESISTÊNCIA À MULTIPLAS DROGAS (MDR)

Embora a busca pela seletividade represente uma preocupação constante para o avanço da terapia antitumoral, outro aspecto limitante na utilização de quimioterápicos que tem sido essencialmente relacionado com o prognóstico de morte, é o desenvolvimento ou presença de resistência a múltiplas drogas (MDR) por células tumorais. Dentre os mecanismos propostos para o surgimento deste fenótipo, a expressão aumentada de bombas de efluxo de drogas (transportadores da superfamília ABC) é considerada um dos fatores mais importantes (ECKFORD; SHAROM, 2009; DE SOUZA *et al.*, 2011; KATHAWALA *et al.*, 2015).

O sucesso de determinadas quimioterapias antitumorais requer, dentre diversos fatores, que os compostos utilizados atinjam concentrações intracelulares necessárias para exercer seus efeitos (XIONG *et al.*, 2005; FUKUDA; SCHUETZ, 2012). Neste sentido, Dano, em 1973, demonstrou que células de carcinoma de Erlich resistentes a daunomicina apresentavam menor concentração intracelular deste composto, quando comparado ao carcinoma não resistente, sugerindo que a MDR seria consequência da ação de transportadores celulares. Evidências como o acúmulo do quimioterápico na presença de drogas estruturalmente análogas (indicando possível inibição competitiva) e sua manutenção contra um gradiente químico, reforçaram a proposição do pesquisador. Três anos mais tarde, foi identificada a primeira bomba de efluxo de drogas, pertencente à superfamília ABC, relacionada com o fenótipo MDR (DANØ, 1973; FUKUDA; SCHUETZ, 2012).

Dos aproximados 15 transportadores ABC descritos como exportadores de quimioterápicos *in vitro*, somente Pg-p (glicoproteína P), MRP1 (proteína 1

associada à resistência a múltiplas drogas) e ABCG2 (proteína de resistência ao câncer de mama) demonstraram associação com o surgimento de MDR *in vivo* (ECKFORD; SHAROM, 2009; MO; ZHANG, 2012). Dentre estes, Pg-p foi o primeiro transportador identificado, sendo detectado como uma glicoproteína de membrana com 170-kDa em células de ovário de hamster chinês resistentes a colchicina (JULIANO; LING, 1976; WU, HSIEH, *et al.*, 2011; FUKUDA; SCHUETZ, 2012). Posteriormente, a partir de análises de expressão diferencial utilizando construções de bibliotecas de cDNA de células resistentes e sua parentais, identificou-se MRP1 e ABCG2 em linhagens de câncer de pulmão resistentes a doxorubicina (H69AR) (COLE *et al.*, 1992; WU, HSIEH, *et al.*, 2011; FUKUDA; SCHUETZ, 2012) e câncer de mama resistente a adriamicina (MCF-7/AdrVp) (ALLIKMETS *et al.*, 1998; DOYLE *et al.*, 1998; WU, HSIEH, *et al.*, 2011; FUKUDA; SCHUETZ, 2012), respectivamente.

Diversos estudos têm destacado que características do microambiente tumoral podem contribuir para o desenvolvimento celular do fenótipo de MDR, particularmente no que diz respeito às alterações na vascularização e produção de citocinas, quimiocinas ou fatores de crescimento pelo estroma tumoral (MILANE *et al.*, 2011; WU, HSIEH, *et al.*, 2011). Neste sentido, Comerford *et al.* (2002) demonstraram que a indução de hipóxia em células de carcinoma colorretal T84 e Caco 2 promoveu aumento no efluxo, sensível a verapamil (inibidor de Pg-p), de digoxina e rodamina 123 (substratos de Pg-p), além de induzir o aumento nos níveis de mRNA desta proteína. Os autores ainda evidenciaram que o tratamento da linhagem Caco2 com oligonucleotídeos anti-senso para HIF1- α reduziu a expressão de Pg-p em condições de hipóxia, sendo identificada, posteriormente, uma região de ligação ao HIF1- α no promotor do gene do transportador. Também foram observados aumento na expressão e atividade de ABCG2 com o tratamento de IL-1 β e TNF- α em linhagem de câncer de mama MCF-7 (MOSAFFA *et al.*, 2009), assim como para MRP1 em linhagem de hepatocarcinoma HepG2 tratada com IL-1 β e IL-6 (LEE; PIQUETTE-MILLER, 2003).

O surgimento do fenótipo MDR muitas vezes pode ocorrer durante ou após a realização de ciclos de quimioterapia, o que muitas vezes está associado à seleção e subsequente expansão clonal de células MDR pré-existentes no tumor. Por outro lado, a exposição aguda a determinados quimioterápicos também pode resultar no aparecimento do fenótipo MDR, como exemplificado pelo aumento nos níveis de mRNA codificante para Pg-p em tumores metastáticos de pulmões humanos

tratados com doxorrubicina (ABOLHODA *et al.*, 1999). Em concordância, tem-se observado a amplificação gênica de bombas de efluxo através do tratamento prolongado de linhagens tumorais com determinados compostos. Esta estratégia tem sido frequentemente utilizada para o desenvolvimento de linhagens superexpressando transportadores ABC (CALCAGNO; AMBUDKAR, 2010).

O aumento na expressão de Pg-p está associado com um prognóstico desfavorável, particularmente em relação à sobrevivência ou reincidência tumoral após tratamento quimioterápico de portadores de leucemias (PIRKER *et al.*, 1991), cânceres de mama (BURGER *et al.*, 2003), ovário (PENSON *et al.*, 2004), rabdiosarcomas e sarcomas indiferenciados (CHAN *et al.*, 1990), osteosarcoma (CHAN *et al.*, 1997), neuroblastoma (HABER *et al.*, 2006) e hepatocarcinoma (NG *et al.*, 2000; AKIMOTO *et al.*, 2006), como citado anteriormente. Para ABCG2 a mesma associação foi encontrada em leucemias (BENDERRA *et al.*, 2004), carcinoma de pulmão (KIM *et al.*, 2009; OTA *et al.*, 2009), e embora com relevância clínica ainda não estabelecida, Diestra *et al.* (2002) demonstraram uma grande prevalência na expressão deste transportador em adenocarcinomas do trato digestivo, endométrio, pulmão e melanoma. Níveis aumentados de MRP1 estão associados com a diminuição da sobrevivência de pacientes portadores de neuroblastoma (HABER *et al.*, 2006) ou leucemia (LAUPEZE *et al.*, 2002; LEGRAND *et al.*, 2009), além de aumento tanto na reincidência de tumores de mama, quanto na invasividade e agressividade de tumores de próstata.

Em geral, os transportadores ABC possuem uma região consenso de ligação ao ATP (domínio NBD), encontrada no citoplasma e de aproximadamente 90-110 aminoácidos, que inclui dois motivos Walker (A e B) e um motivo com a sequência de assinatura ABC (assinatura C) (GOTTESMAN; AMBUDKAR, 2001; ECKFORD; SHAROM, 2009; KATHAWALA *et al.*, 2015). Além disso, possuem domínios transmembrana (TMDs) não conservados, responsáveis pela ligação e extrusão do substrato (ERNST *et al.*, 2010) (FIGURA 5). A diferença entre os transportadores está na estrutura modular e número de domínios, que junto à falta de conservação dos domínios TMDs, resulta em diferente especificidade a substratos (GOTTESMAN; AMBUDKAR, 2001; MO; ZHANG, 2012; MONTANARI; ECKER, 2015).

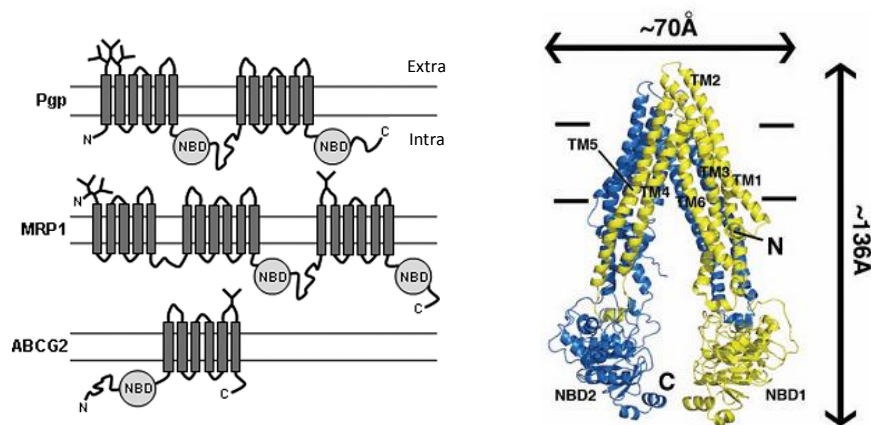


FIGURA 5: TOPOLOGIA E ESTRUTURA DE TRANSPORTADORES ABC

FONTE: ALLER *et al.*, 2009; ECKFORD; SHAROM, 2009 (Copyright 2014 American Chemical Society).

Nota: A topologia dos transportadores ABC está mostrada à esquerda. N e C indicam o grupo amino-terminal e carboxi-terminal. Os retângulos cinza dispostos na vertical indicam as hélices do domínio transmembrana. NBD indica o domínio de ligação ao ATP, voltado para o citoplasma. Ao lado direito está representada a estrutura do transportador Pgp de rato obtida por cristalografia de raios-X. TM(n) indica a posição das hélices do domínio transmembrana.

Diversos compostos antitumorais, não necessariamente relacionados estruturalmente, podem ser substratos de Pgp, MRP1 e ABCG2 (TABELA 1). Este transporte é resultado de mudanças conformacionais, induzidas pela ligação de substratos aos domínios TMDs, e consequente aumento na hidrólise do ATP nos NBDs, permitindo a passagem de compostos, no sentido extracelular, pela região transmembrana do transportador (HIGGINS; LINTON, 2004). Quatro domínios são requeridos para funcionalidade dos transportadores ABC, sendo 2 NBDs e 2 TMDs. Em eucariotos, a maioria destes transportadores é sintetizada em um único polipeptídeo contendo as quatro unidades funcionais. Entretanto, alguns são sintetizados como hemi-transportadores (ABCG2, por exemplo), sendo necessária a dimerização para formação de uma unidade funcional (WILKENS, 2015).

TABELA 1- ANTITUMORAIS SUBSTRATOS DE TRANSPORTADORES ABC

COMPOSTO ANTITUMORAL	Pg-p	MRP1	ABCG2
Antraciclinas			
<i>Doxorrubicina</i>	+	+	+
<i>Daunorrubicina</i>	+	+	+
<i>Epirubicina</i>	+	+	+
<i>Mitoxantrona</i>	+	+	+
Inibidores da topoisomerase			
<i>Etoposídeo</i>	+	+	+
<i>Teniposídeo</i>	+	+	+
<i>Topotecano</i>	+		+
<i>Irinotecano e seu metabólito SN-38</i>	+	+	+
<i>Indolocarbazol NB-506 e J-107088</i>			+
Alcalóides da Vinca			
<i>Vincristina</i>	+	+	
<i>Vinblastina</i>	+	+	
<i>Vinorelbina</i>	+	+	
Alcalóides			
<i>Cefarantina</i>	+		
<i>Homoharrintonina</i>	+		
Taxanos			
<i>Paclitaxel</i>	+		
<i>Docetaxel</i>	+		
Antibióticos Antitumorais			
<i>Actinomicina D</i>	+	+	
<i>Mitomicina C</i>	+	+	
Antimetabólitos			
<i>Citarabina</i>	+		
<i>Metotrexato</i>	+	+	+
Acridinas			
<i>Ansacrina</i>	+		
Antracenos			
<i>Bisantreno</i>	+		+
<i>Flavopiridol</i>			+
Outros			
<i>Cisplatina</i>		+	
<i>Arsenito</i>		+	

Fonte: GOTTESMAN *et al.*, 2002; SCHINKEL; JONKER, 2003; ECKFORD; SHAROM, 2009; COLEY, 2010; TAMAKI *et al.*, 2011

2.3.1 Inibidores de transportadores ABC

A inibição dos transportadores ABC tem sido considerada por muitos pesquisadores uma estratégia simples e direta para restauração da sensibilidade de células resistentes (LEE, 2010; SHUKLA *et al.*, 2011; WU, HSIEH, *et al.*, 2011). Nesta abordagem, o bloqueio do efluxo do quimioterápico permitiria seu acúmulo e distribuição intracelular em concentrações necessárias para promoção do efeito antitumoral (WU, OHNUMA, *et al.*, 2011). Até o momento, entretanto, não existem inibidores disponíveis para utilização clínica, fato decorrente da elevada toxicidade intrínseca associada a estas moléculas (LECERF-SCHMIDT *et al.*, 2013; KATHAWALA *et al.*, 2015). Além disto, os transportadores ABC são altamente expressos, de maneira fisiológica, em importantes órgãos do metabolismo (fígado e rins) e barreiras de proteção (intestino, barreira hematoencefálica, hematoplacentária, hematotesticular), impedindo o acúmulo de toxinas em determinadas estruturas do organismo, ou ainda facilitando sua excreção. Neste contexto, a inibição destes transportadores também poderia resultar em toxicidade sistêmica, no entanto acredita-se que a atividade de outras proteínas ABC, ou mesmo a modulação de sua expressão, possa atenuar este efeito, tornando essencial a busca por inibidores altamente seletivos (LECERF-SCHMIDT *et al.*, 2013; NIGAM, 2015).

2.3.1.1 Inibidores de ABCG2

Diferentes classes de compostos tem demonstrado inibir fortemente, e de maneira relativamente específica, a atividade de ABCG2 *in vitro*, como *fumitremorgin C* (obtido da fermentação de *Aspergillus fumigatus*) (RABINDRAN *et al.*, 2000) e seus análogos sintéticos (Ko132, Ko134 e Ko 143) (VAN LOEVEZIJN *et al.*, 2001; ALLEN *et al.*, 2002) (FIGURA 6); derivados do tariquidar (KUHNLÉ *et al.*, 2009) e elacridar (gerando acridonas e cromonas), reconhecidos inibidores de Pgp (BOUMENDJEL *et al.*, 2007; VALDAMERI *et al.*, 2012a); derivados de grupos pertencentes a classe dos flavonoides, como flavonas (6-prenilcrisina e 3',4',7-trimetoxiflavona) (AHMED-BELKACEM *et al.*, 2005; KATAYAMA *et al.*, 2007) e chalconas (VALDAMERI *et al.*, 2012b; WINTER *et al.*, 2014) e derivados do resveratrol (gerando metóxi-estilbenos) (VALDAMERI *et al.*, 2012c). Entretanto,

poucos trabalhos tem demonstrado a reversão do fenótipo MDR *in vivo*. Neste sentido, Allen *et al.* (2002) demonstraram a atividade inibitória de Ko143 (10 mg/Kg) em ABCG2 localizado no epitélio intestinal de camundongos. Naquele estudo observou-se aumento de 6 vezes nos níveis plasmáticos de topotecano, um substrato do transportador, após administração oral de Ko143 em animais com deleção no gene de Pgp. Além disto, não foram observados sinais de neurotoxicidade após administração oral do inibidor em concentrações até 50 mg/Kg. Por outro lado, demonstrou-se recentemente que Ko143 foi rapidamente metabolizado em plasma de ratos *in vitro* (redução de 50% em ~12 min), e que seu derivado carboxílico é capaz de inibir a atividade de ABCG2, em linhagem embrionária de rim humano (HEK293) superexpressando o transportador, somente em elevadas concentrações (> 100 µM) (WEIDNER *et al.*, 2015).

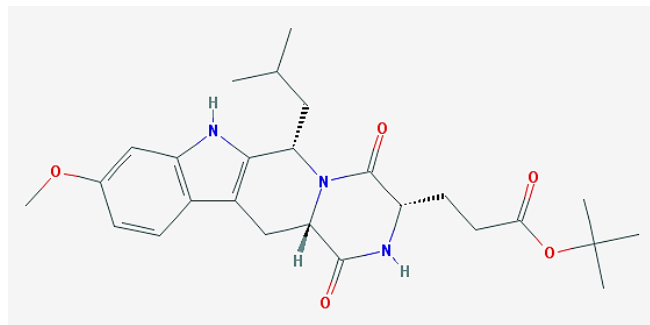


FIGURA 6: ESTRUTURA MOLECULAR DO Ko143

FONTE: Adaptado de NCBI, 2015b

NOTA: Nome químico: Tert-Butil 3-((3S,6S,12aS)-6-isobutil-9-metoxi-1,4-dioxi-1,2,3,4,6,7,12,12a-octahidropirazina[1',2':1,6]pirido[3,4-b]indol-3-il)propanoato. Representação da estrutura molecular em 2D.

Arnaud *et al.* (2011) evidenciaram o efeito de um inibidor derivado de acridona, MBLI-87 (5µM), ao constatar o acúmulo do quimioterápico irinotecano em linhagem embrionária de rim humano HEK293 superexpressando ABCG2. Em tumores xenográficos induzidos com a mesma linhagem, os autores observaram aumento na sensibilização do irinotecano em camundongos tratados intraperitonalmente com 2,4 mg/Kg do inibidor. Os autores não observaram alterações nos parâmetros farmacocinéticos do quimioterápico, quando na presença de MBLI-87.

Através de uma seleção utilizando uma biblioteca química de inibidores de ABCG2, Yamazaki *et al.* (2001) descobriram um derivado de acrinolitrina, denominado YHO-13177, com potente propriedade quimiossensibilizadora. Foi observada reversão da resistência aos antitumorais substratos de ABCG2 (SN-38, mitoxantrona e topotecano) em células HCT-116 e A549 superexpressando o transportador e tratadas com 1 $\mu\text{mol/L}$ do derivado. O mesmo efeito foi observado em diferentes linhagens com expressão intrínseca de ABCG2, sem apresentar citotoxicidade quando utilizado isoladamente. Os autores também avaliaram a reversão da resistência *in vivo* utilizando a pró-droga de YHO-13177, YHO-13351, nos tumores ascíticos HCT116/ABCG2 ou P388/ABCG2 implantados em camundongos. Observou-se um aumento de $\sim 100\%$ na sobrevivência dos animais (P388/ABCG2) tratados com YHO-13351 (200 mg/Kg – i.p.), na presença do quimioterápico irinotecano, quando comparado aos tratados somente com o quimioterápico. Além disto, a coadministração de YHO-13351 (200 mg/Kg - via oral) e irinotecano reduziu em $\sim 50\%$ o crescimento de tumores HCT116/ABCG2, quando comparado com tratamento somente com o quimioterápico.

O composto MBL-II-141 (FIGURA 7), uma cromona substituída derivada do elacridar, tem sido considerado o inibidor de ABCG2 mais promissor até o momento. Este derivado possui uma alta e seletiva afinidade pelo transportador, apresentando IC_{50} de $\sim 0,05$ e $0,11\ \mu\text{M}$ para linhagens H460 selecionadas com mitoxantrona e HEK293/ABCG2, respectivamente, além de baixa citotoxicidade ($\text{IG}_{50} > 100\ \mu\text{M}$ em HEK293) (VALDAMERI *et al.*, 2012a; WINTER *et al.*, 2013). Recentemente, Honorat *et al.* (2014) avaliaram o efeito de MBL-II-141 (10 mg/Kg), na presença de irinotecano, em camundongos com tumores ascíticos de HEK293/ABCG2, demonstrando intensa redução no crescimento tumoral ($\sim 90\%$), assim como aumento de até $\sim 90\%$ no tempo de sobrevivência daqueles animais. O efeito de redução tumoral também foi observado após o tratamento de tumores com maior tempo de estabelecimento.

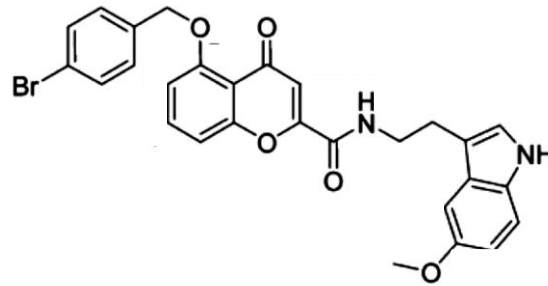


FIGURA 7: ESTRUTURA MOLECULAR DO MBLII-141

FONTE: Adaptado de WINTER *et al.*, 2013 .Copyright 2013 American Chemical Society.

NOTA: Nome químico: 5-(4-bromobenziloxi)-2-(2-(5-metoxindolil)etil-1-carbonil)-4H-cromen-4-ona.

Diversos trabalhos têm demonstrado que inibidores de proteínas quinases são capazes de reverter o fenótipo MDR através da modulação de ABCG2 *in vitro*, como resultado da diminuição de sua expressão ou inibição de sua atividade, ou ainda de ambos (WANG *et al.*, 2014). Entretanto, nenhum destes estudos caracterizou precisamente o tipo de inibição induzida por estes compostos. Neste contexto, Hegedus *et al.* (2012) demonstraram que gefitinibe (10 μM), um derivado de quinozalina com propriedade antitumoral decorrente da inibição do receptor do fator de crescimento epidérmico (EGFR), pode restaurar a sensibilidade de células de carcinoma epidermóide A431/ABCG2 a mitoxantrona, em níveis similares ao inibidor de referência Ko143 (1 μM). Ensaio de citotoxicidade com a mesma linhagem, quando comparados aos das células parentais não resistentes, demonstraram que gefitinibe pode ser transportado por ABCG2 (HEGEDUS *et al.*, 2012), além de estimular sua atividade ATPásica em membrana enriquecidas com a proteína (OZVEGY-LACZKA *et al.*, 2004; HEGEDUS *et al.*, 2012). Estes dados sugerem que gefitinibe promova uma inibição competitiva em ABCG2, indicando sua ligação aos sítios de reconhecimento de substratos, localizados no domínio TMD. A inibição de EGFR, por sua vez, resulta da competição de gefitinibe pelos sítios de ligação ao ATP, localizados na porção citoplasmática da quinase (KRAUSE; VAN ETEN, 2005).

A inibição de ABCG2 por gefitinibe também foi demonstrada *in vivo*. Naquele trabalho o inibidor aumentou a sobrevivência de camundongos transplantados com células de leucemia linfóica murina P388 superexpressando ABCG2 (P388/BCRP), quando tratados intraperitonealmente com irinotecano (antitumoral substrato de

ABCG2) e gefitinibe (150 mg/Kg). Por outro lado, este mesmo inibidor restaurou a sensibilidade a quimioterápicos via inibição de Pgp *in vitro*, demonstrando baixa seletividade para ABCG2 (YANASE *et al.*, 2004).

Importantes quimioterápicos inibidores da proteína tirosina-quinase BCR-ABL (imatinibe, nilotinibe e dasatinibe) e de receptores tirosina-quinase (Sunitinibe), além de inibidores de serina/treonina-quinases (indolocarbazóis e bis-indolilmaleimidas), interagem diretamente com ABCG2, no sítio de ligação a substratos, e aumentam sua atividade ATPásica (BRENDEL *et al.*, 2007; ROBEY *et al.*, 2007; SHUKLA *et al.*, 2009). Estas alterações foram associadas com o transporte dos inibidores de tirosina quinase (com exceção de Sunitinib, para o qual não se investigou este parâmetro), resultando em quimiosensibilização de células tumorais provavelmente por inibição competitiva. Embora não se tenha observado o transporte direto dos inibidores de serina/treonina quinases, sua interação com o sítio de ligação a substratos de ABCG2 promoveu mudanças conformacionais igualmente capazes de restaurar a sensibilidade a quimioterápicos.

Os domínios de ligação ao ATP presentes em ABCG2 também tem sido considerados alvos para inibição do transportador, considerando que derivados de auroa, uma classe de moléculas pertencentes ao grupo dos flavonoides, parecem inibir Pgp através desta interação (BOUMENDJEL *et al.*, 2002). Em concordância, compostos contendo auroa em seu núcleo demonstram inibir proteínas serina-treonina quinases CDK (quinase dependente de ciclina) através da interação com os domínios de ligação ao ATP (SCHOEPFER *et al.*, 2002). Este conhecimento motivou Sim *et al.* (2008) a avaliarem a modulação de ABCG2 utilizando derivados de 4,6-dimetoxiauronas. Os autores observaram que algumas auronas reverteram completamente a resistência a mitoxantrona em células de adenocarcinoma mamário humano tratadas com 0,5 μ M, entretanto os mecanismos envolvidos na inibição não foram analisados.

Embora inibidores com alta afinidade tenham sido desenvolvidos através de estudos de relação estrutura-atividade, a ausência de caracterização da estrutura tridimensional de ABCG2 em alta resolução tem dificultado a identificação precisa de seus sítios de ligação, assim como os de ligação aos substratos. Além disto, a maioria dos trabalhos tem explorado de forma especulativa o tipo de inibição promovida por estes compostos. O maior progresso em relação à descoberta de promissores inibidores de ABCG2 ocorreu nos últimos 12 anos, sendo esperado que

as próximas pesquisas determinem dentro de poucos anos o real impacto clínico destes inibidores para reversão de MDR (LECERF-SCHMIDT *et al.*, 2013).

2.4 ATIVIDADES BIOLÓGICAS DE INDENO[1,2-*b*]INDÓIS

Os indenoindóis constituem uma classe de compostos de origem sintética ou natural, possuindo uma estrutura elementar de quatro anéis fundidos, resultante da combinação dos anéis indol e indeno. Em geral, o esqueleto indenoindol possui dez isômeros, sendo o indeno[1,2-*b*]indol amplamente utilizado como base para síntese de moléculas com diferentes atividades biológicas, dentre as quais se destacam a antioxidante e antitumoral (RONGVED *et al.*, 2013).

Dois compostos contendo o núcleo indeno[1,2-*b*]indol foram investigados devido a sua ação antioxidante. O derivado H290/51 (cis-5, 5a, 6, 10b-tetrahydro-9-metóxi-7-metilindeno[2,1-*b*]indo) foi capaz de reduzir a lipoperoxidação com potência superior a vitamina E em diferentes modelos de estudo (lecitina de soja isolada, lipoproteínas, tecidos animais) (WESTERLUND *et al.*, 1996). Em corações de rato perfundidos, o composto melhorou parâmetros relacionados à injúria cardíaca (como pressão ventricular, fluxo coronariano, liberação de LDH, substâncias reativas ao ácido tiobarbitúrico, edema e isquemia) associada à isquemia ou oxidação induzida por peróxido de hidrogênio, nas concentrações de 10 µM (tempo de perfusão de 20 min) e 1 µM (tempo de perfusão de 10 min), respectivamente (NAGY *et al.*, 1996; NAGY *et al.*, 2001). Ensaios *in vivo* evidenciaram a ação cardioprotetora de H290/51 em porcos submetidos à isquemia e reperfundidos por 30 min com 1µM do derivado (SHIMIZU *et al.*, 1998). O segundo composto, denominado DHII (5,10-dihidroindeno[1,2-*b*]indol), diminuiu a presença de marcadores sorológicos de hepatotoxicidade (alanina aminotransferase, ornitina transcarbamilase e fosfatase alcalina) induzida por tetracloreto de carbono em camundongos tratados intraperitonealmente com 25 mg/Kg da molécula (SHERTZER; SAINSBURY, 1988). Além disto, em culturas primárias de miócitos de ratos mantidas por 14 dias, DHII diminuiu em até 23 % (40 µM) a presença de lipofuscina (MARZABADI *et al.*, 1995), uma estrutura granular fluorescente formada por proteínas oxidadas e lipídios nos lisossomos, considerada um indicativo de envelhecimento celular (TERMAN; BRUNK, 2004). A propriedade antioxidante do DHII foi justificada pela presença de um carbono deficiente de elétrons capaz de estabilizar radicais livres (SHERTZER;

SAINSBURY, 1988). Entretanto, alguns trabalhos demonstraram que DHII pode ativar o receptor para aril hidrocarbonetos em células de fígado, induzindo a expressão de diversas enzimas, incluindo glutathione S-transferase, que contribuem para manutenção da homeostase redox (LIU *et al.*, 1994).

Alguns trabalhos têm apontado a interação de derivados indeno[1,2-*b*]indóis com a enzima anidrase carbônica, receptores de estrogênio e canais de potássio (RONGVED *et al.*, 2013), porém, com exceção do estudo aqui apresentado (ARTIGO 2 e 3) não há relatos de sua interação com transportadores ABC.

Efeitos citotóxicos ou antiproliferativos *in vitro* também têm sido demonstrados com a utilização de diferentes grupos substituintes no núcleo indeno[1,2-*b*]indol. Neste sentido, Hong *et al.* (2006) sintetizaram e selecionaram cinco indenoindóis substituídos com metoxila, hidroxila ou amina, que apresentaram atividade antiproliferativa maior que 90% em células de carcinoma nasofaríngeo (HONE-1) e adenocarcinoma gástrico (NUGC-3) (20 µg/mL – 72h). Kashyap *et al.* (2012) observaram a redução da viabilidade celular ($IG_{50} \sim 18-50 \mu M$) associada à apoptose, em células embrionárias de rim humano (HEK293), após 24h de tratamento com cinco indenoindóis substituídos com metoxila, fenila ou flúor.

Até o momento, apenas dois mecanismos de ação foram associados ao efeito citotóxico promovido pelos indenoindóis. Bal *et al.* (2004) sugeriram que a inibição da enzima topoisomerase II por derivados apresentando diferentes substituintes (metoxila, metila, etila, alquila, propinila) está relacionada com a atividade citotóxica ($IG_{50} \sim 40-50 \text{ nM} - 72\text{h}$) destes compostos em células de leucemia humana (K562). Ainda neste estudo os autores demonstraram completa remissão tumoral em camundongos implantados com adenocarcinoma de cólon (C38) e tratados intravenosamente com um derivado contendo um grupo metila no anel B do núcleo indenoindol (25 mg/Kg). Kashyap *et al.* (2003) também sintetizaram uma série de 45 derivados indenoindóis e selecionaram cinco com significativa citotoxicidade em HEK 293 ($IG_{50} \sim 4-17 \mu M - 48\text{h}$), a qual também foi associada com a inibição de topoisomerase II. O segundo mecanismo sugerido envolve a inibição de CK2, uma serina/treonina-quinase de expressão ubíqua relacionada à sobrevivência celular, e cuja atividade encontra-se elevada em diferentes tipos de células tumorais (HANIF *et al.*, 2010). De fato, a inibição desta enzima tem

fundamentado o mecanismo de ação de diferentes compostos desta classe (ALCHAB *et al.*, 2015).

A investigação da atividade inibitória dos indenoindóis sobre a CK2 justifica-se pelas similaridades do núcleo indenoindol com os inibidores competitivos de CK2. Ambos são heterocíclicos planares de pequeno tamanho e capazes de interagir com sítios de ligação para nucleotídeos. Neste contexto, Hundsdörfer *et al.* (2002b) sintetizaram duas moléculas contendo um núcleo indeno[1,2-*b*]indol quiônico e demonstraram que a adição de um grupo fenila ou isopropila a este núcleo resultou em forte inibição de CK2 ($IC_{50} \sim 1,4 - 5 \mu M$), além da inibição de ARK5 ($\sim 0,5 - 3,7 \mu M$), uma proteína quinase ativada por AMP associada ao crescimento tumoral (SUZUKI *et al.*, 2004). Ambos compostos promoveram importante atividade citotóxica ($IG_{50} \sim 1,3 - 4,1 \mu M - 18h$) em carcinoma (5736) e papiloma (RT4) de bexiga, adenocarcinoma cervical (SISO) e mamário (MCF-7) e carcinoma esofágico (KYSE-70). Em outros trabalhos, moléculas derivadas dos núcleos indeno[1,2-*b*]indol cetônico e quinônico foram selecionados como potentes inibidores competitivos (em relação ao ATP) de CK2 ($IC_{50} \sim 0,11$ e $0,17$, respectivamente), porém seus potenciais citotóxicos não foram avaliados (HUNDSDORFER *et al.*, 2012a; ALCHAB *et al.*, 2015).

3 JUSTIFICATIVA E OBJETIVOS

Considerando a escassez de quimioterápicos disponíveis para o tratamento do HCC (BUPATHI *et al.*, 2015), a participação de ABCG2 na promoção da resistência ao tratamento do HCC (SUN *et al.*, 2010) e outros tipos de cânceres, além da ausência de inibidores de ABCG2 apresentando baixa citotoxicidade, um requisito essencial para sua utilização clínica (LECERF-SCHMIDT *et al.*, 2013), o objetivo geral deste trabalho consistiu na investigação de moléculas promissoras para o tratamento do HCC e inibidores de ABCG2, estabelecendo uma relação estrutura-atividade destes inibidores.

Inicialmente avaliou-se a citotoxicidade de quatro derivados 1,3,4-tiadiazóis mesoiônicos em células de HCC (HepG2) e cultura primária de hepatócitos ratos, como modelo não-tumoral. A inibição e a capacidade de serem efluxados também foram avaliadas sobre os principais transportadores ABC responsáveis pelo desenvolvimento clínico de resistência a quimioterápicos (Pgp, ABCG2 e MRP1). Os resultados estão apresentados na sessão 4.1, no formato exigido pela revista onde o artigo correspondente foi publicado (PLoS One).

Para o desenvolvimento de novos inibidores de ABCG2, foram conduzidos estudos de relação estrutura-atividade de moléculas sintetizadas a partir do núcleo indeno[1,2-b]indol presente em inibidores da proteína quinase II (CK2). (Resultados apresentados na sessão 4.2, no formato exigido pela revista onde o artigo correspondente foi publicado: *Journal of Medicinal Chemistry*). Para aumentar a potência e seletividade destes compostos, foram realizadas modificações das funções orgânicas presentes no núcleo indeno[1,2-b]indol (Resultados apresentados na sessão 4.3, no formato exigido pela revista onde o artigo correspondente foi publicado: *Drug Design, Development and Therapy*).

4 ARTIGOS CIENTÍFICOS

4.1 ARTIGO 1- Publicado na Revista PLoS One, volume 10, número 6, p. e0130046. Junho, 2015 (doi: 10.1371/journal.pone.0130046).

Gozzi GJ, Pires ARAP, Valdameri G, Rocha MEM, Martinez GR, Noleto GR, Acco A, Souza CEAS, Echevarria A, Reis CMR, Di Pietro A, Cadena SMSC. (2015) Selective Cytotoxicity of 1,3,4-Thiadiazolium Mesoionic Derivatives on Hepatocarcinoma Cells (HepG2). PLoS ONE 10(6): e0130046. doi:10.1371

Link:<http://journals.plos.org/plosone/article?id=10.1371/journal.pone.0130046/journal.pone.0130046>

Selective cytotoxicity of 1,3,4-thiadiazolium mesoionic derivatives on hepatocarcinoma cells (HepG2)

Gustavo Jabor Gozzi^{1¶}, Amanda do Rocio Andrade Pires^{1¶}, Glaucio Valdameri¹, Maria Eliane Merlin Rocha¹, Glauca Regina Martinez¹, Guilhermina Rodrigues Noleto¹, Alexandra Acco², Carlos Eduardo Alves de Souza², Aurea Echevarria³, Camilla Moretto dos Reis³, Attilio Di Pietro⁴, Sílvia Maria Suter Correia Cadena^{1,*}

¹Departamento de Bioquímica e Biologia Molecular, Universidade Federal do Paraná, Curitiba, Paraná, Brazil

²Departamento de Farmacologia, Universidade Federal do Paraná, Curitiba, Paraná, Brazil

³Departamento de Química, Universidade Federal Rural do Rio de Janeiro, Rio de Janeiro, Brazil

⁴Equipe Labellisée Ligue 2014, BMSSI UMR 5086 CNRS/Université Lyon 1, IBCP, Lyon, France.

¶These authors contributed equally to this work

ABSTRACT

In this work, we evaluated the cytotoxicity of mesoionic 4-phenyl-5-(2-Y, 4-X or 4-X-cinnamoyl)-1,3,4thiadiazolium-2-phenylamine chloride derivatives (MI-J: X=OH, Y=H; MI-D: X=NO₂, Y=H; MI-4F: X=F, Y=H; MI-2,4diF: X=Y=F) on human hepatocellular carcinoma (HepG2), and non-tumor cells (rat hepatocytes) for comparison. MI-J, MI-4F and MI-2,4diF reduced HepG2 viability by ~ 50% at 25 μM after 24-h treatment, whereas MI-D required a 50 μM concentration, as shown by 3-(4,5-dimethylthiazol-2-yl)-2,5-diphenyltetrazolium bromide assays. The cytotoxicity was confirmed with lactate dehydrogenase assay, of which activity was increased by 55, 24 and 16% for MI-J, MI-4F and MI-2,4diF respectively (at 25 μM after 24 h). To identify the death pathway related to cytotoxicity, the HepG2 cells treated by mesoionic compounds were labeled with both annexin V and PI, and analyzed by flow cytometry. All compounds increased the number of doubly-stained cells at 25 μM after 24 h: by 76% for MI-J, 25% for MI-4F and MI-2,4diF, and 11% for MI-D. It was also verified that increased DNA fragmentation occurred upon MI-J, MI-4F and MI-2,4diF treatments (by 12%, 9% and 8%, respectively, at 25 μM after 24 h). These compounds were only weakly, or not at all, transported by the main multidrug transporters, P-glycoprotein, ABCG2 and MRP1, and were able to slightly inhibit their drug-transport activity. It may be concluded that 1,3,4-thiadiazolium compounds, especially the hydroxy derivative MI-J, constitute promising candidates for future investigations on *in-vivo* treatment of hepatocellular carcinoma.

Keywords: 1,3,4-thiadiazolium mesoionic derivatives, HepG2 cancer cells, rat hepatocytes; cell death, multidrug resistance.

4.1.1 Introduction

Liver cancer is the third most common cause of cancer-related death worldwide (PADHYA *et al.*, 2013; SHI *et al.*, 2014). Hepatocellular carcinoma (HCC), specifically, represents the major histological subtype among primary liver cancer (JEMAL *et al.*, 2011; SHI *et al.*, 2014), being one of the most prevalent malignant tumor worldwide (SHI *et al.*, 2014). Surgical resection and transplantation still remain the first choice of HCC treatment with potential cure, but this procedure must be used only in patients with early stages of HCC (CHENG; LV, 2013; UHL *et al.*, 2014). Unfortunately, diagnosis often occurs in HCC advanced stages (PADHYA *et al.*, 2013), and there is then only one - drug approved by Food and Drug Administration (FDA) that can be used as a systemic therapeutic agent for HCC treatment (REATAZA; IMAGAWA, 2014). Other drug-based therapies have promisingly emerged as alternatives for early- and advanced- HCC treatment, which has motivated the research of new compounds to be used in patients who are not

candidates to surgical treatment (CHENG; LV, 2013; LOONG; YEO, 2014; REATAZA; IMAGAWA, 2014). The high toxicity of drugs toward non-tumoral cells and the resistance to treatment constitute great problems in present chemotherapy (KRATZ *et al.*, 2008; HOLOHAN *et al.*, 2013). Drug toxicity usually limits the concentration usable for the treatments, as well as the frequency of administrations, further affecting curing efficiency (WU *et al.*, 2014). Additionally, tumor cells may become resistant to drugs through different mechanisms. The most notable one is the overexpression of ATP-binding cassette transporters, such as P-glycoprotein (Pgp) (ENDICOTT; LING, 1989), multidrug resistance protein 1 (MRP1) (COLE *et al.*, 1992) and breast cancer resistant protein (ABCG2) (DOYLE *et al.*, 1998), which efflux several types of drugs with unrelated structures and mechanisms (NOGUCHI *et al.*, 2014). This feature is a main obstacle to effectiveness of chemotherapy against HCC (BRITO *et al.*, 2014). Indeed, several studies have demonstrated a relationship between overexpression of these efflux pumps and either poor prognosis or aggressive tumor phenotype in patients with HCC (SEO *et al.*, 2007; VANDER BORGHT *et al.*, 2008; SUKOWATI *et al.*, 2012). Mesoionic compounds with a 1,3,4-thiadiazolium ring have shown important biological activities as antibiotic (CHANDRAKANTHA *et al.*, 2014), antiparasitic (CARVALHO *et al.*, 2004), antiviral (XIAOHE *et al.*, 2010), anticonvulsant (ARCHANA *et al.*, 2004), antidepressant (JUBIE *et al.*, 2012), antioxidant (KHAN *et al.*, 2010), analgesic, antiinflammatory (KUMAR *et al.*, 2008) and antitumoral (SENFF-RIBEIRO *et al.*, 2003) agents. We have specifically studied several 1,3,4-thiadiazolium-2-phenylamine chlorides mesoionic derivatives, only differing through the substituents of the cinnamoyl ring: MI-D, X=NO₂; MI-J, X=OH; MI-4F, X=F; MI-2,4diF, X=Y=F (Fig. 1). Some of them have demonstrated antitumoral effects against carcinoma, sarcoma (GRYNBERG *et al.*, 1997) and melanoma (SENFF-RIBEIRO *et al.*, 2003; SENFF-RIBEIRO *et al.*, 2004b) tumors *in vivo*, and cytotoxic activities against several types of tumor cells have been described *in vitro* (SENFF-RIBEIRO *et al.*, 2004a). Otherwise, it has been shown that these derivatives promote functional and structural alterations in isolated rat liver mitochondria, up to different degrees depending on cinnamoyl ring substitution (CADENA *et al.*, 1998; 2002; PIRES *et al.*, 2010; PIRES, A. R. *et al.*, 2011). We evaluated the cytotoxicity of MI-D, MI-J, MI-4F and MI-2,4diF on human hepatocellular carcinoma cells (HepG2), and primary rat hepatocytes as a non-tumoral model, and their effects on the multidrug resistance proteins Pgp, ABCG2

and MRP1. It was found that these compounds might represent new alternatives for HCC chemotherapeutic treatments, overcoming important limiting problems such as drug resistance and toxicity toward non-tumoral cells.

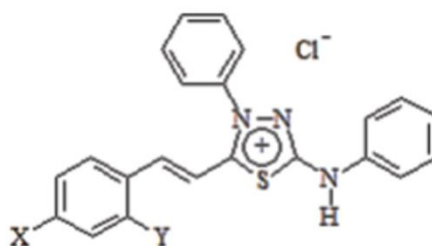


FIGURE 1: CHEMICAL STRUCTURE OF THE 4-PHENYL-5-(2-Y-4-X-CINNAMOYL)-1,3,4-THIADIAZOLIUM-2-PHENYLAMINE CHLORIDE DERIVATIVES

Note: MI-D (X=NO₂; Y=H), MI-J (X=OH; Y=H), MI-4F (X=F; Y=H), and MI-2,4diF (X=Y=F).

4.1.2 Materials and Methods

4.1.2.1 Chemicals

High-glucose Dulbecco's modified Eagle's medium (DMEM) was obtained from Cultilab (Campinas, Brazil) and fetal bovine serum (FBS) was purchased from Gibco. Dimethylsulfoxide (DMSO) was obtained from Merck (São Paulo, SP, Brazil). Annexin V Apoptosis Detection Kit was purchased from BD Bioscience (São Paulo, SP, Brazil). Lactate dehydrogenase (LDH) detection kit (Liquiform) was obtained from Labtest (Lagoa Santa, MG, Brazil). Bovine serum albumin (BSA), 3-(4,5-dimethylthiazol-2-yl)-2,5-diphenyltetrazolium bromide (MTT) and 4-(2-hydroxyethyl)-1-piperazine ethanesulfonic acid (HEPES) were purchased from Sigma. All other reagents were commercial products of the highest available purity grade. The mesoionic derivatives, MI-D (4-phenyl-5-(4-nitrocinnamoyl)-1,3,4-thiadiazolium-2-phenylamine chloride), MI-J (4-phenyl-5-(4-hydroxycinnamoyl)-1,3,4-thiadiazolium-2-phenylamine chloride), MI-4F (4-phenyl-5-(4-fluorocinnamoyl)-1,3,4-thiadiazolium-2-phenylamine chloride), MI-2,4diF (4-phenyl-5-(2,4-fluorocinnamoyl)-1,3,4-

thiadiazolium-2-phenylamine chloride), were synthesized by the Department of Chemistry of the Federal Rural University of Rio de Janeiro, Brazil, and their structures were confirmed by ^1H NMR, ^{13}C NMR and mass spectrometry (SANTOS; ECHEVARRIA, 2001). For this study, the derivatives were dissolved in DMSO and then further diluted with the assay medium. Controls with DMSO (maximal 0.7%, v/v) were carried out in each assay.

4.1.2.2 HepG2 cell culture

The human hepatocarcinoma HepG2 cell line (from the American Type Culture Collection – ATCC) was maintained in high-glucose DMEM supplemented with 10% FBS, 100 UI/mL penicillin G and 100 $\mu\text{g}/\text{mL}$ streptomycin, 20 mmol/L 4-(2-hydroxyethyl)-1-piperazine ethanesulfonic acid (HEPES), adjusted to pH 7.4 with 1 mol/L sodium bicarbonate. HepG2 cells were grown at 37°C , 5 % CO_2 under controlled humidity. Sub-culturing was performed at approximately 48 h intervals, and cell growth was monitored with an Olympus inverted microscope.

4.1.2.3 Primary culture of rat hepatocytes

a) Animals

Male Wistar rats (180-200 g) were obtained from the Central Animal House of the Federal University of Paraná (PR, Brazil). The animals received a standard laboratory diet (Purina) and tap water. This study was carried out in strict accordance with the recommendations in the Guide for the Care and Use of Laboratory Animals of the National Institutes of Health. The protocol was approved by the Committee on the Ethics of Animal Experiments of the University Federal of Paraná (Permit Number: 548). All surgery was performed under ketamine/xylazine anesthesia, and all efforts were made to minimize suffering.

b) Isolation and culture of hepatocytes

The hepatocytes were obtained by monovascular liver perfusion of Wistar rats, as described previously by (SEGLEN, 1976; BRACHT A., 2003) with some

modifications. The male rats were weighed and anesthetized intraperitoneally with a mixture of ketamine (60 mg/kg) and xylazine (7.5 mg/kg). Following laparotomy, 100 μ L of sodium heparin (5000 U/mL) were injected into the abdominal cava vein. The portal and thoracic cava veins were cannulated, and the liver was perfused for 10-15 min with Krebs solution (2.4 mol/L NaCl, 96 mmol/L KCl, 24 mmol/L KH_2PO_4 , 24 mmol/L MgSO_4 , 480 mmol/L NaHCO_3 and 1 mol/L HEPES buffer, pH 7.4) containing 1.3 mol/L CaCl_2 , 20 mg collagenase (types IA and IV) and carbogen (95% O_2 :5% CO_2). The liver was excised, and the cells were released by mechanical action, filtered through 50- μ m nylon membranes and centrifuged at 400 rpm for 5 min at 4°C. Subsequently, the cells were centrifuged four times with Krebs solution supplemented with 20% BSA and treated with carbogen. The cells were suspended in high-glucose DMEM supplemented with FBS (10%), insulin (100 nmol/L), glucagon (10 nmol/L), epidermal growth factor (10 ng/mL), dexamethasone (50 nmol/L), penicillin (100 U/mL) and streptomycin (100 ng/mL). Cell viability was determined using the Trypan blue (0.4%, w/v) exclusion method as previously described by Philips (PHILIPS, 1973). Only the cell suspensions with viabilities higher than 80% were plated (1×10^6 cells/plate on a 60 mm plate) and cultured for further experiments. For 4h after plating, the medium was replaced by Hepatozyme with or without mesoionic compounds. Considering some delays during the isolation procedure and the time required for further assays (e.g. viability assays), the time of treatment was from 18 to 24h. It is important to remark that no differences in the results were observed during this interval.

4.1.2.4 Culture of multiple drugs resistant cells

The human embryonic kidney (HEK293) cells stably transfected with *ABCG2* (HEK293*ABCG2*) (VALDAMERI *et al.*, 2012) or *MRP1* (HEK293*ABCC1*), and their respective parental HEK293 (wild-type) or HEK293*pcDNA5* (empty-vector) cells, were maintained at 37 °C (5% CO_2) in high-glucose DMEM medium, supplemented with 10% fetal bovine serum, 1% penicillin/streptomycin. The mouse embryonic fibroblasts, of either wild-type (NIH3T3) or overexpressing Pgp (NIH3T3*ABCB1*) (MARTINEZ *et al.*, 2014), were maintained under the same conditions. The cell culture media were drug supplemented with either 0.75 mg/mL G418

(HEK293ABCG2), 200 µg/mL hygromycin B (HEK293pcDNA5 and HEK293ABCC1) or 60 ng/mL colchicin (NIH3T3ABCB1).

4.1.2.5 Cell viability assays

a) MTT reduction

HepG2 cells were seeded at a density of 1×10^4 cells/well into 96-well culture plates. After 24 h, the cells were treated with mesoionic compounds at concentrations of 5, 25 and 50 µM for 24 h. Hepatocytes were seeded at 1×10^6 cells/plate in 60-mm plates, and treated with compounds at 25 µM up to 18-24 h. Cell viability was evaluated through the MTT assay (REILLY *et al.*, 1998; CHEUNG *et al.*, 2007), and the absorbance was determined at 550 nm. The results were expressed as a percentage of viable cells in comparison to the control (taken as 100%). All HEK293 cells were seeded at a density of 1×10^4 cells/well into 96-well culture plates, and incubated for 24 h at 37 °C in 5% CO₂. NIH-3T3 and NIH-3T3ABCB1 cells were seeded at a density of 3.5×10^3 and 5.0×10^3 cells/well, respectively, and maintained under the same conditions before treatment. The cells were treated with mesoionic derivatives for 72 h; then, 20 µL of MTT solution (5 mg/mL) were added to each well and incubated for 4 h at 37 °C. The culture medium was discarded, and 100 µL of a DMSO:ethanol (1:1) solution was added into each well and mixed by gently shaking for 10 min. Absorbance was measured in a microplate reader at 570 nm, from which the value measured at 690 nm was subtracted.

b) Lactate dehydrogenase release

HepG2 and hepatocytes cells were plated and treated as described in the item 4.1.2.5-a. Aliquots (50 µL) of culture medium were centrifuged at 1000 rpm for 5 min, and LDH activity was measured by monitoring the decrease of NADH at 340 nm, with the LDH kit assay, according to manufacturer instructions.

c) Annexin-V and propidium iodide staining

HepG2 cells were seeded at a density of 1×10^6 cells in 60-mm plates, and treated with mesoionic derivatives at 25 μM for 24 h. At the end of exposure, cells were collected by trypsinization, centrifuged at 300xg for 5 min at 4 °C and suspended in 500 μL of binding buffer (10 mM HEPES, pH 7.4, 150 mM NaCl, 5mM KCl, 1 mM MgCl_2 and 1.8 mM CaCl_2). Aliquots (100 μl) of the cell suspension were incubated with 5 μl of the reagent mixture containing annexin V-FITC conjugate (BD Pharmingen) and 10 μl of propidium iodide (PI) (50 $\mu\text{g}/\text{mL}$) for 15 min at 25 °C. After incubation, 400 μl of binding buffer were added and the cells were analyzed by flow cytometry (RAZA *et al.*, 2011). Positive controls were separately stained with Annexin V alone (channel FL-1), PI alone (channel FL-2), and both markers, for compensation settings of the two signals. Flow cytometric analysis was carried out on a FACSCalibur flow cytometer (BD Biosciences Pharmingen, San Diego, CA, USA). In each sample, 10.000 events were recorded and analysis was performed using the WinMDI 2.9 software. Three independent experiments were performed for each treatment condition. Hepatocytes were seeded at 1×10^6 cells/plate in 60-mm plates, and treated with compounds at 25 μM up to 18-24 h. The culture medium was then replaced by the binding buffer containing 5 μl of annexin-V FITC and 0.8 mg/mL of PI. Cells were analyzed by fluorescence microscopy (AXIOVERT 40CSFL) with a 10X objective, in either absence (visible) or presence of annexin filter - FL1: 515-530 nm or PI-FL2: 560-580 nm.

4.1.2.6 Morphology assays

HepG2 cells (1×10^5 cells/well) were seeded in 24-well plates with glass slides on the bottom, and incubated in a humidified incubator with 5% CO_2 and at 37 °C for 24 h. After adhesion, the medium was replaced by new medium with or without mesoionic derivatives at 5 μM for 3 h. The cells were fixed with Bouin solution (formaldehyde at 4% (v/v):saturated picric acid:glacial acetic acid, 4:15:1) for 5 min at ambient temperature. Then, the cells were washed with ultrapure water, and stained with hematoxylin and eosin. They were dehydrated with acetone and xylol solutions, and assembled with Entelan (Merck). The morphological alterations were viewed in

Bel Fotonics microscope with 40 X and 100 X magnification, and the images were captured by a photographic camera Sony Cyber-Shot at 13.5 mega pixels. Hepatocytes were seeded at 1×10^6 cells/plate in 60-mm and treated with compounds at 25 μ M up to 18-24 h. After exposure, the morphology was analyzed by optical microscopy (AXIOVERT 40CSFL) with a 20X objective.

4.1.2.7 DNA fragmentation

The fragmented DNA content was determined by flow cytometry using PI (DARZYNKIEWICZ *et al.*, 1992; DOUGLAS *et al.*, 1995; BALASUBRAMANIYAN *et al.*, 2007). For these assays, 1×10^6 cells were dispensed in 60-mm plates, and incubated for 24 h for adhesion at 37 °C in 5% CO₂. The culture medium was then replaced by fresh medium without (control) or with 25 μ M derivatives, or the corresponding volumes of DMSO, and further incubated for 6 and 24 h. After incubation, the culture medium and cells were collected in a Falcon tube by trypsinization, and the samples were centrifuged at 2000 rpm for 5 min. The precipitate was suspended in phosphate buffered saline (PBS) and centrifuged again under the same conditions. The cells were suspended in 0.3 mL of a solution composed of 50 μ g/mL of propidium iodide and 0.1% Triton X -100 in PBS. After labeling, the cells were kept in the dark and analyzed by flow cytometry with the FACSCalibur (BD) apparatus using Cell Quest program. The data acquisition was done using the FL2 filter (yellow fluorescence), and analyzed as histograms (FL2 *versus* number of events). The number of cells in each phase of the cell cycle was expressed as a percentage of total events (10.000 cells). Histograms were analyzed using the WinMDI 2.9 software

4.1.2.8 Protein concentration assay

Protein concentration was determined by the method of Bradford (BRADFORD, 1976) using bovine serum albumin BSA as a standard.

4.1.2.9 Inhibition of drug efflux in multiple drug resistant cells

HEK293ABCG2 cells were seeded at a density of 1.0×10^5 cells/well into 24-well culture plates. After 72-h incubation, they were exposed to 5 μM mitoxantrone for 30 min at 37 °C, in the presence or absence of each derivative, and then washed with PBS and trypsinized. The intracellular fluorescence was monitored with a FACSCalibur cytometer (Becton Dickinson), using the FL4 channel and at least 10,000 events were collected. The percentage of inhibition was calculated relatively to 1 μM Ko143 which produced a complete inhibition. NIH-3T3ABCB1 were seeded at a density of 6×10^4 cells/well into 24-well culture plates and incubated for 48 h at 37 °C, whereas HEK293 cells transfected with ABCC1 were seeded at 2.5×10^5 cells/well for 72 h. The cells were respectively exposed to rhodamine 123 (0.5 μM) or calcein-AM (0.2 μM) for 30 min at 37 °C, in the presence or absence of each derivative, then washed with PBS and trypsinized. The intracellular fluorescence was monitored using the FL1 channel. The inhibition was measured relatively to 5 μM GF120918 or 35 μM verapamil, respectively, producing complete inhibitions. The percentage of inhibition was calculated by using the following equation:

$$\% \text{ inhibition} = (C - M) / (C_{ev} - M) \times 100,$$

where C corresponds to the intracellular fluorescence of resistant cells in the presence of compounds and fluorescent substrate, M to the intracellular fluorescence of resistant cells with the fluorescent substrate alone, and C_{ev} corresponds to the intracellular fluorescence of cells inhibited with standard inhibitor in the presence of fluorescent substrate.

4.1.2.10 Statistical Analysis

Results were expressed as mean \pm standard deviation, and subjected to analysis of variance (ANOVA) and Tukey test for comparison of means. A *P*-value lower than 0.05 was considered significant. All analyses and graphs were performed using GraphPad Prism Software version 6.0.

4.1.3 Results

4.1.3.1 Cytotoxicity of 1,3,4-thiadiazolium derivatives on HepG2 and rat hepatocytes

The viability of HepG2 cells was determined after 24 h of treatment with derivatives at 5, 25 and 50 μM , by both MTT and LDH-release assays. As observed in Fig. 2, upper panel, MI-J, MI-4F and MI-2,4diF reduced HepG2 cells viability by about 50% at 25 μM when analyzed by MTT. MI-D only reduced by 28% the cell viability, requiring 50 μM to reach 50%. The results of the LDH-release assay (Fig. 2, lower panel) also demonstrated the reduction of cell viability by MI-J, MI-4F and MI-2,4diF treatments. The enzymatic activity of the culture medium was increased by 55, 24 and 16%, respectively, for MI-J, MI-4F and MI-2,4diF at 25 μM , in comparison to controls without mesoionic derivative. MI-D, on the contrary, did not significantly affect the LDH activity. The viability of primary hepatocytes was also determined in order to verify the selectivity of derivatives for tumor cells. As observed in Fig. 3, no cytotoxicity was observed in MTT assays (upper panel), except for MI-2,4diF producing a 36% effect (at 25 μM for 18-24 h). However, no increase in LDH activity was observed with any derivative (lower panel). Interestingly, MI-D induced a reduction of LDH activity (\sim 17% at 25 μM).

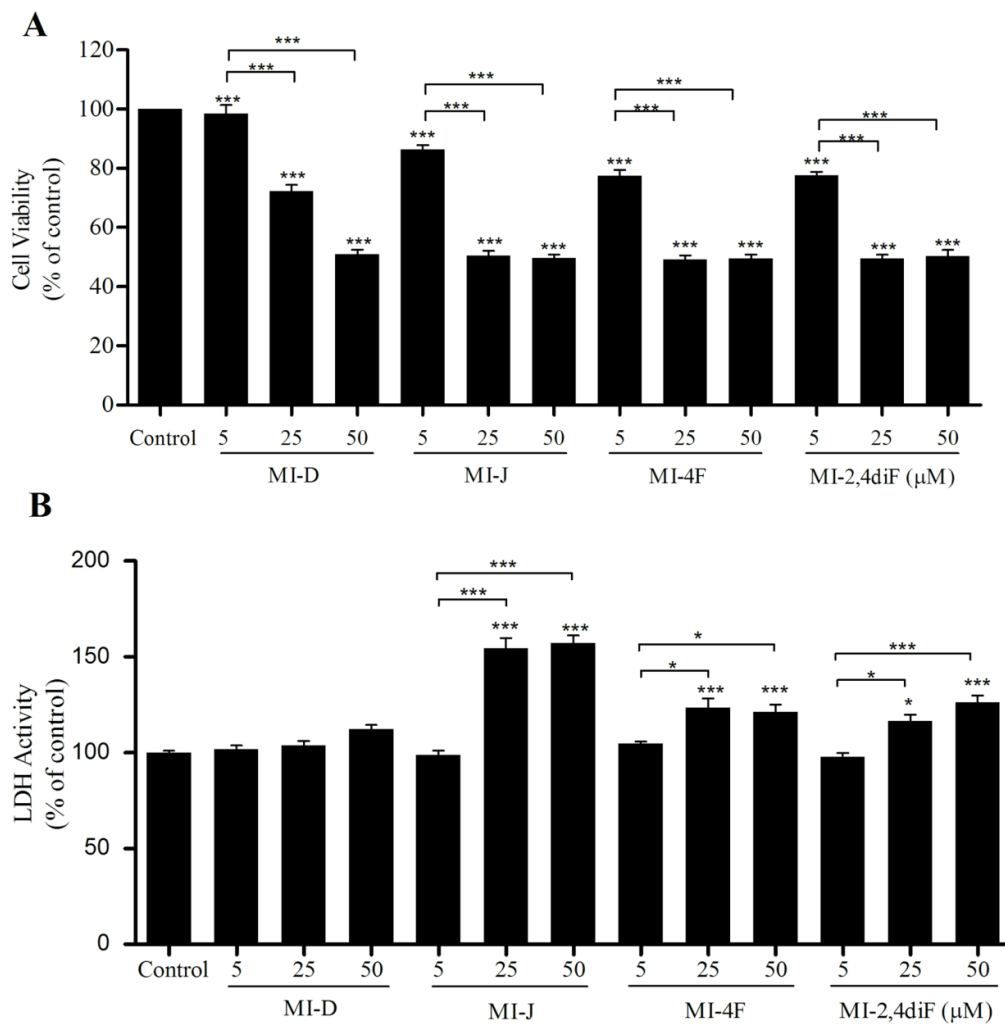


FIGURE 2: CYTOTOXIC EFFECTS OF 1,3,4-THIADIAZOLIUM DERIVATIVES ON HEPG2 CELLS

Note: **A. MTT assay** (the experimental conditions are described in the Materials and Methods section 4.1.2.5-a). The cells were seeded with or without 1,3,4-thiadiazolium derivatives at 5, 25 or 50 μM for 24 h. The results were expressed as % of viability in comparison to control. **B. LDH release assay** (the experimental conditions are described in the Materials and Methods section 4.1.2.5-b). Under the same treatment conditions, as described above, LDH activity was measured in supernatants. Data represent means of four different experiments in quadruplicate. The results were expressed as % of viability in comparison to control. * and *** denote values significantly different from the control or between the different treatments at $P < 0.05$ and $P < 0.0001$, respectively.

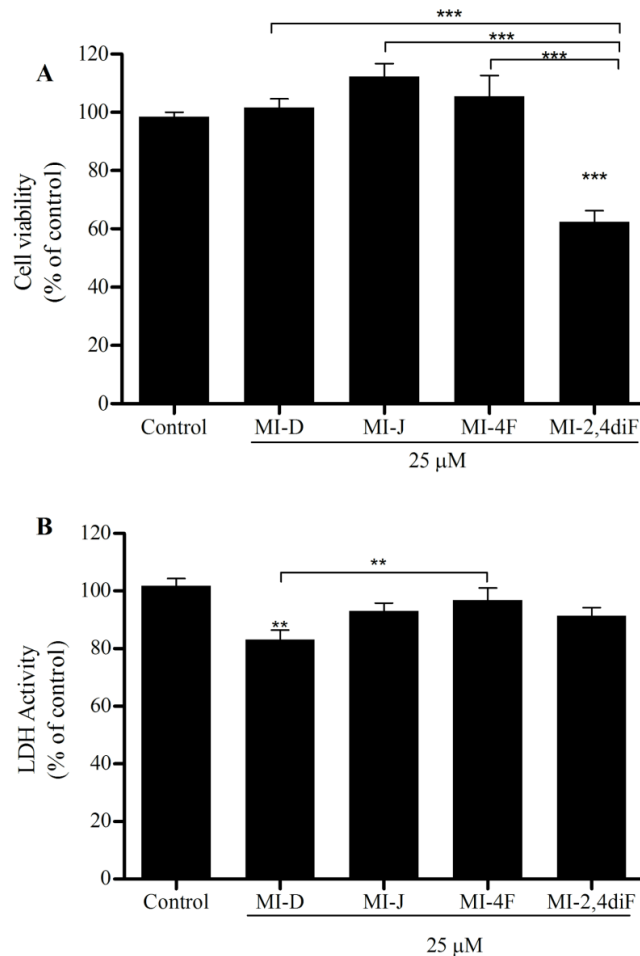


FIGURE 3: CYTOTOXIC EFFECTS OF 1,3,4-THIADIAZOLIUM DERIVATIVES ON HEPATOCYTES

Note: **A. MTT assay** (the experimental conditions are described in the Materials and Methods section 4.1.2.5-a) The cells were seeded with or without 1,3,4-thiadiazolium derivatives at 25 for 18-24 h. The results were expressed as % of viability in comparison to control. **B. LDH release assay** (the experimental conditions are described in the Materials and Methods section 4.1.2.5-b). Under the same treatment conditions described above, LDH activity was measured in the supernatants. Data represent means of four different experiments in quadruplicate. The results were expressed as % of viability in comparison to control. ** and *** denotes values significantly different from the control or between the different treatments at $P < 0.01$ and $P < 0.0001$, respectively.

4.1.3.2 Apoptosis induction by 1,3,4-thiadiazolium derivatives in HepG2 cancer cells but not in control hepatocytes

Considering the significant toxicity of the derivatives on HepG2 cells (Fig. 2), we evaluated the induction of apoptosis in these cells by DNA fragmentation, a key event of cells undergoing apoptosis (ORRENIUS *et al.*, 2011). After 24 h of treatment with MI-J, MI-4F and MI-2,4diF (Fig. 4C-E), approximate increases of 12%, 9% and 8%, respectively, were observed, as evidenced by the higher number of cells in sub-

G1 region. MI-D under the same conditions did not promote any significant alteration in DNA fragmentation, but increased the number of cells in G2/M phase (Fig. 4B). The G1/G0 and G2/M phases were not significantly changed by the other derivatives.

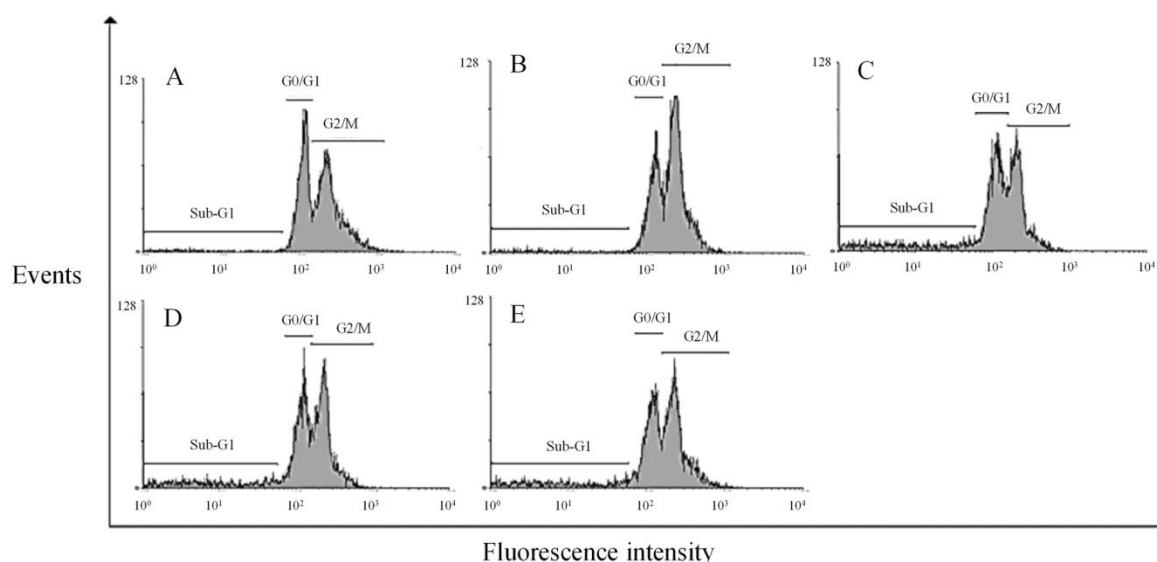


FIGURE 4: DNA FRAGMENTATION IN HEPG2 CELLS, AS INDUCED BY 1,3,4-THIADIAZOLIUM DERIVATIVES

Note: The experimental conditions are described in the Materials and Methods section 4.1.2.7. The cells were seeded with or without 1,3,4-thiadiazolium derivatives at 25 μ M for 24 h. For each sample, 10.000 events were analyzed by flow cytometry using FL2 filter. (A) control, (B) MI-D, (C) MI-J, (D) MI-4F and (E) MI-2,4diF. The histograms represent three different experiments in triplicate.

To further investigate the induction of apoptosis by mesoionic derivatives, HepG2 cells were simultaneously stained with FITC-conjugated annexin V and PI, and analyzed by flow cytometry (Fig. 5). All compounds (at 25 μ M for 24 h) increased the number of doubly-stained cells in comparison to control, reaching up to 76% for MI-J, 36% and 25% for MI-4F and MI-2,4diF, while a lower value of 11% was observed for MI-D. In addition, MI-J and MI-2,4diF promoted a slight increase (around 2.4%) in the number of PI-labeled cells.

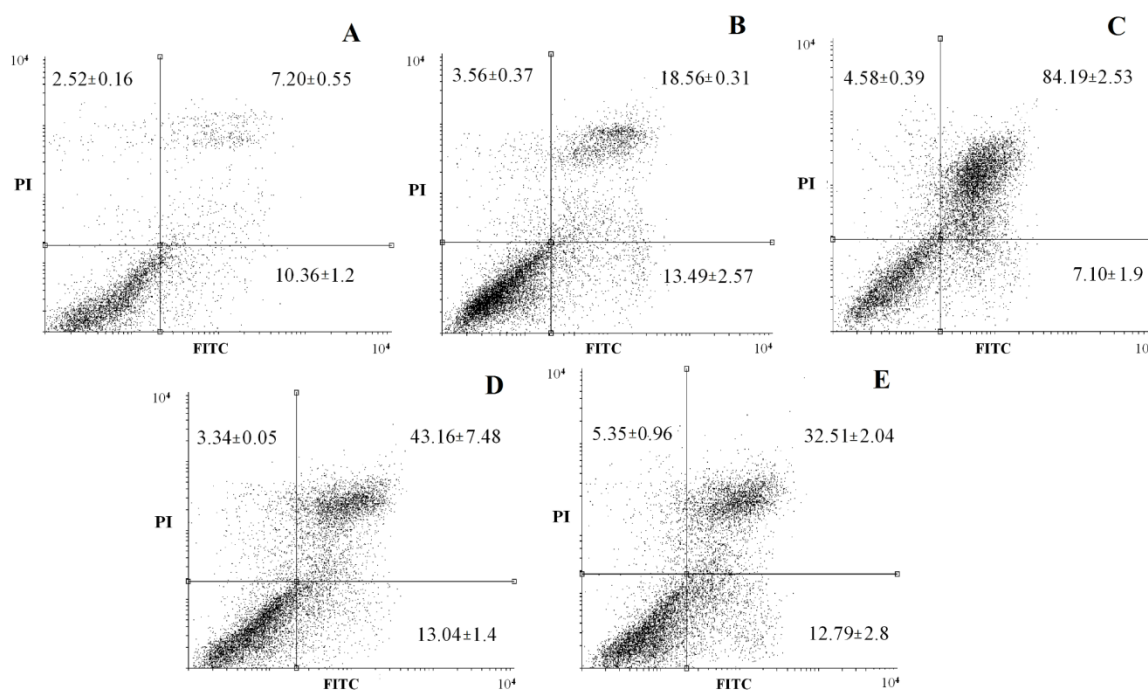


FIGURE 5: ANNEXIN V-FITC AND PROPIDIUM IODIDE STAINING OF HEPG2 TREATED WITH 1,3,4-THIADIAZOLIUM DERIVATIVES

Note: The experimental conditions are described in the Materials and Methods section 4.1.2.5-c. The cells were seeded with or without 1,3,4-thiadiazolium derivatives at 25 μ M for 18-24 h. Then, the cells were collected with trypsin and 10.000 events were analyzed by flow cytometry by FL2 and FL1 filters. (A) control, (B) MI-D, (C) MI-J, (D) MI-4F and (E) MI-2,4diF. The figures show representative dot-plot with the different cell populations: left-bottom = labeled cells; left-top = PI labeled; right-top = doubly labeled; right-bottom = annexin V labeled. The results were expressed as mean \pm SD of three independents experiments.

Since the differentiation between apoptosis and necrosis was not possible with such an assay, short incubation time (3 h) and reduced concentration (5 μ M) were used for morphological analyzes (ORRENIUS *et al.*, 2011). Apoptotic bodies (blebs) were observed, and loss of cellular organization in monolayer was elicited for all compounds even at low concentration (Fig. 6). Other characteristics of apoptosis induction, such as vacuolization, cellular shrinkage (with MI-D, MI-J and MI-4F) and nuclear pyknosis (with MI-4F and MI-2,4diF), were also observed. All together, these results suggest that apoptosis may be the death pathway induced by 1,3,4-thiadiazolium derivatives on HepG2 cells. Cultured hepatocytes were also doubly stained with FITC-conjugated annexin V and PI, and analyzed by fluorescence microscopy (Fig. 7), but no increase in annexin-FITC and PI labeling was observed for any compound (at 25 μ M for 18-24 h) when compared to treatment with acetylsalicylic acid (at 20 mM for 18-24 h), used as a positive control (HOSSAIN *et*

al., 2012). The hepatocytes morphology was also verified: no alterations in normal characteristics of primary hepatocytes, as cubic form, monolayer organization and multinucleation was observed, supporting previous results suggesting that these derivatives slightly or not at all affected hepatocytes viability (Fig. 8).

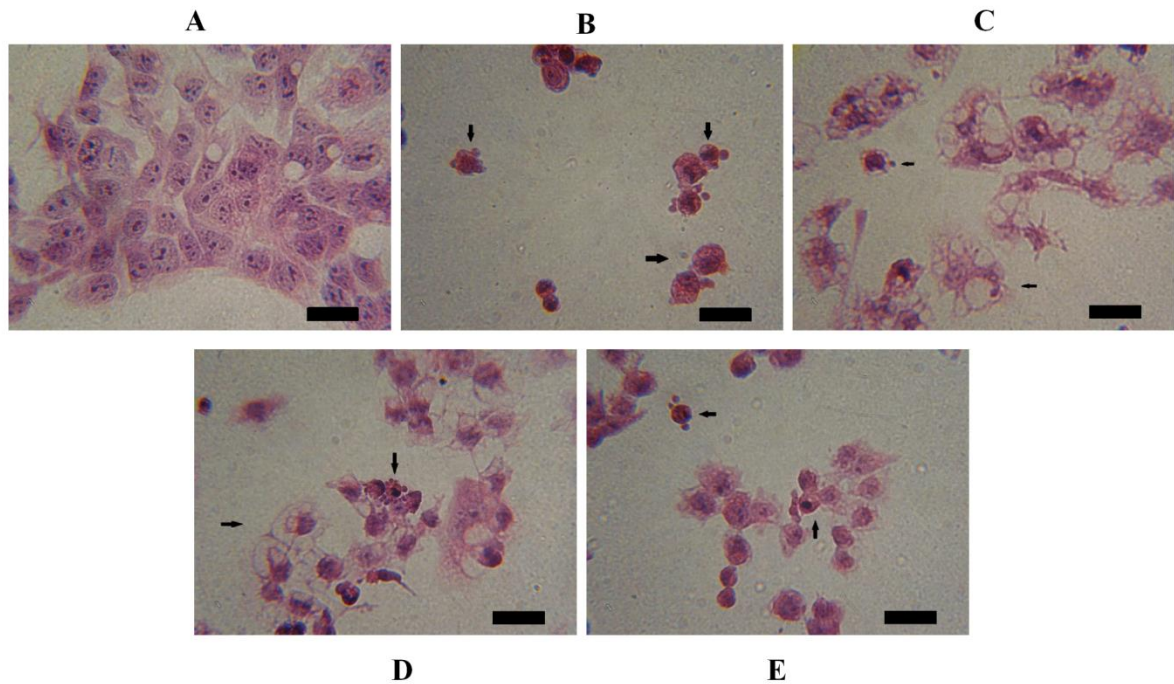


FIGURE 6: EFFECTS OF 1,3,4-THIADIAZOLIUM DERIVATIVES ON HEPG2 CELL MORPHOLOGY

Note: The experimental conditions are described in the Materials and Methods section 4.1.2.6. The cells were seeded with or without 1,3,4-thiadiazolium derivatives at 5 μ M for 3 h. The images were captured with a 100X magnification; they correspond to control (**A**), MI-D (**B**), MI-J (**C**), MI-4F (**D**) and MI-2,4diF (**E**). The scale is indicated by black bars representing 0.02 mm. The arrows show morphological modifications as blebs, increased volume and vacuolization. The photographs represent three different experiments in triplicate.

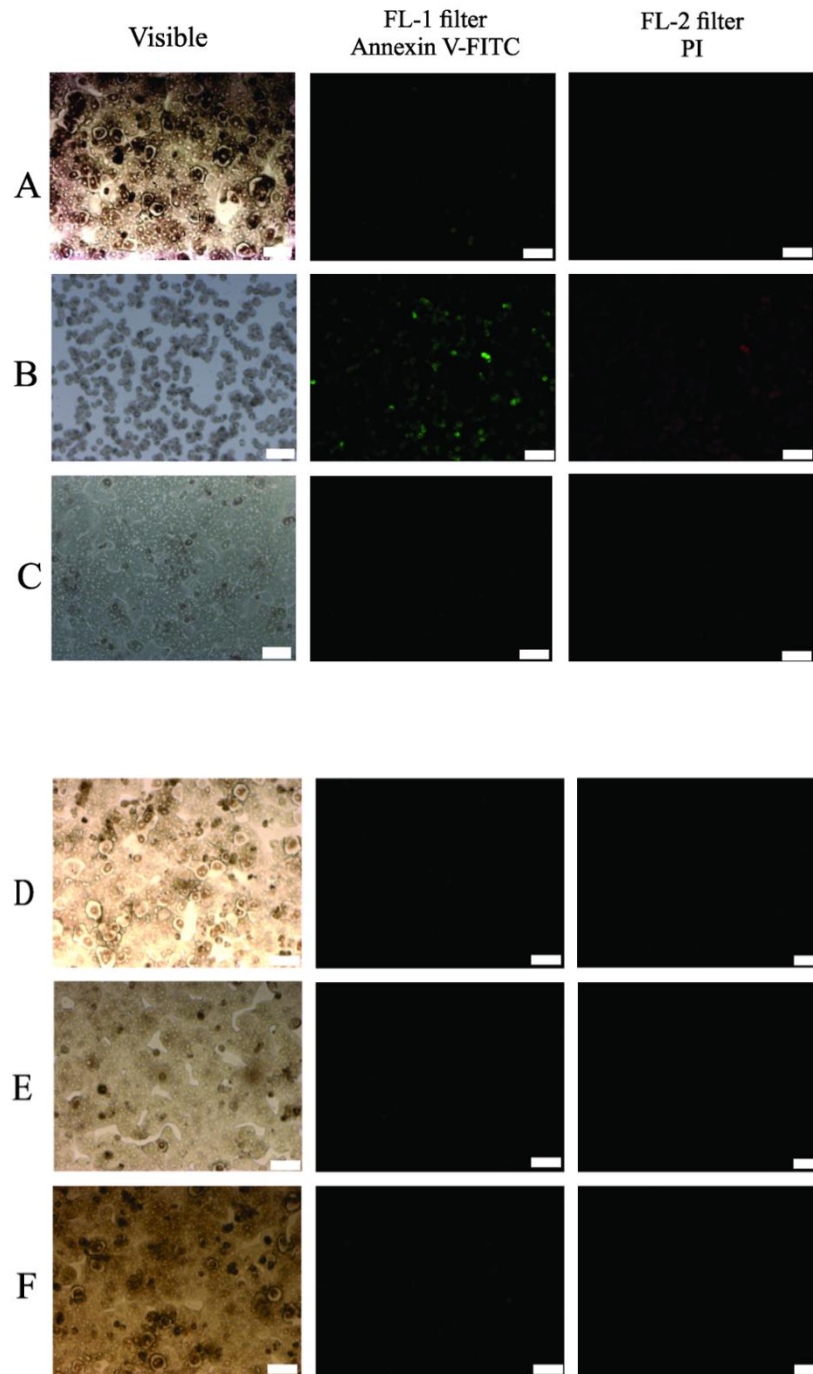


FIGURE 7: ANNEXIN V-FITC AND PROPIDIUM IODIDE STAINING OF HEPATOCYTES TREATED BY 1,3,4-THIADIAZOLIUM DERIVATIVES

Note: The experimental conditions are described in the Materials and Methods section 4.1.2.5-c. Hepatocytes were incubated with derivatives at 25 μ M for 20 h. The images (10X magnification) were captured with an AXIOVERT 40CSFL fluorescence microscope. The scale is indicated by white bars representing 100 μ m. The annexin V-FITC-positive cells are stained in green, and the PI-positive cells in red. The images represent (A) control (untreated cells), (B) ASA positive control at 20 mM, (C) MI-D, (D) MI-J, (E) MI-4F and (F) MI-2,4diF. The figures represent three different experiments in triplicate.

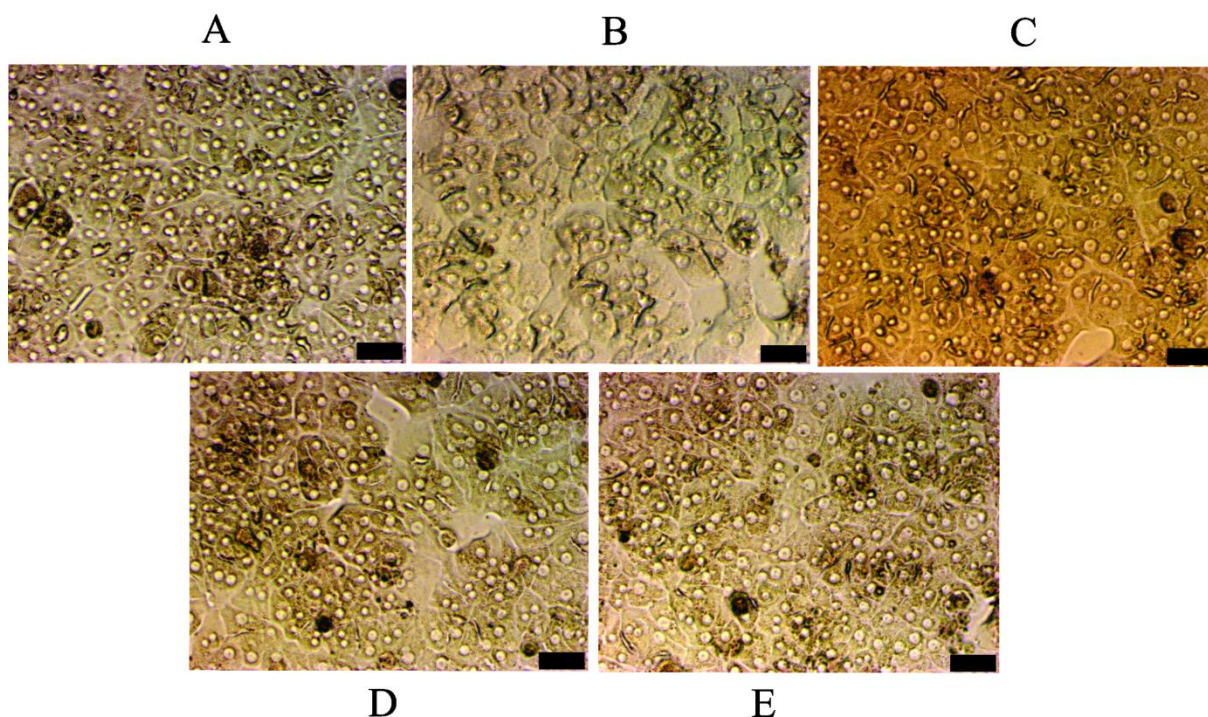


FIGURE 8: EFFECTS OF 1,3,4-THIADIAZOLIUM DERIVATIVES ON HEPATOCYTES MORPHOLOGY

Note: The experimental conditions are described in the Materials and Methods section 4.1.2.6. Hepatocytes were incubated with the derivatives at 25 μ M for 24 h. The images were obtained using inverted microscope. A: control (untreated cells); B-E: treatments by MI-D, MI-J, MI-4F and MI-2,4diF, respectively. The scale is indicated by black bars representing 50 μ m. The photographs represent three different experiments in triplicate.

4.1.3.3 Effects of 1,3,4-thiadiazolium derivatives on multiple drugs resistant (MDR) cells

The effects of 1,3,4-thiadiazolium derivatives were checked on cells overexpressing multidrug ABC transporters, in order to establish their capacity to inhibit the transport of substrate drugs and/or to be transported themselves. Flow cytometry was used to analyze their capacity to induce accumulation of fluorescent substrates. Table 1 shows that, among the different mesoionic derivatives, only MI-J was able to significantly inhibit the Pgp-mediated efflux of rhodamine 123, with 13% inhibition (at 25 μ M upon 30-min incubation) as compared to the control which was fully inhibited by 5 μ M elacridar. The ability of the derivatives to be transported by Pgp was evaluated by the resistance ratio (RR), which was obtained by dividing the IG₅₀ values estimated from survival MTT assays for transfected cells overexpressing the multidrug transporter and its parental, sensitive line, with RR values > 1

suggesting transporter-mediated efflux (HALL *et al.*, 2009). Except for MI-J which was not to be transported by Pgp, with a RR value even <1 , the other derivatives indeed appeared to be transported, with high RR values of 5.2 for MI-2,4diF, and in the range 2.4-2.8 for MI-D and MI-4F.

TABLE 1. EFFECTS OF 1,3,4-THIADIAZOLIUM DERIVATIVES ON MDR CELL PARAMETERS

	Pgp			
	EC ₅₀ (μ M)	%inhibition	^a IG ₅₀ (μ M)	^b IG ₅₀ (μ M)
MI-D	n.d.	1.0	24.9 \pm 5.7	9.0 \pm 0.2
MI-J	n.d.	13.6 \pm 6.3	9.8 \pm 2.0	10.6 \pm 0.5
MI-4F	n.d.	0	3.3 \pm 0.1	1.4 \pm 0.1
MI-2,4diF	n.d.	0.15	5.2 \pm 0.2	1.0 \pm 0.1
	ABCG2			
MI-D	24.3 \pm 9.6	36.7 \pm 14.4	7.0 \pm 0.1	8.9 \pm 1.0
MI-J	8.5 \pm 4.8	21.5 \pm 12.1	7.9 \pm 0.1	6.0 \pm 0.1
MI-4F	n.d.	11.7 \pm 3.9	4.7 \pm 0.2	5.7 \pm 0.3
MI-2,4diF	n.d.	17.7 \pm 12.6	3.3 \pm 0.3	4.6 \pm 0.9
	MRP1			
MI-D	n.d.	8.1 \pm 4.2	9.4 \pm 0.5	7.5 \pm 1.0
MI-J	n.d.	36.2 \pm 24.7	4.9 \pm 0.2	5.8 \pm 0.1
MI-4F	n.d.	10.1 \pm 6.6	6.2 \pm 0.1	6.0 \pm 0.1
MI-2,4diF	n.d.	21.0 \pm 13.1	4.7 \pm 0.5	5.5 \pm 0.5

Note: The experimental conditions are described in the Materials and Methods, sections 4.1.2.5-a and 4.1.2.9. The efficiency of each mesoionic derivative to inhibit the efflux of fluorescent substrates was determined by flow cytometry, relatively to controls (either parental cells, or the same transfected cells fully inhibited with reference inhibitors). The EC₅₀ values (μ M) were determined by using increasing derivatives concentrations, up to 50 μ M, and calculated as derivatives concentrations producing half-maximal inhibition of drug efflux. The IG₅₀ values (μ M) were obtained by MTT assays upon treatment for 72 h with mesoionic derivatives at 0-100 μ M; they were calculated as derivatives concentrations producing half-maximal inhibition of growth. ^aIG₅₀ obtained with resistant transfected cells; ^bIG₅₀ obtained with control, sensitive, cells; *n.d.* not determined.

The same parameters were evaluated for the two other multidrug transporters, ABCG2 and MRP1. All derivatives significantly inhibited the ABCG2-mediated efflux of mitoxantrone: the extent observed at 25 μ M after 30-min incubation was higher with MI-D containing a NO₂ (~ 37%), but the affinity appeared better for MI-J containing a OH (EC₅₀ value of 8.5 μ M *versus* 24.3 μ M). The two fluorinated derivatives (MI-4F and MI-2,4diF) displayed a lower inhibition (11.7-17.7%). No apparent transport by ABCG2 was observed, except for a weak possible

effect of MI-J, with a RR value slightly > 1. No cross resistance at all was observed with MRP1-overexpressing cells, with RR values very close to unity. The different derivatives also inhibited MRP1-mediated drug efflux, using calcein-AM as a substrate, but with different structure-activity relationships when compared to ABCG2 since OH substitution in MI-J was much more efficient than NO₂ in MI-D (36.2% *versus* 8.1% inhibition) while the fluorinated derivatives MI-4F and MI-2,4diF displayed intermediate potency (10-20% inhibition).

4.1.4 Discussion and conclusions

The present work reports a small series of new compounds as promising candidates for future assays of HCC treatment. The different mesoionic derivatives were cytotoxic to HepG2 cells, as demonstrated by MTT assays, with MI-J, MI-4F and MI-2,4diF being the most efficient to reduce their viability whereas MI-D required a 2-fold higher concentration. These results were confirmed by an increase in LDH activity of cell culture supernatants induced by all derivatives, with however some quantitative differences. The survival of non-tumoral hepatocytes in the presence of mesoionic derivatives demonstrated that MI-D, MI-J and MI-4F were not cytotoxic for these cells. By difference, a significant apparent cytotoxicity was observed with MI-2,4diF, in MTT assays, but no increase was produced on LDH activity. The absence of cytotoxicity was further confirmed by the lack of labeling with annexin V or PI, and by morphological analysis. Pires *et al.* (2010) demonstrated that the alterations produced by 1,3,4-thiadiazolium derivatives on mitochondrial bioenergetics were associated with their hydrophobic properties: MI-2,4diF displayed the most pronounced effects, probably due to its high Hansh constant ($\pi = 0,28$) as compared to MI-4F, MI-D and MI-J. Therefore, the significant reduction of non-tumoral cell viability observed with MI-2,4diF in the MTT assay, which is based on the activity of mitochondrial dehydrogenases (TAKAHASHI *et al.*, 2002), might be related to its effects on mitochondrial bioenergetics. Induction of apoptosis by chemotherapeutics is one of the most significant effects related to inhibition of tumor growth (RAYCHAUDHURI, 2010). When HepG2 cells were labeled here with annexin V and PI to monitor such an event, all mesoionic derivatives were indeed able to induce a significant double labeling. Annexin V is known to specifically bind to phosphatidylserine, a lipid which is translocated to the outer leaflet of the cell during

apoptosis and can be identified through FITC fluorescence associated to annexin V (VERMES *et al.*, 1995). PI is impermeable to cell membrane and its binding to DNA is dependent on the increased membrane permeability observed in the late stages of apoptosis or necrosis (RIEGER *et al.*, 2011). The results obtained with mesoionic compounds indicated that they induced a late apoptosis or necrosis in HepG2 cells. In order to better characterize the cytotoxicity pathway promoted, the HepG2 cells were incubated with the mesoionic derivatives, and the morphological analyses in earliest times of incubation indicated apoptosis features. These data were also confirmed by DNA fragmentation assays. Similar morphological alterations on melanoma cells MEL-85 were demonstrated with MI-D treatment (25-50 μ M for 2 h), which also reduced the viability of the cells to ~ 40% at 25 μ M for 24 h (SENFF-RIBEIRO *et al.*, 2004a). In this work, we used primary culture of rat hepatocytes instead human cells due the scarce availability of fresh human liver samples, the logistic and time required by the overall procedure, as well as the high cost related to the procedure. As performed in this work, other studies (CASTANEDA; KINNE, 2000; TIAN *et al.*, 2007; LIU; ZENG, 2009) also have used rat primary hepatocytes in culture as an alternative to verify differential cytotoxicity of antitumoral compounds on human cancer. Nevertheless, the absence of cytotoxicity in rat cells observed in this work must be further confirmed on human cells. For new drugs intended to be used in clinical trials, several absorption, distribution, metabolism, excretion and toxicity assays are required, and the FDA has recommended initial *in vitro* tests to establish the effects of these drug candidates on MDR transporters, which could either promote their efflux or be inhibited by them, thus changing the bioavailability of other drugs used concomitantly (FDA, 2012). We experimentally observed that mesoionic derivatives were not substrates of ABCG2 and MRP1, whereas they might indeed be transported by Pgp (except for MI-J), which could limit their use against resistant tumors overexpressing this efflux pump. This however would not prevent their utilization in nonresistant tumor treatment: for example, the chemotherapeutic agent 5-fluoracil is recognized as a first-choice treatment for nonresistant HCC in advanced stage (UCHIBORI *et al.*, 2012), although displaying a high RR value of 53 on Pgp-overexpressing resistant HepG2 cells (ZHENG *et al.*, 2008). Some drugs with antitumoral and pump-efflux inhibitory activities, as also observed here for most 1,3,4-thiadiazolium derivatives, have indeed given promising results *in vivo*. As an example, the tyrosine kinase inhibitor BIBF120, which has reached phase III clinical

trials of cancers treatments, also demonstrated a capacity to inhibit the ABCG2 transporter; however, the direct correlation between such an inhibition and the success of resistant-tumor treatment was not actually established (XIANG *et al.*, 2011). The weak extent of inhibition by 1,3,4-thiadiazolium derivatives might still represent an advantage, taking into account the reduced probability of bioavailability alterations in polytherapy, and of diminution in the physiological protective role of these efflux pumps (STACY *et al.*, 2013). In conclusion, we showed that the 1,3,4-thiadiazolium derivatives MI-D, MI-J, MI-4F and MI-2,4diF were selectively cytotoxic to HepG2 cells, by promoting cell death with apoptosis characteristics, while not affecting the viability of non-tumoral hepatocytes. Furthermore, the 1,3,4-thiadiazolium derivatives were only slightly, or not at all, transported by resistant cells overexpressing ABCG2 and MRP1, while they even produced inhibition of these transporters. Such mesoionic compounds, especially the hydroxy derivative MI-J, might be considered as promising candidates to HCC treatment, either resistant or not, and should encourage new investigations about their mechanisms of action for future clinical tests.

REFERENCES

- ARCHANA; SRIVASTAVA, V. K.; KUMAR, A. Synthesis of some newer derivatives of substituted quinazolinonyl-2-oxo/thiobarbituric acid as potent anticonvulsant agents. **Bioorg Med Chem**, v. 12, n. 5, p. 1257-64, 2004.
- BALASUBRAMANIYAN, V. et al. Mouse recombinant leptin protects human hepatoma HepG2 against apoptosis, TNF-alpha response and oxidative stress induced by the hepatotoxin-ethanol. **Biochim Biophys Acta**, v. 1770, n. 8, p. 1136-44, 2007.
- BRACHT A., I.-I. E. L. K.-B., A. M. **Métodos de Laboratório em Bioquímica**. São Paulo: Editora Manole, 2003.
- BRADFORD, M. M. A rapid and sensitive method for the quantitation of microgram quantities of protein utilizing the principle of protein-dye binding. **Anal Biochem**, v. 72, p. 248-54, 1976.
- BRITO, A. F. et al. Positron Emission Tomography Diagnostic Imaging in Multidrug-Resistant Hepatocellular Carcinoma: Focus on 2-Deoxy-2-(18F)Fluoro-D-Glucose. **Mol Diagn Ther**, 2014.
- CADENA, S. M. et al. Effect of MI-D, a new mesoionic compound, on energy-linked functions of rat liver mitochondria. **FEBS Lett**, v. 440, n. 1-2, p. 46-50, 1998.
- CADENA, S. M. Interference of MI-D, a new mesoionic compound, on artificial and native membranes. **Cell Biochem Funct**, v. 20, n. 1, p. 31-7, 2002.
- CARVALHO, S. A. et al. Synthesis and antitrypanosomal profile of new functionalized 1,3,4-thiadiazole-2-arylhydrazone derivatives, designed as non-mutagenic megalozin analogues. **Bioorg Med Chem Lett**, v. 14, n. 24, p. 5967-70, 2004.
- CASTANEDA, F.; KINNE, R. K. Cytotoxicity of millimolar concentrations of ethanol on HepG2 human tumor cell line compared to normal rat hepatocytes in vitro. **J Cancer Res Clin Oncol**, v. 126, n. 9, p. 503-10, 2000.
- CHANDRAKANTHA, B. et al. Synthesis and biological evaluation of novel substituted 1,3,4-thiadiazole and 2,6-di aryl substituted imidazo [2,1-b] [1,3,4] thiadiazole derivatives. **Eur J Med Chem**, v. 71, p. 316-23, 2014.
- CHENG, J. W.; LV, Y. New progress of non-surgical treatments for hepatocellular carcinoma. **Med Oncol**, v. 30, n. 1, p. 381, 2013.
- CHEUNG, C. S. et al. Leachianone A as a potential anti-cancer drug by induction of apoptosis in human hepatoma HepG2 cells. **Cancer Lett**, v. 253, n. 2, p. 224-35, 2007.
- COLE, S. P. et al. Overexpression of a transporter gene in a multidrug-resistant human lung cancer cell line. **Science**, v. 258, n. 5088, p. 1650-4, 1992.
- DARZYNKIEWICZ, Z. et al. Features of apoptotic cells measured by flow cytometry. **Cytometry**, v. 13, n. 8, p. 795-808, 1992.

DOUGLAS, R. S. et al. A simplified method for the coordinate examination of apoptosis and surface phenotype of murine lymphocytes. **J Immunol Methods**, v. 188, n. 2, p. 219-28, 1995.

DOYLE, L. A. et al. A multidrug resistance transporter from human MCF-7 breast cancer cells. **Proc Natl Acad Sci U S A**, v. 95, n. 26, p. 15665-70, 1998.

ENDICOTT, J. A.; LING, V. The biochemistry of P-glycoprotein-mediated multidrug resistance. **Annu Rev Biochem**, v. 58, p. 137-71, 1989.

FDA. **Drug Interaction Studies — Study Design, Data Analysis, Implications for Dosing, and Labeling Recommendations** 2012.

GRYNBERG, N.; SANTOS, A. C.; ECHEVARRIA, A. Synthesis and in vivo antitumor activity of new heterocyclic derivatives of the 1,3,4-thiadiazolium-2-aminide class. **Anticancer Drugs**, v. 8, n. 1, p. 88-91, 1997.

HALL, M. D.; HANDLEY, M. D.; GOTTESMAN, M. M. Is resistance useless? Multidrug resistance and collateral sensitivity. **Trends in Pharmacological Sciences**, v. 30, n. 10, p. 546-556, 2009.

HOLOHAN, C. et al. Cancer drug resistance: an evolving paradigm. **Nat Rev Cancer**, v. 13, n. 10, p. 714-26, 2013.

HOSSAIN, M. A. et al. Aspirin induces apoptosis in vitro and inhibits tumor growth of human hepatocellular carcinoma cells in a nude mouse xenograft model. **Int J Oncol**, v. 40, n. 4, p. 1298-304, 2012.

JEMAL, A. et al. Global cancer statistics. **CA Cancer J Clin**, v. 61, n. 2, p. 69-90, 2011.

JUBIE, S. et al. Synthesis, antidepressant and antimicrobial activities of some novel stearic acid analogues. **Eur J Med Chem**, v. 54, p. 931-5, 2012.

KHAN, I. et al. Synthesis, antioxidant activities and urease inhibition of some new 1,2,4-triazole and 1,3,4-thiadiazole derivatives. **Eur J Med Chem**, v. 45, n. 11, p. 5200-7, 2010.

KRATZ, F. et al. Prodrug strategies in anticancer chemotherapy. **ChemMedChem**, v. 3, n. 1, p. 20-53, 2008.

KUMAR, H. et al. 1,3,4-Oxadiazole/thiadiazole and 1,2,4-triazole derivatives of biphenyl-4-yloxy acetic acid: synthesis and preliminary evaluation of biological properties. **Eur J Med Chem**, v. 43, n. 12, p. 2688-98, 2008.

LIU, Z. H.; ZENG, S. Cytotoxicity of ginkgolic acid in HepG2 cells and primary rat hepatocytes. **Toxicol Lett**, v. 187, n. 3, p. 131-6, 2009.

LOONG, H. H.; YEO, W. Microtubule-targeting agents in oncology and therapeutic potential in hepatocellular carcinoma. **Onco Targets Ther**, v. 7, p. 575-585, 2014.

MARTINEZ, L. et al. Understanding polyspecificity within the substrate-binding cavity of the human multidrug resistance P-glycoprotein. **FEBS J**, v. 281, n. 3, p. 673-82, 2014.

NOGUCHI, K.; KATAYAMA, K.; SUGIMOTO, Y. Human ABC transporter ABCG2/BCRP expression in chemoresistance: basic and clinical perspectives for molecular cancer therapeutics. **Pharmgenomics Pers Med**, v. 7, p. 53-64, 2014.

ORRENIUS, S.; NICOTERA, P.; ZHIVOTOVSKY, B. Cell death mechanisms and their implications in toxicology. **Toxicol Sci**, v. 119, n. 1, p. 3-19, 2011.

PADHYA, K. T.; MARRERO, J. A.; SINGAL, A. G. Recent advances in the treatment of hepatocellular carcinoma. **Curr Opin Gastroenterol**, v. 29, n. 3, p. 285-92, 2013.

PHILIPS, H. J., Ed. **Dye exclusion test for cell viability** Tissue culture methods and applications. New York: Academic Press, p.406-408, Tissue culture methods and applicationsed. 1973.

PIRES, A. R. et al. Comparative study of the effects of 1,3,4-thiadiazolium mesoionic derivatives on energy-linked functions of rat liver mitochondria. **Chem Biol Interact**, v. 186, n. 1, p. 1-8, 2010.

PIRES, A. R. et al. Interaction of 1,3,4-thiadiazolium mesoionic derivatives with mitochondrial membrane and scavenging activity: Involvement of their effects on mitochondrial energy-linked functions. **Chem Biol Interact**, v. 189, n. 1-2, p. 17-25, 2011.

RAYCHAUDHURI, S. How can we kill cancer cells: Insights from the computational models of apoptosis. **World J Clin Oncol**, v. 1, n. 1, p. 24-8, 2010.

RAZA, H.; JOHN, A.; BENEDICT, S. Acetylsalicylic acid-induced oxidative stress, cell cycle arrest, apoptosis and mitochondrial dysfunction in human hepatoma HepG2 cells. **Eur J Pharmacol**, v. 668, n. 1-2, p. 15-24, 2011.

REATAZA, M.; IMAGAWA, D. K. Advances in managing hepatocellular carcinoma. **Front Med**, 2014.

REILLY, T. P. et al. Comparison of the in vitro cytotoxicity of hydroxylamine metabolites of sulfamethoxazole and dapsone. **Biochem Pharmacol**, v. 55, n. 6, p. 803-10, 1998.

RIEGER, A. M. et al. Modified annexin V/propidium iodide apoptosis assay for accurate assessment of cell death. **J Vis Exp**, v. 24, n. 50, p. 2597, 2011.

SEGLEN, P. O. Preparation of isolated rat liver cells. **Methods Cell Biol**, v. 13, p. 29-83, 1976.

SEFF-RIBEIRO, A. et al. Cytotoxic effect of a new 1,3,4-thiadiazolium mesoionic compound (MI-D) on cell lines of human melanoma. **Br J Cancer**, v. 91, n. 2, p. 297-304, 2004a.

SEFF-RIBEIRO, A. et al. Effect of a new 1,3,4-thiadiazolium mesoionic compound (MI-D) on B16-F10 murine melanoma. **Melanoma Res**, v. 13, n. 5, p. 465-71, 2003.

SEFF-RIBEIRO, A. et al. Antimelanoma activity of 1,3,4-thiadiazolium mesoionics: a structure-activity relationship study. **Anticancer Drugs**, v. 15, n. 3, p. 269-75, 2004b.

SEO, S. et al. Fluorine-18 fluorodeoxyglucose positron emission tomography predicts tumor differentiation, P-glycoprotein expression, and outcome after resection in hepatocellular carcinoma. **Clin Cancer Res**, v. 13, n. 2 Pt 1, p. 427-33, 2007.

SHI, J. et al. A review on the diagnosis and treatment of hepatocellular carcinoma with a focus on the role of wnts and the dickkopf family of wnt inhibitors. **Journal of Hepatocellular Carcinoma**, v. 1, p. 7, 2014.

SOUZA DOS SANTOS, A. C.; ECHEVARRIA, A. Electronic effects on ¹³C NMR chemical shifts of substituted 1,3,4-thiadiazolium salts. **Magnetic Resonance in Chemistry**, v. 39, n. 4, p. 182-186, 2001.

STACY, A. E.; JANSSON, P. J.; RICHARDSON, D. R. Molecular pharmacology of ABCG2 and its role in chemoresistance. **Mol Pharmacol**, v. 84, n. 5, p. 655-69, 2013.

SUKOWATI, C. H. et al. Gene and functional up-regulation of the BCRP/ABCG2 transporter in hepatocellular carcinoma. **BMC Gastroenterol**, v. 12, p. 160, 2012.

TAKAHASHI, S. et al. Substrate-dependence of reduction of MTT: a tetrazolium dye differs in cultured astroglia and neurons. **Neurochem Int**, v. 40, n. 5, p. 441-8, 2002.

TIAN, Z. et al. Antitumor activity and mechanisms of action of total glycosides from aerial part of *Cimicifuga dahurica* targeted against hepatoma. **BMC Cancer**, v. 7, p. 237, 2007.

UCHIBORI, K. et al. Establishment and characterization of two 5-fluorouracil-resistant hepatocellular carcinoma cell lines. **Int J Oncol**, v. 40, n. 4, p. 1005-10, 2012.

UHL, P. et al. Current status in the therapy of liver diseases. **Int J Mol Sci**, v. 15, n. 5, p. 7500-12, 2014.

VALDAMERI, G. et al. Substituted Chromones as Highly Potent Nontoxic Inhibitors, Specific for the Breast Cancer Resistance Protein. **Journal of Medicinal Chemistry**, v. 55, n. 2, p. 966-970, 2012.

VANDER BORGHT, S. et al. Expression of multidrug resistance-associated protein 1 in hepatocellular carcinoma is associated with a more aggressive tumour phenotype and may reflect a progenitor cell origin. **Liver Int**, v. 28, n. 10, p. 1370-80, 2008.

VERMES, I. et al. A novel assay for apoptosis. Flow cytometric detection of phosphatidylserine expression on early apoptotic cells using fluorescein labelled Annexin V. **J Immunol Methods**, v. 184, n. 1, p. 39-51, 1995.

WU, X. et al. Selective Protection of Normal Cells During Chemotherapy by RY4 Peptides. **Mol Cancer Res**, 2014.

XIANG, Q. F. et al. Effect of BIBF 1120 on reversal of ABCB1-mediated multidrug resistance. **Cell Oncol (Dordr)**, v. 34, n. 1, p. 33-44, 2011.

XIAOHE, Z. et al. Synthesis, biological evaluation and molecular modeling studies of N-aryl-2-arylthioacetamides as non-nucleoside HIV-1 reverse transcriptase inhibitors. **Chem Biol Drug Des**, v. 76, n. 4, p. 330-9, 2010.

ZHENG, L. H. et al. Cantharidin reverses multidrug resistance of human hepatoma HepG2/ADM cells via down-regulation of P-glycoprotein expression. **Cancer Lett**, v. 272, n. 1, p. 102-9, 2008.

4.2 ARTIGO 2- Publicado em Journal of Medicinal Chemistry, volume 58, número 1, p. 265-277. Outubro, 2014 (doi: 10.1021/jm500943z). Copyright 2014 American Chemical Society.

“Reprinted (adapted) with permission from Gustavo Jabor Gozzi, Zouhair Bouaziz, Evelyn Winter, Nathalia Daflon-Yunes, Dagmar Aichele, Abdelhamid Nacereddine, Christelle Marminon, Glaucio Valdameri, Waël Zeinyeh, Andre Bollacke, Jean Guillon, Aline Lacoudre, Noël Pinaud, Silvia M. Cadena, Joachim Jose, Marc Le Borgne, and Attilio Di Pietro. Converting Potent Indeno[1,2-*b*]indole Inhibitors of Protein Kinase CK2 into Selective Inhibitors of the Breast Cancer Resistance Protein ABCG2. 2015 Jan 8;58(1):265-77. 2015 (doi: 10.1021/jm500943z). Epub 2014 Oct 16. Copyright 2014 American Chemical Society”.

Link: <http://pubs.acs.org/doi/abs/10.1021/jm500943z>

Converting Potent Indeno[1,2-*b*]indole Inhibitors of Protein Kinase CK2 into Selective Inhibitors of the Breast Cancer Resistance Protein ABCG2

Gustavo Jabor Gozzi,^{†, ‡, ∇} Zouhair Bouaziz,^{§, ∇} Evelyn Winter,^{†, ||} Nathalia Daflon-Yunes,[†] Dagmar Aichele,[⊥] Abdelhamid Nacereddine,[§] Christelle Marminon,[§] Glaucio Valdameri^{†, ‡}, Waël Zeinyeh,[§] Andre Bollacke,[⊥] Jean Guillon,[#] Aline Lacoudre,[▲] Noël Pinaud,[▲] Silvia M. Cadena,[‡] Joachim Jose,[⊥] Marc Le Borgne,^{§, ○} and Attilio Di Pietro^{†, ○, *}

[†]Equipe Labellisée Ligue 2014, BMSSI UMR 5086 CNRS/Université Lyon 1, IBCP, 69367 Lyon, France

[‡]Department of Biochemistry and Molecular Biology, Federal University of Paraná, Curitiba, Paraná, Brazil

[§]Université de Lyon, Université Lyon 1, Faculté de Pharmacie - ISPB, EA 4446 Biomolécules Cancer et Chimiorésistances, SFR Santé Lyon-Est CNRS UMS3453 - INSERM US7, 8 avenue Rockefeller, F-69373, Lyon Cedex 8, France

^{||}Department of Pharmaceutical Sciences, PGFAR, Federal University of Santa Catarina, Florianopolis, Santa Catarina, Brazil

[⊥] Institute of Pharmaceutical and Medicinal Chemistry, PharmaCampus, Westfälische Wilhelms-University Münster, Corrensstr. 48, 48149 Münster, Germany

[#]Université de Bordeaux, UFR des Sciences Pharmaceutiques, INSERM U869, Laboratoire ARNA, 146 rue Léo Saignat, F-33076 Bordeaux Cedex, France

[▲]ISM - CNRS UMR 5255, Université de Bordeaux, 351 cours de la Libération, F-33405 Talence cedex, France

Author Contributions

[∇]Both researchers equally contributed to the experiments.

[○]Both senior investigators equally contributed to work supervision.

ABSTRACT

A series of indeno[1,2-*b*]indole-9,10-dione derivatives were synthesized as human casein kinase II (CK2) inhibitors. The most potent inhibitors contained a *N*⁶-isopropyl substituent on C-ring. The same series of compounds was found to also inhibit the breast cancer resistance protein ABCG2 but with totally different structure-activity relationships: a *N*⁶-phenethyl substituent was critical, and additional hydrophobic substituents at position 7 or 8 of D-ring or a methoxy at phenethyl position *ortho* or *meta* also contributed to inhibition. The best ABCG2 inhibitors, such as **4c**, **4h**, **4i**, **4j** and **4k**, behaved as very weak inhibitors of CK2, whereas the most potent CK2 inhibitors, such as **4a**, **4p** and **4e**, displayed limited interaction with ABCG2. It was therefore possible to convert, through suited substitutions of the indeno[1,2-*b*]indole-9,10-dione scaffold, potent CK2 inhibitors into selective ABCG2 inhibitors and *vice versa*. In addition, some of the best ABCG2 inhibitors, which displayed a very low cytotoxicity, thus giving a high therapeutic ratio, and appeared not to be transported, constitute promising candidates for further investigations.

4.2.1 Introduction

Human protein kinase casein kinase II (CK2) is a highly pleiotropic serine/threonine protein kinase discovered in 1954.¹ Overexpression of CK2 and its elevated activity are closely related to many human cancers, including breast,² lung,³ pancreas,⁴ and prostate.⁵ Recent studies also confirmed CK2 as a key target in leukemia,⁶ and glioblastoma.⁷ One of the most remarkable features of CK2 is the existence of several forms: (i) catalytic CK2 α subunit and its isoforms CK2 α' and CK2 α'' , (ii) regulatory CK2 β subunit, and (iii) heterotetramer composed of two catalytic subunits and two regulatory subunits.⁸ Both CK2 heterotetrameric holoenzyme and its isolated catalytic subunits are constitutively active. Recent structural insights of CK2 α , CK2 β and CK2 (quaternary structure of CK2) gave further knowledge to perform tailor-made compounds.⁹⁻¹¹ Thus CK2 is becoming an important drug target for the 21st century as mentioned by E.G. Krebs in 1999.¹² Intensive drug discovery chemistry is currently leading to design and synthesis of small molecule CK2 inhibitors targeting ATP-binding pocket or *exosites* at the CK2 α /CK2 β interface.¹³ For example we developed diverse indeno[1,2-*b*]indole- and pyrrolo[1,2-*a*]quinoxaline-based scaffolds^{14,15} as ATP-competitive inhibitors of CK2. Tetracyclic indeno[1,2-*b*]indole derivatives offer great opportunities to functionalize A-, C-, and/or D-rings and so access inhibitors with submicromolar IC₅₀ and antiproliferative activity against cancer cell lines.¹⁶

Protein kinase inhibitors were previously shown to interact with multidrug ABC transporters involved in cancer cells resistance to chemotherapy. Protein kinase C inhibitors were able to inhibit P-glycoprotein/ABCB1 and homologs from yeast and protozoan parasites.¹⁷ A number of tyrosine kinase inhibitors were found to strongly inhibit the breast cancer resistance protein ABCG2: canertinib (CI1033),¹⁸ imatinib,¹⁹ gefitinib,²⁰ N-[4-[(3-bromophenyl)amino]-6-quinazolinyl]-2-butyramide (EKI-785),²¹ nilotinib and dasatinib,²² vandetinib, pelitinib and neratinib,²³ erlotinib,²⁴ sorafenib,²⁵ sunitinib²⁶ and linsitinib.²⁷ Bisindolylmaleimides and indolocarbazoles²⁸ as well as dimethoxyaurones²⁹, which inhibit various serine/threonine kinases, were also found to inhibit ABCG2.

ABCG2 is overexpressed in many types of tumors,³⁰ and is recognized to play a role in their multidrug resistance by catalyzing the efflux of anticancer drugs. Potent, selective and nontoxic inhibitors might constitute a good therapeutic strategy to improve anticancer drugs efficiency by increasing their bioavailability, and then sensitize tumor growth to their cytotoxicity.^{31,32} New inhibitors should therefore be investigated. Our aim was to check the capacity of the newly-synthesized indenoindole inhibitors of CK2 to interact with ABCG2 and inhibit its drug-efflux activity. It is shown that they indeed inhibit ABCG2-mediated mitoxantrone transport but importantly the structure-activity relationships are totally different from those governing CK2 inhibition.

4.2.2 Chemistry

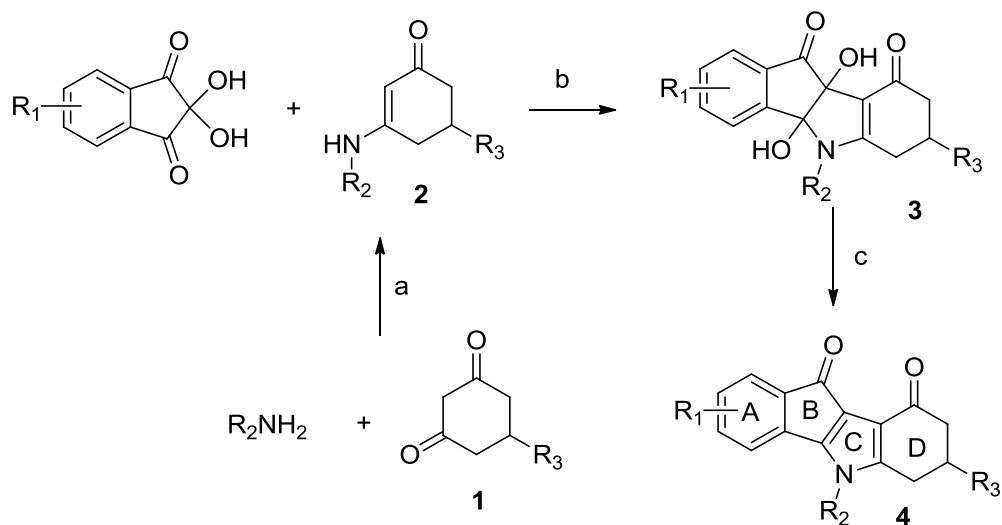
Tetrahydroindeno[1,2-*b*]indole-9,10-diones **4** were synthesized according to a previously reported method,^{14,33} with a modification of the reagent for the deoxygenation of the *vic*-dihydroxyindeno[1,2-*b*]indole-9,10-diones **3**. Usually transition from **3** to **4** is performed with tetramethylthionylamide (TMTA), nevertheless we observed better yields with the tetraethylthionylamide (TETA).³⁴ The latter was prepared by slowly addition of thionyl chloride to 4 equivalents of diethylamine in dry ether at – 40 °C.

The synthetic route started with the preparation of the corresponding enamines **2**, readily available in very good yields by reacting substituted cyclohexane-1,3-diones **1** with primary amines. Subsequent condensation of **2** with 2,2-dihydroxyindane-1,3-diones (ninhydrins) afforded dihydroxyindeno[1,2-*b*]indole-

9,10-diones **3** (Scheme 1).

This protocol provided a useful way to modify the substituents R_1 , R_2 and R_3 in order to establish structure-activity relationships (CK2 inhibition, ABCG2 inhibition, and cytotoxicity). Structural variations on the A-, C- and/or D-ring of the indeno[1,2-*b*]indole scaffold have been carried out thanks to ninhydrins, primary amines and cyclohexane-1,3-diones, respectively.

Scheme 1^a



^aReagents and conditions: (a) Toluene, reflux; (b) MeOH, rt; (c) $(NEt_2)_2SO$ (TETA), DMF, AcOH, rt.

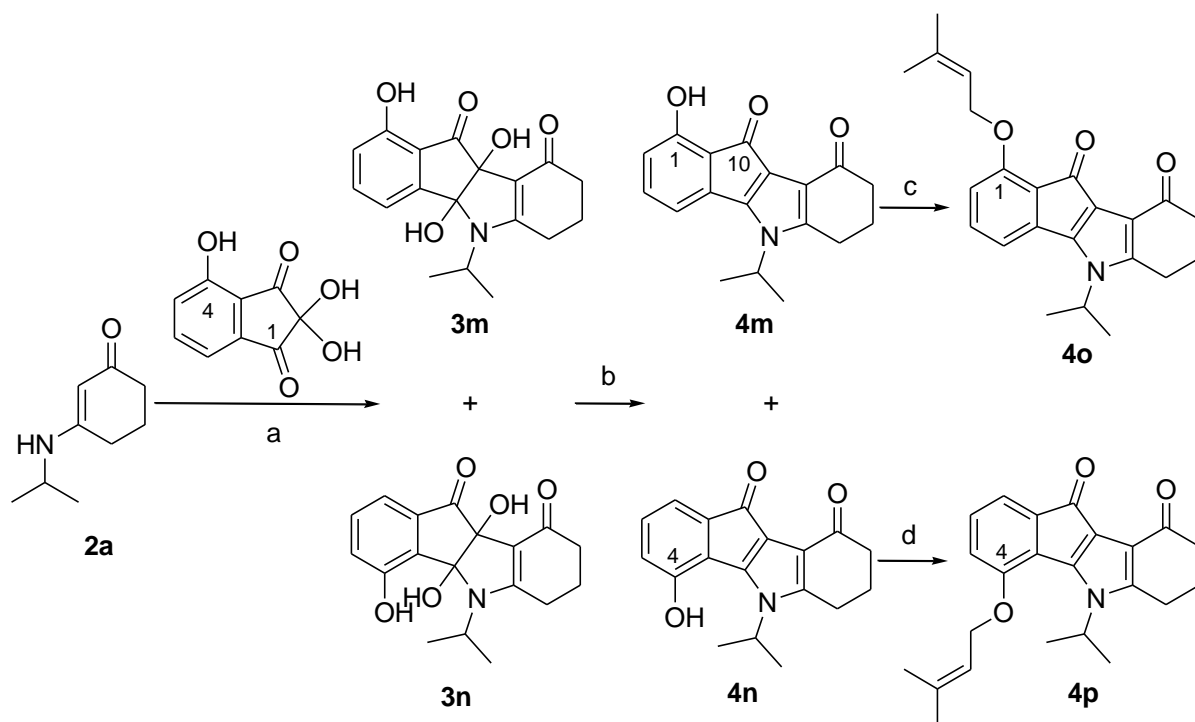
The 1- and 4-hydroxylated indenoindoles **4m** and **4n** (Scheme 2) were prepared from enaminone **2a** and 4-hydroxyninhydrin. The latter was readily prepared in two steps. Firstly, the commercially available dihydrocoumarin reacted with $AlCl_3$ to afford the 4-hydroxyindan-1-one³⁵ which was then oxidized with SeO_2 in dioxane under microwave irradiation (unpublished data).

Condensation of 4-hydroxyninhydrin with enaminon **2a** led to the trihydroxylated derivatives **3m** and **3n** as a mixture of two regioisomers (ratio **3m/3n**: 78/22) which could not be separated under the classical conditions. Deoxygenation procedure of the mixture using TETA was carried out to afford the corresponding hydroxyindenoindoles **4m** and **4n**. At this step, the two regioisomers were easily separated by chromatography column and identified by NMR.

O-Prenylation of the 4-hydroxy derivative **4n** was performed with prenyl bromide in presence of K_2CO_3 in acetone at reflux to provide derivative **4p** with 60%

yield. The reaction with the isomer **4m** was more difficult, probably due to a hydrogen bond between the H of the phenol on the C-1 and the O of ketone C-10 that forms a pseudo 6-membered ring more stable, so more difficult to break. Therefore, O-prenylation of the 1-hydroxy derivative **4m** was carried out by means of K_2CO_3 in dimethylacetamide (DMA) at 80 °C to provide derivative **4o** with 27% yield.

Scheme 2^a

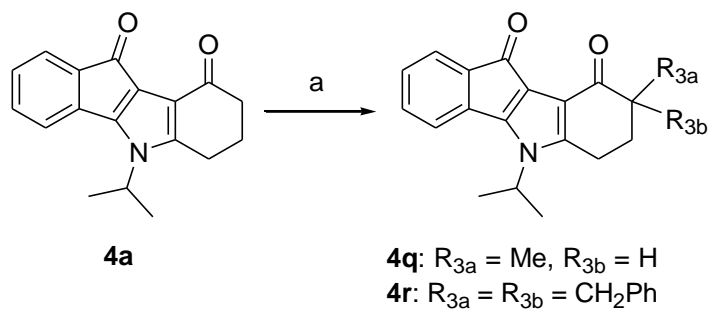


^aReagents and conditions: (a) MeOH, rt; (b) $(NEt_2)_2SO$ (TETA), DMF, AcOH, rt; (c) K_2CO_3 , DMA, 80°C, 24h; (d) K_2CO_3 , acetone, reflux, 8h.

Assignment of regiochemistry was established for each regioisomer by NOESY. Compounds **4q** and **4r** were obtained by alkylation of 5,6,7,8-tetrahydroindeno[1,2-*b*]indole-9,10-dione **4a** with CH_3I and $PhCH_2Br$, respectively, in the presence of a solution of lithium cyclohexylisopropylamide (LCIA)³⁶ prepared from cyclohexylisopropylamine and *n*-BuLi in dry THF at -40 °C (Scheme 3). Attempts to improve the yield of these alkylations by modification of the reaction conditions (nature and amount of the base, amount of the alkylating agent, temperature) proved to be unsuccessful. Moreover, methylation provided the monomethylated compound **4q** with 10% yield and only traces of the dimethylated derivative when benzylation afforded only the disubstituted compound **4r** with 35% yield, the monobenzylated product was not detected. In either case, a large amount

of degradation products was observed.

Scheme 3^a



^aReagents and conditions: (a) Cyclohexylisopropylamine, *n*-BuLi, THF, CH₃I or PhCH₂Br, -40 °C.

All together, 18 indeno[1,2-*b*]indole-9,10-dione derivatives have been synthesized, and their different substituents are shown in Figure 1.

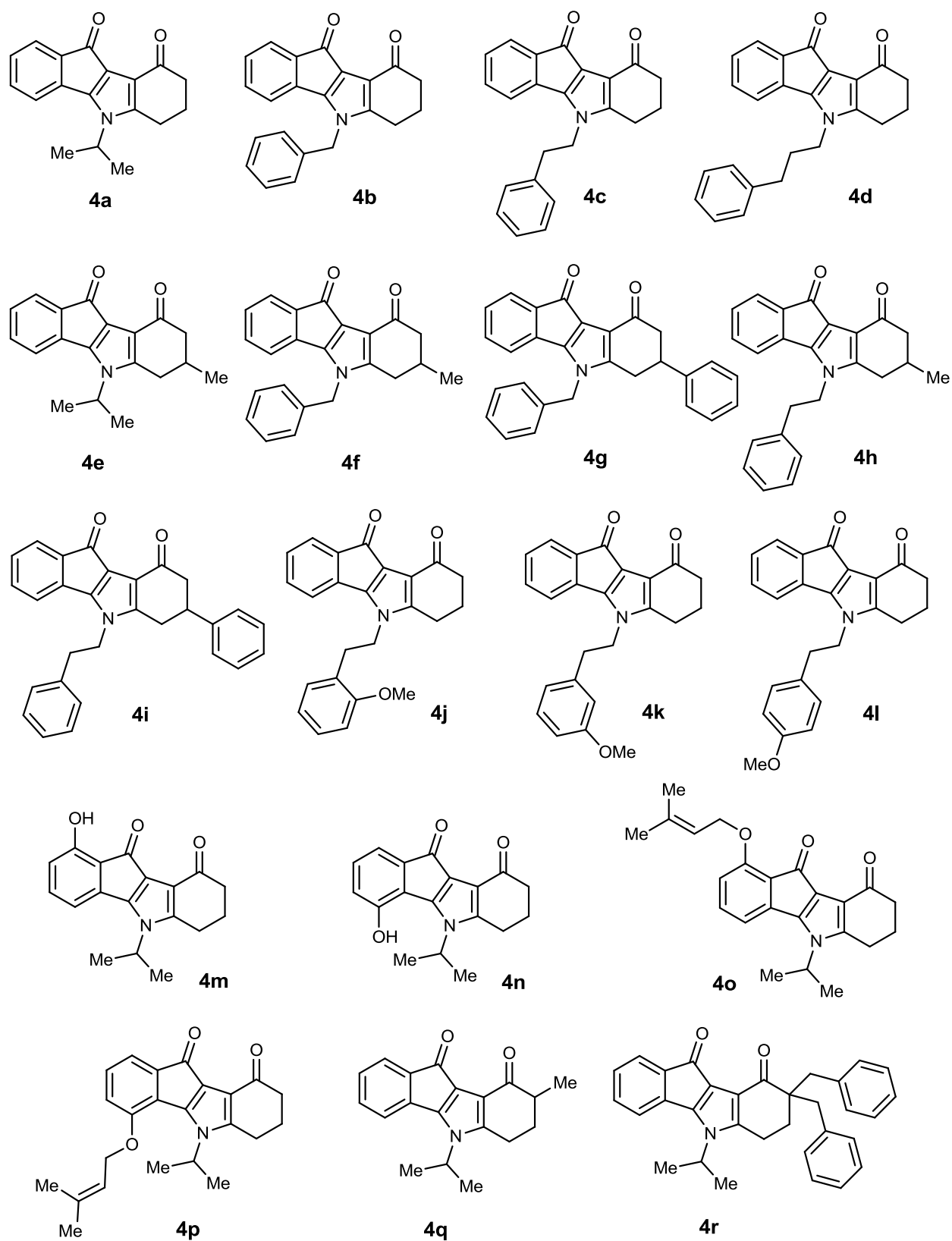


FIGURE 1: SUBSTITUTION PATTERNS OF 4a-r.

Note: compounds **4a-d** and **4f-h** are described in reference 33, and compound **4e** in reference 37.

The 3D structure of **4c** was determined by X-ray crystallography (Figure 2) and confirmed that expected on the basis of IR and ^1H NMR data. The key bond lengths and angles of this indeno[1,2-*b*]indole-9,10-dione **4c** are very similar to those given in the literature for other substituted indenoindole derivatives.^{38,39} The 7,8-dihydro-6*H*-indeno[1,2-*b*]indole-9,10-dione system of **4c** is not planar; a derivation of the C12 and C13 atoms was noticed at 0.1935 (3) Å and 0.4429 (3) Å, respectively, from the plane defined by the heterotetracyclic system. The non-planarity of this tetracyclic system is an important structural characteristic in contrast to planar polycyclic aromatic compounds. The double bonds C1=O1 and C11=O2 of the heterocyclic system of **4c** are confirmed by their respective lengths of 1.218 (3) and 1.221 (3) Å.

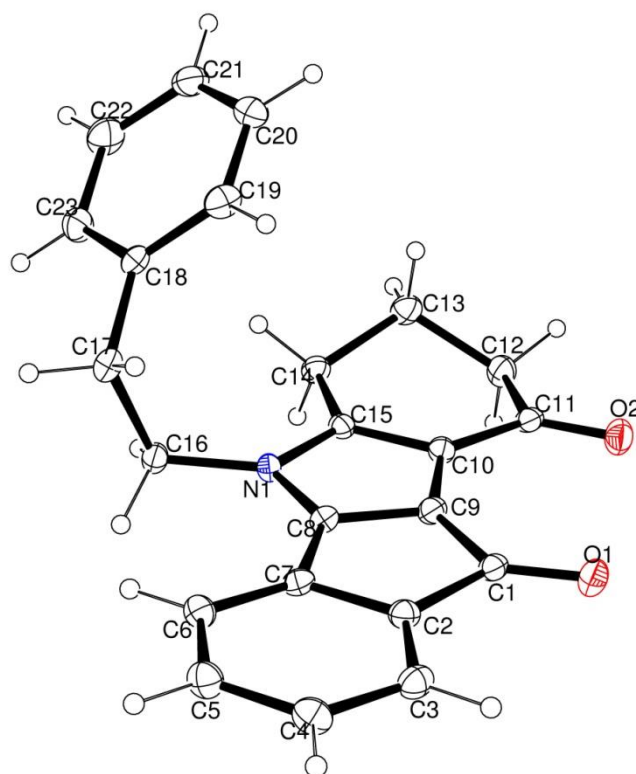


FIGURE 2. VIEW OF THE CRYSTAL STRUCTURE OF **4c** WITH OUR NUMBERING SCHEME, DISPLACEMENT ELLIPSOIDS ARE DRAWN AT THE 30% PROBABILITY LEVEL

Note: the numbering used here is specific to the crystallographic studies, and therefore different from that shown in Table 1 and used all along the text.

4.2.3 Biological evaluation, SARs and discussion

The synthesized indeno[1,2-*b*]indoles were screened for their inhibition capacity, firstly against protein kinase CK2, and then against ABCG2, as summarized here below.

4.2.3.1 Inhibition of human CK2 holoenzyme

Comparison of the results in Table 1 allowed us to draw the following structure-activity relationships: i) compound **4a**, with a *N*⁶-isopropyl-substituted C-ring, produced a complete inhibition at 10 μ M, with a good potency ($IC_{50} = 0.36 \mu$ M); ii) a 14-fold increased potency was observed with **4p** substituted at position 4 of A-ring with *O*-3,3-dimethylallyl ("prenyl"), which was higher than most of the reference inhibitors and approached the extremely potent silmitasertib (CX-4945⁴⁰); by contrast, the same prenyl substituent at position 1 in **4o** dramatically altered the inhibition capacity to 44% at 10 μ M; iii) a 2-fold increased potency was produced by a methyl substituent at position 7 of D-ring in **4e** ($IC_{50} = 0.17 \mu$ M), whereas a strong negative effect was observed at vicinal position 8 with either the same substitution in **4q** or a very hydrophobic and steric substitution by two benzyl groups in **4r** ($IC_{50} \geq 9.2 \mu$ M); iv) replacing the *N*⁶-isopropyl by either a benzyl in **4b**, a phenethyl in **4c** or a phenpropyl in **4d** produced a marked alteration of inhibition (≥ 17 fold) by comparison to **4a**; a partial recovery in potency was produced when substituting with a methoxy the phenethyl at position *ortho* in **4j**, by 5.6-fold relatively to **4c**, while the effects were lower at either position *para* in **4i** or *meta* in **4k**; v) finally, a negative contribution of phenyl substitution at position 7 was observed when comparing **4g** to **4b**, and **4i** to **4c**. The concentration dependence of the inhibition of CK2 activity is illustrated in Figure 3 for the three best indenoindole inhibitors and the most potent reference inhibitor.

TABLE 1. INHIBITION OF HUMAN CK2 HOLOENZYME

Indenoindoles	CK2 inhibition	
	% at 10 μM^a	IC ₅₀ (μM)
4a	99	0.36 ^b
4b	34	(~15) ^c
4c	59	7.0 ^b
4d	62	6.0 ^b
4e	94	0.17 ^b
4f	16	(~35) ^c
4g	9	(~55) ^c
4h	66	2.5 ^b
4i	35	(~15) ^c
4j	87	1.4 ^b
4k	63	5.1 ^b
4l	69	4.1 ^b
4o	44	(~12) ^c
4p	100	0.025 ^b
4q	52	9.2 ^b
4r	48	(~11) ^c
Reference inhibitors		
Silmitasertib ^d	100	0.0037 ^b
Ellagic acid	95	0.04 ^b
TBB ^e	99	0.06 ^b
Emodin	99	0.58 ^b

^aThe percent inhibition of CK2 activity was determined for each compound at a fixed concentration of 10 μM . ^bFor the best compounds producing at least 50% inhibition at 10 μM , the concentration was varied to precisely determine the IC₅₀ values. ^cFor the other, less potent compounds, a rough estimation was obtained from the experimental inhibition produced at 10 μM . ^dSilmitasertib = 5-[(3-chlorophenyl)amino]benzo[c][2,6] naphthyridine-8-carboxylic acid. ^eTBB = 4,5,6,7-tetrabromobenzotriazole.

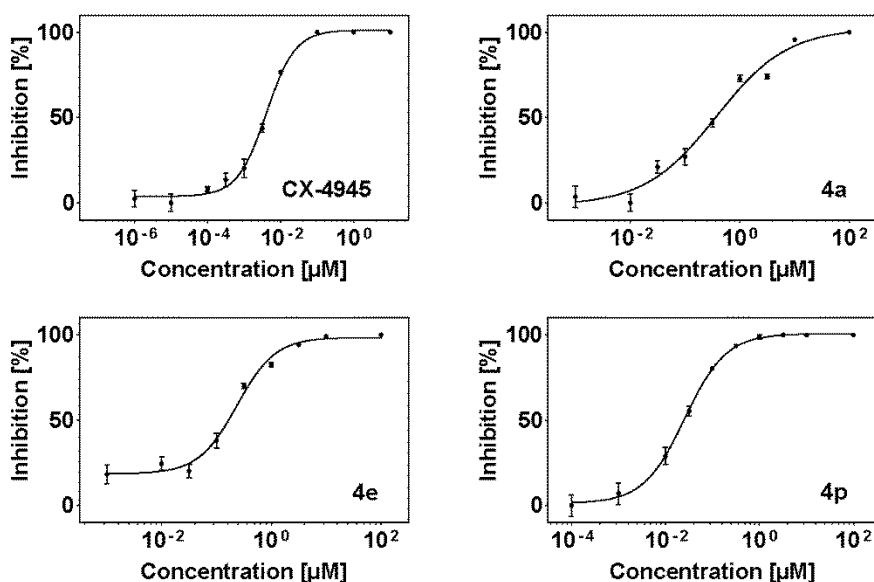


FIGURE 3: CONCENTRATION DEPENDENCE FOR THE MOST POTENT INHIBITORS OF CK2 ACTIVITY

4.2.3.2 Inhibition of MCF-7 cell proliferation by the CK2 inhibitor 4p

The antiproliferative effect of prenyl-substituted indeno[1,2-*b*]indole **4p**, which appeared to be the most potent CK2 inhibitor with an IC_{50} value of 25 nM, was evaluated in MCF-7 breast cancer cells.⁴¹ For this purpose, a commercially-available EdU-click assay was applied, resulting in the incorporation of a TAMRA fluorophore into the nucleic acid of cells performing DNA replication and preparing cell proliferation.⁴² Proliferating cells can be recognized by a violet fluorescence of their nuclei (Figure 4B), and the number of such cells are counted with and without inhibitor and set into relation of the corresponding number of control cells.

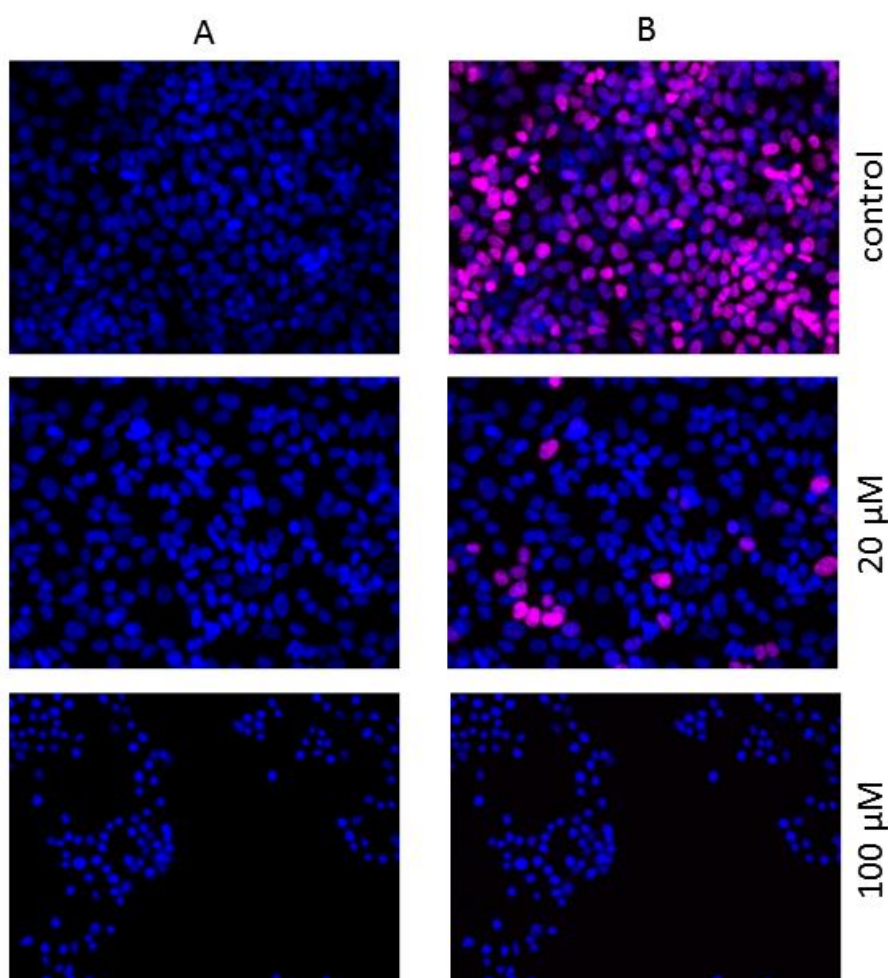


FIGURE 4: FLUORESCENCE IMAGES OF MCF-7 CELLS TREATED WITH DIFFERENT CONCENTRATIONS OF THE INHIBITOR 4p FOR 24 H.

Note: Cell nuclei were double-stained by **1** (blue fluorescence), able to cross the membrane of all cells, and by EdU-assay using 5-TAMRA-PEG3-azide as a coupled fluorophore (violet fluorescence). Cell proliferation was monitored by EdU-assay. **Panel A**: Hoechst-staining of treated MCF-7 cells. **Panel B**: Overlay of the fluorescence images of **1** stained cells and TAMRA-labeled proliferating cells. The cells which are emitting only blue fluorescence are not proliferating, in contrast to those emitting an additional violet fluorescence.

As shown in Figure 5, incubation of MCF-7 cells with 20 μM **4p** for 24 h resulted in a dramatic reduction of the proliferation rate. Only 14% of the cells were still able to synthesize DNA, a ratio that was further decreased after 48 h to 1.3 % (not shown here). When **4p** was used at 100 μM , cell proliferation was completely inhibited even after 24-h exposure. Staining of MCF-7 cells with **1** (Hoechst 33258)⁴³ indicated that the cells were markedly damaged after treatment with **4p** (Figure 4A). Already at 24 h of treatment, the entire number of MCF-7 cells underwent cell death and the total number of detectable cells was strongly reduced, down to 10%. The remaining cells showed characteristic features of apoptosis, such as reduction of nuclear size and condensation of chromatin (Figure 4A). In contrast, **1** staining did not indicate any sign of apoptosis after treatment with 20 μM **4p**. The nuclear morphology of cells under these conditions was similar to DMSO-treated control cells. This clearly indicated that the prenyl-substituted indeno[1,2-*b*]indole **4p** has a distinct antiproliferative effect at 20 μM concentration against MCF-7 breast cancer cells.

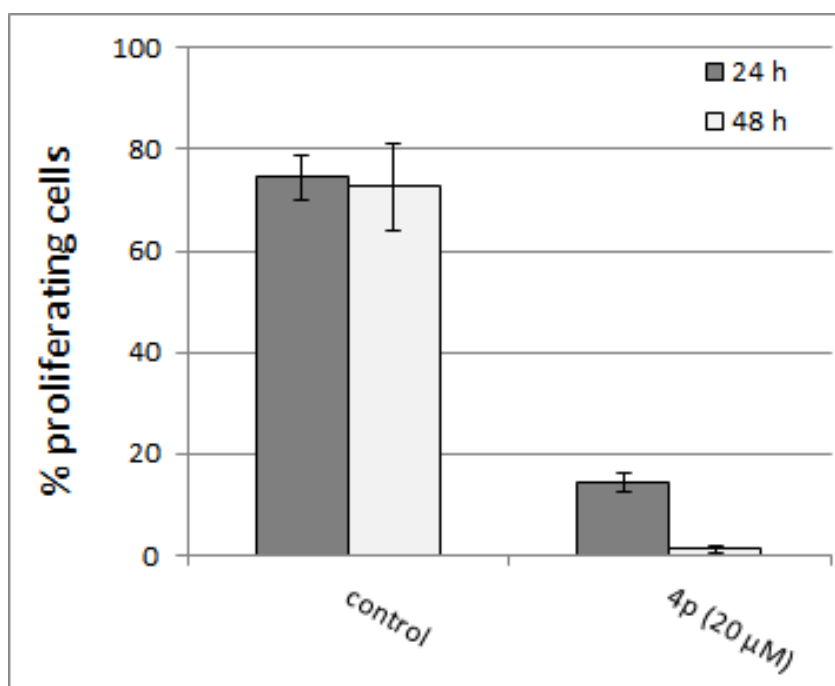


FIGURE 5: ANTIPROLIFERATIVE EFFECT OF THE INHIBITOR **4p** ON MCF-7 CELLS

Note: Results are shown as percent proliferating cells relatively to control cells (with 1% DMSO), and represent the mean (\pm SD) of four assays.

4.2.3.3 Inhibition of ABCG2-Mediated Drug Efflux

The same 16 indeno[1,2-*b*]indole derivatives were assayed for their ability to inhibit ABCG2-mediated mitoxantrone efflux from transfected HEK293 cells. Table 2 shows that the worst CK2 inhibitors appear to be the best ABCG2 inhibitors. Indeed, the *N*⁶-phenethyl substituted compounds produced a complete inhibition, with strong efficiency at submicromolar concentrations, as exemplified by **4c** (IC₅₀ = 0.43 μM). A 2-fold further increase in potency was observed by methyl substitution at position 7 in **4h**, or by methoxy substitution at phenethyl position *ortho* in **4j** whereas an opposite, negative, effect was produced at phenethyl position *para* in **4i** and an intermediate one at phenethyl position *meta* in **4k**.

The concentration dependence of the inhibition of ABCG2-mediated mitoxantrone efflux is illustrated for selected inhibitors in Figure 6.

Increasing the length of the *N*⁶-substituent into phenpropyl in **4d** induced a moderate alteration (2 fold), whereas a dramatic loss of potency was produced by shortening into either benzyl in **4b** or isopropyl in **4a** (approximately 70-100 fold). A main part of this loss in potency could be recovered through hydrophobic substitution by two benzyl groups at position 8 in **4r** versus **4a**, while a partial recovery was observed at vicinal position 7 with either a phenyl group in **4g** versus **4b** or a methyl group in **4e** versus **4a**. A partial recovery of inhibition potency was observed with prenyl substitution not only at position 4 in **4p**, but also at position 1 in **4o**, by comparison to **4a**. The best indenoindole inhibitors were nearly as potent as ABCG2 reference inhibitors, **2** (chromone 1) and **3** (Ko143), assayed under the same conditions.⁴⁴ In some cases, the maximal inhibition, as observed at 10 μM, was not complete (with maximal values of 60-83%) for hydrophobic derivatives such as **4d**, **4g**, **4i** and **4p** (with LogP values of 4.9-6.2) relative to a complete inhibition produced by **4c** and **4j** with a LogP of 4.4, may be partly related to lower water solubility, as suggested for other ABCG2 inhibitors.⁴⁵ However, the fact that **4j**, **4k** and **4i** (with the same LogP of 4.4) gave a variable maximal inhibition indicates that other parameters are critical for inhibition potency, in agreement with known polyspecificity of multidrug transporters, where the number and positions of hydrophobic substituents can modulate the orientation of binding and subsequent inhibition.

TABLE 2. INHIBITION OF MITOXANTRONE EFFLUX IN ABCG2-TRANSFECTED CELLS

Indenoindoles	ABCG2 inhibition		ABCG2/CK2 ^d	Cytotoxicity	
	% at 10 μ M ^a	IC ₅₀ (μ M)		IG ₅₀ (μ M) ^e	TR ^f
4aa	15 \pm 7	~35 ^c	~0.01	nd	
4b	18 \pm 3	~30 ^c	~0.5	nd	
4c	100 \pm 14	0.43 \pm 0.01 ^b	16	30.7 \pm 9.5	71
4d	83 \pm 25	0.79 \pm 0.13 ^b	8	> 100	> 127
4e	65 \pm 17	4.1 \pm 1.1 ^b	~0.04	nd	
4f	33 \pm 14	~15 ^c	~2	nd	
4g	68 \pm 10	0.96 \pm 0.09 ^b	~30	16.9 \pm 6.5	18
4h	100 \pm 21	0.23 \pm 0.02 ^b	11	> 100	> 435
4i	83 \pm 13	0.49 \pm 0.22 ^b	~30	20.1 \pm 4.9	96
4j	106 \pm 22	0.21 \pm 0.07 ^b	7	27.2 \pm 0.7	130
4k	78 \pm 14	0.31 \pm 0.09 ^b	16	12.7 \pm 3.1	41
4l	131 \pm 6	0.70 \pm 0.04 ^b	6	68.5 \pm 0.2	98
4o	74 \pm 12	3.0 \pm 0.5 ^b	~4	nd	
4p	60 \pm 26	1.6 \pm 0.7 ^b	0.02	31.0 \pm 8.4	19
4q	40 \pm 28	20 \pm 14 ^b	~0.46	nd	
4r	90 \pm 20	0.61 \pm 0.1 ^b	~18	6.0 \pm 1.0	10
Reference inhibitors^g					
Chromone 1ⁱ	98 \pm 7	0.13 \pm 0.09		96 \pm 6	
Ko143^j	106 \pm 1	0.09 \pm 0.01		32 \pm 3	
Reference substrates^h					
Mitoxantrone				0.009 \pm 0.005	
SN-38^k				0.005 \pm 0.001	

^aThe percent inhibition of ABCG2-mediated mitoxantrone efflux was determined for each compound at a fixed concentration of 10 μ M. ^bFor the best compounds producing at least 50% inhibition at 10 μ M, the concentration was varied to precisely determine the IC₅₀ values. ^cFor the other, less potent compounds, a rough estimation was obtained from the experimental inhibition produced at 10 μ M. ^dThe ABCG2/CK2 ratio, indicating the inhibitory efficiency of compounds toward ABCG2 relatively to CK2, was calculated by the ratio between the IC₅₀(CK2) values from Table 2 and the IC₅₀(ABCG2) values. ^eThe IG₅₀ values of compounds cytotoxicity were determined after 72 h with MTT cell survival tests. nd, not determined. ^fThe TR ratio was calculated upon dividing the IG₅₀ values of cytotoxicity by corresponding IC₅₀ values of ABCG2 inhibition. ^gOther known inhibitors and ^hcytotoxic substrates have been added for comparison with indenoindoles. ⁱChromone 1 = 5-[(4-bromobenzyl)oxy]-N-[2-(5-methoxy-1*H*-indol-3-yl)ethyl]-4-oxo-4*H*-chromene-2-carboxamide. ^jKo143 = (3*S*,6*S*,12*aS*)-1,2,3,4,6,7,12,12*a*-octahydro-9-methoxy-6-(2-methylpropyl)-1,4-dioxopyrazino[1',2':1,6]pyrido[3,4-*b*]indole-3-propanoic acid 1,1-dimethylethyl ester. ^kSN-38 = 7-ethyl-10-hydroxycamptothecin, active metabolite of the topoisomerase I inhibitor irinotecan.

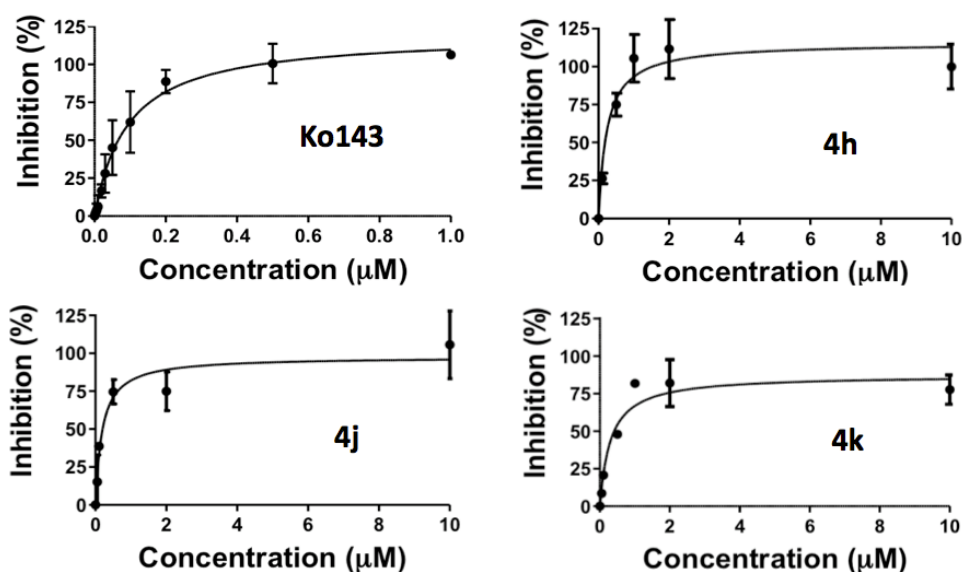


FIGURE 6: CONCENTRATION DEPENDENCE FOR THE MOST POTENT INDENOINDOLE INHIBITORS OF ABCG2 TRANSPORT ACTIVITY

Studies of the intermolecular interactions between ABCG2 and diverse ligands have revealed three important chemical features: hydrogen-bond acceptor (HBA), hydrophobic part (HP) and aromatic ring system (ARS).^{46,47} According to different possible combinations (0-3 HBA + 0-3 HP + 0-2 ARS), various inhibition pharmacophores were designed. Interestingly, a given ligand may adopt different orientations to form its complex with ABCG2. Our lead compound **4h** is mainly characterized by 2 HBAs, 1 HP and 3 ARSs and, according to different pharmacophore models, could indeed interact in variable orientations with the protein target. This point is closely related with the promiscuous nature of polyspecific multidrug transporters such as ABCG2.

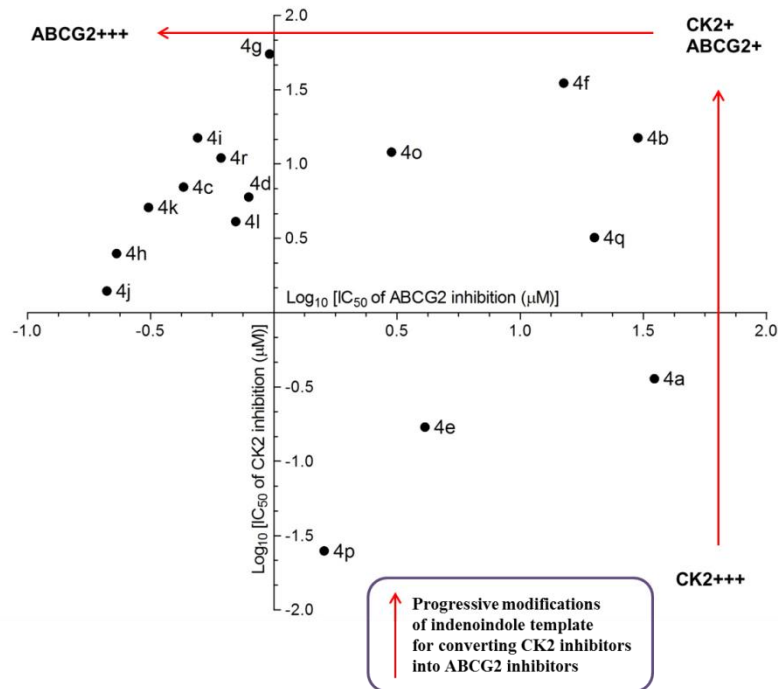
Comparison in Table 2 of the relative ability of each compound to inhibit CK2 and ABCG2 indicates that the best CK2 inhibitors, with a *N*⁶-isopropyl substituent were about two orders of magnitude more selective for CK2 in **4a**, **4e** and **4p** whereas the best ABCG2 inhibitors, with a *N*⁶-phenethyl substituent, **4c**, **4h**, **4i**, **4j**, **4k** and **4l**, were around one order of magnitude more selective for ABCG2. These differences are well illustrated in Figure 7A, also displaying that **4d**, with a longer *N*⁶-substituent, and both **4r** and **4g**, with aromatic substituents on D-ring, were good ABCG2 inhibitors. By contrast, **4b**, **4f**, **4o** and **4q** were only weak inhibitors of both CK2 and ABCG2, whereas no indenoindole derivative was found to potently inhibit

both CK2 and ABCG2. Overall, three orders of magnitude in selectivity were separating the best ABCG2 inhibitors from the best CK2 inhibitors despite they belong to the same indeno[1,2-*b*]indole family of compounds, for example **4c** and **4a** which only differ from the *N*⁵-substitution.

Finally, Table 2 shows that among the best ABCG2 inhibitors, some displayed a very low cytotoxicity characterized by IG_{50} values higher than 100 μ M, for **4h** and **4d**, or of 69 μ M for **4l**, whereas other derivatives appeared more cytotoxic, such as **4r** ($IG_{50} = 6 \mu$ M), and others were moderately cytotoxic such as **4k**, **4g**, **4j** and **4c** ($IG_{50} = 13-31 \mu$ M). A similar low or moderate cytotoxicity was observed with the reference inhibitors **2** and **3**, by difference with known cytotoxic substrates such as mitoxantrone and SN-38¹⁸ ($IG_{50} = 5-9 \text{ nM}$). For indenoindole inhibitors, comparison between cytotoxicity and potency of ABCG2 inhibition showed a very high therapeutic ratio, >435, for **4h**, compatible with future *in vivo* assays in animal models; three other derivatives, **4j**, **4l** and **4d**, with a therapeutic ratio around 100, might also be used. Some of the compounds displaying a moderate cytotoxicity, such as **4j** and **4h**, when assayed under 72-h cell survival MTT tests in both control HEK293 cells and ABCG2-transfected cells indicated no significant difference in IG_{50} values (not shown here); this indicated the absence of apparent ABCG2-mediated cross resistance, which suggested the absence of transport of the inhibitors.

Diverse structural modifications were performed on indeno[1,2-*b*]indoles to design new CK2 inhibitors. The *N*⁵-isopropyl derivative **4a** was progressively modified,^{14,16,37} and the introduction of a prenyl group on position 4 of A-ring was extremely favorable (CK2+++; $IC_{50} = 0.025 \mu$ M) (Figure 7A). Its analogue **4o**, with shifted substitution at position 1, gave significant information by (i) the emergence of ABCG2 inhibitory activity (ABCG2+) and (ii) the loss of CK2 inhibitory activity (CK2-). New pharmacomodulations allowed us to access to nine potent ABCG2 inhibitors (**4g**, **4d**, **4l**, **4r**, **4i**, **4c**, **4k**, **4j**, and **4h**) exhibiting submicromolar IC_{50} values (ABCG2+++).

A



B

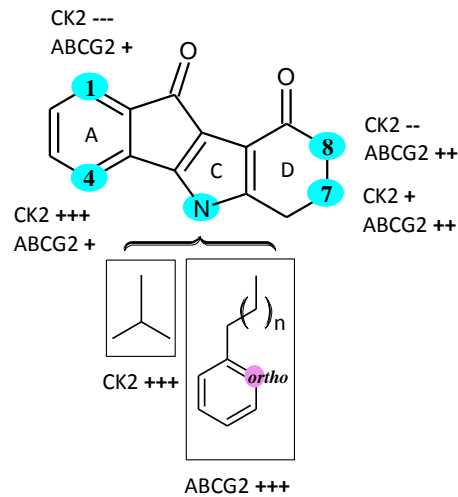


FIGURE 7: RELATIONSHIPS BETWEEN CK2 INHIBITORS AND ABCG2 INHIBITORS

Note. *Panel A*: graphical representation as a function of relative IC_{50} values. *Panel B*: structural modifications of indenoindoles for exploring CK2 or ABCG2 inhibitors.

The main structure-activity relationships of indeno[1,2-*b*]indoles for either CK2 inhibitors or ABCG2 inhibitors are schematically represented in Figure 7B. Quite interestingly, the different critical substitutions concerned the same positions, but

generally with opposite effects of substituents, as following: 1) at N^6 position, the preferred substituent was isopropyl (20-fold over phenethyl) for CK2 inhibition, whereas phenethyl was the best (70 to 100-fold over benzyl and isopropyl) for ABCG2 inhibition; 2) at position 8, hydrophobic substitutions by a methyl and a set of two benzyl groups were highly negative (30-fold *versus* H) for CK2 inhibition whereas they were highly positive (up to 60-fold) for ABCG2 inhibition; 3) at vicinal position 7, a hydrophobic phenyl was negative (3-fold *versus* H) for CK2 inhibition but quite positive (up to 30-fold) for ABCG2 inhibition. Position 7 for methyl substitution and phenethyl position *ortho* for methoxy substitution, produced similar effects on both CK2 and ABCG2, namely a 2 to 5-fold increase in potency. Prenyl substitution produced similar positive effects at position 4 (up to 20-fold increase in potency); however, it was highly selective for CK2 inhibition relatively to position 1, by contrast to ABCG2 inhibition where a positive contribution was also observed. Finally, the ABCG2 inhibitory site appeared more hydrophobic and able to bind bigger indeno[1,2-*b*]indole derivatives than the CK2 inhibitory site. This fully agrees with the fact that the ABCG2 binding site is expected to be located in close proximity to the hydrophobic drug-binding sites, as for previously characterized for various heterocyclic inhibitors,^{31,32} as recently reviewed,^{48,49} by contrast to the CK2 inhibitory site which has been shown to widely overlap the hydrophilic ATP-binding site.¹⁶

4.2.4 Experimental section

4.2.4.1 Chemistry

Melting points were determined on an Electrothermal 9200 capillary apparatus. The IR spectra were recorded on a Perkin Elmer Spectrum Two IR Spectrometer. The ^1H and ^{13}C NMR spectra were recorded at 400 MHz on a Bruker DRX 400 spectrometer. Chemical shifts are expressed in ppm (δ) downfield from internal tetramethylsilane and coupling constants J are reported in hertz (Hz). The following abbreviations are used: s: singlet; bs: broad singlet; d: doublet; t: triplet; dd: doubled doublet; dt: doubled triplet; q: quartet; m: multiplet; Cquat: quaternary carbons. The mass spectra were performed by direct ionization (EI or CI) on a ThermoFinnigan MAT 95 XL apparatus. Chromatographic separations were performed on silica gel columns by column chromatography (Kieselgel 300–400

mesh). All reactions were monitored by TLC on GF254 plates that were visualized under a UV lamp (254 nm). Evaporation of solvent was performed in vacuum with rotating evaporator. The purity of the final compounds (greater than 95%) was determined by uHPLC/MS on an Agilent 1290 system using a Agilent 1290 Infinity ZORBAX Eclipse Plus C18 column (2.1 x 50 mm, 1.8 μ m particle size) with a gradient mobile phase of H₂O/CH₃CN (90:10, v/v) with 0.1% of formic acid to H₂O/CH₃CN (10:90, v/v) with 0.1% of formic acid at a flow rate of 0.5 mL/min, with UV monitoring at the wavelength of 254 nm with a runtime of 10 min.

4.2.4.2 General Procedure for the Synthesis of Compounds 2

A solution containing 10.62 mmol of primary amine and 10.62 mmol of the corresponding cyclohexane-1,3-dione dissolved in 60 mL of toluene was refluxed in a Dean-Stark trap until the separation of H₂O had finished. The solvent was then evaporated under vacuum and the resultant residue was taken up in EtOAc to give a yellow solid that was isolated by filtration. Further purification was then accomplished by silica gel column chromatography with CH₂Cl₂/acetone (1:3, v/v) as the eluent.

5-Phenyl-3-(2-phenylethylamino)cyclohex-2-enone (2i). Yellow solid. Yield 75%. mp 117 °C. IR (ν cm⁻¹): 3240, 1698, 1660, 1601. ¹H NMR (CDCl₃, 400 MHz) δ : 7.33-7.20 (m, 10H, Harom), 5.30 (s, 1H, H-2), 5.00 (s, 1H, NH), 3.44-3.31 (m, 3H, H-5 and CH₂), 2.94 (t, 2H, J = 7.0 Hz, CH₂), 2.70-2.40 (m, 4H, 2 CH₂). ¹³C NMR + DEPT (CDCl₃, 100 MHz) δ : 196.60 (C=O), 163.52 (Cquat), 143.41 (Cquat), 138.35 (Cquat), 129.11 (2 CH), 129.02 (2 CH), 128.93 (2 CH), 127.22 (CH), 127.12 (CH), 127.02 (2 CH), 96.97 (CH), 44.24 (CH₂), 43.79 (CH₂), 40.24 (CH), 37.57 (CH₂), 34.62 (CH₂). HRMS calcd for C₂₀H₂₂NO [M + H]⁺ 292.1696, found 292.1692.

3-[2-(2-Methoxyphenyl)ethylamino]cyclohex-2-enone (2j). Yellow solid. Yield 90%. mp 105 °C. IR (ν cm⁻¹): 3253, 1600, 1569, 1533. ¹H NMR (CDCl₃, 400 MHz) δ : 7.22 (dt, 1H, J_1 = 1.7 Hz, J_2 = 8.2 Hz, Harom), 7.10 (dd, 1H, J_1 = 1.6 Hz, J_2 = 7.3 Hz, Harom), 6.92-6.86 (m, 2H, Harom), 5.15 (s, 1H, H-2), 5.1 (s, 1H, NH), 3.84 (s, 3H, OMe), 3.29 (m, 2H, CH₂), 2.89 (t, 2H, J = 6.8 Hz, CH₂), 2.29-2.24 (m, 4H, 2 CH₂), 1.93 (m, 2H, CH₂). ¹³C NMR + DEPT (CDCl₃, 100 MHz) δ : 197.43 (C=O), 164.50 (Cquat), 157.64 (Cquat), 130.85 (CH), 128.46 (CH), 127.21 (Cquat), 121.21 (CH), 110.78 (CH), 96.98 (CH), 55.57 (CH₃), 43.59 (CH₂), 36.71 (CH₂), 30.14 (CH₂), 29.59 (CH₂), 22.28 (CH₂). HRMS calcd for C₁₅H₂₀NO₂ [M + H]⁺ 246.1489, found 246.1489.

3-[2-(3-Methoxyphenyl)ethylamino]cyclohex-2-enone (2k). Beige solid. Yield 80%. mp 94 °C. IR (ν cm⁻¹): 3256, 1601, 1570, 1531. ¹H NMR (CDCl₃, 400 MHz) δ : 7.22 (t, 1H, J = 7.9 Hz, Harom), 6.79-6.75 (m, 2H, Harom), 6.71 (m, 1H, Harom), 5.17 (s, 1H, H-2), 4.73 (s, 1H, NH), 3.79 (s, 3H, OMe), 3.44 (m, 2H, CH₂), 2.85 (t, 2H, J = 7.0 Hz, CH₂), 2.31-2.26 (m, 4H, 2 CH₂), 1.93 (m, 2H, CH₂). ¹³C NMR + DEPT (CDCl₃, 100 MHz) δ : 197.63 (C=O), 164.36 (Cquat), 160.20 (Cquat), 140.04 (Cquat), 130.11 (CH), 121.22 (CH), 114.77 (CH), 112.24 (CH), 97.36 (CH), 55.51 (CH₃), 43.91 (CH₂), 36.75 (CH₂), 34.67 (CH₂), 30.11 (CH₂), 22.60 (CH₂). HRMS calcd for C₁₅H₂₀NO₂ [M + H]⁺ 246.1489, found 246.1494.

3-[2-(4-Methoxyphenyl)ethylamino]cyclohex-2-enone (2l). Yellow solid. Yield 90%. mp 89 °C. IR (ν cm⁻¹): 3247, 1596, 1531, 1511. ¹H NMR (CDCl₃, 400 MHz) δ : 7.08 (d, 2H, J = 8.6 Hz, Harom), 6.84 (d, 2H, J = 8.6 Hz, Harom), 5.16 (s, 1H, H-2), 4.79 (s, 1H, NH), 3.78 (s, 3H, OMe), 3.30 (m, 2H, CH₂), 2.82 (t, 2H, J = 7.0 Hz, CH₂), 2.30-2.26 (m, 4H, 2 CH₂), 1.93 (m, 2H, CH₂). ¹³C NMR + DEPT (CDCl₃, 100 MHz) δ : 197.54 (C=O), 164.43 (Cquat), 158.74 (Cquat), 130.37 (Cquat), 129.88 (2 CH), 114.47 (2 CH), 97.28 (CH), 55.57 (CH₃), 44.24 (CH₂), 36.75 (CH₂), 30.77 (CH₂), 30.08 (CH₂), 22.26 (CH₂). HRMS calcd for C₁₅H₂₀NO₂ [M + H]⁺ 246.1489, found 246.1483.

4.2.4.3 General Procedure for the Synthesis of Compounds 3

A solution containing 6.86 mmol of enaminone **2** and 6.86 mmol of ninhydrin dissolved in 25 mL of MeOH was stirred at room temperature for 8 h. Generally, a precipitate of compound **3** was formed. It was recovered and washed with MeOH. A second quantity was obtained from the filtrate by purification by silica gel column chromatography with CH₂Cl₂/acetone (1:3, v/v) as the eluent.

4b,9b-Dihydroxy-7-phenyl-5-(2-phenylethyl)-4b,5,6,7,8,9b-hexahydroindeno[1,2-b]indole-9,10-dione (3i). White solid. Yield 84%. mp 128 °C. IR (ν cm⁻¹): 3471, 1714, 1603, 1521. ¹H NMR (CDCl₃, 400 MHz) δ : 7.95-7.87 (m, 2H, Harom), 7.77 (m, 1H, Harom), 7.57 (m, 1H, Harom), 7.36-7.20 (m, 8H, Harom), 7.09-7.03 (m, 2H, Harom), 4.11 (m, 1H, NCH₂), 3.82 (m, 1H, NCH₂), 3.25 (m, 1H, CH₂Ph), 3.11 (m, 1H, H-7), 2.99 (m, 1H, CH₂Ph), 2.61-2.11 (m, 4H, CH₂-6 and CH₂-8). ¹³C NMR + DEPT (CDCl₃, 100 MHz) δ : 197.78 (d, C=O), 191.10 (d, C=O), 166.84 (d, Cquat), 148.51 (d, Cquat),

143.01 (d, Cquat), 138.70 (d, Cquat), 136.10 (d, CH), 135.52 (d, Cquat), 130.80 (d, CH), 129.51 (d, 2 CH), 129.20 (d, 2 CH), 128.99 (d, 2 CH), 127.32 (d, 2 CH), 127.12 (d, 2 CH), 125.12 (d, CH), 124.52 (d, CH), 105.37 (d, Cquat), 96.87 (d, Cquat), 83.12 (d, Cquat), 44.88 (d, CH₂), 44.11 (d, CH₂), 40.42 (d, CH), 37.83 (s, CH₂), 30.84 (d, CH₂). HRMS calcd for C₂₉H₂₆NO₄ [M + H]⁺ 452.1856, found 452.1840.

4b,9b-Dihydroxy-5-[2-(2-methoxyphenyl)ethyl]-4b,5,6,7,8,9b-hexahydroindeno[1,2-b]indole-9,10-dione (3j). Yellow solid. Yield 93%. mp 114 °C. IR (ν cm⁻¹): 3465, 1716, 1656, 1601, 1524. ¹H NMR (CDCl₃, 400 MHz) δ: 7.92 (d, 1H, *J* = 7.8 Hz, Harom), 7.85 (d, 1H, *J* = 7.6 Hz, Harom), 7.73 (m, 1H, Harom), 7.54 (m, 1H, Harom), 7.26 (m, 1H, Harom), 7.16 (dd, 1H, *J*₁ = 1.7 Hz, *J*₂ = 7.4 Hz, Harom), 6.94 (m, 1H, Harom), 6.89 (d, 1H, *J* = 8.2 Hz, Harom), 4.88 (bs, 1H, OH), 3.98 (m, 1H, NCH₂), 3.77 (m, 1H, NCH₂), 3.13 (m, 1H, CH₂Ph), 2.98 (m, 1H, CH₂Ph), 2.38 (bs, 1H, OH), 2.22 (m, 2H, CH₂), 2.16 (m, 2H, CH₂), 1.84 (m, 1H, CH₂), 1.73 (m, 1H, CH₂). ¹³C NMR + DEPT (CDCl₃, 100 MHz) δ: 198.11 (C=O), 192.39 (C=O), 167.26 (Cquat), 157.84 (Cquat), 148.42 (Cquat), 136.05 (CH), 135.44 (Cquat), 131.28 (CH), 130.75 (CH), 128.83 (CH), 126.71 (Cquat), 125.13 (CH), 124.43 (CH), 121.31 (CH), 110.81 (CH), 105.53 (Cquat), 96.22 (Cquat), 83.01 (Cquat), 55.84 (CH₃), 43.29 (CH₂), 36.64 (CH₂), 32.90 (CH₂), 23.16 (CH₂), 21.88 (CH₂). HRMS calcd for C₂₄H₂₄NO₅ [M + H]⁺ 406.1649, found 406.1641.

4b,9b-Dihydroxy-5-[2-(3-methoxyphenyl)ethyl]-4b,5,6,7,8,9b-hexahydroindeno[1,2-b]indole-9,10-dione (3k). White solid. Yield 94% yield. mp 95 °C. IR (ν cm⁻¹): 3471, 1713, 1655, 1599, 1521. ¹H NMR (DMSO-*d*₆, 400 MHz) δ: 8.04 (d, 1H, *J* = 7.8 Hz, Harom), 7.84 (m, 1H, Harom), 7.74 (d, 1H, *J* = 7.5 Hz, Harom), 7.62 (m, 1H, Harom), 7.29 (m, 1H, Harom), 6.95-6.92 (m, 2H, Harom), 6.90 (bs, 1H, OH), 6.85 (dd, 1H, *J*₁ = 2.6 Hz, *J*₂ = 8.2 Hz, Harom), 5.79 (bs, 1H, OH), 4.01 (m, 1H, NCH₂), 3.75 (m, 1H, NCH₂), 3.40 (s, 3H, OMe), 2.97 (m, 2H, CH₂Ph), 2.24 (m, 2H, CH₂), 2.05 (m, 2H, CH₂), 1.73 (m, 1H, CH₂), 1.65 (m, 1H, CH₂). ¹³C NMR + DEPT (DMSO-*d*₆, 100 MHz) δ: 198.58 (C=O), 189.68 (C=O), 166.22 (Cquat), 160.36 (Cquat), 149.19 (Cquat), 141.49 (Cquat), 136.53 (CH), 135.73 (Cquat), 131.20 (CH), 130.51 (CH), 125.74 (CH), 124.11 (CH), 122.19 (CH), 115.52 (CH), 113.00 (CH), 105.71 (Cquat), 96.60 (Cquat), 84.54 (Cquat), 55.99 (CH₃), 44.37 (CH₂), 37.93 (CH₂), 37.84 (CH₂), 23.24 (CH₂), 22.33 (CH₂). HRMS calcd for C₂₄H₂₄NO₅ [M + H]⁺ 406.1649, found 406.1658.

4b,9b-Dihydroxy-5-[(2-(4-methoxyphenyl)ethyl)-4b,5,6,7,8,9bhexahydroindeno[1,2-b]indole-9,10-dione (3I). Yellow solid. Yield 97%. mp 116 °C. IR (ν cm⁻¹): 3489, 1713, 1660, 1605, 1577, 1539, 1509. ¹H NMR (CDCl₃, 400 MHz) δ : 7.89-7.84 (m, 2H, Harom), 7.73 (m, 1H, Harom), 7.54 (m, 1H, Harom), 7.13-7.10 (m, 2H, Harom), 6.89-6.85 (m, 2H, Harom), 5.53 (bs, 1H, OH), 5.14 (bs, 1H, OH), 3.99 (m, 1H, NCH₂), 3.80 (s, 3H, OMe), 3.72 (m, 1H, NCH₂), 2.99 (m, 2H, CH₂Ph), 2.23 (m, 2H, CH₂), 2.12 (m, 2H, CH₂), 1.87 (m, 1H, CH₂), 1.71 (m, 1H, CH₂). ¹³C NMR + DEPT (CDCl₃, 100 MHz) δ : 197.88 (C=O), 192.44 (C=O), 167.17 (Cquat), 158.92 (Cquat), 148.53 (Cquat), 136.04 (CH), 135.49 (Cquat), 130.73 (CH), 130.62 (Cquat), 130.32 (2 CH), 125.16 (CH), 124.43 (CH), 114.60 (2 CH), 105.64 (Cquat), 96.22 (Cquat), 83.19 (Cquat), 55.68 (CH₃), 45.02 (CH₂), 36.97 (CH₂), 36.59 (CH₂), 23.35 (CH₂), 21.82 (CH₂). HRMS calcd for C₂₄H₂₄NO₅ [M + H]⁺ 406.1649, found 406.1638.

4.2.4.4 General Procedure for the Synthesis of Compounds 4i-n

A solution containing 4.43 mmol of **3** and 8.86 mmol (2 equiv) of TETA dissolved in 15 mL of DMF and 2.5 mL of AcOH was stirred at room temperature for 22 h. The solution was then poured into 300 mL of ice and water and stirred for 1 h. The resulting precipitate was filtered and washed with water and dried to give a first quantity of **4**. The filtrate was evaporated and the residue was diluted with H₂O. The solution was basified with NaHCO₃ and extracted with CH₂Cl₂. The organic phase was dried over anhydrous Na₂SO₄ and evaporated in vacuum to give a second quantity of **4** which was purified by silica gel column chromatography with CH₂Cl₂/acetone (95:5, v/v) as the eluent.

7-Phenyl-5-(2-phenylethyl)-5,6,7,8-tetrahydroindeno[1,2-b]indole-9,10-dione (4i). Orange solid. Yield 95%. mp 228 °C. IR (ν cm⁻¹): 1698, 1660, 1603, 1520. ¹H NMR (CDCl₃, 400 MHz) δ : 7.47 (d, 1H, *J* = 6.8 Hz, Harom), 7.33-7.22 (m, 7H, Harom), 7.14 (m, 1H, Harom), 7.07 (d, 2H, *J* = 7.0 Hz, Harom), 6.98-6.93 (m, 3H, Harom), 4.15 (m, 2H, NCH₂), 3.08- 3.00 (m, 3H, H-7 and CH₂Ph), 2.60 (dd, 1H, *J*₁ = 4.0 Hz, *J*₂ = 16.4 Hz, H-6 or H-8), 2.51 (dd, 1H, *J*₁ = 12.6 Hz, *J*₂ = 16.4 Hz, H-6 or H-8), 2.25 (dd, 1H, *J*₁ = 4.8 Hz, *J*₂ = 16.4 Hz, H-6 or H-8), 2.10 (dd, 1H, *J*₁ = 11.6 Hz, *J*₂ = 16.4 Hz, H-6 or H-8). ¹³C NMR + DEPT (CDCl₃, 100 MHz) δ : 191.47 (C=O), 184.55 (C=O), 152.81 (Cquat), 150.27 (Cquat), 142.97 (Cquat), 139.04 (Cquat), 137.01 (Cquat), 135.09 (Cquat), 132.75 (CH), 129.43 (2 CH), 129.30 (2 CH), 128.99 (2 CH), 128.73 (CH),

127.76 (CH), 127.38 (CH), 127.01 (2 CH), 124.16 (CH), 120.39 (Cquat), 117.42 (CH), 117.16 (Cquat), 47.76 (CH₂), 44.90 (CH₂), 41.64 (CH), 37.22 (CH₂), 29.94 (CH₂). HRMS calcd for C₂₉H₂₄NO₂ [M + H]⁺ 418.1802, found 418.1791.

5-[2-(2-Methoxyphenyl)ethyl]-5,6,7,8-tetrahydroindeno[1,2-b]indole-9,10-dione (4j). Orange solid. Yield 83%. mp 198 °C. IR (ν cm⁻¹): 1698, 1664, 1605, 1531. ¹H NMR (CDCl₃, 400 MHz) δ: 7.40 (d, 1H, *J* = 7.0 Hz, Harom), 7.22-7.17 (m, 2H, Harom), 7.08 (m, 1H, Harom), 6.98 (d, 1H, *J* = 7.1 Hz, Harom), 6.90 (d, 1H, *J* = 6.4 Hz, Harom), 6.83-6.79 (m, 2H, Harom), 4.12 (t, 2H, *J* = 6.9 Hz, NCH₂), 3.79 (s, 3H, OMe), 3.06 (t, 2H, *J* = 6.9 Hz, CH₂Ph), 2.34 (m, 2H, CH₂-6 or CH₂-8), 2.27 (m, 2H, CH₂-6 or CH₂-8), 1.90 (m, 2H, CH₂-7). ¹³C NMR + DEPT (CDCl₃, 100 MHz) δ: 192.63 (C=O), 184.63 (C=O), 157.73 (Cquat), 153.04 (Cquat), 150.91 (Cquat), 139.08 (Cquat), 135.25 (Cquat), 132.53 (CH), 131.05 (CH), 129.15 (CH), 128.49 (CH), 125.05 (Cquat), 123.92 (CH), 121.14 (CH), 120.06 (Cquat), 117.52 (Cquat), 117.36 (CH), 110.54 (CH), 55.57 (CH₃), 46.08 (CH₂), 38.05 (CH₂), 32.16 (CH₂), 23.28 (CH₂), 21.74 (CH₂). HRMS calcd for C₂₄H₂₂NO₃ [M + H]⁺ 372.1594, found 372.1590.

5-[2-(3-Methoxyphenyl)ethyl]-5,6,7,8-tetrahydroindeno[1,2-b]indole-9,10-dione (4k). Orange solid. Yield 60%. mp 176 °C. IR (ν cm⁻¹): 1696, 1661, 1594. ¹H NMR (CDCl₃, 400 MHz) δ: 7.43 (dd, 1H, *J*₁ = 0.6 Hz, *J*₂ = 7.1 Hz, Harom), 7.22-7.08 (m, 3H, Harom), 6.88 (d, 1H, *J* = 7.1 Hz, Harom), 6.75 (m, 1H, Harom), 6.57 (d, 1H, *J* = 7.6 Hz, Harom), 6.49 (m, 1H, Harom), 4.14 (t, 2H, *J* = 6.5 Hz, NCH₂), 3.69 (s, 3H, OMe), 3.03 (t, 2H, *J* = 6.5 Hz, CH₂Ph), 2.33 (m, 2H, CH₂-6 or CH₂-8), 2.09 (m, 2H, CH₂-6 or CH₂-8), 1.85 (m, 2H, CH₂-7). ¹³C NMR + DEPT (CDCl₃, 100 MHz) δ: 192.58 (C=O), 184.54 (C=O), 160.25 (Cquat), 152.53 (Cquat), 151.04 (Cquat), 139.07 (Cquat), 138.50 (Cquat), 135.12 (Cquat), 132.63 (CH), 130.35 (CH), 128.65 (CH), 124.14 (CH), 121.45 (CH), 120.47 (Cquat), 117.60 (Cquat), 117.27 (CH), 114.86 (CH), 113.01 (CH), 55.54 (CH₃), 47.71 (CH₂), 38.02 (CH₂), 37.29 (CH₂), 23.22 (CH₂), 21.90 (CH₂). HRMS calcd for C₂₄H₂₂NO₃ [M + H]⁺ 372.1594, found 372.1601.

5-[2-(4-Methoxyphenyl)ethyl]-5,6,7,8-tetrahydroindeno[1,2-b]indole-9,10-dione (4l). Orange solid. Yield 87%. mp 181 °C. IR (ν cm⁻¹): 1697, 1660, 1605, 1511. ¹H NMR (CDCl₃, 400 MHz) δ: 7.44 (d, 1H, *J* = 7.1 Hz, Harom), 7.20 (m, 1H, Harom), 7.11 (m, 1H, Harom), 6.90-6.87 (m, 3H, Harom), 6.79-6.76 (m, 2H, Harom), 4.12 (t, 2H, *J* = 6.5 Hz, NCH₂), 3.73 (s, 3H, OMe), 3.01 (t, 2H, *J* = 6.5 Hz, CH₂Ph), 2.33 (m, 2H, CH₂-6 or CH₂-8), 2.10 (m, 2H, CH₂-6 or CH₂-8), 1.85 (m, 2H, CH₂-7). ¹³C NMR + DEPT

(CDCl₃, 100 MHz) δ : 192.65 (C=O), 184.60 (C=O), 159.31 (Cquat), 152.54 (Cquat), 150.96 (Cquat), 139.11 (Cquat), 135.17 (Cquat), 132.61 (CH), 130.31 (2 CH), 128.88 (Cquat), 128.65 (CH), 124.16 (CH), 120.52 (Cquat), 117.62 (Cquat), 117.28 (CH), 114.65 (2 CH), 55.67 (CH₃), 47.96 (CH₂), 38.04 (CH₂), 36.39 (CH₂), 23.26 (CH₂), 21.95 (CH₂). HRMS calcd for C₂₄H₂₁NNaO₃ [M + Na]⁺ 394.1414, found 394.1403.

1-Hydroxy-5-isopropyl-5,6,7,8-tetrahydroindeno[1,2-b]indole-9,10-dione (**4m**).

Orange solid. Yield 81%. mp = 167 °C. IR (ν cm⁻¹): 3214, 1696, 1672, 1623. ¹H NMR (DMSO-*d*₆, 400 MHz) δ : 9.74 (s, 1H, OH), 7.22 (m, 1H, H-3), 6.91 (d, 1H, *J* = 7.3 Hz, H-4), 6.71 (d, 1H, *J* = 8.5 Hz, H-2), 4.74 (m, 1H, CHMe₂), 2.93 (t, 2H, *J* = 5.6 Hz, CH₂-6 or CH₂-8), 2.35 (t, 2H, *J* = 5.8 Hz, CH₂-6 or CH₂-8), 2.06 (m 2H, CH₂-7), 1.54 (d, 6H, *J* = 9.3 Hz, CHMe₂). ¹³C NMR + DEPT (DMSO-*d*₆, 100 MHz) δ : 192.25 (C=O), 185.44 (C=O), 156.24 (2 Cquat), 151.19 (Cquat), 150.40 (Cquat), 136.57 (Cquat), 135.64 (CH), 120.62 (CH), 120.14 (Cquat), 117.56 (Cquat), 113.15 (CH), 50.02 (CH), 38.58 (2 CH₂), 23.75 (CH₂), 22.15 (2 CH₃). HRMS calcd for C₁₈H₁₇NNaO₃ [M + Na]⁺ 318.1101, found 318.1094.

4-Hydroxy-5-isopropyl-5,6,7,8-tetrahydroindeno[1,2-b]indole-9,10-dione (**4n**). Pink solid. Yield 19%. mp = 309 °C. IR (ν cm⁻¹): 2642, 1698, 1596. ¹H RMN (DMSO-*d*₆, 400 MHz) δ : 10.58 (s, 1H, OH), 7.08 (m, 1H, H-2), 6.92 (d, 1H, *J* = 8.3 Hz, H-1 or H-3), 6.89 (d, 1H, *J* = 6.8 Hz, H-1 or H-3), 5.91 (m, 1H, CHMe₂), 2.93 (t, 2H, *J* = 5.7 Hz, CH₂-6), 2.38 (t, 2H, *J* = 6.1 Hz, CH₂-8), 2.07 (m, 2H, CH₂-7), 1.56 (d, 6H, *J* = 6.8 Hz, CHMe₂). ¹³C NMR + DEPT (DMSO-*d*₆, 100 MHz) δ : 191.33 (C=O), 183.21 (C=O), 149.75 (Cquat), 147.94 (Cquat), 140.20 (Cquat), 131.60 (Cquat), 131.51 (Cquat), 130.00 (CH), 128.64 (Cquat), 123.40 (CH), 118.61 (Cquat), 115.10 (CH), 50.66 (CH), 41.42 (CH₂), 37.68 (2 CH₂), 21.60 (2 CH₃). HRMS calcd for C₁₈H₁₈NO₃ [M + H]⁺ 296.1281, found 296.1279.

5-Isopropyl-1-(3-methylbut-2-enyloxy)-5,6,7,8-tetrahydroindeno[1,2-b]indole-9,10-dione (**4o**). A mixture of 1-hydroxyindenoindole **4m** (1 mmol), K₂CO₃ (3 mmol), and prenyl bromide (1.5 mmol) in DMA was heated at 80 °C for 24 h. The mixture was then poured into H₂O and extracted with CH₂Cl₂. The organic layers were washed with H₂O, dried over Na₂SO₄, filtered and concentrated. The residue was purified by flash chromatography using acetone/CH₂Cl₂ (2:10, v/v) as the eluent to provide compound **4o**. Orange solid. Yield 27%. mp = 212 °C. IR (ν cm⁻¹): 1698, 1659, 1588, 1503. ¹H NMR (CDCl₃, 400 MHz) δ : 7.17 (m, 1H, H-3), 6.77 (d, 1H, *J* = 7.3 Hz, H-2 or

H-4), 6.73 (d, 1H, $J = 8.6$ Hz, H-2 or H-4), 5.49 (m, 1H, $\text{Me}_2\text{C}=\underline{\text{CH}}$), 4.67 (d, 2H, $J = 6.5$ Hz, OCH_2), 4.61 (m, 1H, $\underline{\text{CH}}\text{Me}_2$), 2.83 (t, 2H, $J = 6.0$ Hz, CH_2 -6 or CH_2 -8), 2.46 (t, 2H, $J = 5.8$ Hz, CH_2 -6 or CH_2 -8), 2.14 (m, 2H, CH_2 -7), 1.73 (d, 3H, $J = 1.0$ Hz, $\underline{\text{Me}_2\text{C}=\text{CH}}$), 1.71 (s, 3H, $\underline{\text{Me}_2\text{C}=\text{CH}}$), 1.62 (d, 6H, $J = 7.1$ Hz, $\underline{\text{CHMe}_2}$). ^{13}C NMR + DEPT (CDCl_3 , 100 MHz) δ : 192.30 (C=O), 183.33 (C=O), 157.24 (Cquat), 149.61 (Cquat), 148.91 (Cquat), 138.06 (Cquat), 137.99 (Cquat), 134.10 (CH), 123.87 (Cquat), 121.64 (Cquat), 120.20 (CH), 117.90 (Cquat), 117.46 (CH), 112.71 (CH), 66.90 (CH_2), 49.60 (CH), 38.18 (CH_2), 26.07 (CH_3), 23.95 (CH_2), 23.61 (CH_2), 22.13 (2 CH_3), 18.67 (CH_3). HRMS calcd for $\text{C}_{23}\text{H}_{25}\text{NNaO}_3$ [$\text{M} + \text{Na}$] $^+$, 386.1727, found 386.1711.

5-Isopropyl-4-(3-methylbut-2-enyloxy)-5,6,7,8-tetrahydroindeno[1,2-*b*]indole-9,10-dione (**4p**). A solution of 4-hydroxyindenoindole **4n** (0.677 mmol, 1 equiv), K_2CO_3 (2.03 mmol, 3 equiv) and prenyl bromide (2.03 mmol, 3 equiv) in acetone (20 mL) was refluxed for 8 h. The mixture was then filtered and concentrated. The residue was purified by flash chromatography using acetone/ CH_2Cl_2 (2:10, v/v) as the eluent to provide compound (**4p**). Red solid. Yield 60%. mp = 167 °C. IR (ν cm^{-1}): 1694, 1660, 1642, 1598. ^1H RMN ($\text{DMSO}-d_6$, 400 MHz) δ : 7.20-7.18 (m, 2H, H-1 and H-3), 6.98 (m, 1H, H-2), 5.84 (bs, 1H, $\text{Me}_2\text{C}=\underline{\text{CH}}$), 5.52 (m, 1H, $\underline{\text{CH}}\text{Me}_2$), 4.68 (d, 2H, $J = 7.1$ Hz, OCH_2), 2.98 (t, 2H, $J = 5.87$ Hz, CH_2 -6 or CH_2 -8), 2.37 (t, 2H, $J = 5.74$ Hz, CH_2 -6 or CH_2 -8), 2.06 (m, 2H, CH_2 -7), 1.82 (s, 3H, $\underline{\text{Me}_2\text{C}=\text{CH}}$), 1.77 (d, 3H, $J = 0.9$ Hz, $\underline{\text{Me}_2\text{C}=\text{CH}}$), 1.49 (d, 6H, $J = 7.1$ Hz, $\underline{\text{CHMe}_2}$). ^{13}C NMR + DEPT ($\text{DMSO}-d_6$, 100 MHz) δ : 192.30 (C=O), 184.03 (C=O), 154.19 (Cquat), 151.07 (Cquat), 150.01 (Cquat), 140.61 (Cquat), 140.28 (Cquat), 131.35 (CH), 122.29 (Cquat), 120.86 (CH), 119.57 (CH), 119.12 (Cquat), 118.66 (Cquat), 117.10 (CH), 66.13 (CH_2), 51.74 (CH), 38.65 (CH_2), 26.42 (CH_3), 25.37 (CH_2), 24.31 (CH_2), 22.47 (2 CH_3), 18.88 (CH_3). HRMS calcd for $\text{C}_{23}\text{H}_{25}\text{NNaO}_3$ [$\text{M} + \text{Na}$] $^+$ 386.1727, found 386.1718.

4.2.4.5 General Procedure for the Synthesis of Compounds 4q and 4r.

A solution of **4a** (1.79 mmol, 1 equiv) in dry THF (10 mL) was added dropwise under argon to a solution of LCIA prepared from cyclohexylisopropylamine (2 equiv) and *n*-BuLi (2.82 equiv) in dry THF (4.2 mL) at -20 °C. The resulting solution was cooled at -40 °C and stirred for 5 h. Then, alkylating agent (16 equiv) was added dropwise and stirring was continued at -40 °C for 2 h. The reaction

mixture was warmed to room temperature and stirred overnight. After the addition of 2 M HCl (4 mL), the reaction mixture was extracted with AcOEt. The combined organic layers were washed with water and brine successively and dried over anhydrous Na₂SO₄. The solvent was then evaporated under vacuum and the resultant residue was purified by silica gel column chromatography using EtOAc/cyclohexane (1:1, v/v) as the eluent.

5-Isopropyl-8-methyl-5,6,7,8-tetrahydroindeno[1,2-b]indole-9,10-dione (**4q**).

Orange solid. Yield 10%. mp 209 °C. IR (ν cm⁻¹): 1702, 1665, 1601, 1525. ¹H NMR (CDCl₃, 400 MHz) δ : 7.45 (m, 1H, Harom), 7.22 (m, 1H, Harom), 7.12-7.08 (m, 2H, Harom), 4.59 (m, 1H, CHMe₂), 2.87 (m, 2H, CH₂-6), 2.47 (m, 1H, H-7), 2.22 (m, 1H, H-7), 1.90 (m, 1H, H-8), 1.63 (d, 3H, *J* = 7.0 Hz, CHMe₂), 1.64 (d, 3H, *J* = 7.0 Hz, CHMe₂), 1.21 (d, 3H, *J* = 7.0 Hz, CH₃-8). ¹³C NMR + DEPT (CDCl₃, 100 MHz) δ : 194.87 (C=O), 184.54 (C=O), 152.00 (Cquat), 148.58 (Cquat), 139.32 (Cquat), 135.76 (Cquat), 132.40 (CH), 128.41 (CH), 124.14 (CH), 121.11 (Cquat), 118.97 (CH), 117.74 (Cquat), 49.57 (CH), 41.56 (CH), 31.51 (CH₂), 23.19 (CH₂), 22.33 (CH₃), 22.21 (CH₃), 15.33 (CH₃). HRMS calcd for C₁₉H₁₉NNaO₂ [M + Na]⁺ 316.1308, found 316.1310.

8,8-Dibenzyl-5-isopropyl-5,6,7,8-tetrahydroindeno[1,2-b]indole-9,10-dione (**4r**).

Orange solid. Yield 35%. mp 236 °C. IR (ν cm⁻¹): 1707, 1654, 1604, 1527. ¹H NMR (CDCl₃, 400 MHz) δ : 7.48 (d, 1H, *J* = 7.1 Hz, Harom), 7.22-7.06 (m, 13H, Harom), 4.45 (m, 1H, CHMe₂), 3.34 (d, 2H, *J* = 13.4 Hz, CH₂Ph), 2.70 (m, 2H, CH₂-6 or CH₂-7), 2.62 (d, 2H, *J* = 13.6 Hz, CH₂Ph), 1.93 (m, 2H, CH₂-6 or CH₂-7), 1.53 (d, 6H, *J* = 7.1 Hz, CHMe₂). ¹³C NMR + DEPT (CDCl₃, 100 MHz) δ : 194.72 (C=O), 184.28 (C=O), 152.20 (Cquat), 147.40 (Cquat), 139.19 (Cquat), 137.84 (3 Cquat), 135.40 (Cquat), 132.17 (CH), 131.12 (4 CH), 128.29 (CH), 128.07 (4 CH), 126.44 (2 CH), 124.01 (CH), 118.78 (CH), 65.99 (CH₂), 50.66 (2 Cquat), 42.53 (2 CH₂), 29.50 (CH₂), 21.96 (2 CH₃), 15.50 (CH). HRMS calcd for C₃₂H₂₉NNaO₂ [M + Na]⁺ 482.2091, found 482.2106.

4.2.4.6 X-ray Data

The structure of compounds **4c** has been established by X-ray crystallography (Figure 2). Orange/red single crystal (0.20 x 0.10 x 0.01 mm³) of **4c** was obtained after 24 h at 21 °C from a closed methanol/chloroform (25/75) solution

preliminary heated at 37 °C during 1 h followed by instantaneous cooling at – 20 °C during 20 sec: orthorhombic, space group P2₁2₁2, *a*= 15.3192(7) Å, *b*= 21.1897(10) Å, *c*= 5.4407(2) Å, $\alpha=90^\circ$, $\beta=90^\circ$, $\gamma=90^\circ$, *V*= 1766.10(13) Å³, *Z*=4, $\delta(\text{calcd})=1.284 \text{ Mg.m}^{-3}$, *FW*=341.39 for C₂₃H₁₉NO₂, *F*(000)=720. Crystallographic data were acquired on a Bruker APEX 2 DUO. Full crystallographic results have been deposited at the Cambridge Crystallographic Data Centre (CCDC-867623), UK, as supplementary Material.⁵⁰ The data were corrected for Lorentz and polarization effects, and for empirical absorption correction.⁵¹ The structure was solved by direct methods Shelx 97 and refined using Shelx 97 suite of programs.⁵²

4.2.4.7 Biology and Biochemistry

a) Preparation of recombinant human CK2 holoenzyme

Recombinant human CK2 holoenzyme was prepared according to a modified protocol of Grankowski *et al.*⁵³ as described earlier.⁵⁴ Human CK2 α - (CSNK2A1) and human CK2 β -subunit (CSNK2B) were expressed separately using a pT7-7 expression system in *Escherichia coli* BL21(DE3). In detail, freshly transformed starter cultures were grown overnight at 37 °C in LB-medium until the stationary phase was reached. Fresh LB-medium, inoculated with the separate starter cultures for both subunits, was cultivated until an OD₅₀₀ of 0.6 was reached. Protein expression was induced by the addition of IPTG (1 mM final concentration) and further incubation of the cultures at 30 °C for 5-6 h for the CK2 α - and for 3 h for the CK2 β -subunit. Bacterial cells were harvested by centrifugation (6000×g for 10 min at 4 °C) and disrupted by sonification (3 times 30 s on ice). Cell debris was removed by centrifugation and the bacterial extracts were combined prior to purification by a three-column procedure. Fractions showing CK2 activity were combined and analyzed by SDS-PAGE and Western Blot. The purity of the CK2 holoenzyme was superior to 99 %.¹⁵

b) Capillary electrophoresis based assay for the testing of inhibitors of the human CK2

Testing of the inhibitors of the human CK2 was performed by the recently established capillary electrophoresis based CK2 activity assay of Gratz *et al.*⁵⁵ 2 μL

of the dissolved inhibitors (stock solution in DMSO) mixed with 78 μL of kinase buffer (50 mM Tris/HCl (pH 7.5), 100 mM NaCl, 10 mM MgCl_2 and 1 mM DTT) containing 1 μg CK2 were preincubated at 37 $^\circ\text{C}$ for 10 min. CK2 reaction was initiated by the addition of 120 μL of likewise preincubated assay buffer (25 mM Tris/HCl (pH 8.5), 150 mM NaCl, 5 mM MgCl_2 , 1 mM DTT, 100 μM ATP and 0.19 mM of the substrate peptide RRRDDDSDDD). After 15 min the reaction was stopped by the addition of 4 μL EDTA (0.5 M). The reaction mixture was supplied to a PA800 plus capillary electrophoresis system (Beckman Coulter, Krefeld, Germany) using acetic acid (2 M, adjusted with conc. HCl to pH 2.0) as the background electrolyte. The separated substrate and product peptide were detected at 214 nm using a DAD detector. Samples containing pure DMSO served as a control for 0 % inhibition and samples additionally lacking the CK2 holoenzyme served as a control for 100 % inhibition. For the initial testing a final inhibitor concentration of 10 μM was applied. Compounds that exhibited at least 50 % inhibition at this concentration were subjected to an IC_{50} determination. For this purpose, nine inhibitor concentrations in appropriate intervals ranging from 0.001 μM to 100 μM were used. IC_{50} values were calculated from the resulting dose-response curves.

c) Cell culture and proliferation

MCF-7 breast cancer cells (kindly provided by the Department of Clinical Radiology of the University Hospital Münster, Germany), were cultured in RPMI 1640 medium - GlutaMaxTM (Life Technologies) and 10% fetal calf serum.⁴¹ They were seeded at a density of 5.0×10^4 cells per well into 24-well culture plates. After overnight incubation, seeding medium was removed and replaced with fresh medium containing the inhibitor at 20 μM or 100 μM . DMSO, at a final concentration of 1%, served as a control. Cells were incubated for 24 h or 48 h at 37 $^\circ\text{C}$ in a humidified atmosphere (5% CO_2). Cell proliferation was quantified by the EdU-click assay (baseclick BCK-EdU555-1, Baseclick GmbH, Munich, Germany): the nucleoside analog 5-ethynyl-2'-deoxyuridine is incorporated during active DNA synthesis and the 5-TAMRA-PEG3-azide fluorophore, used for detection, is coupled by click reaction; afterwards, nuclear DNA is stained using the DNA fluorophore **1** (500 μL of 3 $\mu\text{g}/\text{mL}$ in methanol) and cells were incubated for 30 min at room temperature in the dark, washed and finally overlayed with PBS.⁴² Cellular fluorescence was monitored with a

Keyence BZ-9000 fluorescence microscope (Keyence Corporation, Osaka, Japan) with the “hard-coated” TRITC filter (excitation 543/22 nm; emission 593/40 nm) for TAMRA detection and the “hard coated” DAPI BP filter (excitation 377/50 nm; emission 447/60 nm) for 1 detection. The number of cells exhibiting an active DNA synthesis (staining with Fluorophore 5-TAMRA-PEG3-azide) and the total number of cells (Hoechst staining) were counted. The results were expressed as a percent ratio of proliferating cells *versus* total number of cells.

d) Compounds

Mitoxantrone was purchased from Sigma Aldrich (France). All commercial reagents were of the highest available purity grade. The compounds were dissolved in DMSO, and then diluted in Dulbecco’s modified Eagle’s medium (DMEM high glucose). The stock solutions were stored at – 20 °C, and warmed to 25 °C just before use.

e) Cell Cultures

The human fibroblast HEK293 cell line was transfected with ABCG2 (HEK293-ABCG2) as previously described.⁴⁴ The cells were maintained in DMEM high glucose supplemented with 10% fetal bovine serum (FBS), 1% penicillin/streptomycin and 0.75 mg/mL G418 at 37 °C, 5% CO₂ under controlled humidity.

f) ABCG2-Mediated Mitoxantrone Efflux and Inhibition

As previously,⁴⁴ cells were seeded at a density of 1.0×10^5 cells/well into 24-well culture plates. After 72 h incubation, the cells were exposed to 5 μ M mitoxantrone for 30 min at 37 °C, in the presence or absence of each compound, and then washed with phosphate buffer saline (PBS) and trypsinized. The intracellular fluorescence was monitored with a FACS Calibur cytometer (Becton Dickinson) equipped with a 635-nm red laser, using the FL4 channel and at least 10,000 events were collected. The percentage of inhibition was calculated by using the following equation: $\% \text{ inhibition} = (C - M) / (C_{ev} - M) \times 100$, where C is the intracellular

fluorescence of resistant cells (HEK293-*ABCG2*) in the presence of compounds and mitoxantrone, M the intracellular fluorescence of resistant cells with only mitoxantrone, and C_{ev} the intracellular fluorescence of control cells (the same HEK293-*ABCG2* cells 100% inhibited with 1 μ M Ko143).

g) Intrinsic Cytotoxicity of the Inhibitory Compounds

Cell viability was evaluated through the MTT colorimetric assay.⁵⁶ Wild-type HEK293 cells were seeded at a density of 1×10^4 cells/well, into 96-well culture plates. After overnight incubation, the cells were treated with the compounds (0-250 μ M) for 72 h. To assess the viability, the cells were exposed to 0.5 mg/mL of MTT and incubated for 4 h at 37 °C. The culture medium was discarded, and 100 μ L of a DMSO/ethanol (1:1) solution was added into each well and mixed by gently shaking for 10 min. Absorbance was measured at 570 nm using a microplate reader at 570 nm, and the value measured at 690 nm was subtracted. Data are the mean \pm SD of at least three independent experiments.

4.2.5 Acknowledgements

G.J.G., E.W. and G.V. were recipients of mobility doctoral fellowships from the Brazilian CNPq-CAPES (Science without Borders Program 245762/2012-4) and CAPES (Process numbers 8792127 and 2303/10-8), respectively. N.D.Y. was recipient of a postdoctoral fellowship for the Control of Cancer-CNPq (Science without Borders Program). A.N. thanks the Algerian Ministry of Foreign Affairs and the Institut Français d'Algérie for his doctoral fellowship. Financial support was provided by the CNRS and Université Lyon 1 (UMR 5086), the Ligue Nationale Contre le Cancer (Equipe labellisée Ligue 2014), an international grant from French ANR and Hungarian NIH (2010-INT-1101-01). The Aquitaine Region is thanked for supporting equipment set up in CESAMO. We would like to thank M. Duong Minh Quang and Mrs. Thi Huong Nguyen for their assistance during the preparation of compounds **4j**, **4l** and **4o**, and Dr. Anthony Coleman for improving the english.

REFERENCES

- (1) Burnett, G.; Kennedy, E. P. The enzymatic phosphorylation of proteins. *J. Biol. Chem.* **1954**, *211*, 969-980.
- (2) Giusiano, S.; Cochet, C.; Filhol, O.; Duchemin-Pelletier, E.; Secq, V.; Bonnier, P.; Carcopino, X.; Boubli, L.; Birnbaum, D.; Garcia, S.; Iovanna, J.; Charpin, C. Protein kinase CK2 α subunit over-expression correlates with metastatic risk in breast carcinomas: quantitative immunohistochemistry in tissue microarrays. *Eur. J. Cancer* **2011**, *47*, 792-801.
- (3) Zhao, T.; Jia, H.; Li, L.; Zhang, G.; Zhao, M.; Cheng, Q.; Zheng, J.; Li, D. Inhibition of CK2 enhances UV-triggered apoptotic cell death in lung cancer cell lines. *Oncol. Rep.* **2013**, *30*, 377-384.
- (4) Giroux, V.; Dagorn, J. C.; Iovanna, J. L. A review of kinases implicated in pancreatic cancer. *Pancreatology* **2009**, *9*, 738-754.
- (5) Yao, K.; Youn, H.; Gao, X.; Huang, B.; Zhou, F.; Li, B.; Han, H. Casein kinase 2 inhibition attenuates androgen receptor function and cell proliferation in prostate cancer cells. *Prostate* **2012**, *72*, 1423-1430.
- (6) Borgo, C.; Cesaro, L.; Salizzato, V.; Ruzzene, M.; Massimino, M. L.; Pinna, L. A.; Donella-Deana, A. Aberrant signalling by protein kinase CK2 in imatinib-resistant chronic myeloid leukaemia cells: biochemical evidence and therapeutic perspectives. *Mol. Oncol.* **2013**, *7*, 1103-1115.
- (7) Zheng, Y.; McFarland, B. C.; Drygin, D.; Yu, H.; Bellis, S. L.; Kim, H.; Bredel, M.; Benveniste, E. N. Targeting protein kinase CK2 suppresses prosurvival signaling pathways and growth of glioblastoma. *Clin. Cancer Res.* **2013**, *19*, 6484-6494.
- (8) Papinutto, E.; Ranchio, A.; Lolli, G.; Pinna, L. A.; Battistutta, R. Structural and functional analysis of the flexible regions of the catalytic α -subunit of protein kinase CK2. *J. Struct. Biol.* **2012**, *177*, 382-391.
- (9) Kinoshita, T.; Nakaniwa, T.; Sekiguchi, Y.; Sogabe, Y.; Sakurai, A.; Nakamura, S.; Nakanishi, I. Crystal structure of human CK2 α at 1.06 Å resolution. *J. Synchrotron Radiat.* **2013**, *20*, 974-979.
- (10) Cao J. Y.; Shire, K.; Landry, C.; Gish, G. D.; Pawson, T.; Frappier, L. Identification of a novel protein interaction motif in the regulatory subunit of casein kinase 2. *Mol. Cell. Biol.* **2014**, *34*, 246-258.
- (11) Raaf, J.; Guerra, B.; Neundorff, I.; Bopp, B.; Issinger, O. G.; Jose, J.; Pietsch, M.; Niefind, K. First structure of protein kinase CK2 catalytic subunit with an effective CK2 β -competitive ligand. *ACS Chem. Biol.* **2013**, *17*, 901-907.
- (12) Dobrowolska, G.; Lozeman, F. J.; Li, D.; Krebs, E. G. CK2, a protein kinase of the next millennium. *Mol. Cell. Biochem.* **1999**, *191*, 3-12.

- (13) Prudent, R.; Sautel, C. F.; Cochet, C. Structure-based discovery of small molecules targeting different surfaces of protein-kinase CK2. *Biochim. Biophys. Acta* **2010**, *1804*, 493-498.
- (14) Hundsdörfer, C.; Hemmerling, H. J.; Götz, C.; Totzke, F.; Bednarski, P.; Le Borgne, M.; Jose, J. Indeno[1,2-*b*]indole derivatives as novel class of potent human protein kinase CK2 inhibitors. *Bioorg. Med. Chem.* **2012**, *20*, 2282-2289.
- (15) Guillon, J.; Le Borgne, M.; Rimbault, C.; Moreau, S.; Savrimoutou, S.; Pinaud, N.; Baratin, S.; Marchivie, M.; Roche, S.; Bollacke, A.; Pecci, A.; Alvarez, L.; Desplat, V.; Jose, J. Synthesis and biological evaluation of novel substituted pyrrolo[1,2-*a*]quinoxaline derivatives as inhibitors of the human protein kinase CK2. *Eur. J. Med. Chem.* **2013**, *65*, 205-222.
- (16) Hundsdörfer, C.; Hemmerling, H. J.; Hamberger, J.; Le Borgne, M.; Bednarski, P.; Götz, C.; Totzke, F.; Jose, J. Novel indeno[1,2-*b*]indoloquinones as inhibitors of the human protein kinase CK2 with antiproliferative activity towards a broad panel of cancer cell lines. *Biochem. Biophys. Res. Commun.* **2012**, *424*, 71-75.
- (17) Conseil, G.; Perez-Victoria, J. M.; Jault, J.-M.; Gamarro, F.; Goffeau, A.; Hofmann, J.; Di Pietro, A. Protein kinase C effectors bind to multidrug ABC transporters and inhibit their activity. *Biochemistry* **2001**, *40*, 2564-2571.
- (18) Erlichman, C.; Boerner, S. A.; Hallgren, C. G.; Spieker, R.; Wang, X. Y.; James, C. D.; Scheffer, G. L.; Maliepaard, M.; Ross, D. D.; Bible, K. C.; Kaufmann, S. H. The HER tyrosine kinase inhibitor C11033 enhances cytotoxicity of 7-ethyl-10-hydroxycamptothecin and topotecan by inhibiting breast cancer resistance protein-mediated drug efflux. *Cancer Res.* **2001**, *61*, 739-748.
- (19) Houghton, P. J.; Germain, G. S.; Harwood, F. C.; Schuetz, J. D.; Stewart, C. F.; Buchdunger, E.; Traxler, P. Imatinib mesylate is a potent inhibitor of the ABCG2 (BCRP) transporter and reverses resistance to topotecan and SN-38 in vitro. *Cancer Res.* **2004**, *64*, 2333-2337.
- (20) Yanase, K.; Tsukahara, S.; Asada, S.; Ishikawa, E.; Imai, Y.; Sugimoto, Y. Gefitinib reverses breast cancer resistance protein-mediated drug resistance. *Mol. Cancer Ther.* **2004**, *3*, 1119-1125.
- (21) Ozvegy-Laczka, C.; Hegedus, T.; Varady, G.; Ujhelly, O.; Schuetz, J. D.; Varadi, A.; Keri, G.; Orfi, L.; Nemet, K.; Sarkadi, B. High-affinity interaction of tyrosine kinase inhibitors with the ABCG2 multidrug transporter. *Mol. Pharmacol.* **2004**, *65*, 1485-1495.
- (22) Dohse, M.; Scharenberg, C.; Shukla, S.; Robey, R. W.; Volkmann, T.; Deeken, J. F.; Brendel, C.; Ambudkar, S. V.; Neubauer, A.; Bates, S. E. Comparison of ATP-binding cassette transporter interactions with the tyrosine kinase inhibitors imatinib, nilotinib, and dasatinib. *Drug Metab. Dispos.* **2010**, *38*, 1371-1380.
- (23) Hegedus, C.; Truta-Feles, K.; Antalffy, G.; Varady, G.; Nemet, K.; Ozvegy-Laczka, C.; Keri, G.; Orfi, L.; Szakacs, G.; Varadi, A.; Sarkadi, B. Interaction of the EGFR inhibitors gefitinib, vandetanib, pelitinib and neratinib with the ABCG2 multidrug transporter: implications for the emergence and reversal of cancer drug

resistance. *Biochem. Pharmacol.* **2012**, *84*, 260-267.

(24) Lainey, E.; Sébert, M.; Thépot, S.; Scoazec, M.; Bouteloup, C.; Leroy, C.; De Botton, S.; Galluzzi, L.; Fenaux, P.; Kroemer, G. Erlotinib antagonizes ABC transporters in acute myeloid leukemia. *Cell Cycle* **2012**, *11*, 4079-4092.

(25) Mazard, T.; Causse, A.; Simony, J.; Leconet, W.; Vezzio-Vie, N.; Torro, A.; Jarlier, M.; Evrard, A.; Del Rio, M.; Assenat, E.; Martineau, P.; Ychou, M.; Robert, B.; Gongora, C. Sorafenib overcomes irinotecan resistance in colorectal cancer by inhibiting the ABCG2 drug-efflux pump. *Mol. Cancer Ther.* **2013**, *12*, 2121-2134.

(26) Bilbao-Meseguer, I.; Jose, B. S.; Lopez-Gimenez, L. R.; Gil, M. A.; Serrano, L.; Castano, M.; Sautua, S.; Basagoiti, A. D.; Belaustegui, A.; Baza, B.; Baskaran, Z.; Bustinza, A. Drug interactions with sunitinib. *J. Oncol. Pharm. Pract.* **2014**, January 8, doi: 10.1177/1078155213516158.

(27) Zhang, H.; Kathawala, R. J.; Wang, Y. J.; Zhang, Y. K.; Patel, A.; Shukla, S.; Robey, R. W.; Talele, T. T.; Ashby, C. R. Jr.; Ambudkar, S. V.; Bates, S. E.; Fu, L. W.; Chen, Z. S. Linsitinib (OSI-906) antagonizes ATP-binding cassette subfamily G member 2 and subfamily C member 10-mediated drug resistance. *Int. J. Biochem. Cell Biol.* **2014**, *51C*, 111-119.

(28) Robey, R. W.; Shukla, S.; Steadman, K.; Obrzut, T.; Finley, E. M.; Ambudkar, S. V.; Bates, S. E. Inhibition of ABCG2-mediated transport by protein kinase inhibitors with a bisindolylmaleimide or indolocarbazole structure. *Mol. Cancer Ther.* **2007**, *6*, 1877-1885.

(29) Sim, H.-M.; Lee, C.-Y.; Ee, P. L. R.; Go, M.-L. Dimethoxyaurones: potent inhibitors of ABCG2 (breast cancer resistance protein). *Eur. J. Pharm. Sci.* **2008**, *35*, 293-306.

(30) Diestra, J. E.; Scheffer, G. L.; Català, I.; Maliepaard, M.; Schellens, J. H.; Scheper, R. J.; Germà-Lluch, J. R.; Izquierdo, M. A. Frequent expression of the multi-drug resistance-associated protein BCRP/MXR/ABCP/ABCG2 in human tumors detected by the BXP-21 monoclonal antibody in paraffin-embedded material. *J. Pathol.* **2002**, *198*, 213-219.

(31) Allen, J. D.; van Loevezijn, A.; Lakhai, J. M.; van der Valk, M.; van Tellingen, O.; Reid, G.; Schellens, J. H. M.; Koomen, G.-J.; Schinkel, A. H. Potent and specific inhibition of the breast cancer resistance protein multidrug transporter *in vitro* and in mouse intestine by a novel analogue of fumitremorgin C. *Mol. Cancer Ther.* **2002**, *1*, 417-425.

(32) Kühnle, M.; Egger, M.; Müller, C.; Mahringer, A.; Bernhardt, G.; Fricker, G.; König, B.; Buschauer, A. Potent and selective inhibitors of breast cancer resistance protein (ABCG2) derived from the p-glycoprotein (ABCB1) modulator tariquidar. *J. Med. Chem.* **2009**, *52*, 1190-1197.

(33) Hemmerling, H. J.; Reiss, G. Partially saturated indeno[1,2-*b*]indole derivatives via deoxygenation of heterocyclic α -hydroxy-N,O-hemiaminals. *Synthesis* **2009**, *6*, 985-999.

- (34) Richey, H. G.; Farkas, J. Sulfamides and sulfonamides as polar aprotic solvents. *J. Org. Chem.* **1987**, *52*, 479-483.
- (35) Lui, W.; Buck, M.; Chen, N.; Shang, M.; Talor, N. J.; Asoud, J.; Wu, X.; Hasinoff, B. B.; Dmitrienko, G. I. Total synthesis of isoprekinamycin: structural evidence for enhanced diazonium ion character and growth inhibitory activity toward cancer cells. *Org. Lett.* **2007**, *19*, 2915-2918.
- (36) Matsuo, K.; Ishida, S. Synthesis of Murrayaquinone-A. *Chem. Pharm. Bull.* **1994**, *42*, 1325-1327.
- (37) Alchab, F.; Ettouati, L.; Bouaziz, Z.; Bollacke, A.; Delcros, J-G.; Gertzen, C. G. W.; Gohlke, H.; Pinaud, N.; Marchivie, M.; Guillon, J.; Fenet, B.; Jose, J.; Le Borgne, M. Unpublished results.
- (38) Janreddy, D.; Kavala, V.; Bosco, J. W. J.; Kuo, C.-W.; Yao, C.-F. An easy access to carbazolones and 2,3-disubstituted indoles. *Eur. J. Org. Chem.* **2011**, *12*, 2360-2365.
- (39) Bill, K.; Black, G. G.; Falshaw, C. P.; Sainsbury, M. The coupling reactions of 3-acylindoles and proof of structure of the palladium (II) acetate mediated cyclisation reaction product of 3-benzoyl-1-methylindole. *Heterocycles* **1983**, *20*, 2433-2436.
- (40) Gray, G. K.; McFarland, B. C.; Rowse, A. L.; Gibson, S. A.; Benveniste, E. N. Therapeutic CK2 inhibition attenuates diverse prosurvival signaling cascades and decreases cell viability in human breast cancer cells. *Oncotarget* **2014**, *5*, 6484-6496.
- (41) Xue, L.; Chiu, S.; Oleinick, N. L. Staurosporine-induced death of MCF-7 human breast cancer cells: a distinction between caspase-3-dependent steps of apoptosis and the critical lethal lesions. *Exp. Cell Res.* **2003**, *283*, 135-145.
- (42) Salic, A.; Mitchinson, T. J. A chemical method for fast and sensitive detection of DNA synthesis in vivo. *Proc. Natl. Acad. Sci. USA* **2008**, *105*, 2415-2420.
- (43) Latt, S. A.; Stetten, G.; Juergens, L. A.; Willard, H. F.; Scher, C. D. Recent developments in the detection of deoxyribonucleic acid synthesis by 33258 Hoescht fluorescence. *J. Histochem. Cytochem.* **1975**, *23*, 493-505.
- (44) Winter, E.; Lecerf-Schmidt, F.; Jabor Gozzi, G.; Peres, B.; Lightbody, M.; Gauthier, C.; Ozvegy-Laczka, C.; Szakacs, G.; Sarkadi, B.; Creczynski-Pasa, T.; Boumendjel, A.; Di Pietro, A. Structure-activity relationships of chromone derivatives toward mechanism of interaction with, and inhibition of, breast cancer resistance protein ABCG2. *J. Med. Chem.* **2013**, *56*, 9849-9860.
- (45) Ochoa-Puentes, C.; Höcherl, P.; Kühnle, M.; Bauer, S.; Bürger, K.; Bernhardt, G.; Buschauer, A.; König, B. Solid-phase synthesis of tariquidar-related modulators of breast cancer resistance protein (ABCG2). *Bioorg. Med. Chem. Lett.* **2011**, *21*, 3654-3657.
- (46) Matsson, P.; Englund, G.; Ahlin, G.; Bergström, C. A. S.; Norinder, U.; Artursson, P. A global drug inhibition pattern for the human ATP-binding cassette transporter breast cancer resistance protein (ABCG2). *J. Pharmacol. Exp. Ther.* **2007**, *323*, 19-

30.

(47) Ding, Y.-L.; Shih, Y.-H.; Tsai, F.-H.; Leong, M. K. In silico prediction of inhibition of promiscuous breast cancer resistance protein (BCRP/ABCG2). *PLoS ONE* **2014**, *9*, e90689.

(48) Stacy, A. E.; Jansson, P. J.; Richardson, D. R. Molecular pharmacology of ABCG2 and its role in chemoresistance. *Mol. Pharmacol.* **2013**, *84*, 655-669.

(49) Lecerf-Schmidt, F.; Peres, B.; Valdameri, G.; Gauthier, C.; Winter, E.; Payen, L.; Di Pietro, A.; Boumendjel, A. ABCG2: recent discovery of potent and highly selective inhibitors. *Future Med. Chem.* **2013**, *5*, 1037-1045.

(50) Supplementary X-ray crystallographic data: Cambridge Crystallographic Data Centre, University Chemical Lab, Lensfield Road, Cambridge, CB2 1EW, UK; e-mail: deposit@chemcrys.cam.ac.uk.

(51) Sheldrick G. M. (1996) SADABS, University of Göttingen, Germany.

(52) Sheldrick, G. M. A short history of SHELX. *Acta Crystallogr. Sect. A* **2008**, *64*, 112-122.

(53) Grankowski, N.; Boldyreff, B.; Issinger, O. G. Isolation and characterization of recombinant human casein kinase II subunits α and β from bacteria. *Eur. J. Biochem.* **1991**, *198*, 25-30.

(54) Olgen, S.; Götz, C.; Jose, J. Synthesis and biological evaluation of 3-(substituted-benzylidene)-1,3-dihydroindolin derivatives as human protein kinase CK2 and p60(c-Src) tyrosine kinase inhibitors. *Biol. Pharm. Bull.* **2007**, *30*, 715-718.

(55) Gratz, A.; Götz, C.; Jose, J. A CE-based assay for human protein kinase CK2 activity measurement and inhibitor screening. *Electrophoresis* **2010**, *31*, 634-640.

(56) Mosmann T. Rapid colorimetric assay for cellular growth and survival. Application to proliferation and cytotoxicity assays. *J. Immunol. Methods* **1983**, *65*, 55-63.

4.3 ARTIGO 3- Publicado em Drug Design, Development and Therapy, volume 9, p. 3481-95. Julho, 2015 (doi: 10.2147/DDDT.S84982).

“Republished with permission of Dove Press Limited, from Phenolic indeno[1,2-*b*]indoles as ABCG2-selective potent and nontoxic inhibitors stimulating basal ATPase activity, authors: Gustavo Jabor Gozzi; Zouhair Bouaziz; Evelyn Winter; Nathalia Daflon-Yunes; Mylène Honorat; Nathalie Guragossian; Christelle Marminon; Glaucio Valdameri; Andre Bollacke; Jean Guillon; Noël Pinaud; Mathieu Marchivie; Silvia M. Cadena; Joachim Jose; Marc Le Borgne and Attilio Di Pietro, volume 2015:9, 2015; permission conveyed through Copyright Clearance Center, Inc.”
Link: <https://dx.doi.org/10.2147/DDDT.S84982>

Phenolic indeno[1,2-*b*]indoles as ABCG2-selective potent and nontoxic inhibitors stimulating basal ATPase activity

Gustavo Jabor Gozzi^{1,2,#}, Zouhair Bouaziz^{3,#}, Evelyn Winter^{1,4}, Nathalia Daflon-Yunes¹, Mylène Honorat¹, Nathalie Guragossian³, Christelle Marminon³, Glaucio Valdameri^{1,2}, Andre Bollacke⁵, Jean Guillon⁶, Noël Pinaud⁷, Mathieu Marchivie⁸, Silvia M. Cadena², Joachim Jose⁵, Marc Le Borgne^{3,§}, and Attilio Di Pietro^{1,§,*}

¹Equipe Labellisée Ligue 2014, BMSSI UMR 5086 CNRS/Université Lyon 1, IBCP, 69367 Lyon, France

²Department of Biochemistry and Molecular Biology, Federal University of Paraná, Curitiba, Paraná, Brazil

³Université de Lyon, Université Lyon 1, Faculté de Pharmacie - ISPB, EA 4446 Biomolécules Cancer et Chimiorésistances, SFR Santé Lyon-Est CNRS UMS3453 - INSERM US7, 69373 Lyon Cedex 8, France

⁴Department of Pharmaceutical Sciences, PGFAR, Federal University of Santa Catarina, Florianopolis, Santa Catarina, Brazil

⁵Institute of Pharmaceutical and Medicinal Chemistry, PharmaCampus, Westfälische Wilhelms-University Münster, 48149 Münster, Germany

⁶Université de Bordeaux, UFR des Sciences Pharmaceutiques, INSERM U869, Laboratoire ARNA, 33076 Bordeaux Cedex, France

⁷ISM - CNRS UMR 5255, Université de Bordeaux, 33405 Talence Cedex, France

⁸Université de Bordeaux, ICMCB CNRS-UPR 9048, 33608 Pessac Cedex, France

#Both researchers equally contributed to the experiments.

§Both senior investigators equally contributed to work supervision.

ABSTRACT

Ketonic indeno[1,2-*b*]indole-9,10-dione derivatives, initially designed as human casein kinase II (CK2) inhibitors, were recently shown to be converted into efficient inhibitors of drug efflux by the breast cancer resistance protein ABCG2 upon suited substitutions including a *N*⁶-phenethyl on C-ring and hydrophobic groups on D-ring. A series of 10 phenolic and 7 *p*-quinonic derivatives were synthesized and screened for inhibition of both CK2 and ABCG2 activities. The best phenolic inhibitors were about 3-fold more potent against ABCG2 than the corresponding ketonic derivatives, and showed low cytotoxicity. They were selective for ABCG2 over both P-glycoprotein and MRP1, whereas the ketonic derivatives also interacted with MRP1, and they additionally displayed a lower interaction with CK2. Quite interestingly, they strongly stimulated ABCG2 ATPase activity, in contrast to ketonic derivatives, suggesting distinct binding sites. In contrast, the *p*-quinonic indenoindoles were cytotoxic and poor ABCG2 inhibitors, whereas a partial inhibition recovery could be reached upon hydrophobic substitutions on D-ring, similarly to the ketonic derivatives.

Keywords: Multidrug resistance, cancer cells, ABCG2/BCRP, indenoindole inhibitors, structure-activity relationships, ATPase activity.

4.3.1 Introduction

A major obstacle of tumor treatment by chemotherapy is cancer cell multidrug resistance, which may be caused by several factors including overexpression of multidrug ATP-binding cassette (ABC) transporters. These transmembrane proteins work as efflux pumps reducing the intracellular concentration of drugs.¹ Among the 48 human genes encoding ABC transporters, only three are recognized to be associated to low prognostic in cancer patients: ABCB1/Pgp (P-glycoprotein), ABCC1/MRP1 (multidrug resistance protein 1) and ABCG2/BCRP (breast cancer resistance protein).² Pgp was the first multidrug ABC transporter to be discovered, and has been extensively studied,³ while MRP1 was later associated to multidrug resistance,⁴ and ABCG2 was more recently identified.⁵⁻⁷

One of the strategies aimed at eliminating resistant tumors is to use inhibitors of the multidrug ABC transporters. Combination of inhibitors with anticancer drugs should increase the intracellular accumulation of drugs and their availability to cellular targets. A number of Pgp inhibitors have been optimized *in vitro*, up to third/fourth-generation compounds, but their intrinsic toxicity and low *in vivo* activity prevented the achievement of clinical trials.^{8,9}

ABCG2 is a “half-transporter” of 655 aminoacids, containing one cytosolic nucleotide-binding domain (NBD) and one transmembrane domain (TMD) with six α -

helical spans, which needs to at least dimerize to be functional (Figure 1). This transporter is present in various membrane barriers protecting sensitive organs, as well as in many types of cancer cells.^{10,11} Selective inhibitors are interesting for two main reasons: i) *in vitro* to study the specific role of the transporter, and ii) *in vivo*, hopefully up to clinical trials, to use very low concentrations to inhibit each targeted transporter because most potent P-glycoprotein inhibitors, such as elacridar or tariquidar, also inhibited ABCG2 but at much higher concentrations expected to induce cytotoxicity and related side effects. The first specific ABCG2 inhibitor, of natural origin, was fumitremorgin C (FTC) which unfortunately displayed serious neurotoxicity.¹² Synthetic derivatives were developed, resulting in the highly potent Ko143 inhibitor, which however still retained significant residual toxicity.¹³ Screening of different classes of flavonoids identified interesting inhibitors such as hydrophobic flavones, acridones, chromones, asymmetric chalcones and symmetric *bis*-chalcones,¹⁴ some of them being active *in vivo* in mouse models.^{15,16}

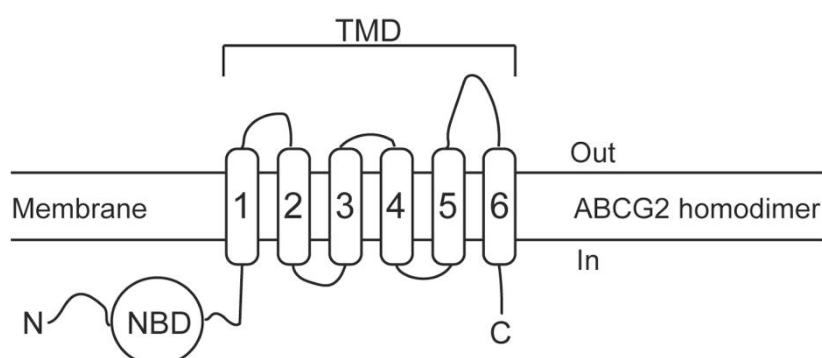


FIGURE 1: STRUCTURAL ARRANGEMENT OF ABCG2

A different type of ABCG2-selective inhibitors was recently developed as a series of ketonic indenoindoles, upon appropriate substitutions of potent inhibitors of casein kinase II (CK2), such as the replacement of isopropyl by phenethyl at N^5 position of C-ring, and the addition of hydrophobic substituents on D-ring.¹⁷ The present work was aimed at further modifying the D-ring, by replacing the ketone by either a phenol or a *p*-quinone, and reinvestigating the effects of substituents (Figure 2). The results showed that phenolic indenoindoles, independently of hydrophobic substituents, were better inhibitors of ABCG2-mediated drug efflux than the previously described ketonic derivatives, through higher potency and selectivity, and

the ability to strongly stimulate ATPase activity. In contrast, the *p*-quinonic derivatives displayed reduced inhibition capacity and significant cytotoxicity.

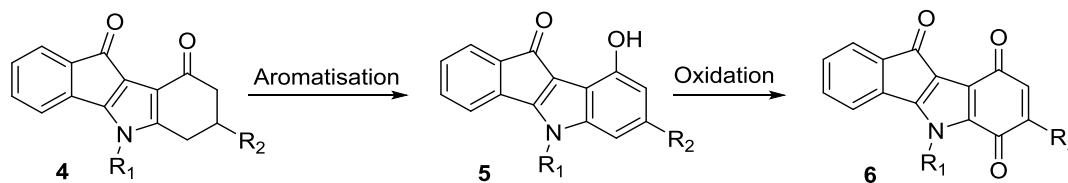


FIGURE 2: PREPARATION OF THE TARGET COMPOUNDS 5 AND 6 FROM KETONES 4

4.3.2 Material and Methods

4.3.2.1 Chemistry

Melting points were determined on an Electrothermal 9200 capillary apparatus. The IR spectra were recorded on a Perkin Elmer Spectrum Two IR Spectrometer. The ^1H and ^{13}C NMR spectra were recorded at 400 MHz on a Bruker DRX 400 spectrometer. Chemical shifts are expressed in ppm (δ) downfield from internal tetramethylsilane and coupling constants J are reported in hertz (Hz). The following abbreviations are used: s: singlet; bs: broad singlet; d: doublet; t: triplet; dd: doubled doublet; dt: doubled triplet; q: quartet; m: multiplet; Cquat: quaternary carbons. The mass spectra were performed by direct ionization (EI or CI) on a ThermoFinnigan MAT 95 XL apparatus. Chromatographic separations were performed on silica gel columns by column chromatography (Kieselgel 300-400 mesh). All reactions were monitored by TLC on GF254 plates that were visualized under a UV lamp (254 nm). Evaporation of solvent was performed in vacuum with rotating evaporator. The purity of the final compounds (greater than 95%) was determined by uHPLC/MS on an Agilent 1290 system using a Agilent 1290 Infinity ZORBAX Eclipse Plus C18 column (2.1 x 50 mm, 1.8 μm particle size) with a gradient mobile phase of $\text{H}_2\text{O}/\text{CH}_3\text{CN}$ (90:10, v/v) with 0.1% of formic acid to $\text{H}_2\text{O}/\text{CH}_3\text{CN}$ (10:90, v/v) with 0.1% of formic acid at a flow rate of 0.5 mL/min, with UV monitoring at the wavelength of 254 nm with a runtime of 10 min.

a) General procedure for the synthesis of compounds 5

To a solution of compound **4** (2.4 mmol) in Ph₂O (15 mL) was added 0.48 g of 10% Pd-C. Then, the mixture was heated to reflux for 6 h. After cooling, 25 mL of MeOH were added and the solution filtered on celite. Evaporation of the solvent left a residue which was purified by silica gel column chromatography using EtOAc/cyclohexane (1:2, v/v) as the eluent.

Compound 5c: 9-Hydroxy-5-(2-phenylethyl)-5H-indeno[1,2-b]indol-10-one

Red solid. Yield 53%. mp 144 °C. IR (ν cm⁻¹): 3232, 1660, 1602, 1581. ¹H NMR (CDCl₃, 400 MHz) δ : 7.31 (m, 1H, Harom), 7.25-7.12 (m, 3H, Harom), 7.10-7.03 (m, 5H, Harom), 6.75-6.72 (m, 2H, Harom), 6.67 (dd, 1H, $J_1 = 0.4$ Hz, $J_2 = 7.8$ Hz, Harom), 6.45 (bs, 1H, OH), 4.36 (t, 2H, $J = 7.1$ Hz, CH₂N), 3.14 (t, 2H, $J = 7.1$ Hz, CH₂Ph). ¹³C NMR + DEPT (CDCl₃, 100 MHz) δ : 186.20 (Cquat), 157.04 (Cquat), 150.29 (Cquat), 143.65 (Cquat), 140.55 (Cquat), 137.40 (Cquat), 135.91 (Cquat), 132.41 (CH), 129.62 (CH), 129.19 (2CH), 129.10 (2CH), 127.55 (CH), 125.72 (CH), 123.56 (CH), 118.72 (CH), 115.14 (Cquat), 113.48 (Cquat), 108.33 (CH), 103.41 (CH), 47.92 (CH₂), 36.71 (CH₂). HRMS calcd for C₂₃H₁₇NNaO₂ [M + Na]⁺ 362.1151, found 362.1140.

Compound 5d: 9-Hydroxy-5-(3-phenylpropyl)-5H-indeno[1,2-b]indol-10-one

Red solid. Yield 64%. mp 146 °C. IR (ν cm⁻¹): 3441, 1665, 1603. ¹H NMR (DMSO-*d*₆, 400 MHz) δ : 9.53 (bs, 1H, OH), 7.34-7.23 (m, 8H, Harom), 7.10-6.96 (m, 3H, Harom), 6.62 (m, 1H, Harom), 4.39 (t, 2H, $J = 7.3$ Hz, NCH₂CH₂CH₂Ph), 2.74 (t, 2H, $J = 7.5$ Hz, NCH₂CH₂CH₂Ph), 2.12 (m, 2H, NCH₂CH₂CH₂Ph). ¹³C NMR + DEPT (DMSO-*d*₆, 100 MHz) δ : 183.62 (Cquat), 157.76 (Cquat), 152.13 (Cquat), 144.96 (Cquat), 141.82 (Cquat), 141.17 (Cquat), 134.98 (Cquat), 133.25 (CH), 130.36 (CH), 129.36 (2CH), 129.31 (2CH), 126.98 (CH), 125.34 (CH), 123.31 (CH), 119.76 (CH), 114.35 (Cquat), 113.59 (Cquat), 109.01 (CH), 103.67 (CH), 45.28 (CH₂), 32.98 (CH₂), 32.61 (CH₂). HRMS calcd for C₂₄H₁₉NNaO₂ [M + Na]⁺ 376.1308, found 376.1299.

Compound 5f: 9-Hydroxy-7-methyl-5-(2-phenylethyl)-5H-indeno[1,2-b]indol-10-one

Dark red solid. Yield 44%. mp 154 °C. IR (ν cm^{-1}): 3433, 1667, 1646, 1602. ^1H NMR (DMSO- d_6 , 400 MHz) δ : 9.41 (s, 1H, OH), 7.27-7.12 (m, 9H, Harom), 6.82 (s, 1H, H-6 or H-8), 6.45 (s, 1H, H-6 or H-8), 4.57 (t, 2H, $J = 7.0$ Hz, $\underline{\text{CH}_2\text{N}}$), 3.11 (t, 2H, $J = 7.0$ Hz, $\underline{\text{CH}_2\text{Ph}}$), 2.54 (s, 3H, CH_3 -7). ^{13}C NMR + DEPT (DMSO- d_6 , 100 MHz) δ : 183.70 (Cquat), 157.84 (Cquat), 151.60 (Cquat), 144.88 (Cquat), 140.92 (Cquat), 138.58 (Cquat), 135.11 (Cquat), 134.98 (Cquat), 132.98 (CH), 129.97 (2CH), 129.90 (CH), 129.24 (2CH), 127.52 (CH), 122.91 (CH), 119.45 (CH), 114.17 (Cquat), 111.51 (Cquat), 110.56 (CH), 103.97 (CH), 47.30 (CH_2), 36.45 (CH_2), 22.48 (CH_3). HRMS calcd for $\text{C}_{24}\text{H}_{19}\text{NNaO}_2$ [$\text{M} + \text{Na}$] $^+$ 376.1308, found 376.1295.

Compound 5g: 9-Hydroxy-7-phenyl-5-(2-phenylethyl)-5H-indeno[1,2-b]indol-10-one

Dark red solid. Yield 55%. mp 168 °C. IR (ν cm^{-1}): 3428, 1665, 1633, 1600. ^1H NMR (CDCl_3 , 400 MHz) δ : 7.53 (d, 2H, $J = 7.3$ Hz, Harom), 7.44 (t, 2H, $J = 7.3$ Hz, Harom), 7.38-7.03 (m, 9H, Harom), 6.91 (s, 1H, H-6 or H-8), 6.82 (s, 1H, H-6 or H-8), 6.72 (d, 1H, $J = 6.5$ Hz, Harom), 6.42 (bs, 1H, OH), 4.36 (t, 2H, $J = 7.1$ Hz, $\underline{\text{CH}_2\text{N}}$), 3.14 (t, 2H, $J = 7.1$ Hz, $\underline{\text{CH}_2\text{Ph}}$). ^{13}C NMR + DEPT (CDCl_3 , 100 MHz) δ : 186.11 (Cquat), 157.42 (Cquat), 150.08 (Cquat), 144.05 (Cquat), 141.75 (Cquat), 140.47 (Cquat), 139.64 (Cquat), 137.41 (Cquat), 135.82 (Cquat), 132.44 (CH), 129.59 (CH), 129.17 (2CH), 129.12 (2CH), 129.06 (2CH), 127.55 (4CH), 123.50 (CH), 118.73 (CH), 114.91 (Cquat), 112.58 (Cquat), 108.09 (CH), 102.29 (CH), 47.81 (CH_2), 36.74 (CH_2). HRMS calcd for $\text{C}_{29}\text{H}_{22}\text{NO}_2$ [$\text{M} + \text{H}$] $^+$ 416.1645, found 416.1635.

Compound 5h: 9-Hydroxy-5-[2-(2-methoxyphenyl)ethyl]-5H-indeno[1,2-b]indol-10-one

Red solid. Yield 51%. mp 166 °C. IR (ν cm^{-1}): 3408, 1666, 1642, 1603. ^1H NMR (CDCl_3 , 400 MHz) δ : 7.34 (dd, 1H, $J_1 = 1.0$ Hz, $J_2 = 7.0$ Hz, Harom), 7.21-6.99 (m, 6H, Harom), 6.85-6.80 (m, 3H, Harom), 6.67 (d, 1H, $J = 7.8$ Hz, Harom), 6.45 (bs, 1H, OH), 4.37 (t, 2H, $J = 7.6$ Hz, $\underline{\text{CH}_2\text{N}}$), 3.86 (s, 3H, OCH_3), 3.16 (t, 2H, $J = 7.6$ Hz, $\underline{\text{CH}_2\text{Ph}}$). ^{13}C NMR + DEPT (CDCl_3 , 100 MHz) δ : 186.19 (Cquat), 157.83 (Cquat), 157.16 (Cquat), 150.24 (Cquat), 143.95 (Cquat), 140.82 (Cquat), 136.09 (Cquat), 132.39 (CH), 131.04 (CH), 129.65 (CH), 129.03 (CH), 125.60 (CH), 125.53 (Cquat),

123.55 (CH), 121.20 (CH), 118.96 (CH), 115.01 (Cquat), 113.49 (Cquat), 110.67 (CH), 108.22 (CH), 103.51 (CH), 55.57 (CH₃), 46.12 (CH₂), 32.12 (CH₂). HRMS calcd for C₂₄H₁₉NNaO₃ [M + Na]⁺ 392.1257, found 392.1248.

Compound 5i: 9-Hydroxy-5-[2-(3-methoxyphenyl)ethyl]-5H-indeno[1,2-b]indol-10-one

Red solid. Yield 50%. mp 138 °C. IR (ν cm⁻¹): 3461, 1671, 1604, 1582. ¹H NMR (CDCl₃, 400 MHz) δ: 7.32 (d, 1H, *J* = 6.2 Hz, Harom), 7.16-7.04 (m, 4H, Harom), 6.75-6.65 (m, 5H, Harom), 6.55 (bs, 1H, OH), 6.45 (s, 1H, Harom), 4.36 (t, 2H, *J* = 7.1 Hz, CH₂N), 3.67 (s, 3H, OCH₃), 3.10 (t, 2H, *J* = 7.1 Hz, CH₂Ph). ¹³C NMR + DEPT (CDCl₃, 100 MHz) δ: 186.18 (Cquat), 160.26 (Cquat), 157.10 (Cquat), 150.32 (Cquat), 143.66 (Cquat), 140.52 (Cquat), 138.93 (Cquat), 135.93 (Cquat), 132.40 (CH), 130.27 (CH), 129.61 (CH), 125.74 (CH), 123.55 (CH), 121.37 (CH), 118.75 (CH), 115.12 (Cquat), 115.06 (CH), 113.48 (Cquat), 112.77 (CH), 108.36 (CH), 103.43 (CH), 55.52 (CH₃), 47.84 (CH₂), 36.67 (CH₂). HRMS calcd for C₂₄H₁₉NNaO₃ [M + Na]⁺ 392.1257, found 392.1258.

Compound 5j: 9-Hydroxy-5-[2-(4-methoxyphenyl)ethyl]-5H-indeno[1,2-b]indol-10-one

Red solid. Yield 47%. mp 150 °C. IR (ν cm⁻¹): 3422, 1667, 1601, 1512. ¹H NMR (CDCl₃, 400 MHz) δ: 7.31 (m, 1H, Harom), 7.10-7.03 (m, 3H, Harom), 6.96-6.93 (m, 2H, Harom), 6.76-6.66 (m, 5H, Harom), 6.45 (bs, 1H, OH), 4.31 (t, 2H, *J* = 7.0 Hz, CH₂N), 3.69 (s, 3H, OCH₃), 3.07 (t, 2H, *J* = 7.0 Hz, CH₂Ph). ¹³C NMR + DEPT (CDCl₃, 100 MHz) δ: 186.20 (Cquat), 159.20 (Cquat), 157.13 (Cquat), 150.28 (Cquat), 143.65 (Cquat), 140.56 (Cquat), 135.92 (Cquat), 132.35 (CH), 130.13 (2CH), 129.56 (CH), 129.44 (Cquat), 125.69 (CH), 123.50 (CH), 118.77 (CH), 115.06 (Cquat), 114.61 (2CH), 113.50 (Cquat), 108.32 (CH), 103.46 (CH), 55.62 (CH₃), 48.17 (CH₂), 35.81 (CH₂). HRMS calcd for C₂₄H₁₉NNaO₃ [M + Na]⁺ 392.1257, found 392.1252.

b) General procedure for the synthesis of compounds 6

A solution containing 0.63 mmol of **5** and 0.013 g of salcomine (Co-Salen) in 13 mL of DMF was stirred under oxygen atmosphere at room temperature for 24 h.

The solution was then poured into 100 mL of ice and water and stirred for 1 h. The resulting precipitate was filtered and washed with water and dried to give a first quantity of **6**. The filtrate was extracted with CH₂Cl₂. The organic phase was dried over sodium sulfate and evaporated in vacuum to give a second quantity of **6** which was purified by silica gel column chromatography with EtOAc/cyclohexane (1:2, v/v) as the eluent.

Compound 6c: 5-(2-Phenylethyl)-5H-indeno[1,2-b]indole-6,9,10-trione

Dark red solid. Yield 70%. mp 263 °C. IR (ν cm⁻¹): 1709, 1663, 1645, 1594, 1526. ¹H NMR (CDCl₃, 400 MHz) δ : 7.58 (dd, 1H, $J_1 = 1.0$ Hz, $J_2 = 7.2$ Hz, Harom), 7.34-7.16 (m, 7H, Harom), 7.04 (dd, 1H, $J_1 = 1.0$ Hz, $J_2 = 6.9$ Hz, Harom), 6.63 (AB, 2H, H-7 and H-8), 4.77 (t, 2H, $J = 7.2$ Hz, CH₂N), 3.18 (t, 2H, $J = 7.2$ Hz, CH₂Ph). ¹³C NMR + DEPT (CDCl₃, 100 MHz) δ : 186.40 (Cquat), 183.79 (Cquat), 181.95 (Cquat), 178.45 (Cquat), 155.80 (Cquat), 140.04 (Cquat), 137.47 (CH), 136.81 (Cquat), 136.70 (CH), 133.74 (Cquat), 133.58 (CH), 130.47 (CH), 129.26 (2CH), 129.23 (2CH), 127.68 (CH), 124.96 (CH), 122.96 (Cquat), 120.79 (Cquat), 119.44 (CH), 49.76 (CH₂), 37.28 (CH₂). HRMS calcd for C₂₃H₁₅NNaO₃ [M + Na]⁺ 376.0944, found 376.0936.

Compound 6d: 5-(3-Phenylpropyl)-5H-indeno[1,2-b]indole-6,9,10-trione

Red solid. Yield 30%. mp 205 °C. IR (ν cm⁻¹): 1709, 1662, 1647, 1589, 1526. ¹H NMR (CDCl₃, 400 MHz) δ : 7.55 (dd, 1H, $J_1 = 0.9$ Hz, $J_2 = 7.2$ Hz, Harom), 7.36-7.18 (m, 7H, Harom), 6.61 (AB, 2H, H-7 and H-8), 6.52 (d, 1H, $J = 7.0$ Hz, Harom), 4.52 (t, 2H, $J = 7.9$ Hz, CH₂N), 2.82 (t, 2H, $J = 7.1$ Hz, CH₂Ph), 2.24 (m, 2H, CH₂CH₂CH₂). ¹³C NMR + DEPT (CDCl₃, 100 MHz) δ : 183.69 (Cquat), 181.84 (Cquat), 178.50 (Cquat), 155.46 (Cquat), 140.47 (Cquat), 140.11 (Cquat), 137.44 (CH), 136.65 (CH), 133.87 (Cquat), 133.74 (CH), 136.61 (Cquat), 130.43 (CH), 129.07 (2CH), 128.97 (2CH), 126.88 (CH), 124.94 (CH), 122.80 (Cquat), 120.82 (Cquat), 119.71 (CH), 47.41 (CH₂), 33.04 (CH₂), 32.21 (CH₂). HRMS calcd for C₂₄H₁₇NNaO₃ [M + Na]⁺ 390.1101, found 390.1094.

Compound 6e: 5-Benzyl-7-phenyl-5H-indeno[1,2-b]indole-6,9,10-trione

Red solid. Yield 40%. mp 255 °C. IR (ν cm⁻¹): 1715, 1646, 1585. ¹H NMR (CDCl₃, 400 MHz) δ : 7.61 (d, 1H, $J = 6.8$ Hz, Harom), 7.43-7.27 (m, 12H, Harom),

7.16 (d, 1H, $J = 7.1$ Hz, Harom), 6.73 (s, 1H, H-8), 5.88 (s, 2H, NCH_2Ph). ^{13}C NMR + DEPT (CDCl_3 , 100 MHz) δ : 183.78 (Cquat), 181.71 (Cquat), 177.86 (Cquat), 156.49 (Cquat), 146.86 (Cquat), 140.20 (Cquat), 135.14 (Cquat), 134.29 (Cquat), 133.86 (Cquat), 133.85 (CH), 133.71 (CH), 133.34 (Cquat), 130.62 (CH), 130.10 (CH), 129.81 (2CH), 129.49 (2CH), 128.65 (2CH), 128.63 (CH), 126.85 (2CH), 125.02 (CH), 123.26 (Cquat), 120.66 (Cquat), 119.96 (CH), 51.21 (CH_2). HRMS calcd for $\text{C}_{28}\text{H}_{17}\text{NNaO}_3$ [$\text{M} + \text{Na}$] $^+$ 438.1101, found 438.1086.

Compound 6f: 7-Methyl-5-(2-phenylethyl)-5H-indeno[1,2-b]indole-6,9,10-trione

Red solid. Yield 80%. mp 228 °C. IR (ν cm^{-1}): 1717, 1645, 1609, 1532. ^1H NMR (CDCl_3 , 400 MHz) δ : 7.53 (dd, 1H, $J_1 = 0.7$ Hz, $J_2 = 7.1$ Hz, Harom), 7.32-7.15 (m, 7H, Harom), 7.01 (d, 1H, $J = 7.3$ Hz, Harom), 6.48 (q, 1H, $J = 1.6$ Hz, H-8), 4.74 (t, 2H, $J = 7.3$ Hz, CH_2N), 3.17 (t, 2H, $J = 7.3$ Hz, CH_2Ph), 2.07 (d, 3H, $J = 1.6$ Hz, Me-7). ^{13}C NMR + DEPT (CDCl_3 , 100 MHz) δ : 183.81 (Cquat), 181.95 (Cquat), 178.89 (Cquat), 155.72 (Cquat), 146.31 (Cquat), 140.04 (Cquat), 136.91 (Cquat), 133.99 (Cquat), 133.85 (Cquat), 133.51 (CH), 133.45 (CH), 130.28 (CH), 129.27 (2CH), 129.17 (2CH), 127.58 (CH), 124.79 (CH), 123.30 (Cquat), 120.39 (Cquat), 119.35 (CH), 49.78 (CH_2), 37.25 (CH_2), 16.19 (CH_3). HRMS calcd for $\text{C}_{24}\text{H}_{17}\text{NNaO}_3$ [$\text{M} + \text{Na}$] $^+$ 390.1102, found 390.1097.

Compound 6g: 7-Phenyl-5-(2-phenylethyl)-5H-indeno[1,2-b]indole-6,9,10-trione

Red solid. Yield 74%. mp 190 °C. IR (ν cm^{-1}): 1713, 1655, 1583. ^1H NMR (CDCl_3 , 400 MHz) δ : 7.59 (d, 1H, $J = 7.3$ Hz, Harom), 7.52-7.21 (m, 12H, Harom), 7.10 (d, 1H, $J = 7.1$ Hz, Harom), 6.76 (s, 1H, H-8), 4.85 (t, 2H, $J = 7.3$ Hz, CH_2N), 3.25 (t, 2H, $J = 7.3$ Hz, CH_2Ph). ^{13}C NMR + DEPT (CDCl_3 , 100 MHz) δ : 183.87 (Cquat), 181.83 (Cquat), 177.91 (Cquat), 156.17 (Cquat), 146.93 (Cquat), 140.11 (Cquat), 137.01 (Cquat), 134.13 (Cquat), 133.86 (Cquat), 133.75 (CH), 133.67 (CH), 133.53 (Cquat), 130.48 (CH), 130.20 (CH), 129.91 (2CH), 129.40 (2CH), 129.25 (2CH), 128.79 (2CH), 127.69 (CH), 124.91 (CH), 123.19 (Cquat), 120.34 (Cquat), 119.59 (CH), 49.94 (CH_2), 37.29 (CH_2). HRMS calcd for $\text{C}_{29}\text{H}_{20}\text{NO}_3$ [$\text{M} + \text{H}$] $^+$ 430.1438, found 430.1426.

c) X-ray data

The structure of compound **5c** has been established by X-ray crystallography at 170K. Red single crystal (0.25 x 0.25 x 0.03 mm³) of **5c** was obtained after 20 h at 17 °C from a CS₂/chloroform (70/30) solution: monoclinic, space group P1 21/c 1, a = 10.4901(3) Å, b = 10.1187(3) Å, c = 15.8195(4) Å, $\alpha = 90^\circ$, $\beta = 91.6571(11)^\circ$, $\gamma = 90^\circ$, V = 1678.48(8) Å³, Z = 4, $\delta(\text{calcd}) = 1.343 \text{ Mg}\cdot\text{m}^{-3}$, FW = 339.38 for C₂₃H₁₇NO₂, F(000) = 712. Crystallographic data were acquired at ICMCB (UPR 9048) on a Bruker K-CCD APEX 2. Full crystallographic results have been deposited at the Cambridge Crystallographic Data Centre (CCDC-991361), UK, as supplementary Material.¹⁸ The data were corrected for Lorentz and polarization effects and for empirical absorption correction.¹⁹ The structure was solved by direct methods Shelx 2013 and refined using Shelx 2013 suite of programs²⁰ found in the integrated OLEX2 package.²¹

4.3.2.2 Biology and biochemistry

a) Compounds

Mitoxantrone was purchased from Sigma Aldrich (France). All commercial reagents were of the highest available purity grade. The compounds were dissolved in DMSO, and then diluted in Dulbecco's modified Eagle's medium (high-glucose DMEM). The stock solutions were stored at - 20 °C, and warmed to 25 °C just before use.

b) Cell cultures

The human fibroblast HEK293 cell line was transfected with ABCG2 (HEK293-ABCG2) or its empty vector (HEK293-*pcDNA3*),²² as well as MRP1 (HEK293-*ABCC1*) and its empty vector (HEK293-*pcDNA5*). The cells were maintained in high-glucose DMEM supplemented with 10% fetal bovine serum (FBS), 1% penicillin/streptomycin at 37 °C, 5% CO₂ under controlled humidity. The mouse embryonic fibroblast wild-type (NIH3T3) and Pgp-overexpressing (NIH3T3-*ABCB1*) were maintained in the same conditions. The cell culture medium was supplemented with either 0.75 mg/mL G418 (HEK293-*ABCG2*), 200 µg/mL hygromycin B

(HEK293*pcDNA5* and HEK293*ABCC1*) or 60 ng/mL colchicin (NIH3T3).

c) ABCG2-mediated mitoxantrone efflux and inhibition

As previously described,²² cells were seeded at a density of 1.0×10^5 cells/well into 24-well culture plates. After 72 h incubation, the cells were exposed to 5 μ M mitoxantrone for 30 min at 37 °C, in the presence or absence of each compound, and then washed with phosphate buffer saline (PBS) and trypsinized. The intracellular fluorescence was monitored with a FACS Calibur cytometer (Becton Dickinson) equipped with a 635-nm red laser, using the FL4 channel and at least 10,000 events were collected. The percentage of inhibition was calculated by using the following equation: $\% \text{ inhibition} = (C - M) / (C_{ev} - M) \times 100$, where C is the intracellular fluorescence of resistant cells (HEK293-*ABCG2*) in the presence of compounds and mitoxantrone, M the intracellular fluorescence of resistant cells with only mitoxantrone, and C_{ev} the intracellular fluorescence of control cells (the same HEK293-*ABCG2* cells 100% inhibited with 1 μ M Ko143).

d) Intrinsic cytotoxicity of the inhibitory compounds

Cell viability was evaluated through the MTT colorimetric assay.²³ Wild-type HEK293 cells were seeded at a density of 1×10^4 cells/well, into 96-well culture plates. After overnight incubation, the cells were treated with the compounds (0-250 μ M) for 72 h. To assess the viability, the cells were exposed to 0.5 mg/mL of MTT and incubated for 4 h at 37 °C. The culture medium was discarded, and 100 μ L of a DMSO/ethanol (1:1) solution was added into each well and mixed by gently shaking for 10 min. Absorbance was measured at 570 nm using a microplate reader at 570 nm, and the value measured at 690 nm was subtracted. Data are the mean \pm SD of at least three independent experiments.

e) Inhibition of Pgp- and MRP1-mediated drug efflux

NIH3T3-*ABCB1* were seeded at a density of 6×10^4 cells/well into 24-well culture plates and incubated for 48 h at 37 °C, whereas HEK293 cells transfected with *ABCC1* were seeded at 2.5×10^5 cells/well for 72 h. The cells were respectively

exposed to rhodamine 123 (0.5 μM) or calcein-AM (0.2 μM) for 30 min at 37 °C, in the presence or absence of each compound, then washed with PBS and trypsinized. The intracellular fluorescence was monitored with a FACS Calibur cytometer (Becton Dickinson) using the FL1 channel and at least 10,000 events were collected. The percentage of inhibition was calculated relatively to 5 μM GF120918 or 35 μM verapamil, respectively, using similar equation as demonstrated to ABCG2 inhibition.

f) Effects on ABCG2 ATPase activity²⁴

Vanadate-sensitive ATPase activity was measured colorimetrically by determining the liberation of inorganic phosphate from ATP. The Sf9 membranes were prepared as previously and loaded with cholesterol. The incubation was performed in 96-well plates. Sf9 insect cell membranes (1 mg/mL) were incubated in a 50 mM Tris-HCl, 50 mM NaCl buffer (pH 8.0) containing sodium azide (3.3 mM) in the absence (with or without sodium orthovanadate at 0.33 mM) or presence of tested compounds (2 μM). The reaction was started by the addition of ATP-Mg (3.9 mM) and the plates were incubated for 30 min at 37 °C. The reaction was stopped with sodium dodecylsulfate (10%) and revealed with a mixture of ammonium molybdate reagent and 10% ascorbic acid (1:4). The absorbance was measured after 30-min incubation at 880 nm using a reader plate.

g) Preparation of recombinant human CK2 holoenzyme and assay of inhibitors activity

The human protein kinase CK2 holoenzyme was prepared as previously described.^{25,26} In brief, human CK2 α - (CSNK2A1) and CK2 β - subunits (CSNK2B) were expressed separately in *Escherichia coli* BL21(DE3) cells using the pT7-7 vector. Freshly-transformed cultures were grown over night at 37 °C in LB-medium until the stationary phase was reached. LB medium was inoculated with the starter cultures (1:100), and protein expression was induced by IPTG addition (1 mM final concentration) when an OD₅₀₀ of 0.6 was reached. The cultures were further incubated at 30 °C during 5-6 h for the CK2 α -subunit, or 3 h for the CK2 β -subunit. After harvesting the bacterial cells by centrifugation (6000xg for 10 min at 4 °C) and disruption by sonication (3 x 30 s on ice), cell debris were removed by another

centrifugation at 15.000xg (10 min, 4 °C). Both extracts were combined and CK2 holoenzyme was purified by a three-column procedure. Fractions were analyzed by SDS-PAGE and Western Blot. Those containing CK2 and showing CK2 activity were pooled and stored at - 80 °C as aliquots, which obtained CK2 holoenzyme with a purity higher than 99%.²⁷

For testing the compounds on CK2 inhibition, a capillary electrophoresis-based CK2 activity assay²⁸ was used. Briefly, 2 µL of the inhibitors solutions in DMSO were mixed with 78 µL of kinase buffer (50 mM Tris/HCl (pH 7.5), 100 mM NaCl, 10 mM MgCl₂ and 1 mM DTT) containing 1 µg CK2, and preincubated at 37 °C for 10 min. The CK2 reaction was initiated by the addition of preincubated assay buffer (25 mM Tris/HCl (pH 8.5), 150 mM NaCl, 5 mM MgCl₂, 1 mM DTT, 100 µM ATP and 190 µM of the CK2 substrate peptide RRRDDDSDDD), carried on for 15 min at 37 °C and was stopped by addition of 4 µL of 0.5 M EDTA. Subsequently, the reaction samples were fed to a PA800 plus capillary electrophoresis system (Beckman Coulter, Krefeld, Germany) using acetic acid (2 M, adjusted to pH 2.0 with concentrated HCl) as the background electrolyte. Detection of the separated CK2 reaction substrate and product peptide at 214 nm was accomplished by a DAD detector. As controls for 0% and 100% inhibition, samples containing pure DMSO instead of inhibitor and samples additionally lacking the CK2 holoenzyme respectively, were treated under identical conditions. Compounds which showed more than 50% inhibition in the initial test at a final inhibitor concentration of 10 µM were subjected to IC₅₀ determination. For this purpose, nine final inhibitor concentrations in suitable intervals ranging from 0.001 µM to 100 µM were tested. IC₅₀ values were calculated from the resulting dose-response curves using GraphPadPrism 5.02 (La Jolla, CA, USA).

4.3.3 Results

4.3.3.1 Chemistry

The access to 5,6,7,8-tetrahydroindeno[1,2-*b*]indole-9,10-diones **4** was previously detailed.¹⁷ Their syntheses started by the reaction of a cyclohexane-1,3-dione with the appropriate primary amine to form the enaminone derivatives, which were then condensed with ninhydrin. The resulting *vic*-dihydroxyindeno[1,2-*b*]indole-

9,10-diones were deoxygenated with tetraethylthionylamide (TETA) to afford compounds **4**.

9-Hydroxy-5*H*-indeno[1,2-*b*]indol-10-ones **5** were prepared by dehydrogenation of **4** with 10% Pd-C in refluxing diphenyl ether.²⁹ Subsequent oxidation with molecular dioxygen in the presence of salcomine³⁰ (Co-Salen), at room temperature, gave 5*H*-indeno[1,2-*b*]indole-6,9,10-triones **6** (Figure 3).

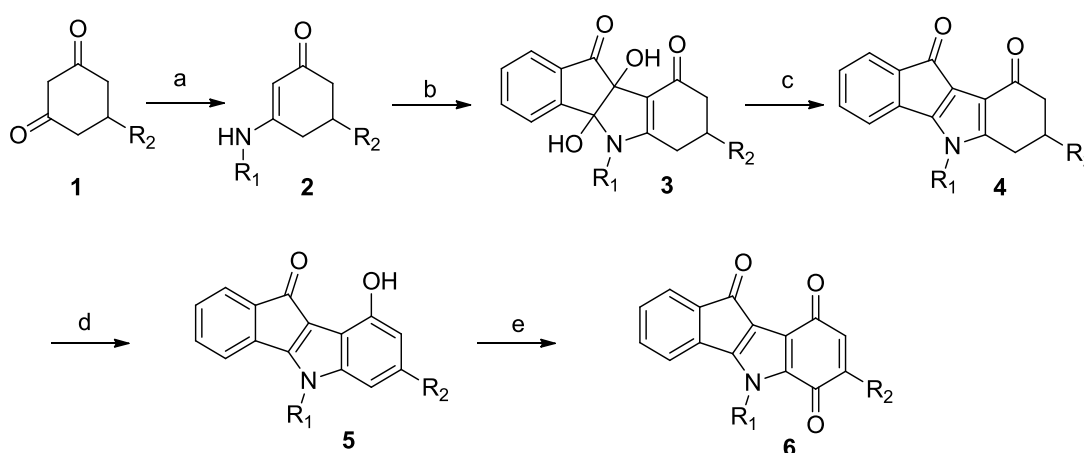


FIGURE 3: REAGENTS AND CONDITIONS

Notes: (a) R_1NH_2 , Toluene, reflux; (b) ninhydrin, MeOH, rt; (c) $(NEt_2)_2SO$ (TETA), DMF, AcOH, rt; (d) 10% Pd-C, Ph₂O, reflux, 6 h; (e) Co-Salen, DMF, O₂, rt, 24 h.

It is known that oxidation of phenols with Fremy's salt represents an excellent synthetic method for the preparation of *p*-quinones under mild conditions and usually in good yield.³¹ For this reason, we applied these conditions to oxidize compounds **5c** and **5g** (Figure 4), but very low yields of the desired products were obtained. This was presumably due to steric effects of R_1 and R_2 , or/and electronic destabilization of the radical intermediates. Accordingly, we preferred the method of oxidation with O_2 /salcomine that we applied for the synthesis of all *p*-quinones mentioned in this work.

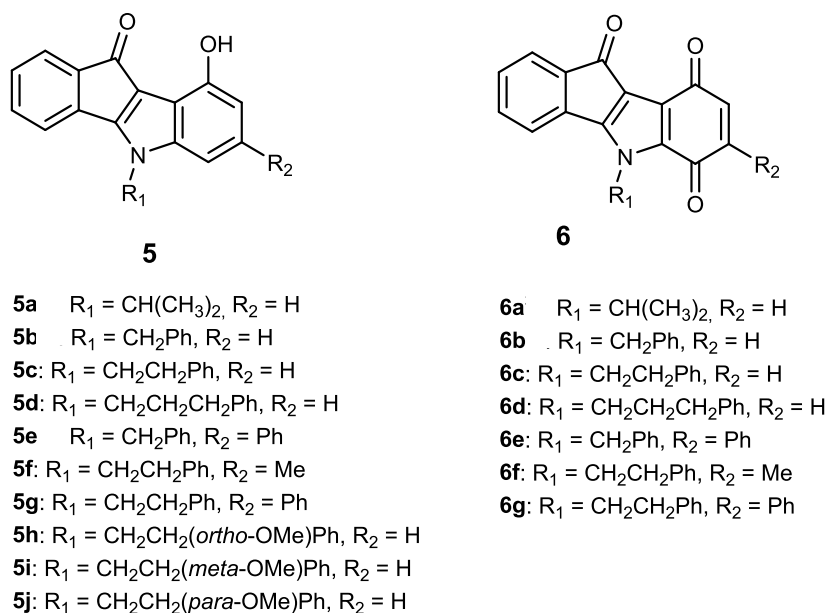


FIGURE 4: STRUCTURES OF THE INVESTIGATED INDENOINDOLE SERIES 5 AND 6

Note: 5a⁴¹; 5b⁴¹; 6a³⁰ and 6b³⁰

In total, ten phenols (series **5**) and seven quinones (series **6**) have been synthesized, and their structures are shown in Figure 4. The 3D spatial determinations of **5c** were established by X-ray crystallography, and confirmed the structure in the solid state as anticipated on the basis of IR and ¹H NMR data (Figure 5). The key bond lengths and angles of this indeno[1,2-*b*]indolone are very similar to those given in the literature for other substituted indenoindole derivatives.^{32,33} The indeno[1,2-*b*]indolone system of **5c** is nearly planar with a mean out-of-plane deviation of 0.027 Å and the largest deviation of 0.062(2) Å for atom C7. The C4=O1 double bond was noticed at 1.231 (2) Å.

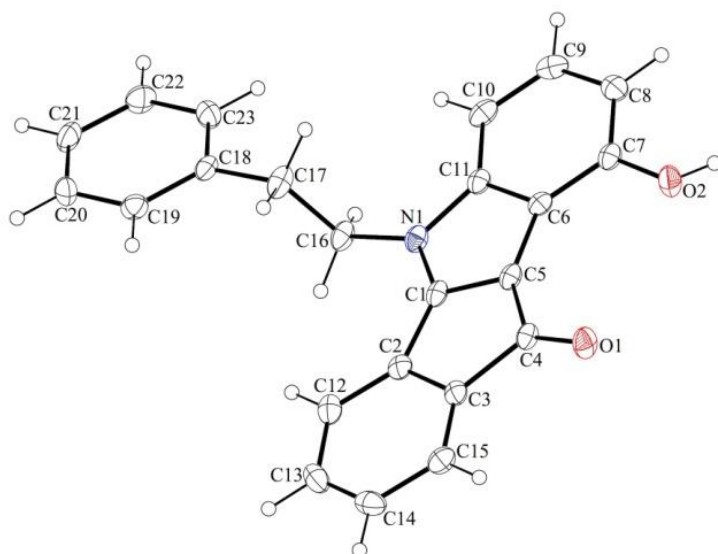


FIGURE 5: VIEW OF THE CRYSTAL STRUCTURE OF 5C WITH OUR NUMBERING SCHEME

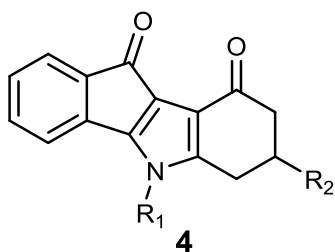
Notes: Displacement ellipsoids are drawn at the 30% probability level; the numbering used here is specific for crystallographic studies, and therefore different from that used detailed in the Experimental Section.

4.3.3.2 Biological evaluation and SARs

The newly-synthesized phenolic- and *p*-quinonic- indenoindoles were assayed for their capacity to modulate ABCG2 and CK2 activities, and for their cytotoxicity.

a) Inhibition of ABCG2-mediated mitoxantrone efflux, and cytotoxicity

The new series of compounds **5** and **6** were firstly screened for their ABCG2-inhibitory activities using mitoxantrone as a substrate, and the inhibitory potency was compared to the recently-characterized ketonic derivative **4c**¹⁷ (Figure 6). Other reference inhibitors of mitoxantrone efflux, used here as positive controls, were chromone 6g and Ko143 with IC₅₀ values of 0.11-0.13 μM and 0.09 μM, respectively.^{22,34}



- 4c:** R₁ = CH₂Ph, R₂ = H
4d: R₁ = CH₂CH₂CH₂Ph, R₂ = H
4h: R₁ = CH₂CH₂Ph, R₂ = Me
4j: R₁ = CH₂CH₂(*ortho*-OMe)Ph, R₂ = H
4k: R₁ = CH₂CH₂(*meta*-OMe)Ph, R₂ = H
4l: R₁ = CH₂CH₂(*para*-OMe)Ph, R₂ = H

FIGURE 6: STRUCTURES OF KETONIC INDENOINDOLES (SERIES 4).¹⁷

Table 1 shows that the corresponding phenolic derivative **5c**, without any substituent on both D-ring and *N*⁵-phenethyl, was about 3-fold more potent (IC₅₀ = 0.16 μM *versus* 0.43 μM). In contrast to ketonic indenoindoles,¹⁷ addition of hydrophobic methyl and phenyl substituents on D-ring did not further increase inhibition, producing either no effect or a negative contribution, as in **5f** (0.16 μM) and **5g** (0.51 μM) *versus* **5c**. Replacement of *N*⁵-phenethyl by a shorter linker drastically decreased the inhibitory potency, as evidenced from **5g** (full inhibition, with IC₅₀ = 0.51 μM) to **5e** (only 56% inhibition at 10 μM), as well as from **5c** (0.16 μM) to **5b** (68% inhibition). However, changing the *N*⁵-phenethyl substituent by a longer linker only slightly reduced the inhibitory potency, in **5d** (0.64 μM) *versus* **5c** (0.16 μM). Methoxy substitution of the *N*⁵-phenethyl phenolic-indenoindole core structure (**5c**), at either position *ortho* in **5h** (0.15 μM), *para* in **5j** (0.20 μM) or *meta* in **5i** (0.37 μM) did not show substantial improvement on activity. Phenyl substitution of D-ring was not able to recover any activity for *N*⁵-benzyl derivatives (**5e** *versus* **5b**). In sharp contrast, *p*-quinonic derivatives were very poor inhibitors when comparing **6c** (18% inhibition) to **5c** (and **4c**), **6d** (33% inhibition) to **5d**, and **6b** (10% inhibition) to **5b**. However, hydrophobic substitutions of D-ring allowed a partial recovery of inhibition potency, as illustrated for methyl and phenyl additions in **6f** (0.84 μM) and **6g** (0.43 μM) *versus* **6c**, and in **6e** (41% inhibition) *versus* **6b**.

TABLE 1. INHIBITION OF MITOXANTRONE EFFLUX IN ABCG2-TRANSFECTED CELLS, AND CYTOTOXICITY

Reference ketonic indenoindole	ABCG2 inhibition		Cytotoxicity IG ₅₀ (μM) ^d	TR ^e
	% at 10 μM ^a	IC ₅₀ (μM)		
4c	100 ± 14	0.43 ± 0.01 ^b	30.7 ± 9.5	71
Phenolic derivatives				
5a	45	~12 ^c	> 10	≥ 1
5b	68	~7 ^c	> 4	≥ 1
5c	81 ± 5	0.16 ± 0.02 ^b	42.7 ± 9.7	267
5d	98 ± 25	0.64 ± 0.23 ^b	> 100	> 156
5e	56	~9 ^c	4.8 ± 0.9	< 1
5f	92 ± 22	0.16 ± 0.01 ^b	42.3 ± 2.8	264
5g	111 ± 2	0.51 ± 0.09 ^b	> 100	> 196
5h	85 ± 11	0.15 ± 0.01 ^b	54 ± 14	360
5i	100 ± 10	0.37 ± 0.09 ^b	45.7 ± 6.1	124
5j	111 ± 14	0.20 ± 0.01 ^b	0.8 ± 0.1	4
p-Quinonic derivatives				
6a	36	~14 ^c	1.3 ± 0.4	< 1
6b	10	~50 ^c	0.53 ± 0.15	< 1
6c	18	~30 ^c	6.9 ± 2.1	< 1
6d	33	~15 ^c	6.8 ± 0.5	< 1
6e	41	~13 ^c	7.1 ± 1.1	< 1
6f	99 ± 9	0.84 ± 0.31 ^b	15.6 ± 5.9	19
6g	128 ± 6	0.43 ± 0.01 ^b	3.7 ± 2.2	9

Notes: ^aThe percent inhibition of ABCG2-mediated mitoxantrone efflux was determined for each compound at a fixed concentration of 10 μM. ^bFor the best compounds producing at least 50% inhibition at 10 μM, a concentration range was analyzed in order to precisely determine the IC₅₀ values. ^cFor the other, less potent compounds, a rough estimation was obtained from the experimental inhibition produced at 10 μM. ^dThe IG₅₀ values of compounds cytotoxicity were determined after 72 h of treatment with the MTT cell-survival method. ^eThe therapeutic ratio (TR) was calculated by dividing the IG₅₀ values of cytotoxicity with the corresponding IC₅₀ values of ABCG2 inhibition.

Since the root cause of *in vivo* and preclinical trial failures of potent ABCG2 inhibitors are their intrinsic cytotoxic effects, one valuable complementary approach is to evaluate the *in vitro* cytotoxicity of new inhibitors. The ratio between cytotoxicity and inhibitory potency of the inhibitor, defined here as therapeutic ratio (TR), gives a valuable information to guide future *in vivo* trials. The phenolic leads, **5c**, **5f** and **5h** (IC₅₀ = 0.15-0.16 μM), as well as **5d**, **5g** and **5i** (IC₅₀ = 0.37-0.64 μM), displayed a low cytotoxicity, with IG₅₀ values > 42 μM, and even > 100 μM in two cases. Such IG₅₀

values were similar to those previously observed with ketonic derivatives.¹⁷ This gave high therapeutic ratio (TR) values, up to 360, assumed to be quite promising for further investigations. The only exception was **5j**, which displayed an unexpectedly high cytotoxicity, possibly due to strong interaction with unknown critical cellular target(s). Similarly, shortening the phenethyl substituent into either benzyl (in **5b** and **5e**) or isopropyl (in **5a**) drastically increased cytotoxicity, leading to very low TR values (around 1). All *p*-quinonic derivatives were much more cytotoxic than phenolic compounds, except for **6e** where the already high toxicity of **5e** was not further increased, with IG₅₀ values in the 0.5-15 μ M range, and gave very low TR values (< 20, and often < 1). No cross-resistance was ever observed in ABCG2-transfected cells *versus* the control cell line (data not shown), indicating that both phenolic- and *p*-quinonic- indenoindoles were apparently not transported by ABCG2.

b) Selectivity toward ABCG2 inhibition

The most potent indenoindole inhibitors of ABCG2 were tested against the two other major multidrug ABC transporters of cancer cells, namely Pgp/ABCB1 and MRP1 (multidrug resistance protein 1)/ABCC1. Figure 7 shows that none of the selected compounds, including phenolic-, *p*-quinonic- and ketonic- derivatives were able to induce any inhibition of Pgp-mediated rhodamine 123 efflux, as compared to the reference inhibitor GF120918/elacridar. A differential pattern was obtained with MRP1-mediated calcein efflux: while the phenolic derivatives (**5c**, **5f** and **5h**) and *p*-quinonic derivatives (**6f** and **6g**) produced a very limited, if any, inhibition, in contrast the ketonic derivatives (**4h**, **4j** and **4k**)¹⁷ (Figure 7) significantly inhibited at 2 μ M and, in two cases, as efficiently as verapamil at 10 μ M. Therefore, phenolic- and *p*-quinonic-, but not ketonic-, inhibitors could be considered as ABCG2 selective over MRP1.

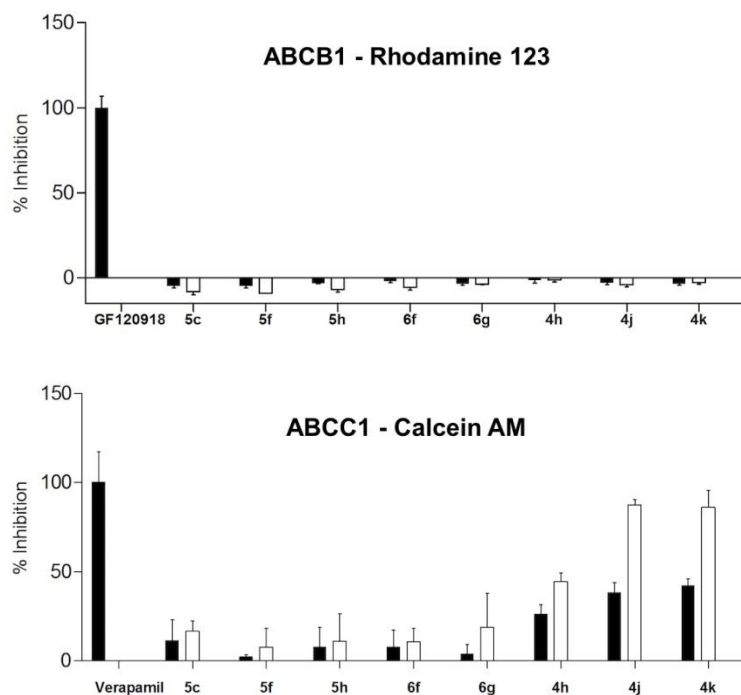


FIGURE 7: ABILITY OF LEADS OF THE DIFFERENT SERIES OF INDENOINDOLES TO INHIBIT DRUG EFFLUX BY ABCB1 OR ABCC1

Notes: Each indenoindole derivative was assayed at either 2 μM (black bars) or 10 μM (white bars) for its ability to alter the efflux of either rhodamine 123 by ABCB1 (upper panel) or calcein by ABCC1 (lower panel) assayed by flow cytometry, as for the efflux of mitoxantrone by ABCG2 in Table 1. The inhibition produced by the two reference inhibitors, 5 μM GF120918 and 35 μM verapamil, was taken as 100%.

A higher selectivity of phenolic indenoindoles, relatively to the ketonic derivatives, was also observed toward the CK2 protein kinase (Table 2). Indeed, the phenolic derivatives inhibited CK2 activity with a limited potency, never reaching a complete inhibition at 10 μM . The high values of the ABCG2/CK2 ratio, in the range 70-75 for **5f** and **5j**, were 7-to-12-fold higher than those previously obtained (in the range 6-11) for the corresponding ketonic derivatives (**4h** and **4i**)¹⁷ (Figure 6). A significant effect was also observed with **5d** and **5i**, giving a ratio value around 31, which was 2-to-4-fold higher than for the respective ketonic indenoindoles **4d** and **4k** (Figure 4). In the case of *p*-quinonic derivatives, the potency to inhibit CK2 was also lower, by about 2-fold, as compared to the ketonic ones, such as for **6c** (IC_{50} ~13 μM) *versus* **4c** (7.0 μM), and **6f** (4.1 μM) *versus* **4h** (2.5 μM),¹⁷ but their very low capacity to inhibit ABCG2 gave extremely low ABCG2/CK2 ratio values (< 1), except for the two more active compounds, **6f** and **6g**, containing hydrophobic substituents on D-ring (5-27).

TABLE 2: INHIBITION OF HUMAN CK2 HOLOENZYME AND COMPARISON WITH ABCG2

Reference ketonic indenoindole	CK2 inhibition		AGCG2/CK2 ^d
	% at 10 μ M ^a	IC ₅₀ (μ M)	
4c	59	7.0 ^b	16
Phenolic derivatives			
5a	72	2.0 ^b	< 1
5b	20	~25 ^c	~4
5c	57	7.5 ^b	47
5d	27	~20 ^c	~31
5e	48	~10.5 ^c	~1
5f	42	~12 ^c	~75
5g	45	~11 ^c	~22
5h	78	1.3 ^b	9
5i	44	~11.5 ^c	~31
5j	38	~14 ^c	~70
<i>p</i>-Quinonic derivatives			
6a	60	5.5 ^b	< 1
6b	70	2.2 ^b	< 1
6c	40	~13 ^c	< 1
6d	60	6.4 ^b	< 1
6e	40	~13 ^c	< 1
6f	65	4.1 ^b	5
6g	44	~11.5 ^c	~27

Notes: ^aThe percent inhibition of CK2 activity was determined, for each compound, at 10 μ M. ^bFor the best compounds, producing at least 50% inhibition at 10 μ M, the concentration was varied in order to precisely determine the IC₅₀ values. ^cFor the other, less potent compounds, a rough estimation was obtained from the experimental inhibition produced at 10 μ M. ^dThe ABCG2/CK2 ratio, indicating the inhibitory efficiency of compounds toward ABCG2 relatively to CK2, was calculated by dividing the IC₅₀(CK2) values with the IC₅₀(ABCG2) values of Table 1.

The interest of phenolic indenoindoles as ABCG2 inhibitors, *versus* ketonic- and *p*-quinonic- derivatives, is illustrated in Figure 8, where five phenolic leads, namely **5c**, **5d**, **5f**, **5g** and **5i**, display both a good selectivity, with a lower interaction toward CK2 than ketonic derivatives such as **4c** (Figure 8A), and a low cytotoxicity by difference with all *p*-benzoquinonic derivatives (Figure 8B).

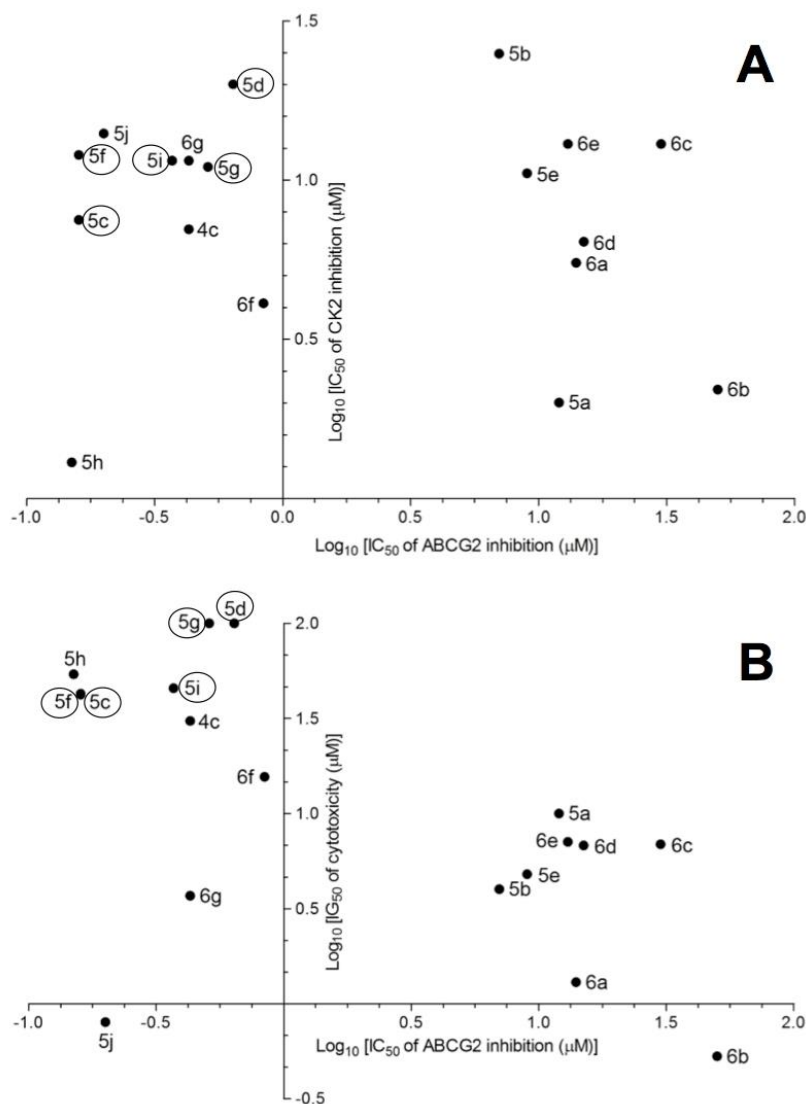


FIGURE 8. PHENOLIC INDENOINDOLES AS BETTER ABCG2 INHIBITORS OVER KETONIC- AND *P*-QUINONIC- DERIVATIVES.

Notes: ABCG2 inhibition *versus* CK2 inhibition (a) and *versus* cytotoxicity (b).

c) Effects on ABCG2 basal ATPase activity

The phenolic indenoindoles could also be distinguished from both ketonic- and *p*-quinonic- derivatives on the basis of their differential modulation of ABCG2 ATPase activity, which provided indirect information about the binding sites of the different compounds. Figure 9 shows that the vanadate-sensitive ATPase activity of insect-cell plasma membranes overexpressing human ABCG2 was strongly stimulated by the most potent phenolic inhibitors of mitoxantrone efflux: a 2- to 4.5-fold stimulation was observed with **5c**, **5d**, **5f**, **5g**, **5h**, **5i** and **5j**, in contrast to the very

low stimulation observed with much less active **5e** (cf. Table 1). Addition of hydrophobic methoxy substitution on N^5 -phenethyl at position *ortho* did not further stimulate the ATPase activity, as in **5c** versus **5h**. However, shifting the methoxy substituent to position *meta* significantly increased the ATPase activity (**5i**), a maximal stimulation being observed for compound **5j**, with a methoxy substituent at position *para*. A similar lack of positive effects was observed by lengthening the linker at N^5 -phenethyl when comparing **5c** to **5d**. However, changing the N^5 -phenethyl substituent into a shorter linker, from **5g** to **5e**, was quite detrimental to stimulation. Methyl substitution of D-ring was not able to increase the ATPase stimulation activity (**5c** versus **5f**); however, changing the methyl into phenyl (**5f** versus **5g**) induced a 2-fold increased stimulation.

In addition, the *p*-quinonic derivative **6f**, as well as **6c** and **6e** (not shown here), did not produce any effect, while a very limited stimulation was observed for compound **6g** (Figure 9). This lack of effect on ATPase activity was also observed with the four ketonic derivative leads, **4c**, **4h**, **4j** and **4k**, which did not induce any significant stimulation, suggesting either distinct binding sites or different induced conformational changes associated to inhibition of ABCG2-mediated mitoxantrone efflux. All indenoindole derivatives behaved differently than the reference inhibitors, Ko143 and chromone 1, which strongly inhibited ATPase activity.

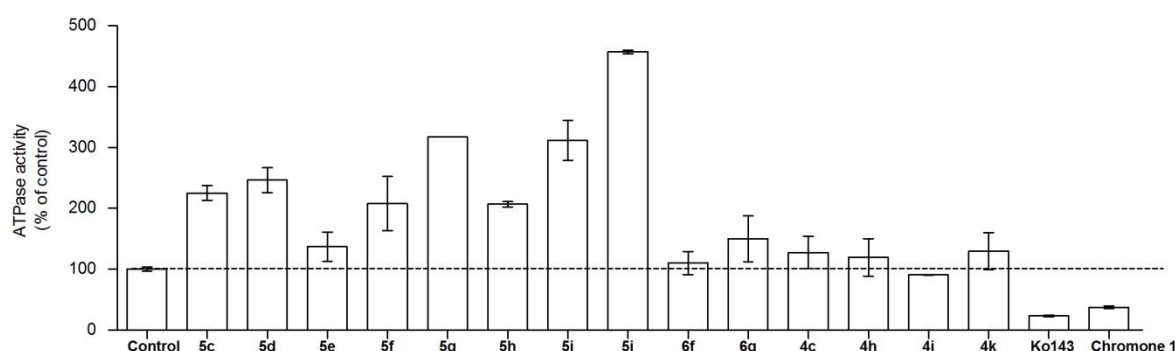


FIGURE 9: MODULATION OF BASAL ATPase ACTIVITY BY INDENOINDOLES

Notes: The effects of 2 μ M compounds from the different series on the vanadate-sensitive ATPase activity of ABCG2 were tested on 10 μ g of ABCG2-containing membrane vesicles (prepared from Sf9 cells overexpressing human ABCG2, and loaded with cholesterol). The specific basal ATPase activity of the control without inhibitor, taken as 100%, was 7.0 ± 0.4 nmol ATP hydrolyzed/min x mg of proteins. Two reference inhibitors, Ko143¹³ and chromone 1,³⁵ were used under the same conditions for comparison.

4.3.4 Discussion

This paper shows that phenolic indenoindoles constitute quite interesting ABCG2 modulators as potent and selective inhibitors, with low cytotoxicity. They strongly stimulate ATPase activity, by difference with ketonic derivatives and reference inhibitors.

4.3.4.1 Phenolic indenoindoles as better ABCG2 inhibitors than ketonic derivatives

The advantages of the phenolic-, over the ketonic-, derivatives are related to three main aspects. Firstly, a higher potency (about 3-fold) in inhibition of drug-efflux activity: such an increase might be due to a higher reactivity of the phenol- *versus* the ketone- group rather than to the planarity of the indenoindole core, since the inhibition was markedly altered in planar *p*-quinonic derivatives. Secondly, a higher selectivity for ABCG2 among MDR transporters and CK2: this was monitored through the absence of interaction with MRP1, and a 3-fold lower interaction with CK2 giving a 3-7 higher ABCG2/CK2 ratio; this further confirms the possibility to convert CK2 inhibitors into ABCG2 inhibitors upon appropriate substitutions, as previously observed with ketonic derivatives,¹⁷ and extends the differences to high ABCG2/CK2 ratio values, of 70-75, for **5f** and **5j**. Thirdly, a strong modulation, up to 4.5-fold, of the basal ATPase activity: this allows considering the possibility of depleting intracellular ATP from ABCG2-overexpressing cells, with the aim of promoting selective cell death, as proposed for the Pgp-dependent collateral sensitivity observed in the presence of verapamil.³⁵⁻³⁷ Such a stimulation of ATPase activity contrasts with the lack of effect observed with both ketonic and *p*-quinonic derivatives, and the inhibition produced by the reference inhibitors chromone 1 and Ko143,²² as well as fumitremorgin C.³⁸

Among the six best phenolic derivatives, toward both potency of ABCG2 inhibition (IC₅₀ values in the range 0.16-0.64 μM) and selectivity (ABCG2/CK2 ratio values in the range 22-75), one compound, namely **5j**, appeared to be cytotoxic. The five remaining leads, namely **5c**, **5d**, **5f**, **5g** and **5i**, which displayed high TR values, in the range 124-267, constitute good candidates for additional experiments to check their suitability in future assays in animal models.

4.3.4.2 Molecular mechanism and polyspecificity

The different modulation of ABCG2 basal ATPase activity by phenolic indenoindoles *versus* non-stimulatory ketonic derivatives and inhibitory reference inhibitors suggests distinct binding sites. A similar situation was previously observed with methoxy *trans*-stilbenes which, in combination with GF120918, prazosin or nilotinib, produced additive inhibitory effects on drug efflux³⁹. Although the inhibitor binding sites are probably distant from the cytosolic nucleotide-binding domain, they are indeed able to modulate the ATPase activity; this suggests the existence of allosteric interactions, between transmembrane and cytosolic domains of the transporter, controlling the strict coupling between ATP binding/hydrolysis and drug transport.

The common *N*⁵-phenethyl substituent found in all active indenoindole derivatives, as illustrated in Figure 10, should however induce partial overlapping of the binding sites. The hydrophobic substituents shown to increase the binding affinity of ketonic indenoindoles, produced similar effects in *p*-quinonic derivatives, where they partially compensated the strongly-negative contribution of the second ketone group, at *para* position *versus* the first one, within the quinone moiety. In contrast, the phenol group appeared to interact with a distinct, although likely overlapping, subsite associated to ATPase-stimulation effects. A similar overlapping of binding sites was previously observed for ABCG2-selective acridones in comparison with GF120918/elacridar, a dual inhibitor strongly interacting with Pgp.⁴⁰



FIGURE 10: TENTATIVE REPRESENTATION OF PARTLY-OVERLAPPING SITES FOR INDENOINDOLES, WITHIN ABCG2, ALLOWING BINDING OF, AND INHIBITION BY, THE DIFFERENT TYPES OF DERIVATIVES

Notes: *Left*, ketonic 4h; *middle*, phenolic 5c and *right*, *p*-quinonic 6g. The common phenethyl group, which is essential for ABCG2 inhibition and selectivity, is framed in orange; the other substituents positively contributing to inhibition are framed in either red (hydrophobic methyl or phenyl) or green (phenol) whereas the negatively-contributing *p*-quinone is framed in blue.

Finally, these diverse binding sites, located close each other and partly overlapping, constitute a new demonstration of ABCG2 polyspecificity toward inhibitors, similarly to that better known for substrates.

4.3.5 Acknowledgments

E.W. and G.V. were recipients of mobility doctoral fellowships from the Brazilian CNPq-CAPES (Science without Borders Program 245762/2012-4) and CAPES (Process numbers 8792127 and 2303/10-8), respectively. N.D.Y. was recipient of a postdoctoral fellowship for the Control of Cancer-CNPq (Science without Borders Program). Financial support was provided by the CNRS and Université Lyon 1 (UMR 5086), the Ligue Nationale Contre le Cancer (Equipe labellisée Ligue 2014), an international grant from French ANR and Hungarian NIH (2010-INT-1101-01). The Aquitaine Region is thanked for supporting equipment set up in CESAMO and at ICMCB. C. Ozvegy-Laczka and B. Sarkadi are acknowledged for providing the insect cell membranes overexpressing human ABCG2, L. Luku Tchamabe for technical assistance, and Dr. A. Coleman for improving the English.

REFERENCES

1. Gottesman MM. Mechanisms of cancer drug resistance. *Annu Rev Med.* 2002; 53: 615-627.
2. Szakács G, Paterson JK, Ludwig JA, Booth-Genthe C, Gottesman MM. Targeting multidrug resistance in cancer. *Nat Rev Drug Discov.* 2006; 5(3): 219-234.
3. Juliano RL, Ling V. A surface glycoprotein modulating drug in chinese hamster ovary cell mutants. *Biochim Biophys Acta.* 1976; 455(1): 152-162.
4. Cole SP, Bhardwaj G, Gerlach JH, Mackie JE, Grant CE, Almquist KC, Stewart AJ, Kurz EU, Duncan AMV, Deeley RG. Overexpression of a transporter gene in a multidrug-resistant human lung cancer cell line. *Science.* 1992; 258(5088): 1650-1654.
5. Allikmets R, Schriml LM, Hutchinson A, Romano-Spica V, Dean M. A human placenta-specific ATP-binding cassette gene (ABCP) on chromosome 4q22 that is involved in multidrug resistance. *Cancer Res.* 1998; 58(23): 5337-5339.
6. Doyle LA, Yang W, Abruzzo LV, Krogmann T, Gao Y, Rishi AK, Ross DD. A multidrug resistance transporter from human MCF-7 breast cancer cells. *Proc Natl Acad Sci USA.* 1998; 95(26): 15665-15670.
7. Miyake K, Mickley L, Litman T, Zhan Z, Robey R, Cristensen B, Brangi M, Greenberger L, Dean M, Fojo T, Bates SE. Molecular cloning of cDNAs which are highly overexpressed in mitoxantrone-resistant cells: demonstration of homology to ABC transport genes. *Cancer Res.* 1999; 59(1): 8-13.
8. Cripe LD, Uno H, Paietta EM, Litzow MR, Ketterling RP, Bennett JM, Rowe JM, Lazarus HM, Luger S, Tallman MS. Zosuquidar, a novel modulator of P-glycoprotein does not improve the outcome of older patients with newly diagnosed acute myeloid leukemia: a randomized, placebo-controlled trial of the Eastern Cooperative Oncology Group 3999. *Blood.* 2010; 116(20): 4077-4085.
9. Darby RA, Callaghan R, Mc Mahon RM. P-glycoprotein Inhibition: The past, the present and the future. *Curr Drug Metab.* 2011; 12(8): 722-731.
10. Vlaming ML, Lagas JS, Schinkel AH. Physiological and pharmacological roles of ABCG2 (BCRP): recent findings in Abcg2 knockout mice. *Adv Drug Deliv Rev.* 2009; 61(1): 14-25.
11. Natarajan K, Xie Y, Baer MR, Ross DD. Role of breast cancer resistance protein (BCRP/ABCG2) in cancer drug resistance. *Biochem Pharmacol.* 2012; 83(8): 1084-1103.
12. Rabindran SK, He H, Singh M, Brown E, Collins KI, Annable T, Greenberger LM. Reversal of a novel multidrug resistance mechanism in human colon carcinoma cells by fumitremorgin C. *Cancer Res.* 1998; 58(24): 5850-5858.

13. Allen JD, van Loevezijn A, Lakhai JM, van der Valk M, van Tellingen O, Reid G, Schellens JHM, Koomen GJ, Schinkel AH. Potent and specific inhibition of the breast cancer resistance protein multidrug transporter in vitro and in mouse intestine by a novel analogue of fumitremorgin C. *Mol Cancer Ther.* 2002; 1(6): 417-425.
14. Winter E, Devantier Neuenfeldt P, Chiaradia-Delatorre LD, Gauthier C, Yunes RA, Nunes RJ, Creczynski-Pasa TB, Di Pietro A. Symmetric bis-chalcones as a new type of breast cancer resistance protein inhibitors with a different mechanism than chromones. *J Med Chem.* 2014; 57(7): 2930-2941.
15. Arnaud O, Boumendjel A, Geze A, Honorat M, Mattera E, Stein WD, Bates SE, Falson P, Dumontet C, Di Pietro A, Payen L. The acridone derivative MBLI-87 reverses breast cancer resistance protein-mediated resistance to irinotecan in xenografts. *Eur J Cancer.* 2011; 47(4): 640-648.
16. Honorat M, Guitton J, Gauthier C, Bouard C, Lecerf-Schmidt F, Peres B, Terreux R, Gervot H, Rioufol C, Boumendjel A, Puisieux A, Di Pietro A, Payen L. MBL-II-141, a chromone derivative, enhances irinotecan anticancer efficiency in ABCG2-positive xenografts. *Oncotarget.* 2014; 5(23): 11957-11970.
17. Gozzi GJ, Bouaziz Z, Winter E, Daflon-Yunes N, Aichele D, Nacereddine A, Marminon C, Valdameri G, Zeinyeh W, Bollacke A, Guillon J, Lacoudre A, Pinaud N, Cadena SM, Jose J, Le Borgne M, Di Pietro A. Converting potent indeno[1,2-*b*]indole inhibitors of protein kinase CK2 into selective inhibitors of the breast cancer resistance protein ABCG2. *J Med Chem.* 2015; 58(1): 265-277.
18. Supplementary X-ray crystallographic data: Cambridge Crystallographic Data Centre, University Chemical Lab, Lensfield Road, Cambridge, CB2 1EW, UK; E-mail: deposit@chemcrys.cam.ac.uk.
19. Sheldrick GM. 1996; SADABS, University of Göttingen, Germany.
20. Sheldrick GM. A short history of SHELX. *Acta Crystallogr Sect A.* 2008; 64(Pt 1): 112-122.
21. Dolomanov OV, Bourhis LJ, Gildea RJ, Howard JAK, Puschmann H. OLEX2: a complete structure solution, refinement and analysis program. *J Appl Cryst.* 2009; 42: 339-341.
22. Winter E, Lecerf-Schmidt F, Gozzi GJ, Peres B, Lightbody M, Gauthier C, Ozvegy-Laczka C, Szakacs G, Sarkadi B, Creczynski-Pasa TB, Boumendjel A, Di Pietro A. Structure-activity relationships of chromone derivatives toward mechanism of interaction with, and inhibition of, breast cancer resistance protein ABCG2. *J Med Chem.* 2013; 56(24): 9849-9860.
23. Mosmann T. Rapid colorimetric assay for cellular growth and survival. Application to proliferation and cytotoxicity assays. *J Immunol Methods.* 1983; 65(1-2): 55-63.

24. Telbisz A, Muller M, Ozvegy-Laczka C, Homolya L, Szente L, Varadi A, Sarkadi B. Membrane cholesterol selectively modulates the activity of the human ABCG2 multidrug transporter. *Biochim Biophys Acta*. 2007; 1768(11): 2698-2713.
25. Olgen S, Götz C, Jose J. Synthesis and biological evaluation of 3-(substituted-benzylidene)-1,3-dihydroindolin derivatives as human protein kinase CK2 and p60(c-Src) tyrosine kinase inhibitors. *Biol Pharm Bull*. 2007; 30(4): 715-718.
26. Grankowski N, Boldyreff B, Issinger OG. Isolation and characterization of recombinant human casein kinase II subunits α and β from bacteria. *Eur J Biochem*. 1991; 198(1): 25-30.
27. Guillon J, Le Borgne M, Rimbault C, Moreau S, Savrimoutou S, Pinaud N, Baratin S, Marchivie M, Roche S, Bollacke A, Pecci A, Alvarez L, Desplat V, Jose J. Synthesis and biological evaluation of novel substituted pyrrolo[1,2-a]quinoxaline derivatives as inhibitors of the human protein kinase CK2. *Eur J Med Chem*. 2013; 65: 205-222.
28. Gratz A, Götz C, Jose J. A CE-based assay for human protein kinase CK2 activity measurement and inhibitor screening. *Electrophoresis*. 2010; 31(4): 634-640.
29. Poumaroux A, Bouaziz Z, Domard M, Fillion H. Regiospecific hetero Diels-Alder synthesis of pyrido[2,3-b]- and [3,2-b]carbazole-5,11-diones. *Heterocycles*. 1997; 45: 585-596.
30. Hundsdörfer C, Hemmerling HJ, Hamberger J, Le Borgne M, Bednarski P, Goetz C, Totzke F, Jose J. Novel indeno[1,2-b]indoloquinones as inhibitors of the human protein kinase CK2 with antiproliferative activity towards a broad panel of cancer cell lines. *Biochem Biophys Res Commun*. 2012; 424(1): 71-75.
31. Zimmer H, Lankin DC, Horgan SW. Oxidations with potassium nitrosodisulfonate (Fremy's radical). The Teuber reaction. *Chem Rev*. 1971; 71(2): 229-246.
32. Janreddy D, Kavala V, Bosco JWJ, Kuo C-W, Yao C-F. An easy access to carbazolones and 2,3-disubstituted indoles. *Eur J Org Chem*. 2011; 12: 2360-2365.
33. Bill K, Black GG, Falshaw CP, Sainsbury M. The coupling reactions of 3-acylindoles and proof of structure of the palladium (II) acetate mediated cyclisation reaction product of 3-benzoyl-1-methylindole. *Heterocycles*. 1983; 20: 2433-2436.
34. Valdameri G, Genoux-Bastide E, Peres B, Gauthier C, Guitton J, Terreux, R, Winnischofer SM, Rocha ME, Boumendjel A., Di Pietro A. Substituted chromones as highly potent nontoxic inhibitors, specific for the breast cancer resistance protein. *J Med Chem*. 2012; 55(2): 966-970.

35. Karwatsky J, Lincoln MC, Georges E. A mechanism for P-glycoprotein-mediated apoptosis as revealed by verapamil hypersensitivity. *Biochemistry*. 2003; 42(42): 12163-12173.
36. Hall MD, Handley MD, Gottesman MM. Is resistance useless? Multidrug resistance and collateral sensitivity. *Trends Pharmacol Sci*. 2009; 30(10): 546-556.
37. Szakacs G, Hall M, Gottesman MM, Boumendjel A, Kachadourian R, Day BJ, Baubichon-Cortay H, Di Pietro A. Targeting the Achilles heel of multidrug-resistant cancer by exploiting the fitness cost of resistance. *Chem Rev*. 2014; 114(11): 5753-5774.
38. Ozvegy C, Litman T, Szakacs G, Nagy Z, Bates SE, Varadi A, Sarkadi B. Functional characterization of the human multidrug transporter, ABCG2, expressed in insect cells. *Biochem Biophys Res Commun*. 2001; 285(1): 111-117.
39. Valdameri G, Pereira Rangel L, Spatafora C, Guitton J, Gauthier C, Arnaud O, Ferreira-Pereira A, Falson P, Winnischofer SM, Rocha ME, Tringali C, Di Pietro A. Methoxy stilbenes as potent, specific, untransported, and nontoxic inhibitors of breast cancer resistance protein. *ACS Chem Biol*. 2012; 7(2): 322-330.
40. Boumendjel A, Macalou S, Valdameri G, Pozza A, Gauthier C, Arnaud O, Nicolle E, Magnard S, Falson P, Terreux R, Carrupt P-A, Payen L, Di Pietro A. Targeting the multidrug ABCG2 transporter with flavonoidic inhibitors: *in vitro* optimization and *in vivo* validation. *Curr Med Chem*. 2011; 18(22): 3387-3401.
41. Hundsdörfer C, Hemmerling HJ, Götz C, Totzke F, Bednarski P, Le Borgne M, Jose J. Indeno[1,2-b]indole derivatives as novel class of potent human protein kinase CK2 inhibitors. *Bioorg Med Chem*. 2012; 20(7): 2282-2289.

5. CONCLUSÕES

Com os resultados obtidos neste trabalho pode-se concluir que MI-J é o composto mais promissor para futuras investigações *in vivo* visando o tratamento do HCC. Este derivado apresentou destacada atividade citotóxica, quando comparado aos outros derivados 1,3,4-tiadiazóis mesoiônicos, sem afetar a viabilidade das células não-tumorais (hepatócitos de ratos). Além disto, MI-J foi o único composto capaz de inibir, embora fracamente, a atividade de Pgp, não sendo transportado por esta proteína. Estes efeitos o tornam um bom candidato para o tratamento do HCC com resistência mediada por Pgp; sugestão bastante relevante ao considerar o importante papel desta proteína no desenvolvimento de MDR em pacientes portadores de HCC.

Também conclui-se que potentes e seletivos inibidores de ABCG2 são obtidos através de substituições nos anéis do núcleo indeno[1,2-*b*]indol presente em inibidores de CK2, sendo as substituições na posição N⁵ do núcleo cetônico indeno[1,2-*b*]indol críticas para afinidade por ABCG2 ou CK2, e a utilização de um núcleo fenólico indeno[1,2-*b*]indol importante para obtenção de inibidores de ABCG2 com maior seletividade sobre CK2 ou outros transportadores ABC. Estas modificações permitem o desenvolvimento de inibidores com baixa citotoxicidade intrínseca e alta atividade inibitória de ABCG2, resultando em índices terapêuticos desejáveis para utilização em modelos *in vivo*.

REFERÊNCIAS

- ABOLHODA, A. et al. Rapid activation of MDR1 gene expression in human metastatic sarcoma after in vivo exposure to doxorubicin. **Clin Cancer Res**, v. 5, n. 11, p. 3352-6, 1999.
- AHMED-BELKACEM, A. et al. Flavonoid structure-activity studies identify 6-prenylchrysin and tectochrysin as potent and specific inhibitors of breast cancer resistance protein ABCG2. **Cancer Res**, v. 65, n. 11, p. 4852-60, 2005.
- AKIMOTO, M. et al. Relationship between therapeutic efficacy of arterial infusion chemotherapy and expression of P-glycoprotein and p53 protein in advanced hepatocellular carcinoma. **World J Gastroenterol**, v. 12, n. 6, p. 868-73, 2006.
- ALCHAB, F. et al. Synthesis, Biological Evaluation and Molecular Modeling of Substituted Indeno[1,2-b]indoles as Inhibitors of Human Protein Kinase CK2. **Pharmaceuticals (Basel)**, v. 8, n. 2, p. 279-302, 2015.
- ALLEN, J. D. et al. Potent and specific inhibition of the breast cancer resistance protein multidrug transporter in vitro and in mouse intestine by a novel analogue of fumitremorgin C. **Mol Cancer Ther**, v. 1, n. 6, p. 417-25, 2002.
- ALLER, S. G. et al. Structure of P-glycoprotein reveals a molecular basis for poly-specific drug binding. **Science**, v. 323, n. 5922, p. 1718-22, 2009.
- ALLIKMETS, R. et al. A human placenta-specific ATP-binding cassette gene (ABCP) on chromosome 4q22 that is involved in multidrug resistance. **Cancer Res**, v. 58, n. 23, p. 5337-9, 1998.
- ALVES, R. C. et al. Advanced hepatocellular carcinoma. Review of targeted molecular drugs. **Ann Hepatol**, v. 10, n. 1, p. 21-7, 2011.
- ARCHANA; SRIVASTAVA, V. K.; KUMAR, A. Synthesis of some newer derivatives of substituted quinazolinonyl-2-oxo/thiobarbituric acid as potent anticonvulsant agents. **Bioorg Med Chem**, v. 12, n. 5, p. 1257-64, 2004.
- ARNAUD, O. et al. The acridone derivative MBLI-87 sensitizes breast cancer resistance protein-expressing xenografts to irinotecan. **European Journal of Cancer**, v. 47, n. 4, p. 640-648, 2011.
- ATTWA, M. H.; EL-ETREBY, S. A. Guide for diagnosis and treatment of hepatocellular carcinoma. **World J Hepatol**, v. 7, n. 12, p. 1632-51, 2015.
- BALASUBRAMANIYAN, V. et al. Mouse recombinant leptin protects human hepatoma HepG2 against apoptosis, TNF-alpha response and oxidative stress induced by the hepatotoxin-ethanol. **Biochim Biophys Acta**, v. 1770, n. 8, p. 1136-44, 2007.

BENDERRA, Z. et al. Breast cancer resistance protein and P-glycoprotein in 149 adult acute myeloid leukemias. **Clin Cancer Res**, v. 10, n. 23, p. 7896-902, 2004.

BOUMENDJEL, A. et al. 4-Hydroxy-6-methoxyaurones with high-affinity binding to cytosolic domain of P-glycoprotein. **Chem Pharm Bull (Tokyo)**, v. 50, n. 6, p. 854-6, 2002.

BOUMENDJEL, A. et al. Acridone derivatives: design, synthesis, and inhibition of breast cancer resistance protein ABCG2. **Bioorg Med Chem**, v. 15, n. 8, p. 2892-7, 2007.

BRACHT A., I.-I. E. L. K.-B., A. M. **Métodos de Laboratório em Bioquímica**. São Paulo: Editora Manole, 2003.

BRADFORD, M. M. A rapid and sensitive method for the quantitation of microgram quantities of protein utilizing the principle of protein-dye binding. **Anal Biochem**, v. 72, p. 248-54, 1976.

BRENDEL, C. et al. Imatinib mesylate and nilotinib (AMN107) exhibit high-affinity interaction with ABCG2 on primitive hematopoietic stem cells. **Leukemia**, v. 21, n. 6, p. 1267-75, 2007.

BRITO, A. F. et al. Positron Emission Tomography Diagnostic Imaging in Multidrug-Resistant Hepatocellular Carcinoma: Focus on 2-Deoxy-2-(18F)Fluoro-D-Glucose. **Mol Diagn Ther**, 2014.

BRUIX, J.; SALA, M.; LLOVET, J. M. Chemoembolization for hepatocellular carcinoma. **Gastroenterology**, v. 127, n. 5 Suppl 1, p. S179-88, 2004.

BUPATHI, M. et al. Hepatocellular carcinoma: Where there is unmet need. **Mol Oncol**, 2015.

BURGER, H. et al. RNA expression of breast cancer resistance protein, lung resistance-related protein, multidrug resistance-associated proteins 1 and 2, and multidrug resistance gene 1 in breast cancer: correlation with chemotherapeutic response. **Clin Cancer Res**, v. 9, n. 2, p. 827-36, 2003.

CADENA, S. M. et al. Effect of MI-D, a new mesoionic compound, on energy-linked functions of rat liver mitochondria. **FEBS Lett**, v. 440, n. 1-2, p. 46-50, 1998.

CADENA, S. M. et al. Interference of MI-D, a new mesoionic compound, on artificial and native membranes. **Cell Biochem Funct**, v. 20, n. 1, p. 31-7, 2002.

CADENA, S. M. S. C. **Contribuição ao conhecimento ao mecanismo de ação dos compostos 1,3,4-tiadiazóis mesoiônicos**. Curitiba, Tese (Doutorado em Bioquímica), Setor de Ciências Biológicas, Universidade Federal do Paraná, Curitiba, 1999.

CALCAGNO, A. M.; AMBUDKAR, S. V. Molecular mechanisms of drug resistance in single-step and multi-step drug-selected cancer cells. **Methods Mol Biol**, v. 596, p. 77-93, 2010.

CARVALHO, S. A. et al. Synthesis and antitrypanosomal profile of new functionalized 1,3,4-thiadiazole-2-arylhydrazone derivatives, designed as non-mutagenic megalin analogues. **Bioorg Med Chem Lett**, v. 14, n. 24, p. 5967-70, 2004.

CASTANEDA, F.; KINNE, R. K. Cytotoxicity of millimolar concentrations of ethanol on HepG2 human tumor cell line compared to normal rat hepatocytes in vitro. **J Cancer Res Clin Oncol**, v. 126, n. 9, p. 503-10, 2000.

CHAN, H. S. et al. P-glycoprotein expression: critical determinant in the response to osteosarcoma chemotherapy. **J Natl Cancer Inst**, v. 89, n. 22, p. 1706-15, 1997.

CHAN, H. S. et al. Immunohistochemical detection of P-glycoprotein: prognostic correlation in soft tissue sarcoma of childhood. **J Clin Oncol**, v. 8, n. 4, p. 689-704, 1990.

CHANDRAKANTHA, B. et al. Synthesis and biological evaluation of novel substituted 1,3,4-thiadiazole and 2,6-di aryl substituted imidazo [2,1-b] [1,3,4] thiadiazole derivatives. **Eur J Med Chem**, v. 71, p. 316-23, 2014.

CHENG, A. L. et al. Efficacy and safety of sorafenib in patients in the Asia-Pacific region with advanced hepatocellular carcinoma: a phase III randomised, double-blind, placebo-controlled trial. **Lancet Oncol**, v. 10, n. 1, p. 25-34, 2009.

CHENG, J. W.; LV, Y. New progress of non-surgical treatments for hepatocellular carcinoma. **Med Oncol**, v. 30, n. 1, p. 381, 2013.

CHENG, X. et al. Transarterial (chemo)embolization for curative resection of hepatocellular carcinoma: a systematic review and meta-analyses. **J Cancer Res Clin Oncol**, v. 140, n. 7, p. 1159-70, 2014.

CHEUNG, C. S. et al. Leachianone A as a potential anti-cancer drug by induction of apoptosis in human hepatoma HepG2 cells. **Cancer Lett**, v. 253, n. 2, p. 224-35, 2007.

CHO, Y. K. et al. Systematic review of randomized trials for hepatocellular carcinoma treated with percutaneous ablation therapies. **Hepatology**, v. 49, n. 2, p. 453-9, 2009.

CHOU, J.-Y. et al. Investigation of anticancer mechanism of thiadiazole-based compound in human non-small cell lung cancer A549 cells. **Biochemical Pharmacology**, v. 66, n. 1, p. 115-124, 2003.

COLE, S. P. et al. Overexpression of a transporter gene in a multidrug-resistant human lung cancer cell line. **Science**, v. 258, n. 5088, p. 1650-4, 1992.

COLEY, H. M. Overcoming multidrug resistance in cancer: clinical studies of p-glycoprotein inhibitors. **Methods Mol Biol**, v. 596, p. 341-58, 2010.

COMERFORD, K. M. et al. Hypoxia-inducible factor-1-dependent regulation of the multidrug resistance (MDR1) gene. **Cancer Res**, v. 62, n. 12, p. 3387-94, 2002.

DANØ, K. Active outward transport of daunomycin in resistant ehrlich ascites tumor cells. **Biochimica et Biophysica Acta (BBA) - Biomembranes**, v. 323, n. 3, p. 466-483, 1973.

DARZYNKIEWICZ, Z. et al. Features of apoptotic cells measured by flow cytometry. **Cytometry**, v. 13, n. 8, p. 795-808, 1992.

DE SOUZA, A. C. et al. Defining the molecular basis of tumor metabolism: a continuing challenge since Warburg's discovery. **Cell Physiol Biochem**, v. 28, n. 5, p. 771-92, 2011.

DIESTRA, J. E. et al. Frequent expression of the multi-drug resistance-associated protein BCRP/MXR/ABCP/ABCG2 in human tumours detected by the BXP-21 monoclonal antibody in paraffin-embedded material. **Journal of Pathology**, v. 198, n. 2, p. 213-219, 2002.

DOUGLAS, R. S. et al. A simplified method for the coordinate examination of apoptosis and surface phenotype of murine lymphocytes. **J Immunol Methods**, v. 188, n. 2, p. 219-28, 1995.

DOYLE, L. A. et al. A multidrug resistance transporter from human MCF-7 breast cancer cells. **Proc Natl Acad Sci U S A**, v. 95, n. 26, p. 15665-70, 1998.

EASL-EORTC. European Association for the Study of the Liver (EASL)- European Organisation for Research and Treatment of Cancer (EORTC). Clinical practice guidelines: management of hepatocellular carcinoma. **J Hepatol**, v. 56, n. 4, p. 908-43, 2012.

ECKFORD, P. D.; SHAROM, F. J. ABC efflux pump-based resistance to chemotherapy drugs. **Chem Rev**, v. 109, n. 7, p. 2989-3011, 2009.

ENDICOTT, J. A.; LING, V. The biochemistry of P-glycoprotein-mediated multidrug resistance. **Annu Rev Biochem**, v. 58, p. 137-71, 1989.

ERNST, R. et al. Multidrug efflux pumps: substrate selection in ATP-binding cassette multidrug efflux pumps--first come, first served? **FEBS J**, v. 277, n. 3, p. 540-9, 2010.

FDA. **Drug Interaction Studies — Study Design, Data Analysis, Implications for Dosing, and Labeling Recommendations** 2012.

FITZMORRIS, P. et al. Management of hepatocellular carcinoma. **J Cancer Res Clin Oncol**, v. 141, n. 5, p. 861-76, 2015.

FUKUDA, Y.; SCHUETZ, J. D. ABC transporters and their role in nucleoside and nucleotide drug resistance. **Biochemical Pharmacology**, v. 83, n. 8, p. 1073-1083, 2012.

GE, P. L.; DU, S. D.; MAO, Y. L. Advances in preoperative assessment of liver function. **Hepatobiliary Pancreat Dis Int**, v. 13, n. 4, p. 361-70, 2014.

GOTTESMAN, M. M.; AMBUDKAR, S. V. Overview: ABC transporters and human disease. **J Bioenerg Biomembr**, v. 33, n. 6, p. 453-8, 2001.

GOTTESMAN, M. M.; FOJO, T.; BATES, S. E. Multidrug resistance in cancer: role of ATP-dependent transporters. **Nat Rev Cancer**, v. 2, n. 1, p. 48-58, 2002.

GRYNBERG, N.; SANTOS, A. C.; ECHEVARRIA, A. Synthesis and in vivo antitumor activity of new heterocyclic derivatives of the 1,3,4-thiadiazolium-2-aminide class. **Anticancer Drugs**, v. 8, n. 1, p. 88-91, 1997.

HABER, M. et al. Association of high-level MRP1 expression with poor clinical outcome in a large prospective study of primary neuroblastoma. **J Clin Oncol**, v. 24, n. 10, p. 1546-53, 2006.

HALL, M. D.; HANDLEY, M. D.; GOTTESMAN, M. M. Is resistance useless? Multidrug resistance and collateral sensitivity. **Trends in Pharmacological Sciences**, v. 30, n. 10, p. 546-556, 2009.

HANIF, I. M. et al. Casein Kinase II: an attractive target for anti-cancer drug design. **Int J Biochem Cell Biol**, v. 42, n. 10, p. 1602-5, 2010.

HATZARAS, I. et al. Treatment options and surveillance strategies after therapy for hepatocellular carcinoma. **Ann Surg Oncol**, v. 21, n. 3, p. 758-66, 2014.

HEGEDUS, C. et al. Interaction of the EGFR inhibitors gefitinib, vandetanib, pelitinib and neratinib with the ABCG2 multidrug transporter: implications for the emergence and reversal of cancer drug resistance. **Biochem Pharmacol**, v. 84, n. 3, p. 260-7, 2012.

HIGGINS, C. F.; LINTON, K. J. The ATP switch model for ABC transporters. **Nat Struct Mol Biol**, v. 11, n. 10, p. 918-26, 2004.

HOLOHAN, C. et al. Cancer drug resistance: an evolving paradigm. **Nat Rev Cancer**, v. 13, n. 10, p. 714-26, 2013.

HONG, B.-C. et al. Synthesis and Cytotoxicity Studies of Cyclohepta[b]indoles, Benzo[6,7]Cyclohepta[1,2-b]Indoles, Indeno[1,2-b]Indoles, and Benzo[a]Carbazoles. **Journal of the Chinese Chemical Society**, v. 53, n. 3, p. 647-662, 2006.

HONORAT, M. et al. MBL-II-141, a chromone derivative, enhances irinotecan (CPT-11) anticancer efficiency in ABCG2-positive xenografts. **Oncotarget**, v. 5, n. 23, p. 11957-70, 2014.

HOSSAIN, M. A. et al. Aspirin induces apoptosis in vitro and inhibits tumor growth of human hepatocellular carcinoma cells in a nude mouse xenograft model. **Int J Oncol**, v. 40, n. 4, p. 1298-304, 2012.

HSU, C. Y. et al. Performance status in patients with hepatocellular carcinoma: determinants, prognostic impact, and ability to improve the Barcelona Clinic Liver Cancer system. **Hepatology**, v. 57, n. 1, p. 112-9, 2013.

HU, Y. et al. 1,3,4-Thiadiazole: synthesis, reactions, and applications in medicinal, agricultural, and materials chemistry. **Chem Rev**, v. 114, n. 10, p. 5572-610, 2014.

HUANG, W. C. et al. BCRP/ABCG2 inhibition sensitizes hepatocellular carcinoma cells to sorafenib. **PLoS One**, v. 8, n. 12, p. e83627, 2013.

HUNSDORFER, C. et al. Indeno[1,2-b]indole derivatives as a novel class of potent human protein kinase CK2 inhibitors. **Bioorg Med Chem**, v. 20, n. 7, p. 2282-9, 2012a.

HUNSDORFER, C. et al. Novel indeno[1,2-b]indoloquinones as inhibitors of the human protein kinase CK2 with antiproliferative activity towards a broad panel of cancer cell lines. **Biochem Biophys Res Commun**, v. 424, n. 1, p. 71-5, 2012b.

JAIN, A. K. et al. 1,3,4-thiadiazole and its derivatives: a review on recent progress in biological activities. **Chem Biol Drug Des**, v. 81, n. 5, p. 557-76, 2013.

JEMAL, A. et al. Global cancer statistics. **CA Cancer J Clin**, v. 61, n. 2, p. 69-90, 2011.

JUBIE, S. et al. Synthesis, antidepressant and antimicrobial activities of some novel stearic acid analogues. **Eur J Med Chem**, v. 54, p. 931-5, 2012.

JULIANO, R. L.; LING, V. A surface glycoprotein modulating drug permeability in Chinese hamster ovary cell mutants. **Biochim Biophys Acta**, v. 455, n. 1, p. 152-62, 1976.

JUSZCZAK, M. et al. The activity of a new 2-amino-1,3,4-thiadiazole derivative 4CIABT in cancer and normal cells. **Folia Histochem Cytobiol**, v. 49, n. 3, p. 436-44, 2011.

KALYAN, A.; NIMEIRI, H.; KULIK, L. Systemic therapy of hepatocellular carcinoma: current and promising. **Clin Liver Dis**, v. 19, n. 2, p. 421-32, 2015.

KASHYAP, M. et al. Scaffold hybridization in generation of indenoindolones as anticancer agents that induce apoptosis with cell cycle arrest at G2/M phase. **Bioorg Med Chem Lett**, v. 22, n. 7, p. 2474-9, 2012.

KASHYAP, M. et al. Indenoindolone derivatives as topoisomerase II-inhibiting anticancer agents. **Bioorg Med Chem Lett**, v. 23, n. 4, p. 934-8, 2013.

KATAYAMA, K. et al. Flavonoids inhibit breast cancer resistance protein-mediated drug resistance: transporter specificity and structure-activity relationship. **Cancer Chemother Pharmacol**, v. 60, n. 6, p. 789-97, 2007.

KATHAWALA, R. J. et al. The modulation of ABC transporter-mediated multidrug resistance in cancer: a review of the past decade. **Drug Resist Updat**, v. 18, p. 1-17, 2015.

KHAN, I. et al. Synthesis, antioxidant activities and urease inhibition of some new 1,2,4-triazole and 1,3,4-thiadiazole derivatives. **Eur J Med Chem**, v. 45, n. 11, p. 5200-7, 2010.

KHAN, K. N. et al. Prospective analysis of risk factors for early intrahepatic recurrence of hepatocellular carcinoma following ethanol injection. **J Hepatol**, v. 32, n. 2, p. 269-78, 2000.

KIER, L. B.; ROCHE, E. B. Medicinal chemistry of the mesoionic compounds. **J Pharm Sci**, v. 56, n. 2, p. 149-68, 1967.

KIM, Y. H. et al. Expression of breast cancer resistance protein is associated with a poor clinical outcome in patients with small-cell lung cancer. **Lung Cancer**, v. 65, n. 1, p. 105-11, 2009.

KRATZ, F. et al. Prodrug strategies in anticancer chemotherapy. **ChemMedChem**, v. 3, n. 1, p. 20-53, 2008.

KRAUSE, D. S.; VAN ETTEN, R. A. Tyrosine kinases as targets for cancer therapy. **N Engl J Med**, v. 353, n. 2, p. 172-87, 2005.

KUHNLE, M. et al. Potent and selective inhibitors of breast cancer resistance protein (ABCG2) derived from the p-glycoprotein (ABCB1) modulator tariquidar. **J Med Chem**, v. 52, n. 4, p. 1190-7, 2009.

KUMAR, D. et al. Synthesis of novel 1,2,4-oxadiazoles and analogues as potential anticancer agents. **Eur J Med Chem**, v. 46, n. 7, p. 3085-92, 2011.

KUMAR, H. et al. 1,3,4-Oxadiazole/thiadiazole and 1,2,4-triazole derivatives of biphenyl-4-yloxy acetic acid: synthesis and preliminary evaluation of biological properties. **Eur J Med Chem**, v. 43, n. 12, p. 2688-98, 2008.

LAUPEZE, B. et al. High multidrug resistance protein activity in acute myeloid leukaemias is associated with poor response to chemotherapy and reduced patient survival. **Br J Haematol**, v. 116, n. 4, p. 834-8, 2002.

LECERF-SCHMIDT, F. et al. ABCG2: recent discovery of potent and highly selective inhibitors. **Future Med Chem**, v. 5, n. 9, p. 1037-45, 2013.

LEE, C. H. Reversing agents for ATP-binding cassette drug transporters. **Methods Mol Biol**, v. 596, p. 325-40, 2010.

LEE, G.; PIQUETTE-MILLER, M. Cytokines alter the expression and activity of the multidrug resistance transporters in human hepatoma cell lines; analysis using RT-PCR and cDNA microarrays. **J Pharm Sci**, v. 92, n. 11, p. 2152-63, 2003.

LEE, J. M.; PARK, J. W.; CHOI, B. I. 2014 KLCSSG-NCC Korea Practice Guidelines for the management of hepatocellular carcinoma: HCC diagnostic algorithm. **Dig Dis**, v. 32, n. 6, p. 764-77, 2014.

LEGRAND, O.; TANG, R.-P.; MARIE, J.-P. Expression, Detection, and Implication of ABC Proteins in Acute Myeloblastic Leukemia. In: (Ed.). **ABC Transporters and Multidrug Resistance**: John Wiley & Sons, Inc., 2009. p.119-141. ISBN 9780470495131.

LIN, S. M. et al. Randomised controlled trial comparing percutaneous radiofrequency thermal ablation, percutaneous ethanol injection, and percutaneous acetic acid injection to treat hepatocellular carcinoma of 3 cm or less. **Gut**, v. 54, n. 8, p. 1151-6, 2005.

LIU, R. M. et al. Regulation of [Ah] gene battery enzymes and glutathione levels by 5,10-dihydroindeno[1,2-b]indole in mouse hepatoma cell lines. **Carcinogenesis**, v. 15, n. 10, p. 2347-52, 1994.

LIU, Z. H.; ZENG, S. Cytotoxicity of ginkgolic acid in HepG2 cells and primary rat hepatocytes. **Toxicol Lett**, v. 187, n. 3, p. 131-6, 2009.

LLOVET, J. M. et al. Arterial embolisation or chemoembolisation versus symptomatic treatment in patients with unresectable hepatocellular carcinoma: a randomised controlled trial. **Lancet**, v. 359, n. 9319, p. 1734-9, 2002.

LLOVET, J. M. et al. Sorafenib in advanced hepatocellular carcinoma. **N Engl J Med**, v. 359, n. 4, p. 378-90, 2008.

LO, C. M. et al. Randomized controlled trial of transarterial lipiodol chemoembolization for unresectable hepatocellular carcinoma. **Hepatology**, v. 35, n. 5, p. 1164-71, 2002.

LOONG, H. H.; YEO, W. Microtubule-targeting agents in oncology and therapeutic potential in hepatocellular carcinoma. **Onco Targets Ther**, v. 7, p. 575-585, 2014.

MAHATO, R.; TAI, W.; CHENG, K. Prodrugs for improving tumor targetability and efficiency. **Adv Drug Deliv Rev**, v. 63, n. 8, p. 659-70, 2011.

MARSH, J. W. et al. Is the pathologic TNM staging system for patients with hepatoma predictive of outcome? **Cancer**, v. 88, n. 3, p. 538-43, 2000.

MARTINEZ, L. et al. Understanding polyspecificity within the substrate-binding cavity of the human multidrug resistance P-glycoprotein. **FEBS J**, v. 281, n. 3, p. 673-82, 2014.

MARZABADI, M. R.; JONES, C.; RYDSTROM, J. Indenoindole depresses lipofuscin formation in cultured neonatal rat myocardial cells. **Mech Ageing Dev**, v. 80, n. 3, p. 189-97, 1995.

MATYSIAK, J. Synthesis and antiproliferative activity of N-substituted 2-amino-5-(2,4-dihydroxyphenyl)-1,3,4-thiadiazoles. **Bioorganic & Medicinal Chemistry**, v. 14, n. 13, p. 4483-4489, 2006a.

MATYSIAK, J. et al. Synthesis and antiproliferative activity of some 5-substituted 2-(2,4-dihydroxyphenyl)-1,3,4-thiadiazoles. **Eur J Med Chem**, v. 41, n. 4, p. 475-82, 2006b.

MENDEZ-SANCHEZ, N. et al. Latin American Association for the Study of the Liver (LAASL) clinical practice guidelines: management of hepatocellular carcinoma. **Ann Hepatol**, v. 13 Suppl 1, p. S4-40, 2014.

MILANE, L. et al. Multi-modal strategies for overcoming tumor drug resistance: hypoxia, the Warburg effect, stem cells, and multifunctional nanotechnology. **J Control Release**, v. 155, n. 2, p. 237-47, 2011.

MO, W.; ZHANG, J. T. Human ABCG2: structure, function, and its role in multidrug resistance. **Int J Biochem Mol Biol**, v. 3, n. 1, p. 1-27, 2012.

MONTANARI, F.; ECKER, G. F. Prediction of drug-ABC-transporter interaction - Recent advances and future challenges. **Adv Drug Deliv Rev**, v. 86, p. 17-26, 2015.

MOSAFFA, F. et al. Interleukin-1 beta and tumor necrosis factor-alpha increase ABCG2 expression in MCF-7 breast carcinoma cell line and its mitoxantrone-resistant derivative, MCF-7/MX. **Inflamm Res**, v. 58, n. 10, p. 669-76, 2009.

MURATA, S. et al. Interventional treatment for unresectable hepatocellular carcinoma. **World J Gastroenterol**, v. 20, n. 37, p. 13453-65, 2014.

NAGY, A. et al. The effect of a low molecular weight inhibitor of lipid peroxidation on ultrastructural alterations to ischemia-reperfusion in the isolated rat heart. **Acta Physiol Hung**, v. 88, n. 2, p. 101-15, 2001.

NAGY, A. et al. Effects of a novel low-molecular weight antioxidant on cardiac injury induced by hydrogen peroxide. **Free Radic Biol Med**, v. 20, n. 4, p. 567-72, 1996.

NCBI. National Center for Biotechnology Information. PubChem Compound Database; CID=216239. Disponível em: <<https://pubchem.ncbi.nlm.nih.gov/compound/216239>>. Acesso em: 6/08/2015a.

NCBI. National Center for Biotechnology Information. PubChem Compound Database; CID=10322450. Disponível em: <http://pubchem.ncbi.nlm.nih.gov/compound/Ko_143#section=Top>. Acesso em: 21/11/2015b.

NG, I. O. et al. Expression of P-glycoprotein in hepatocellular carcinoma. A determinant of chemotherapy response. **Am J Clin Pathol**, v. 113, n. 3, p. 355-63, 2000.

NIGAM, S. K. What do drug transporters really do? **Nat Rev Drug Discov**, v. 14, n. 1, p. 29-44, 2015.

NOGUCHI, K.; KATAYAMA, K.; SUGIMOTO, Y. Human ABC transporter ABCG2/BCRP expression in chemoresistance: basic and clinical perspectives for molecular cancer therapeutics. **Pharmgenomics Pers Med**, v. 7, p. 53-64, 2014.

OLLIS, W. D.; RAMSDEN, C. A. Meso-ionic Compounds*. In: KATRITZKY, A. R. e BOULTON, A. J. (Ed.). **Advances in Heterocyclic Chemistry**: Academic Press, v. Volume 19, 1976. p.1-122. ISBN 0065-2725.

ORRENIUS, S.; NICOTERA, P.; ZHIVOTOVSKY, B. Cell death mechanisms and their implications in toxicology. **Toxicol Sci**, v. 119, n. 1, p. 3-19, 2011.

OTA, S. et al. Immunohistochemical expression of BCRP and ERCC1 in biopsy specimen predicts survival in advanced non-small-cell lung cancer treated with cisplatin-based chemotherapy. **Lung Cancer**, v. 64, n. 1, p. 98-104, 2009.

OZVEGY-LACZKA, C. et al. High-affinity interaction of tyrosine kinase inhibitors with the ABCG2 multidrug transporter. **Mol Pharmacol**, v. 65, n. 6, p. 1485-95, 2004.

PADHYA, K. T.; MARRERO, J. A.; SINGAL, A. G. Recent advances in the treatment of hepatocellular carcinoma. **Curr Opin Gastroenterol**, v. 29, n. 3, p. 285-92, 2013.

PAIVA, R. O. et al. Mesoionic compounds with antifungal activity against *Fusarium verticillioides*. **BMC Microbiol**, v. 15, p. 11, 2015.

PENSON, R. T. et al. Expression of multidrug resistance-1 protein inversely correlates with paclitaxel response and survival in ovarian cancer patients: a study in serial samples. **Gynecol Oncol**, v. 93, n. 1, p. 98-106, 2004.

PHILIPS, H. J., Ed. **Dye exclusion test for cell viability** Tissue culture methods and applications. New York: Academic Press, p.406-408, Tissue culture methods and applications. 1973.

PIRES, A. D. R. A. **Derivados 1,3,4-Tiadiazóis mesoiônicos: Disfunção mitocondrial e toxicidade em células HEPG2**. Curitiba, 157p., Tese (Doutorado em Bioquímica), Setor de Ciências Biológicas, Universidade Federal do Paraná, Curitiba, 2011.

PIRES, A. R. et al. Comparative study of the effects of 1,3,4-thiadiazolium mesoionic derivatives on energy-linked functions of rat liver mitochondria. **Chem Biol Interact**, v. 186, n. 1, p. 1-8, 2010.

PIRES, A. R. et al. Interaction of 1,3,4-thiadiazolium mesoionic derivatives with mitochondrial membrane and scavenging activity: Involvement of their effects on

mitochondrial energy-linked functions. **Chem Biol Interact**, v. 189, n. 1-2, p. 17-25, 2011.

PIRES, A. R. A. et al. Interaction of 1,3,4-thiadiazolium mesoionic derivatives with mitochondrial membrane and scavenging activity: Involvement of their effects on mitochondrial energy-linked functions. **Chem Biol Interact**, v. 189, n. 1-2, p. 17-25, 2011.

PIRKER, R. et al. MDR1 gene expression and treatment outcome in acute myeloid leukemia. **J Natl Cancer Inst**, v. 83, n. 10, p. 708-12, 1991.

RABINDRAN, S. K. et al. Fumitremorgin C reverses multidrug resistance in cells transfected with the breast cancer resistance protein. **Cancer Res**, v. 60, n. 1, p. 47-50, 2000.

RAJAK, H. et al. 2,5-Disubstituted-1,3,4-oxadiazoles/thiadiazole as surface recognition moiety: Design and synthesis of novel hydroxamic acid based histone deacetylase inhibitors. **Bioorganic & Medicinal Chemistry Letters**, v. 21, n. 19, p. 5735-5738, 2011.

RAYCHAUDHURI, S. How can we kill cancer cells: Insights from the computational models of apoptosis. **World J Clin Oncol**, v. 1, n. 1, p. 24-8, 2010.

RAZA, H.; JOHN, A.; BENEDICT, S. Acetylsalicylic acid-induced oxidative stress, cell cycle arrest, apoptosis and mitochondrial dysfunction in human hepatoma HepG2 cells. **Eur J Pharmacol**, v. 668, n. 1-2, p. 15-24, 2011.

REATAZA, M.; IMAGAWA, D. K. Advances in managing hepatocellular carcinoma. **Front Med**, 2014.

REILLY, T. P. et al. Comparison of the in vitro cytotoxicity of hydroxylamine metabolites of sulfamethoxazole and dapsone. **Biochem Pharmacol**, v. 55, n. 6, p. 803-10, 1998.

RIEGER, A. M. et al. Modified annexin V/propidium iodide apoptosis assay for accurate assessment of cell death. **J Vis Exp**, v. 24, n. 50, p. 2597, 2011.

ROBEY, R. W. et al. Inhibition of ABCG2-mediated transport by protein kinase inhibitors with a bisindolylmaleimide or indolocarbazole structure. **Mol Cancer Ther**, v. 6, n. 6, p. 1877-85, 2007.

ROMAO, S. et al. Metabolism of the mesoionic compound (MI-D) by mouse liver microsome, detection of its metabolite in vivo, and acute toxicity in mice. **J Biochem Mol Toxicol**, v. 23, n. 6, p. 394-405, 2009.

RONGVED, P. et al. Indenoindoles and cyclopentacarbazoles as bioactive compounds: synthesis and biological applications. **Eur J Med Chem**, v. 69, p. 465-79, 2013.

SANTOS, A. C. S.; ECHEVARRIA, A. Electronic effects on ¹³C NMR chemical shifts of substituted 1,3,4-thiadiazolium salts. **Magnetic Resonance in Chemistry**, v. 39, n. 4, p. 182-186, 2001.

SCHINKEL, A. H.; JONKER, J. W. Mammalian drug efflux transporters of the ATP binding cassette (ABC) family: an overview. **Adv Drug Deliv Rev**, v. 55, n. 1, p. 3-29, 2003.

SCHOEPFER, J. et al. Structure-based design and synthesis of 2-benzylidene-benzofuran-3-ones as flavopiridol mimics. **J Med Chem**, v. 45, n. 9, p. 1741-7, 2002.

SEGLEN, P. O. Preparation of isolated rat liver cells. **Methods Cell Biol**, v. 13, p. 29-83, 1976.

SENF-FRIBEIRO, A. et al. Cytotoxic effect of a new 1,3,4-thiadiazolium mesoionic compound (MI-D) on cell lines of human melanoma. **Br J Cancer**, v. 91, n. 2, p. 297-304, 2004a.

SENF-FRIBEIRO, A. et al. Effect of a new 1,3,4-thiadiazolium mesoionic compound (MI-D) on B16-F10 murine melanoma. **Melanoma Res**, v. 13, n. 5, p. 465-71, 2003.

SENF-FRIBEIRO, A. et al. Antimelanoma activity of 1,3,4-thiadiazolium mesoionics: a structure-activity relationship study. **Anticancer Drugs**, v. 15, n. 3, p. 269-75, 2004b.

SEO, S. et al. Fluorine-18 fluorodeoxyglucose positron emission tomography predicts tumor differentiation, P-glycoprotein expression, and outcome after resection in hepatocellular carcinoma. **Clin Cancer Res**, v. 13, n. 2 Pt 1, p. 427-33, 2007.

SHERTZER, H. G.; SAINSBURY, M. Protection against carbon tetrachloride hepatotoxicity by 5,10-dihydroindeno[1,2-b]indole, a potent inhibitor of lipid peroxidation. **Food Chem Toxicol**, v. 26, n. 6, p. 517-22, 1988.

SHI, J. et al. A review on the diagnosis and treatment of hepatocellular carcinoma with a focus on the role of wnts and the dickkopf family of wnt inhibitors. **Journal of Hepatocellular Carcinoma**, v. 1, p. 7, 2014.

SHIMIZU, M. et al. The lipid peroxidation inhibitor indenoindole H290/51 protects myocardium at risk of injury induced by ischemia-reperfusion. **Free Radic Biol Med**, v. 24, n. 5, p. 726-31, 1998.

SHUKLA, S.; OHNUMA, S.; AMBUDKAR, S. V. Improving cancer chemotherapy with modulators of ABC drug transporters. **Curr Drug Targets**, v. 12, n. 5, p. 621-30, 2011.

SHUKLA, S. et al. Sunitinib (Sutent, SU11248), a small-molecule receptor tyrosine kinase inhibitor, blocks function of the ATP-binding cassette (ABC) transporters P-glycoprotein (ABCB1) and ABCG2. **Drug Metab Dispos**, v. 37, n. 2, p. 359-65, 2009.

SIM, H. M. et al. Dimethoxyaurones: Potent inhibitors of ABCG2 (breast cancer resistance protein). **Eur J Pharm Sci**, v. 35, n. 4, p. 293-306, 2008.

SINGAL, A. G.; EL-SERAG, H. B. Hepatocellular Carcinoma from Epidemiology to Prevention: Translating Knowledge into Practice. **Clin Gastroenterol Hepatol**, 2015.

STACY, A. E.; JANSSON, P. J.; RICHARDSON, D. R. Molecular pharmacology of ABCG2 and its role in chemoresistance. **Mol Pharmacol**, v. 84, n. 5, p. 655-69, 2013.

SUKOWATI, C. H. et al. Gene and functional up-regulation of the BCRP/ABCG2 transporter in hepatocellular carcinoma. **BMC Gastroenterol**, v. 12, p. 160, 2012.

SUN, J. et al. Synthesis, biological evaluation and molecular docking studies of 1,3,4-thiadiazole derivatives containing 1,4-benzodioxan as potential antitumor agents. **Bioorg Med Chem Lett**, v. 21, n. 20, p. 6116-21, 2011.

SUN, Z. et al. Relevance of two genes in the multidrug resistance of hepatocellular carcinoma: in vivo and clinical studies. **Tumori**, v. 96, n. 1, p. 90-6, 2010.

SUZUKI, A. et al. ARK5 is a tumor invasion-associated factor downstream of Akt signaling. **Mol Cell Biol**, v. 24, n. 8, p. 3526-35, 2004.

TABRIZIAN, P.; ROAYAIE, S.; SCHWARTZ, M. E. Current management of hepatocellular carcinoma. **World J Gastroenterol**, v. 20, n. 30, p. 10223-37, 2014.

TAKAHASHI, S. et al. Substrate-dependence of reduction of MTT: a tetrazolium dye differs in cultured astroglia and neurons. **Neurochem Int**, v. 40, n. 5, p. 441-8, 2002.

TAMAKI, A. et al. The controversial role of ABC transporters in clinical oncology. **Essays Biochem**, v. 50, n. 1, p. 209-32, 2011.

TERMAN, A.; BRUNK, U. T. Lipofuscin. **Int J Biochem Cell Biol**, v. 36, n. 8, p. 1400-4, 2004.

TIAN, Z. et al. Antitumor activity and mechanisms of action of total glycosides from aerial part of *Cimicifuga dahurica* targeted against hepatoma. **BMC Cancer**, v. 7, p. 237, 2007.

UCHIBORI, K. et al. Establishment and characterization of two 5-fluorouracil-resistant hepatocellular carcinoma cell lines. **Int J Oncol**, v. 40, n. 4, p. 1005-10, 2012.

UHL, P. et al. Current status in the therapy of liver diseases. **Int J Mol Sci**, v. 15, n. 5, p. 7500-12, 2014.

VALDAMERI, G. et al. Investigation of chalcones as selective inhibitors of the breast cancer resistance protein: critical role of methoxylation in both inhibition potency and cytotoxicity. **J Med Chem**, v. 55, n. 7, p. 3193-200, 2012b.

VALDAMERI, G. et al. Substituted chromones as highly potent nontoxic inhibitors, specific for the breast cancer resistance protein. **J Med Chem**, v. 55, n. 2, p. 966-70, 2012a.

VALDAMERI, G. et al. Substituted Chromones as Highly Potent Nontoxic Inhibitors, Specific for the Breast Cancer Resistance Protein. **Journal of Medicinal Chemistry**, v. 55, n. 2, p. 966-970, 2012.

VALDAMERI, G. et al. Methoxy stilbenes as potent, specific, untransported, and noncytotoxic inhibitors of breast cancer resistance protein. **ACS Chem Biol**, v. 7, n. 2, p. 322-30, 2012c.

VAN LOEVEZIJN, A. et al. Inhibition of BCRP-mediated drug efflux by fumitremorgin-type indolyl diketopiperazines. **Bioorg Med Chem Lett**, v. 11, n. 1, p. 29-32, 2001.

VANDER BORGHT, S. et al. Expression of multidrug resistance-associated protein 1 in hepatocellular carcinoma is associated with a more aggressive tumour phenotype and may reflect a progenitor cell origin. **Liver Int**, v. 28, n. 10, p. 1370-80, 2008.

VERMES, I. et al. A novel assay for apoptosis. Flow cytometric detection of phosphatidylserine expression on early apoptotic cells using fluorescein labelled Annexin V. **J Immunol Methods**, v. 184, n. 1, p. 39-51, 1995.

WANG, Y. J. et al. Repositioning of Tyrosine Kinase Inhibitors as Antagonists of ATP-Binding Cassette Transporters in Anticancer Drug Resistance. **Cancers (Basel)**, v. 6, n. 4, p. 1925-52, 2014.

WEIDNER, L. D. et al. The Inhibitor Ko143 Is Not Specific for ABCG2. **J Pharmacol Exp Ther**, v. 354, n. 3, p. 384-93, 2015.

WESTERLUND, C. et al. Characterization of novel indenoindoles. Part I. Structure-activity relationships in different model systems of lipid peroxidation. **Biochem Pharmacol**, v. 51, n. 10, p. 1397-402, 1996.

WILHELM, S. M. et al. BAY 43-9006 exhibits broad spectrum oral antitumor activity and targets the RAF/MEK/ERK pathway and receptor tyrosine kinases involved in tumor progression and angiogenesis. **Cancer Res**, v. 64, n. 19, p. 7099-109, 2004.

WILKENS, S. Structure and mechanism of ABC transporters. **F1000Prime Reports**, v. 7, p. 14, 2015.

WINTER, E. et al. Symmetric bis-chalcones as a new type of breast cancer resistance protein inhibitors with a mechanism different from that of chromones. **J Med Chem**, v. 57, n. 7, p. 2930-41, 2014.

WINTER, E. et al. Structure-activity relationships of chromone derivatives toward the mechanism of interaction with and inhibition of breast cancer resistance protein ABCG2. **J Med Chem**, v. 56, n. 24, p. 9849-60, 2013.

WOO, H. Y.; HEO, J. New perspectives on the management of hepatocellular carcinoma with portal vein thrombosis. **Clin Mol Hepatol**, v. 21, n. 2, p. 115-21, 2015.

WU, C. P.; HSIEH, C. H.; WU, Y. S. The emergence of drug transporter-mediated multidrug resistance to cancer chemotherapy. **Mol Pharm**, v. 8, n. 6, p. 1996-2011, 2011.

WU, C. P.; OHNUMA, S.; AMBUDKAR, S. V. Discovering natural product modulators to overcome multidrug resistance in cancer chemotherapy. **Curr Pharm Biotechnol**, v. 12, n. 4, p. 609-20, 2011.

WU, X. et al. Selective Protection of Normal Cells During Chemotherapy by RY4 Peptides. **Mol Cancer Res**, 2014.

XIANG, Q. F. et al. Effect of BIBF 1120 on reversal of ABCB1-mediated multidrug resistance. **Cell Oncol (Dordr)**, v. 34, n. 1, p. 33-44, 2011.

XIAOHE, Z. et al. Synthesis, biological evaluation and molecular modeling studies of N-aryl-2-arylthioacetamides as non-nucleoside HIV-1 reverse transcriptase inhibitors. **Chem Biol Drug Des**, v. 76, n. 4, p. 330-9, 2010.

YAMAZAKI, R. et al. Novel acrylonitrile derivatives, YHO-13177 and YHO-13351, reverse BCRP/ABCG2-mediated drug resistance in vitro and in vivo. **Mol Cancer Ther**, v. 10, n. 7, p. 1252-63, 2011.

YANASE, K. et al. Gefitinib reverses breast cancer resistance protein-mediated drug resistance. **Mol Cancer Ther**, v. 3, n. 9, p. 1119-25, 2004.

YU, S. J.; KIM, Y. J. Effective treatment strategies other than sorafenib for the patients with advanced hepatocellular carcinoma invading portal vein. **World J Hepatol**, v. 7, n. 11, p. 1553-61, 2015.

ZHENG, L. H. et al. Cantharidin reverses multidrug resistance of human hepatoma HepG2/ADM cells via down-regulation of P-glycoprotein expression. **Cancer Lett**, v. 272, n. 1, p. 102-9, 2008.

ANEXOS

ANEXO 1- DIREITO DE REPRODUÇÃO DO ARTIGO 1.....	154
ANEXO 2- DIREITO DE REPRODUÇÃO DO ARTIGO 2.....	155
ANEXO 3- DIREITO DE REPRODUÇÃO DO ARTIGO 3.....	156

ANEXO 1- DIREITO DE REPRODUÇÃO DO ARTIGO 1

Selective Cytotoxicity of 1,3,4-Thiadiazolium Mesoionic Derivatives on Hepatocarcinoma Cells (HepG2)

Gustavo Jabor Gozzi, Amanda do Rocio Andrade Pires, Glauco Valdameri, Maria Eliane Merlin Rocha, Glauca Regina Martinez, ...

Abstract

Introduction

Materials and Methods

Results

Discussion and
Conclusions

Author Contributions

References

Reader Comments (0)

Media Coverage (0)

Figures

Citation: Gozzi GJ, Pires AdRA, Valdameri G, Rocha MEM, Martinez GR, Noleto GR, et al. (2015) Selective Cytotoxicity of 1,3,4-Thiadiazolium Mesoionic Derivatives on Hepatocarcinoma Cells (HepG2). PLoS ONE 10(6): e0130046. doi:10.1371/journal.pone.0130046

Academic Editor: Matias A. Avila, University of Navarra School of Medicine and Center for Applied Medical Research (CIMA), SPAIN

Received: March 3, 2015; **Accepted:** May 15, 2015; **Published:** June 17, 2015

Copyright: © 2015 Gozzi et al. This is an open access article distributed under the terms of the [Creative Commons Attribution License](#), which permits unrestricted use, distribution, and reproduction in any medium, provided the original author and source are credited

Data Availability: All relevant data are within the paper.

Funding: This study was supported by the Brazilian research funding agencies CNPq (Conselho Nacional para o Desenvolvimento Científico e Tecnológico), CAPES (Coordenação de Aperfeiçoamento de Pessoal de Nível Superior), and the French National League against Cancer (Equipe Labellisée 2014), CNRS and University of Lyon 1 (UMR5086). G.J.G. was supported by a sandwich Ph.D. fellowship from the Brazilian Agency (CNPq) (process numbers 245762/2012-4). G.R.M. also received financial support from the Instituto do Milênio: Redoxoma, INCT de Processos Redox em Biomedicina—Redoxoma.

Competing interests: The authors have declared that no competing interests exist.

ANEXO 2- DIREITO DE REPRODUÇÃO DO ARTIGO 2



RightsLink®

Home

Account
Info

Help

ACS Publications
Most Trusted. Most Cited. Most Read.

Title: Converting Potent Indeno[1,2-b]indole Inhibitors of Protein Kinase CK2 into Selective Inhibitors of the Breast Cancer Resistance Protein ABCG2

Author: Gustavo Jabor Gozzi, Zouhair Bouaziz, Evelyn Winter, et al

Publication: Journal of Medicinal Chemistry

Publisher: American Chemical Society

Date: Jan 1, 2015

Copyright © 2015, American Chemical Society

Logged in as:
Gustavo Gozzi
Account #:
3000973833

LOGOUT

PERMISSION/LICENSE IS GRANTED FOR YOUR ORDER AT NO CHARGE

This type of permission/license, instead of the standard Terms & Conditions, is sent to you because no fee is being charged for your order. Please note the following:

- Permission is granted for your request in both print and electronic formats, and translations.
- If figures and/or tables were requested, they may be adapted or used in part.
- Please print this page for your records and send a copy of it to your publisher/graduate school.
- Appropriate credit for the requested material should be given as follows: "Reprinted (adapted) with permission from (COMPLETE REFERENCE CITATION). Copyright (YEAR) American Chemical Society." Insert appropriate information in place of the capitalized words.
- One-time permission is granted only for the use specified in your request. No additional uses are granted (such as derivative works or other editions). For any other uses, please submit a new request.

BACK

CLOSE WINDOW

Copyright © 2016 Copyright Clearance Center, Inc. All Rights Reserved. [Privacy statement](#). [Terms and Conditions](#).
Comments? We would like to hear from you. E-mail us at customer@copyright.com

ANEXO 3- DIREITO DE REPRODUÇÃO DO ARTIGO 3

11/11/2015

Copyright Clearance Center



Note: Copyright.com supplies permissions but not the copyrighted content itself.

1
PAYMENT

2
REVIEW

3
CONFIRMATION

Step 3: Order Confirmation

Thank you for your order! A confirmation for your order will be sent to your account email address. If you have questions about your order, you can call us at +1.855.239.3415 Toll Free, M-F between 3:00 AM and 6:00 PM (Eastern), or write to us at info@copyright.com. This is not an invoice.

Confirmation Number: 11487723
Order Date: 11/11/2015

If you paid by credit card, your order will be finalized and your card will be charged within 24 hours. If you choose to be invoiced, you can change or cancel your order until the invoice is generated.

Payment Information

Gustavo Gozzi
gustavobioquimico@yahoo.com.br
+55 (41)33611664
Payment Method: n/a

Order Details

Drug Design, Development and Therapy

Order detail ID: 68928668
Order License Id: 3746080982539
ISSN: 1177-8881
Publication Type: e-Journal
Volume:
Issue:
Start page:
Publisher: Dove Press Limited

Permission Status: **Granted**
Permission type: Republish or display content
Type of use: Republish in a thesis/dissertation

Requestor type	Academic institution
Format	Print, Electronic
Portion	chapter/article
Title or numeric reference of the portion(s)	Phenolic indeno[1,2-b]indoles as ABCG 2-selective potent and non-toxic inhibitors stimulating basal ATPase activity
Title of the article or chapter the portion is from	N/A
Editor of portion(s)	N/A
Author of portion(s)	N/A
Volume of serial or monograph	N/A
Issue, if republishing an article from a serial	N/A

11/11/2015

Copyright Clearance Center

Page range of portion

Publication date of portion	3 July 2015
Rights for	Main product
Duration of use	Life of current and all future editions
Creation of copies for the disabled	no
With minor editing privileges	no
For distribution to	Worldwide
In the following language(s)	Original language of publication
With incidental promotional use	no
Lifetime unit quantity of new product	Up to 499
Made available in the following markets	Education
The requesting person/organization	Gustavo Jabor Gozzi
Order reference number	
Author/Editor	Gustavo Jabor Gozzi
The standard identifier	Thesis
Title	DERIVADOS 1,3,4-TIADIAZÁIS MESOIÁNICOS E INDENO[1,2-b]INDÁIS: CITOTOXICIDADE E EFEITOS SOBRE TRANSPORTADORES ABC
Publisher	Universidade Federal do Paraná
Expected publication date	Dec 2015
Estimated size (pages)	150
Customer Tax ID	BR87214320

Note: This item will be invoiced or charged separately through CCC's **RightsLink** service. [More info](#) **\$ 0.00**

11/11/2015

Copyright Clearance Center

Total order items: 1

This is not an invoice.

Order Total: 0.00 USD

Confirmation Number: 11487723

Special Rightsholder Terms & Conditions

The following terms & conditions apply to the specific publication under which they are listed

Drug Design, Development and Therapy
Permission type: Republish or display content
Type of use: Republish in a thesis/dissertation

TERMS AND CONDITIONS

The following terms are individual to this publisher:

None

Other Terms and Conditions:

STANDARD TERMS AND CONDITIONS

1. Description of Service; Defined Terms. This Republication License enables the User to obtain licenses for republication of one or more copyrighted works as described in detail on the relevant Order Confirmation (the "Work(s)"). Copyright Clearance Center, Inc. ("CCC") grants licenses through the Service on behalf of the rightsholder identified on the Order Confirmation (the "Rightsholder"). "Republication", as used herein, generally means the inclusion of a Work, in whole or in part, in a new work or works, also as described on the Order Confirmation. "User", as used herein, means the person or entity making such republication.

2. The terms set forth in the relevant Order Confirmation, and any terms set by the Rightsholder with respect to a particular Work, govern the terms of use of Works in connection with the Service. By using the Service, the person transacting for a republication license on behalf of the User represents and warrants that he/she/it (a) has been duly authorized by the User to accept, and hereby does accept, all such terms and conditions on behalf of User, and (b) shall inform User of all such terms and conditions. In the event such person is a "freelancer" or other third party independent of User and CCC, such party shall be deemed jointly a "User" for purposes of these terms and conditions. In any event, User shall be deemed to have accepted and agreed to all such terms and conditions if User republishes the Work in any fashion.

3. Scope of License; Limitations and Obligations.

3.1 All Works and all rights therein, including copyright rights, remain the sole and exclusive property of the Rightsholder. The license created by the exchange of an Order Confirmation (and/or any invoice) and payment by User of the full amount set forth on that document includes only those rights expressly set forth in the Order Confirmation and in these terms and conditions, and conveys no other rights in the Work(s) to User. All rights not expressly granted are hereby reserved.

3.2 General Payment Terms: You may pay by credit card or through an account with us payable at the end of the month. If you and we agree that you may establish a standing account with CCC, then the following terms apply: Remit Payment to: Copyright Clearance Center, Dept 001, P.O. Box 843006, Boston, MA 02284-3006. Payments Due: Invoices are payable upon their delivery to you (or upon our notice to you that they are available to you for downloading). After 30 days, outstanding amounts will be subject to a service charge of 1-1/2% per month or, if less, the maximum rate allowed by applicable law. Unless otherwise specifically set forth in the Order Confirmation or in a separate written agreement signed by CCC, invoices are due and payable on "net 30" terms. While User may exercise the rights licensed immediately upon issuance of the Order Confirmation, the license is automatically revoked and is null and void, as if it had never been issued, if complete payment for the license is not received on a timely basis either from User directly or through a payment agent, such as a credit card company.

3.3 Unless otherwise provided in the Order Confirmation, any grant of rights to User (i) is "one-time" (including the editions and product family specified in the license), (ii) is non-exclusive and non-transferable and (iii) is subject to any and all limitations and restrictions (such as, but not limited to, limitations on duration of use or circulation) included in the Order Confirmation or invoice and/or in these terms and conditions. Upon completion of the licensed use, User shall either secure a new permission for further use of the Work(s) or immediately cease any new use of the Work(s) and shall render inaccessible (such as by deleting or by removing or severing links or other locators) any further copies of the Work (except for copies printed on paper in accordance with this license and still in User's stock at the end of such period).

3.4 In the event that the material for which a republication license is sought includes third party materials (such as photographs, illustrations, graphs, inserts and similar materials) which are identified in such material as having been used by permission, User is responsible for identifying, and seeking separate licenses (under this Service or otherwise) for, any of such third party materials; without a separate license, such third party materials may not be used.

3.5 Use of proper copyright notice for a Work is required as a condition of any license granted under the Service. Unless otherwise provided in the Order Confirmation, a proper copyright notice will read substantially as follows: "Republished with permission of [Rightsholder's name], from [Work's title, author, volume, edition number and year of copyright]; permission conveyed through Copyright Clearance Center, Inc. " Such notice must be provided in a reasonably legible font size and must be placed either immediately adjacent to the Work as used (for example, as part of a by-line or footnote but not as a separate electronic link) or in the place where substantially all other credits or notices for the new work containing the republished Work are located. Failure to include the required notice results in loss to the Rightsholder and CCC, and the User shall be liable to pay liquidated damages for each such failure equal to twice the use fee specified in the Order Confirmation, in addition to the use fee itself and any other fees and charges specified.

3.6 User may only make alterations to the Work if and as expressly set forth in the Order Confirmation. No Work may be used in any way that is defamatory, violates the rights of third parties (including such third parties' rights of copyright, privacy, publicity, or other tangible or intangible property), or is otherwise illegal, sexually explicit or obscene. In addition, User may not conjoin a Work with any other material that may result in damage to the reputation of the Rightsholder. User agrees to inform CCC if it becomes aware of any infringement of any rights in a Work and to cooperate with any reasonable request of CCC or the Rightsholder in connection therewith.

4. Indemnity. User hereby indemnifies and agrees to defend the Rightsholder and CCC, and their respective employees and directors, against all claims, liability, damages, costs and expenses, including legal fees and expenses, arising out of any use of a Work beyond the scope of the rights granted herein, or any use of a Work which has been altered in any unauthorized way by User, including claims of defamation or infringement of rights of copyright, publicity, privacy or other tangible or intangible property.

5. Limitation of Liability. UNDER NO CIRCUMSTANCES WILL CCC OR THE RIGHTSHOLDER BE LIABLE FOR ANY DIRECT, INDIRECT, CONSEQUENTIAL OR INCIDENTAL DAMAGES (INCLUDING WITHOUT LIMITATION DAMAGES FOR LOSS OF BUSINESS PROFITS OR INFORMATION, OR FOR BUSINESS INTERRUPTION) ARISING OUT OF THE USE OR INABILITY TO USE A WORK, EVEN IF ONE OF THEM HAS BEEN ADVISED OF THE POSSIBILITY OF SUCH DAMAGES. In any event, the total liability of the Rightsholder and CCC (including their respective employees and directors) shall not exceed the total amount actually paid by User for this license. User assumes full liability for the actions and omissions of its principals, employees, agents, affiliates, successors and assigns.

6. Limited Warranties. THE WORK(S) AND RIGHT(S) ARE PROVIDED "AS IS". CCC HAS THE RIGHT TO GRANT TO USER THE RIGHTS GRANTED IN THE ORDER CONFIRMATION DOCUMENT. CCC AND THE RIGHTSHOLDER DISCLAIM ALL OTHER WARRANTIES RELATING TO THE WORK(S) AND RIGHT(S), EITHER EXPRESS OR IMPLIED, INCLUDING WITHOUT LIMITATION IMPLIED WARRANTIES OF MERCHANTABILITY OR FITNESS FOR A PARTICULAR PURPOSE. ADDITIONAL RIGHTS MAY BE REQUIRED TO USE ILLUSTRATIONS, GRAPHS, PHOTOGRAPHS, ABSTRACTS, INSERTS OR OTHER PORTIONS OF THE WORK (AS OPPOSED TO THE ENTIRE WORK) IN A MANNER CONTEMPLATED BY USER; USER UNDERSTANDS AND AGREES THAT NEITHER CCC NOR THE RIGHTSHOLDER MAY HAVE SUCH ADDITIONAL RIGHTS TO GRANT.

7. Effect of Breach. Any failure by User to pay any amount when due, or any use by User of a Work beyond the scope of the license set forth in the Order Confirmation and/or these terms and conditions, shall be a material breach of the license created by the Order Confirmation and these terms and conditions. Any breach not cured within 30 days of written notice thereof shall result in immediate termination of such license without further notice. Any unauthorized (but licensable) use of a Work that is terminated immediately upon notice thereof may be liquidated by payment of the Rightsholder's ordinary license price therefor; any unauthorized (and unlicensable) use that is not terminated immediately for any reason (including, for example, because materials containing the Work cannot reasonably be recalled) will be subject to all remedies available at law or in equity, but in no event to a payment of less than three times the Rightsholder's ordinary license price for the most closely analogous licensable use plus Rightsholder's and/or CCC's costs and expenses incurred in collecting such payment.

8. Miscellaneous.

8.1 User acknowledges that CCC may, from time to time, make changes or additions to the Service or to these terms and conditions, and CCC reserves the right to send notice to the User by electronic mail or otherwise for the purposes of notifying User of such changes or additions; provided that any such changes or additions shall not apply to permissions already secured and paid for.

8.2 Use of User-related information collected through the Service is governed by CCC's privacy policy, available online here: <http://www.copyright.com/content/cc3/en/tools/footer/privacypolicy.html>.

8.3 The licensing transaction described in the Order Confirmation is personal to User. Therefore, User may not assign or transfer to any other person (whether a natural person or an organization of any kind) the license created by the Order Confirmation and these terms and conditions or any rights granted hereunder; provided, however, that User may assign such license in its entirety on written notice to CCC in the event of a transfer of all or substantially all of User's rights in the new material which includes the Work(s) licensed under this Service.

8.4 No amendment or waiver of any terms is binding unless set forth in writing and signed by the parties. The Rightsholder and CCC hereby object to any terms contained in any writing prepared by the User or its principals, employees, agents or affiliates and purporting to govern or otherwise relate to the licensing transaction described in the Order Confirmation, which terms are in any way inconsistent with any terms set forth in the Order Confirmation and/or in these terms and conditions or CCC's standard operating procedures, whether such writing is prepared prior to, simultaneously with or subsequent to the Order Confirmation, and whether such writing appears on a copy of the Order Confirmation or in a separate instrument.

8.5 The licensing transaction described in the Order Confirmation document shall be governed by and construed under the law of the State of New York, USA, without regard to the principles thereof of conflicts of law. Any case, controversy, suit, action, or proceeding arising out of, in connection with, or related to such licensing transaction shall be brought, at CCC's sole discretion, in any federal or state court located in the County of New York, State of New York, USA, or in any federal or state court whose geographical jurisdiction covers the location of the Rightsholder set forth in the Order Confirmation. The parties expressly submit to the personal jurisdiction and venue of each such federal or state court. If you have any comments or questions about the Service or Copyright Clearance Center, please contact us at 978-750-8400 or send an e-mail to info@copyright.com.

v 1.1

Close

11/11/2015

Copyright Clearance Center

Confirmation Number: 11487723

Citation Information

Order Detail ID: 68928668

Drug Design, Development and Therapy by Dove Press Limited. Reproduced with permission of Dove Press Limited in the format Republish in a thesis/dissertation via Copyright Clearance Center.

Close